GEOLINKS

INTERNATIONAL CONFERENCE

# CONFERENCE PROCEEDINGS

BOOK 1

VOLUME 3

BIOTECHNOLOGIES

ENVIRONMENTAL GEOLOGY

SOIL SCIENCE

WATER RESOURCES

17-18 MAY 2021 | ONLINE EDITION

## DISCLAIMER

This book contains papers which cover the sections: Biotechnologies, Environmental Geology, Soil Science and Water Resources.

This book contains abstracts, keywords and full papers, which has gone under double blind peer review by the GEOLINKS Review Committee. Authors of the articles are responsible for the content and accuracy.

Opinions expressed might not necessary affect the position of GEOLINKS Committee Members and Scientific Council.

Information in the GEOLINKS 2021 Conference proceedings is subject to change without any prior notice. No parts of this book can by reproduced or transmitted in any form or by any mean without the written confirmation of the Scientific Council of GEOLINKS.


Published by SAIMA CONSULT LTD, Sofia, 1616, st. Beliya Kladenets, 15, fl. 3
Total print 50

ISSN 2603-5472
ISBN 978-619-7495-17-1
DOI 10.32008/GEOLINKS2021/B1/V3

GEOLINKS CONFERENCE
Secretariat Bureau
e-mail: contact@geolinks.info
URL: https://www.geolinks.info

## ORGANIZERS AND SCIENTIFIC PARTNERS OF GEOLINKS INTERNATIONAL CONFERENCE

SLOVAK ACADEMY OF SCIENCES
CZECH ACADEMY OF SCIENCES
NATIONAL ACADEMY OF SCIENCES OF UKRAINE
BULGARIAN ACADEMY OF SCIENCES
POLISH ACADEMY OF SCIENCES
ACADEMY OF SCIENCES OF HUNGARY
SERBIAN ACADEMY OF SCIENCES
TURKISH ACADEMY OF SCIENCES
ACADEMY OF SCIENCES OF MOLDOVA
ISLAMIC WORLD ACADEMY OF SCIENCES
LATVIA ACADEMY OF SCIENCES

## SCIENTIFIC COMMITEE OF GEOLINKS INTERNATIONAL CONFERENCE

ASSOC. PROF. JOZEF MARTINKA, SLOVENIA
PROF. BAIBA RIVZA, LATVIA
PROF. DSC. VOLODYMYR POHREBENNYK, UKRAINE AND POLAND
ASSOC.PROF. ZEYNEL FUAT TOPRAK, TURKEY
PROF. RADA JOAN, ROMANIA
ASSOC. PROF. DSC. GIUSEPPE SAPPA, ITALY
DR. DIMITRIS KALIAMPAKOS, GREECE
PHD. TAKACS ILDIKO-CSILLA, ROMANIA
PROF. ANDON ANDONOV, BULGARIA
DR. PAOLO BAZZOFFI, ITALY
PROF. VRACHNAKIS MICHAIL, GREECE
PROF. MAYA DIMITROVA, BULGARIA
DR. ENG. VLAD MIHAI PASCULESCU, ROMANIA
ASSOC. PROF. PHD ENG. IURES LIANA, ROMANIA
ASSOC. PROF. VADIM ZHMUD, RUSSIA
ASSOC. PROF. POENAR DANIEL PUIU, ROMANIA
PROF. NIKOLAOS SAMARAS, GREECE
ASSOC. PROF. CARMEN-PENELOPI PAPADATU, ROMANIA
DR. AFSOON KAZEROUNI, USA

# CONTENT

## Section BIOTECHNOLOGIES

## Section ENVIRONMENTAL GEOLOGY

## Section SOIL SCIENCE



## Section WATER RESOURCES

Section

# BIOTECHNOLOGIES

Genetic engineering and molecular diagnostic
Bio-energy production and environmental bioremediation
Bio-safety, systems biology and bioethics

# COMPREHENSIVE BIOTECHNOLOGICAL APPROACH TO PROCESSING OF PEA FLOUR FOR FOOD AND FODDER PURPOSES

**Ph.D. Student Denis Kulikov**[1]
**Ph.D. Ruzaliya Ulanova**[2]
**Prof. Dr. Valentina Kolpakova**[3]
[1, 3] All-Russian Research Institute for Starch Products – Branch of V.M. Gorbatov Federal Research Center for Food Systems of Russian Academy of Sciences, Russia
[2] S.N. Vinogradsky Institute of Microbiology, Federal Research Center "Fundamental Foundations of Biotechnology", of Russian Academy of Sciences, Moscow, Russia

## ABSTRACT

Investigations were carried out to optimize the growth parameters of the symbiosis of cultures of the yeast *Saccharomyces cerevisiae* 121 and the fungus *Geotrichum candidum* 977 on whey waters formed from pea flour as a secondary product in the production of protein concentrates after precipitation of proteins at the isoelectric point. The whey remaining after protein precipitation is bioconverted at optimal parameters of crop growth (pH of the medium, amount of inoculum, temperature) with the formation of microbial plant concentrate (MPC) for feed purposes. Serum cultures assimilated stachyose, glucose, maltose, arabinose, and other pentoses. The mass fraction of protein in the concentrate was 57.90-61.68 % of DS. The composition of MPC obtained from biomass is balanced in essential amino acids with a speed of 107-226 %. The fatty acid composition is represented by 97 % fatty acids and 3 % - esters, aldehydes, ketones with the properties of fragrances, photo stabilizers, odor fixers, preservatives and other compounds. The ratio of the sum of saturated and unsaturated acids is 1:3, the content of cis-isomers is 91.1 %, trans-isomers are 5.1 %, omega-6 fatty acids are 19.73 %. The quality and safety indicators indicated that it is promising for use in the diet of animals.

***Keywords:*** *pea flour, processing, serum, bioconversion, microbial-plant concentrate, amino acid composition, fatty acid composition*

## INTRODUCTION

Modern trends in the development of food production indicate that in the coming years, the deficit of protein in human and animal nutrition will not decrease, and the need for new high-quality (dietary) protein sources will increase. The number of hungry people in the world is growing, at the moment it has reached a third of the entire population of the Earth, part of the population is experiencing a deficiency of complete protein [1]. One of the ways to eliminate the deficit is to obtain protein preparations from plant materials. In this case, secondary products of processing raw materials into proteins or starch can be involved in the scheme of processing by the bioconversion method. The biomass of microorganisms can be

used as part of the diets of farm animals to increase their productivity and for human nutrition as new sources of proteins. Known bioconversion products from various types of by-product sources of the food industry and agriculture. Since ancient times, legumes have been used in the diet of people, including those who, for one reason or another, do not eat meat [2], [3]. Of particular interest is one of the traditional leguminous crops for European countries, including Russia, - peas, the use of which makes it possible to create technologies for protein concentrates, flour, isolates and by-products [4]. Information on the processing of secondary products formed from leguminous crops is still limited, despite the interest in this area. Thus, on the basis of a by-product formed during the extraction of pea protein, using filamentous fungi, a food mycoprotein concentrate was synthesized to "replace" meat. Studies were carried out with strains of fungi: *Aspergillus oryzae*, *Fusarium venenatum*, *Monascus purpureus*, *Rhizopus oryzae* fermentation at 35 ± 2 °C for 48 hours. The protein content in the mushroom biomass reached 43.13-59.74 %. It has been shown that the introduction of this process into production will provide about 680 kg of mushroom biomass with 38 % of additional protein for each 1 ton of by-product [5]. We have also proved the possibility of bioconversion of the secondary product (extract) of processing triticale grain into starch together with pea flour, and obtaining a feed concentrate with a mass fraction in% on DS: protein 55.8−75.1, carbohydrates - 18.9−32.83, fat 3.56−13.56, ash 2.05–8.27 [6]. Cultures of microorganisms actively developing on the substrate were selected, and a symbiotic starter culture from the fungus was compiled from them. *Geotrichum candidum* 977 and yeast *Saccharomyces cerevisiae* 121, providing the growth of biomass in a carbohydrate, nitrogen-containing medium. The serum formed after the isolation of concentrated proteins from the composition with pea flour was benign for culture media of microbiological synthesis with fungus and yeast. We also obtained preliminary positive results with this composition of microorganisms using serum formed during the isolation of proteins from chickpea [7] and pea [8] grains according to the scheme using enzyme preparations without optimization of parameters.

The aim of this work was to improve the process of bioconversion of grain whey, formed as a secondary product of the processing of flour from pea grain into protein concentrate, by the symbiosis of the yeast *S. cerevisiae* and the fungus *G. candidum* 977, by optimizing the growth parameters of microorganisms with the subsequent characterization of the feed microbial-plant concentrate.

## MATERIALS AND METHODS

The objects used were pea whey made from flour obtained from Yamal grain with 11.6 % moisture and mass fraction, % of DS: protein (Nx6.25) - 25.7; ash - 2.67; fat - 1.46; starch - 51.50; carbohydrates - 18.76. Enzyme preparations from Novozymes A/S (Denmark) were used to isolate protein concentrates and the secondary product of grain whey from flour: Shearzym 500 L, Viscoferm L, Fungamyl 800 L, AMG 300 L 2500, and Distizym Protacid from Erbslon. The yeast *Saccharomyces cerevisiae* 121 from the collection of the Institute of Microbiology named after S.N. Vinogradskiy and a new strain of the fungus *Geotrichum*

*candidum* 977, the phylogenetic position of which was determined jointly with the State Research Institute of Genetics (Russia) [9].

The amount of protein in the solution was determined by the Lowry method, nitrogenous substances in flour and in MPC - by the Kjeldahl method (GOST 10846-91); moisture - GOST 13586.5-93; ash - GOST 10847-2019; fat - GOST 29033-91, carbohydrates - by the difference between 100 % and the sum of the remaining components. The amino acid composition of MPC was determined on an L-8800 chromatograph (Hitachi, Japan) in the standard mode of analysis of protein hydrolysates with a sulfonated styrene-divinylbenzene copolymer and a stepwise gradient of Na-citrate buffer solution with increasing pH and molarity (GOST 32195-2013). When calculating the rate of essential amino acids, we used the FAO / WHO standard protein scale (2011) [10]. The carbohydrate composition of serum and extracts was investigated on a Shimadzu GCMS 2010 gas chromatograph (Japan), the fatty acid composition of MPC lipids - on a chromatograph with a Simadzu GCMS-QP 2010 Ultra mass detector at 120°C, an injector - 200°C; interface – 205°C, detector – 200 °C on an SLB-IL82 column (30 m, 0.20 mkm, d = 0.25 mm) with a carrier helium at a flow rate of 35.6 cm / s, flow division 1:10. The gradient mode varied from 120°C to 260°C at a rate of 5 °C/min for 2 minutes. Lipids were isolated according to the Folch method, evaporated on a rotary evaporator, dissolved in chloroform, hydrochloric acid methanol (Supelco Methanolic-HCl 0.5 N) was added, sealed in a vial and heated at 90 °C for 1 h. Museum cultures from wort agar were subcultured into a test tube with serum remaining after protein isolation, and cultured for 24 h. Then the culture was subcultured into 300 $cm^3$ flasks with 50 $cm^3$ nutrient medium, grown on a shaker at a rotation speed of 150 $min^{-1}$ and a temperature of 27±1°C for 48 hours. Serum with pH 6.0 - 6.5 was used to prepare nutrient media. The serum was sterilized at a pressure of 0.1 MPa, cooled, a suspension of cultures was introduced into the substrate and grown at different temperatures for 24 - 48 h with stirring on a rocking chair at a rate of 150 min-1. The suspension was inactivated at 95 ± 5°C for 10 - 15 min and cooled for 10 - 15 min at a temperature of 22 ± 2°C. The biomass was separated from the culture liquid by centrifugation at 4000 min – 1 for 10 min. The biomass (KMPK-1) and the biomass with the culture liquid (KMPK-2) were dried on a Hochvacuum HVDTG-50 lyophilizer (Germany) in a vacuum at -80 °C.

The experimental data were processed in the TableCurve 2D 5.1, TableCurve 3D 4.0, Mathematica 10.3, and Statistica 10 programs. The confidence interval of the arithmetic means was calculated according to the significance level p = 0.05.

## RESULTS AND DISCUSSION

The extraction of proteins from the pea suspension was carried out by a biotechnological method using hydrolytic enzyme preparations (EPs) of various actions (cellulases, xylanases, amylases, proteases) in stages. The scheme and parameters of protein extraction for each stage are presented in [8]. The hydromodule 1:15 was used, the EP concentration was 1.5 %/g of protein, the fermentation time was 4 hours, the reaction temperature was 55 ± 1°C, and the stirring speed was 200 $min^{-1}$. After precipitation of the protein at the isoelectric point and centrifugation of the suspension, serum was formed, which was subjected to

bioconversion to synthesize feed protein preparations. The mass fraction of dry substances (DM) in pea whey averaged 3.5±0.5 %, nitrogenous substances (Nx6.25) - 28.35 ± 0.8 %, true proteins - 11.06±0.23 %, in% of DS. Table 1 shows that in the process of protein extraction from flour with amylases, cytases and hemicellulases, the amount of high molecular weight carbohydrates in the dissolved part after the 2nd stage decreased by 2 %, tri-, tetra-disaccharides - almost 2 times, and the amount of glucose, on the contrary, - increased by 36 %, fructose, galactose, xylose - 3 times.

***Table 1.*** *The content of carbohydrates by stages of protein extraction,% of the total content in flour*

| Product | HMWC* | Stachyose Raffinose | Sucrose, maltose | Glucose | Fructose, galactose, xylose | Arabinose |
|---|---|---|---|---|---|---|
| Extract Stage 1 | 23.43 | 23.93 | 0+31.81 | 10.11 | 8.40 | 2.31 |
| Extract Stage 2 | 21.12 | 11.95 | 6.70+12.33 | 20.48 | 24.79 | 2.64 |
| Extract Stage 1 | 14.77 | 20.27 | 8.99+ 10.91 | 13.89 | 28.39 | 2.78 |
| Serum | 32.01 | 26.38 | 0+14.98 | 9.66 | 12.06 | 4.90 |

*Note: HMWC* – High molecular weight compounds*

At the third stage of extraction, under the influence of proteases, the share of HMWC decreased by 37 %, disaccharides - by 38 %, but the amount of monosaccharides (fructose galactose, xylose) increased 3.4 times. Thus, the nutrient medium for the synthesis of substances by microorganisms has been enriched with assimilable low molecular weight carbohydrates.

To determine the optimal conditions for increasing the productivity of the yeast *S. cerevisiae* and the fungus *G. candidum* 977, we studied the effect of the substrate pH, temperature, and the amount of inoculum on biomass synthesis for 3 days. For this, the matrix of the experiment was compiled (Table 2), the results of which were processed in the Statistica 12.5 program.

***Table 2.*** *Matrix for planning the experiment of growth of cultures on serum*

| No. | pH | Temperature, °C | Seed amount, % | Mass fraction of biomass, g/dm$^3$ |
|---|---|---|---|---|
| 1 | 5 | 20 | 3 | 0.611 |
| 2 | 5 | 25 | 2 | 0.816 |
| 3 | 5 | 30 | 1 | 0.757 |
| 4 | 5 | 35 | 4 | 0.570 |
| 5 | 6 | 20 | 4 | 0.776 |
| 6 | 6 | 25 | 3 | 0.774 |
| 7 | 6 | 30 | 2 | 0.711 |
| 8 | 6 | 35 | 1 | 0.573 |
| 9 | 7 | 20 | 1 | 0.791 |
| 10 | 7 | 25 | 4 | 0.811 |
| 11 | 7 | 30 | 3 | 0.708 |
| 12 | 7 | 35 | 2 | 0.413 |
| 13 | 8 | 20 | 2 | 0.616 |
| 14 | 8 | 25 | 1 | 0.751 |
| 15 | 8 | 30 | 4 | 0.553 |
| 16 | 8 | 35 | 3 | 0.313 |

Table 3 shows the values of the regression coefficients and the level of significance p. The equation for the dependence of the mass fraction of biomass md, g/dm$^3$ on influencing factors was as follows:

$$md = -2.94 + 0.544 \cdot pH - 0.0356 \cdot pH^2 + 0.181 \cdot t - 0.003 \cdot t^2$$
$$-0.147 \cdot cm + 0.0276 \cdot cm^2 - 0.00447 \cdot pH \cdot t$$

All coefficients of the equation are significant ($p \leq 0.05$) (Table 3). An adequate description of the data was indicated by the results of the experiment, the data of the calculation by the equation, their absolute error (Table 4) and the correlation graph $R = 0.9644$ (Figure 1).

***Table 3.*** *Regression coefficients and significance level p*

| Factor | Regr. Coefficients; Var.:md; R-sqr=,9644; Adj: 93325 (Spreadsheet1) 3 factors, 1 Blocks, 16 Runs; MS Residual=,0014517 DV: md | | | | | |
|---|---|---|---|---|---|---|
| | Regression Coeff. | Std.Err. | T (8) | p | -95, % Cnf.Limt | +95, % Cnf.Limt |
| Mean/Interc. | -2,93662 | 0,593210 | -4,95040 | 0,001120 | -4,30457 | -1,56868 |
| (1) pH(L) | 0,54434 | 0,133016 | 4,09228 | 0,003475 | 0,23760 | 0,85107 |
| pH(Q) | -0,03563 | 0,009525 | -3,74006 | 0,005705 | -0,05759 | -0,01366 |
| (2)t(L) | 0,18057 | 0,023871 | 7,56456 | 0,000065 | 0,12553 | 0,23562 |
| t(Q) | -0,00304 | 0,000381 | -7,99191 | 0,000044 | -0,00392 | -0,00217 |
| (3)cm(L) | -0,14700 | 0,054163 | -2,71404 | 0,026492 | -0,27190 | -0,02210 |
| cm(Q) | 0,02756 | 0,010471 | 2,63238 | 0,030067 | 0,00342 | 0,05171 |
| 1L by 2L | -0,00447 | 0,001739 | -2,57322 | 0,032962 | -0,00849 | -0,00046 |

***Table 4.*** *Experimental (1), calculated (2) data and absolute error*

| No. | 1 | 2 | Absolute error | No. | 1 | 2 | Absolute error |
|---|---|---|---|---|---|---|---|
| 1 | 0.611 | 0.647450 | -0.036450 | 9 | 0.791 | 0.775625 | 0.015375 |
| 2 | 0.816 | 0.762500 | 0.053500 | 10 | 0.811 | 0.809175 | 0.001825 |
| 3 | 0.757 | 0.780425 | -0.023425 | 11 | 11 | 0.708 | 0.672100 |
| 4 | 0.570 | 0.554225 | 0.015775 | 12 | 12 | 0.413 | 0.437900 |
| 5 | 0.776 | 0.756350 | 0.019650 | 13 | 0.616 | 0.631775 | -0.015775 |
| 6 | 0.774 | 0.793900 | -0.019900 | 14 | 0.751 | 0.734825 | 0.016175 |
| 7 | 0.711 | 0.734325 | -0.023325 | 15 | 0.553 | 0.593750 | -0.040750 |
| 8 | 0.573 | 0.577625 | -0.004625 | 16 | 0.313 | 0.282050 | 0.030950 |

The equation made it possible to determine the dependence of the mass fraction of biomass *md* on the influencing factors and to determine their values for its maximum yield. Figure 2 shows, as an example, the regularity of the change in biomass from the pH value and the temperature of the environment $C^0$ with the amount of seed $cm = 2\%$.

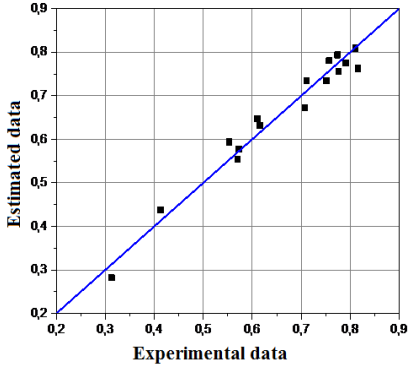


***Fig. 1****. Correlation graph*

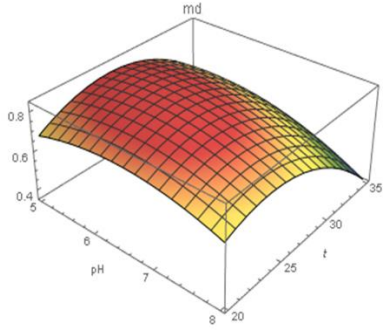


***Fig. 2.*** *Dependence of the mass fraction of biomass on pH and temperature*

From the equation in the Mathematica 12.1 program, the values of the factors for the maximum biomass yield (0.88 g/dm3) are determined: pH of the medium - 6.03, *C*=25.7°, seed quantity *cm*=4%. At lower pH values (4.5-5.0) or higher (7.5-8.0), the growth of microorganisms slowed down. Cultivation of symbiosis of cultures had a positive effect on the accumulation of biomass and protein; for the symbiosis of cultures, the amount of protein in the biomass was 61.68% of DS (Table 5), while from biomass with the culture liquid - 57.90%.

***Table 5.*** *Chemical composition of MPC from biomass on serum*

| Moisture, % | Mass fraction, % of DS | | | |
|---|---|---|---|---|
| | Protein (Nx6.25) | Ash | Lipids | Carbohydrates |
| 6.81±0.4 | 61.68±0.47 | 8.60±0.03 | 8.31±0.36 | 21.41±0.55 |

In the process of synthesis, stachyose, maltose, arabinose were completely absorbed from serum, more than half - glucose and almost all other pentoses (Table 6). The assimilation of stachyose by these yeasts corresponded to the literature data. On the other hand, in the MPC, the number of HMWC has doubled, the nature of which has to be deciphered.

***Table 6.*** *Carbohydrate composition of pea serum (1) and MPC (2),% of the total*

| Product | HMWC | Stachyose | Raffinose | Sucrose, maltose | Glucose | Fructose, galactose, xylose | Arabinose |
|---|---|---|---|---|---|---|---|
| 1 | 32.01 | 26.38 | 0 | 0+14.98 | 9.66 | 12.06 | 4.90 |
| 2 | 68.83 | 0 | 26.21 | 0 | 3.87 | 1.09 | 0 |

The amino acid composition of MPC from biomass and from biomass with culture liquid is mostly represented by glutamic, aspartic acids, glycine, alanine, lysine (Figure 3).

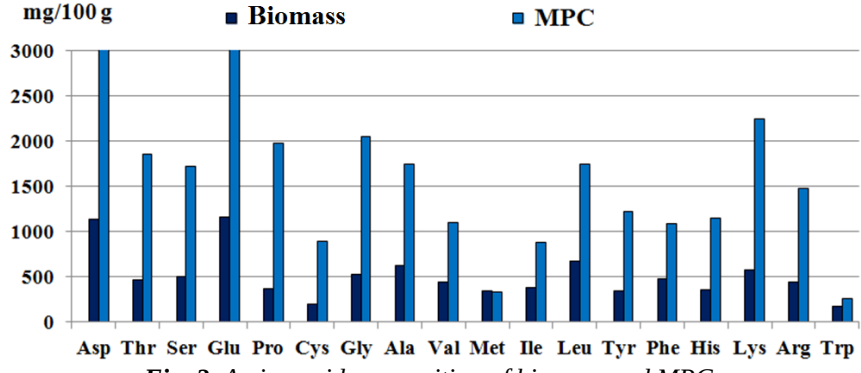


***Fig. 3.*** *Amino acid composition of biomass and MPC*

The amino acid rate of biomass of cultures for all essential acids was 107-226%, for MPC with a culture liquid it was high for histidine, lysine, threonine, sulfur-containing amino acids (81-128%), and for valine, leucine, isoleucine it was not higher 48%. The fatty acid composition (FAC) of MPC is represented by 30 components, among which 97 % are fatty acids that are part of animal fats, vegetable oils, marine organisms, 3 % are esters, aldehydes, ketones with the properties of aromatizing essential oils, metabolites of the human body, photo stabilizer, odor fixatives, preservatives and other compounds. The ratio of the sum of saturated (23.51 %) and unsaturated fatty acids (71.67 %) is 1:3, the content of cis isomers is 91.1 %, trans isomers - 5.1 %, omega-6 fatty acids (linoleic) -

19,73 %. MPC did not have a negative effect on the vital parameters of experimental rats [11], which indicated its safety and prospects for use.

## CONCLUSION

The optimization of the process of biotransformation of the chemical composition of the secondary product of pea flour processing into food protein concentrate (serum) into a microbial-plant concentrate by a symbiosis of cultures of the fungus *G. candidum* 977 and yeast *S. cerevisiae* 121 has been carried out. adequately describing the dependence of the crop biomass yield on technological parameters: pH of the medium, temperature and amount of seed. The microbial-plant concentrate from the biomass of cultures with a protein mass fraction of 57.90 and 61.68 % of DS was biologically valuable (the rate of essential amino acids was 107-226 %), had a high biological efficiency of lipids: out of 30 types of fatty acids, 97 % were acids included in composition of animal fats, vegetable oils and marine organisms. The ratio of saturated (23.51 %) and unsaturated fatty acids (71.67 %) was 1:3, the content of trans isomers was 5.1%, and omega-6 fatty acids (linoleic) were 19.73 %. The use of the concentrate is promising for animal diets.

## REFERENCES

[1] World Health Organization, Food and Agriculture Organization of the United Nations. Driving commitment for nutrition within the UN Decade of Action on Nutrition // WHO/NMH/NHD/17.11, FAO/CA1340EN/1/09.18., 2018. 12 p.

[2] Söderberg J. Functional properties of legume proteins compared to egg proteins and their potential as egg replacers in vegan food // Swedish University of Agricultural Sciences, Uppsala, Sweden Publication, 2013. 37 p.

[3] Singhal A., Karaca A.C., Tyler R., Nickerson M. Pulse Proteins: from processing to structure-function relationships // Grain Legumes, 2016. DOI: 10.5772/64020

[4] Pruter T. Alternative crops for a traditional potato starch producer *69th Starch Convention in Detmold, Germany,* 2018. 35 p.

[5] Pedro F., Souza Filho, Ramkumar B. Nair, Dan Andersson, Patrik R. Lennartsson, Mohammad J. Taherzadeh. Vegan-mycoprotein concentrate from pea-processing industry byproduct using edible filamentous fungi // Fungal Biology and Biotechnology, 2018. No. 5. P. 5-8.

[6] Kolpakova V.V., Ulanova R.V., Kulikov D.S. and al. Grain composites with complementary amino acid composition for food and feed purposes, Food Engineering and Technology, 2019. Vol. 2 (49). P. 301-311. DOI: 10.21603/2074-9414-2019-2-301-311 [In Russian]

[7] Kulikov D., Kolpakova V., Slozhenkina M., Ulanova R., Chumikina L. Biotechnological process for producing protein products from chickpeas with a high biological value // 20th International Scientific Multidisciplinary Conference on Earth and Planetary Sciences SGEM 2020 Conference Period: 18-24 August,

2020 Albena, Bulgaria. Vol. 20, Bk. 6.1, P. 175-182. doi: 10.5593/sgem2020/6.1/s25.023

[8] Kulikov D.S., Kolpakova V.V., Ulanova R.V, Chumikina L.V., Bessonov V.V. Biological processing of pea grain to obtain food and feed protein concentrates // Biotechnology, 2020. Vol. 36. No 4. P. 49-58. DOI: 10.21519/0234-2758-2020-36-4-49-58 [In Russian]

[9] Kolpakova V.V., Ulanova R.V., Kulikov D.S. Modification of secondary products of processing triticale into starch with a new strain of the fungus *Geotrichium candidum* // E3s Web of Conference, 2020. Vol. 224, Article number: 04033. TPACEE-2020 10.1051/e3sconf/202022404033

[10] Dietary protein quality evaluation in human nutrition: Report of an FAO Expert Consultation. Rome: FAO, 2013. 66 p.

[11] Kolpakova V., Kulikov D., Ulanova R., Lukin N., Gaivoronskaya I. Bioconversion of cereal serum – a secondary product for producing protein concentrates from pea and chickpeas. GEOLINKS International Conference on geosciences. Conference proceedings. 23-25 March, 2020, Imperial Hotel, Plovdiv, Bulgaria, Book 1. Vol. 2. P. 59-67.

# CONSIDERATIONS ON SARS-COV-2 DIAGNOSIS IN THE LABORATORY OF UNIVERSITY EMERGENCY CLINICAL HOSPITAL OF CONSTANTA

**Assoc. Prof. Dr. Ramona Stoicescu**[1]
**M.D. Razvan-Alexandru Stoicescu**[2]
**Ph.D. Student Codrin Gheorghe**[3]
**Lecturer Dr. Adina Honcea**[4]
**Lecturer Dr. Iulian Bratu**[5]
**Assoc. Prof. Dr. Verginica Schroder**[6]
[1, 4, 5, 6] Ovidius University of Constanța, Faculty of Pharmacy, Constanta, Romania
[3] Ovidius University of Constanta, Faculty of Medicine, Constanta, Romania
[1] Emergency Clinical County Hospital, Constanta, Romania
[2] Emergency Clinical Hospital, Bucharest, Romania

## ABSTRACT

Coronaviruses are members of the Coronaviridae family. They are enveloped, non-segmented, positive-sense, single-stranded RNA viruses. Their genome size is about 30 kilobases (kb) which consist, at the 5' end, of non-structural open reading frames (ORFs: ORF1a, ORF 1b) which code for 16 non structural proteins, and at the 3' end the genes which code for four structural proteins including membrane (M), envelope (E), spike (S), and nucleocapsid (N) proteins. Due to the rapid spread of COVID-19, a reliable detection method is needed for patient diagnosis especially in the early stages of the disease. WHO has recommended nucleic acid amplification tests such as real-time reverse transcription-polymerase chain reaction (RT-PCR). The assay detects three SARS-CoV-2 RNA targets: the envelope (E) gene, the nucleocapsid (N) gene and a region of the open reading frame (ORF1) of the RNA-dependent RNA polymerase (RdRp) gene from SARS-CoV-2 virus isolate Wuhan-Hu-1. Our study was made in the first 3 months of the year 2021 using the real-time RT PCR results obtained in the Cellular Biology ward of the University Emergency Clinical Hospital. In our lab we are testing the inpatients from the hospital wards (Neurology, Pediatrics, Surgery, Internal medicine, ICU, Cardiology, etc.); we are also testing the outpatients from Dialysis and Oncology, 2 days prior to their therapy; we also test the health care personnel. The number of tests we performed was: in January 1456, with 399 positive results (27.4%), 33 deaths; in February 1273 tests, 221 positive (17.36%), 16 deaths; in March 1471 tests, 373 positive (25.36%), 37 deceased.

***Keywords:*** *SARS-CoV-2, real-time-RT PCR, envelope, nucleocapsid, RdRp genes*

## INTRODUCTION

Coronaviruses are a group of enveloped viruses which can cause diseases in birds and mammals, including humans [1].

Seven coronaviruses have been identified so far which can cause mild to lethal respiratory tract infections in humans [1].

HCoV-229E, HCoV-OC43, HCoV-NL63, and HCoV-HKU1 are the 4 low risk members of *Coronaviridae* family. They generally produce mild upper respiratory tract infections representing up to 30% of cases of common colds in adults. In immunocompromised patients, in infants or elderly people these Corononaviruses can also produce lower respiratory tract infections.

Coronaviruses which are more dangerous and can cause severe infections are SARS-CoV or SARS-CoV1 (Severe acute respiratory syndrome coronavirus), MERS-CoV (Middle East Respiratory Syndrome coronavirus) and SARS-CoV-2 also known as 2019-nCoV [2].

Coronaviruses are enveloped, non-segmented, positive-sense, single-stranded RNA viruses. Their genome consists of non-structural open reading frames (ORFs) and four structural proteins including membrane (M), envelope (E), spike (S), and nucleocapsid (N) proteins [3].

Their name derives from corona appearance, given by club-like spikes that project from their surface [1].

## MATERIALS AND METHODS

Diagnostic tests have been considered as the main alternative for the control of coronavirus disease (COVID-19) as a correct diagnosis allows correct decisions.

The tests can be organized into two main categories: virological diagnosis recommended for the initial detection of the virus, and serological tests, recommended for assessing the disease progression.

Virological diagnosis comprises 3 categories of laboratory detection methods for human coronaviruses: RNA amplification-based detection methods (including RT-PCR, real-time RT-PCR and isothermal amplification-based methods/ nucleic acid-based tests), viral RNA biosensors and whole virus or viral proteins detection assays [1].

The polymerase chain reaction (PCR) technique can synthesize a large number of a specific DNA sequence. It is a three-step cycle that consists of denaturation, annealing and extension [4].

The reverse transcription PCR (RT-PCR) technique was developed for specific RNA detection. The target RNA is converted to cDNA by the reverse transcriptase enzyme. The obtained cDNA is amplified by PCR [4].

Real-time RT-PCR or quantitative RT-PCR (qRT-PCR) is a technique in which amplification and detection steps have been combined together to decrease the detection time and increase the sensitivity and specificity of the method [5].

Serologic tests detect the immune response of the infected patients. Specific IgM starts to develop after 7 days and becomes detectable around 10 days after the infection onset. Specific IgG productions start around 10-14 days after infection and are detectable around day 21 and are maintained for a high level for a longer period of time [6].

A reliable detection method is needed for patient diagnosis especially in the early stages of the disease.WHO has recommended nucleic acid amplification tests (NAAT), such as reverse transcription-polymerase chain reaction (RT-PCR) [7]

In our Cellular Biology Laboratory at the University Emergency Clinical Hospital Constanta, we use real-time RT PCR for SARS-CoV-2 diagnosis. The specimens are represented by oro/nasopharyngeal swabs.

Detection of infection by SARS-CoV-2 relies on the efficient detection of the viral genome using RT PCR.

The assay detects three SARS-CoV-2 RNA targets: the envelope (E) gene, the nucleocapsid (N) gene and a region of the open reading frame (ORF1) of the RNA dependent RNA polymerase (RdRp) gene from SARS-CoV-2 virus isolate Wuhan-Hu-1.

First step is represented by RNA extraction from samples. RNA extraction is a key pre-analytical step in RT-PCR, achieved using commercial kits.

Our laboratory is equipped with 3 extractors: RBC Bioscience using MAGCore automated nucleic acid extraction kit, 1-16 samples per run; Bioneer EXI PREP 16DX using Exi Prep viral RNA kit, 8-16 samples per run, as a multiple of 8; Bioneer EP 48 DX-BXA 057 using Exi prep 48 Viral RNA kit, 8-48 samples per run as a multiple of 8.

Once RNA is extracted the eluates are amplified. The target RNA is converted to cDNA by the reverse transcriptase enzyme. The obtained cDNA is amplified by PCR.

Our lab is equipped with 2 amplifiers: Bioneer Exicycler 96 using Accupower SARS-CoV-2 using Multiplex Real-time RT PCR amplification kit, and Biorad CFX 96 Real-time System using Primer Design/ Gensig amplification kit.

Amplification takes place in a thermal cycler. Each PCR cycle theoretically doubles the amount of targeted sequence in the reaction. Each cycle of PCR includes steps for template denaturation (94°C), primer annealing (40–60°C) and primer extension (70–74°C).

To apply PCR to the study of RNA, the RNA sample must first be converted to cDNA to provide the necessary DNA template for the thermostable polymerase. This process is called reverse transcription (RT), hence the name RT-PCR.

Reverse transcriptases (RTs) are RNA-directed DNA polymerases. RTs catalyzes the synthesis of a DNA copy (cDNA) of the target RNA molecules using a reverse transcription primer, dNTPs (deoxyribonucleotide triphosphate), and $Mg^{2+}$ or $Mn^{2+}$ as a cofactor [8].

## RESULTS AND DISCUSSIONS

Our study was made in the first 3 months of year the 2021 using the real-time RT PCR. The laboratory is testing the inpatients from the hospital wards (Neurology, Pediatrics, Surgery, Internal medicine, ICU, Cardiology, etc); the outpatients from Dialysis and Oncology, 2 days prior to their therapy; the hospital employees (health care personnel, front desk medical clerks, administrative and technical staff, hospital housekeepers).

The number of tested patients were:

In January 1456, with 399 positive results (27.4%)

In February 1273 tests, 221 positive (17.36%)

In March 1471 tests, 373 positive (25.36%).

According to hospital statistics the number of deceased patients in University Clinical Emergency Hospital Constanta due to Covid 19 infections were: 33 deceased patients in January, 16 deceased patients in February, 37 deceased patients in March.

The distribution of positive cases with relation to the month and the hospital wards (for inpatients, outpatients) and hospital staff workplace can be seen in table 1.

***Table 1.*** *Positive cases*

| | January | January | February | February | March | March |
|---|---|---|---|---|---|---|
| Ward | Health care personnel | Patients | Health care personnel | Patients | Health care personnel | Patients |
| Emergency ward | 2 | 241 | 2 | 165 | 2 | 239 |
| Hemodialysis | 0 | 4 | 0 | 1 | 1 | 7 |
| Oncology | 1 | 3 | 0 | 2 | 0 | 7 |
| Internal medicine 1 | 2 | 1 | 0 | 5 | 2 | 17 |
| Internal medicine 2 | 2 | 14 | 0 | 0 | 1 | 12 |
| Nephrology | 0 | 7 | 0 | 6 | 0 | 3 |
| Neurology | 0 | 8 | 0 | 1 | 0 | 6 |
| Gastroenterology | 1 | 2 | 0 | 3 | 3 | 8 |
| ICU | 2 | 11 | 0 | 6 | 0 | 15 |
| Cardiology | 2 | 12 | 0 | 0 | 0 | 7 |
| Orthopedics | 3 | 4 | 2 | 0 | 2 | 0 |

| | | | | | | |
|---|---|---|---|---|---|---|
| Op theater orthopedics | 1 | 0 | 0 | 0 | 1 | 0 |
| Cardiovascular surgery | 4 | 3 | 0 | 1 | 4 | 5 |
| Surgery ward 2 | 1 | 0 | 0 | 0 | 0 | 0 |
| Surgery ward 1 | 1 | 10 | 1 | 6 | 2 | 4 |
| Urology | 0 | 0 | 1 | 2 | 0 | 0 |
| New born | 1 | 0 | 0 | 1 | 0 | 0 |
| Ob/ gynecology ward 2 | 0 | 0 | 0 | 1 | 1 | 0 |
| Ob/gynecology ward 1 | 0 | 1 | 1 | 1 | 0 | 0 |
| Neurosurgery ward | 2 | 5 | 2 | 1 | 2 | 2 |
| Ophthalmology | 0 | 0 | 0 | 0 | 0 | 1 |
| Otorhinolaryngology (ORL) | 1 | 2 | 0 | 0 | 0 | 0 |
| Pediatrics | 0 | 15 | 0 | 1 | 0 | 4 |
| Pediatric surgery | 1 | 0 | 0 | 0 | 1 | 1 |
| Psychiatry | 6 | 4 | 0 | 0 | 0 | 2 |
| Osteoarticular tuberculosis (OATB) ward | 0 | 2 | 0 | 0 | 0 | 1 |
| Palliative care | 0 | 1 | 0 | 0 | 0 | 2 |
| Physical and Rehabilitation Medicine Sanatorium | 0 | 1 | 1 | 2 | 1 | 1 |
| Dermatology | 0 | 3 | 0 | 0 | 0 | 0 |
| Pneumoftisiology | 1 | 2 | 0 | 2 | 0 | 1 |
| Physical and Rehabilitation Medicine | 4 | 1 | 1 | 0 | 0 | 0 |
| Pathology | 1 | 0 | 0 | 0 | 0 | 0 |
| Functional exploration dep. | 0 | 0 | 0 | 0 | 1 | 0 |
| Radiotherapy | 0 | 0 | 0 | 1 | 0 | 0 |
| Ambulatory | 0 | 0 | 2 | 0 | 0 | 0 |
| Hospital Technical staff | 2 | 0 | 0 | 0 | 0 | 0 |
| Hospital administration | 0 | 0 | 0 | 0 | 1 | 0 |
| Medical front desk clerk | 1 | 0 | 0 | 0 | 0 | 0 |
| Center for mental health | 0 | 0 | 0 | 0 | 1 | 0 |
| Hospital housekeeper staff | 0 | 0 | 0 | 0 | 2 | 0 |
| **TOTAL** | **42** | **357** | **13** | **208** | **28** | **345** |

During 3 months there were tested and confirmed positive a number of 993 patients and 83 health care personnel and other professional workers in the hospital.

## CONCLUSION

The University Emergency Clinical Hospital is following WHO recommendation of using nucleic acid amplification tests (NAAT)/ reverse

transcription-polymerase chain reaction (RT-PCR) for diagnosing SARS-Co-V-2 infection (gold standard)

The Hospital's Cellular Biology Laboratory performs real-time RT PCR for inpatients, outpatients from Haemodialysis and Oncology and medical and auxiliary staff.

During 3 months were performed 4200 RT-PCR tests with 993 positive tests for patients and 83 positive tests for hospital employees.

The positivity rate for all tested persons was 27.4% in January, 17.36% in February and 25.36% in March.

The highest positivity rate was for patients from the Emergency ward, representing 60.4% in January, 74.66% in February, 64.07% in March out of all performed tests.

The highest number of positive cases among health care personnel in January was in Psychiatry ward 6 cases, Cardiovascular surgery 4 cases, Physical and Rehabilitation Medicine 4 cases, Orthopedics 3 cases; in February: Emergency ward 2 cases, Orthopedics 2 cases; in March: 4 cases in Cardiovascular surgery, 3 cases Gastroenterology, 2 cases in the Emergency ward, 2 cases in Surgery ward number 2.

The number of infected health care workers was small compared with the number of infected patients due to strict infection control measures (protection equipment, hand hygiene, disinfection) and vaccination campaign which started in December 2020.

## REFERENCES

[1] Ehsan Shabani, Sayeh Dowlatshahi, and Mohammad J. Abdekhodaie, Laboratory detection methods for the human coronaviruses https://www.ncbi.nlm.nih.gov/pmc/articles/PMC7520381/

[2] Ding X. Liu, Jia Q. Liang, and To S. Fung, Human Coronavirus-229E, -OC43, -NL63, and -HKU1 (*Coronaviridae*), Encyclopedia of Virology. 2021 : 428–440.,Published online 2021 Mar 1. doi: 10.1016/B978-0-12-809633-8.21501-X, PMCID: PMC7204879

[3] Chen Y, Liu Q, Guo D. Emerging coronaviruses: genome structure, replication, and pathogenesis. *J Med Virol.* 2020;92:418–423. doi: 10.1002/jmv.25681. [PMC free article] [PubMed] [CrossRef] [Google Scholar]

[4] Wei Zhang,Rong-Hui Du, Bei Li, Xiao-Shuang Zheng, Xing-Lou Yang, Ben Hu, Yan-Yi Wang, Geng-Fu Xiao, Bing Yan, Zheng-Li Shi,and Peng Zhou, Molecular and serological investigation of 2019-nCoV infected patients: implication of multiple shedding routes Emerg Microbes Infect. 2020; 9(1): 386–389. Published online 2020 Feb 17. doi: 10.1080/22221751.2020.1729071

[5] Alireza Tahamtan and Abdollah Ardebili. Expert Rev Mol Diagn. Real-time RT-PCR in COVID-19 detection, Published online 2020 Apr 22. doi: 10.1080/14737159.2020.1757437

[6] Hongyan Hou, Ting Wang, Bo Zhang, Ying Luo, Lie Mao, Feng Wang, Shiji Wuand Ziyong Sun Detection of IgM and IgG antibodies in patients with coronavirus disease 2019, Clin Trans Immunology. 2020; 9(5): e1136. Published online 2020 May 6. doi: 10.1002/cti2.1136PMCID: PMC7202656, PMID: 32382418

[7] World Health Organization (2020) Laboratory testing for 2019 novel coronavirus (2019-nCoV) in suspected human cases

[8] https://www.promega.ro/resources/guides/nucleic-acid-analysis/pcr-amplification/

# DETERMINATION OF THE OPTIMAL CONCENTRATIONS OF PECTIN AND CALCIUM CHLORIDE FOR THE SYNTHESIS OF CHITOSAN-PECTIN MICROPARTICLES

**Prof. Dr. Alla A. Krasnoshtanova**[1]
**Anastasiya D. Bezyeva**[2]
[1, 2] D. Mendeleev University of Chemical Technology of Russia, Moscow, Russia

## ABSTRACT

The oral route of drug inclusion is the most convenient for the patient. In addition to ease of use, this method of drug inclusion has such advantages as non-invasiveness of inclusion, absence of complications during injection; comparative safety for the organism due to the passage of the active substance and auxiliary compounds through the gastrointestinal tract; the possibility of introducing larger doses of the drug at one time. However, despite the obvious advantages, the oral route of inclusion has a number of significant disadvantages that significantly limit its use for a number of drugs. Among them are: relatively slow therapeutic action of the drug with this route of inclusion; the aggressive effect of a number of drugs (for example, antibiotics) on the gastrointestinal tract; low bioavailability of a number of substances (especially high molecular weight hydrophilic compounds), caused by poor permeability of the intestinal epithelium for hydrophilic and large molecules, as well as enzymatic and chemical degradation of the active substance in the gastrointestinal tract.

There are various approaches used in the development of oral drug delivery systems. In particular, for the targeted delivery of drugs, it is proposed to use nano- and microcapsules with mucoadhesive properties. Among the polymers used for the synthesis of these microparticles, it is preferable to use pH-dependent, gelable biopolymers that change their structure depending on the acidity of the environment. Microcapsules obtained from compounds with the above properties are capable of protecting the active substance (or from the active substance) in the stomach environment and ensuring its release in the intestine. These properties are possessed by such polysaccharides as alginate, pectin, carrageenan, xylan, etc. The listed biopolymers are non-toxic, biocompatible, and biodegradable, which makes microparticles containing these polysaccharides promising as oral drug delivery systems. To impart mucoadhesive properties to nanoparticles, complexes of the listed polymers with chitosan are used.

In this research, pectin, a polysaccharide formed mainly by residues of galacturonic acid, was used as a structural polymer. The concentrations of substances in the initial solutions were selected that were optimal for the synthesis of microcapsules. The main parameters for evaluating the resulting microparticles were the size of the capsules (less than 1 μm for oral inclusion), the zeta-potential,

showing the tendency of the microparticles to stick together, and the completeness of the binding of the microparticles to chitosan.

It was found that the optimal solutions for the synthesis of microparticles are: 15.7 ml of a solution of pectin 0.093% by weight, 3.3 ml of a solution of chitosan 0.07% by weight and 1.0 ml of a solution of $CaCl_2$ 20 mM. The diameter of the microparticles obtained by this method was 700-800 nm, and the value of their zetta-potential, equal to - (34 ± 3) mV, does not cross the particle adhesion threshold. It was also found that the synthesis of microparticles at these concentrations of calcium chloride provides the most complete binding of chitosan to their surface, which increases the mucoadhesive properties of microparticles.

***Keywords:*** *pectin, chitosan, microparticles, sorption capacity*

## INTRODUCTION

The oral route of inclusion of drugs is the most convenient in therapy due to the ease of use for the patient, atraumatic introduction into the body and the possibility of taking large doses of the drug [1]. However, this method of drug inclusion also has a number of disadvantages that limit its use. Among them, one can single out low bioavailability for a number of active substances, the effect of aggressive drugs on the gastrointestinal tract (in particular, this item refers to various kinds of antibiotics) [1], the destruction of biological substances of a protein nature under the action of enzymes of the gastrointestinal tract and its aggressive environment [1], [2], low permeability of the intestinal mucosa for high molecular weight compounds [2] and a relatively slow therapeutic effect of the drug with this route of inclusion [1]. Modern advances in biotechnology have led to the possibility of industrial production of protein-based drugs and their widespread use in therapeutic practice [3]. These trends make the search for and development of new oral drug delivery systems a promising topical direction for almost two decades.

There are various approaches used in the development of oral drug delivery systems. In particular, for targeted delivery of drugs, it is proposed to use nano- and microcapsules with mucoadhesive properties [2], [3]. Among the polymers used for the synthesis of these microparticles, it is preferable to use pH-dependent, gelable biopolymers that change their structure depending on the acidity of the environment. Microcapsules obtained from compounds with the above properties are able to protect the active substance (or from the active substance) in the stomach environment and ensure its release in the intestine [3]. These properties are possessed by such polysaccharides as alginate, pectin, carrageenan, xylan, etc. [4]. The listed biopolymers are non-toxic, biocompatible, and biodegradable, which makes microparticles containing these polysaccharides promising as oral drug delivery systems [4]. To impart mucoadhesive properties to nanoparticles, complexes of the listed polymers with chitosan are used [4]. Chitosan is a biodegradable non-toxic polysaccharide consisting of randomly linked β- (1-4) D-glucosamine units and N-acetyl-D-glucosamines (with a predominance of residues of the first monomer in the composition). This biopolymer is capable of forming stable polyelectrolyte complexes with the aforementioned polysaccharides and, due to its mucoadhesive properties, is able to increase the residence time and the amount

of the active substance at the site of adsorption, creating a concentration gradient leading to the rapid absorption of protein molecules through the intestinal mucosa [3].

In this research, pectin, a polysaccharide formed mainly by residues of galacturonic acid, was used as a structural polymer. The scheme of the formation of a polyelectrolyte complex of chitosan-pectin microparticles is shown in Fig. 1-2

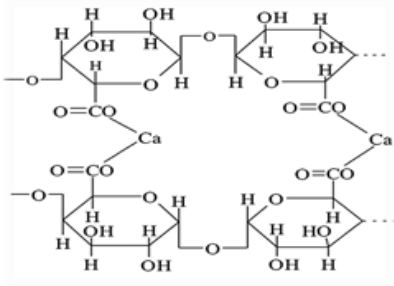

***Fig. 1.*** *Scheme of the formation of calcium bridges between pectin molecules through carboxyl groups*

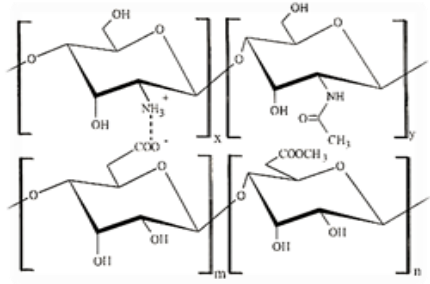

***Fig. 2.*** *Scheme of the formation of the polyelectrolyte complex of chitosan with pectin*

The aim of this work is to determine the optimal ratio of the concentrations of the initial solutions of pectin, chitosan, and calcium chloride for the synthesis of chitosan-pectin microparticles that are effective when therapeutic molecules are included in them.

## MATERIALS AND METHODS

The objects of this investigation were: low molecular weight chitosan (200 kDa) with a degree of diacetylation of 85%, manufactured by Sigma-Aldrich; apple pectin with a molecular weight of 12 kDa and a degree of metaxylation of 66% produced by Cargill (France); lyophilizate of doxorubicin hydrochloride for the preparation of a solution for intravascular and intravesical administration, produced by the pharmaceutical company "Teva".

To synthesize chitosan-pectin microparticles, 7.5 ml of a 22 mM calcium chloride solution was added to 117.5 ml of a 0.094% (mass) pectin solution (pH 4.3) dropwise at a rate of 0.125 ml/min using a peristaltic pump with constant stirring on a magnetic stirrer (stirring speed 800 rpm). At the end of the addition of the chitosan solution to stabilize the microparticles, the prepared suspension of microparticles was stirred on a magnetic stirrer for 30 minutes at a speed of 800 rpm. The separation of microparticles from the solution was carried out by centrifugation at a speed of 10,000 rpm for 30 minutes. To obtain microparticles loaded with a substance (in this investigation doxorubicin was used as an active compound), it was added to the initial pectin solution.

The size and zetta potential of the obtained microparticles were determined using a JEOL 1610LV scanning electron microscope with an SSD X-Max Inca

Energy energy dispersive spectrometer for electron probe microanalysis (JEOL, Japan; Oxford Instruments, Great Britain).

The completeness of the incorporation of chitosan into polyelectrolyte complexes was determined by the method of IR spectroscopy of the supernatant carried out on an IR Fourier spectrometer with an ATR attachment and additional equipment Nicolet 380 (Thermo Fisher Scientific Inc., USA) [5].

The capacity of chitosan-pectin microparticles for doxorubicin was determined by measuring the residual amount of doxorubicin in the supernatant obtained after centrifugation of the suspension. The concentration of doxorubicin was established by determining the optical density of the sample at a wavelength of 475 nm [6].

## RESULTS AND DISCUSSION

The main criteria by which the primary assessment of the obtained chitosan-pectin microparticles was carried out were their size (the permitted size of the preparation for oral administration is up to 1000 microns) [7], the zetta-potential, which characterizes their tendency to sticking together (sticking threshold | 27-29 | mV), as well as the completeness of binding of chitosan to microparticles.

At the first stage, it was necessary to determine the optimal concentration of the initial solution of the structure-forming polysaccharide (pectin) for the synthesis of microparticles. For this purpose, a series of chitosan-pectin microcapsules were prepared by varying the initial concentration of the pectin solution at constant concentration values of solutions of calcium chloride (18 mM) and chitosan (0.07% by weight).

The size of the obtained microparticles and their zeta-potential were measured. The measurement results are presented in Table 1.

***Table 1.*** *Characteristics of chitosan-pectin microparticles synthesized using solutions of pectin with various concentrations at constant concentrations of solutions of chitosan (0.07% by weight) and calcium chloride (18 mM)*

| Pectin concentration,% mass | Microparticle diameter, nm | Zetta potential of microparticles, mV |
|---|---|---|
| 0.042 | 500-600 | -(33±2) |
| 0.085 | 500-600 | -(39±3) |
| 0.093 | 600-700 | -(32±2) |
| 0.102 | 800-900 | -(29±1) |
| 0.111 | 1000-1100 | -(22±1) |

From the presented data, it can be seen that the maximum permissible sizes for oral administration of microparticles are reached at a concentration of a pectin solution of 0.102% by weight, however, these microparticles have a zetta potential close to the sticking threshold. Proceeding from this, the optimal concentration of the solution at which the synthesized polysaccharide microparticles have the

maximum allowable size and do not have a tendency to stick together was taken equal to 0.093%.

The next step was to determine the optimal concentration of the binder solution (calcium chloride) for the synthesis of microparticles. For this purpose, samples of chitosan-pectin microcapsules were prepared by varying the initial concentration of calcium chloride solution at constant concentration values of solutions of pectin (0.093 wt%) and chitosan (0.07 wt%). The size and zetta potential of the synthesized microparticles were measured. The measurement results are presented in Table 2.

The presented data show that an increase in the concentration of the initial solution of calcium chloride leads to an increase in the zetta potential of chitosan-pectin microparticles, that is, their tendency to stick together decreases. All synthesized microparticles have an acceptable range of zetta-potential values. The maximum size of microparticles is reached at solution concentrations of 20 and 22 mM. An increase in the concentration of the binder leads to a decrease in their size. It can be assumed that this is due to the fact that only a small part of chitosan was able to bind to a complex with microparticles.

***Table 2.*** *Characteristics of chitosan-pectin microparticles synthesized using solutions of calcium chloride with various concentrations at constant concentrations of solutions of pectin (0.093% by weight) and chitosan (0.07% by weight)*

| Concentration of $CaCl_2$, mM | Diameter of microparticles, nm | Zetta-potential of microparticles, mV |
|---|---|---|
| 18 | 600-700 | -(32±2) |
| 20 | 700-800 | -(34±3) |
| 22 | 700-800 | -(35±3) |
| 24 | 500-600 | -(36±3) |
| 26 | 500-600 | -(37±3) |

The completeness of the inclusion of chitosan in the polyelectrolyte complex has already been mentioned as one of the key criteria for evaluating the synthesized microparticles. To determine it, the IR spectra of the supernatant liquid obtained after the separation of microparticles were recorded.

As a control, the IR spectrum of a solution containing: 25 ml of a 0.07% chitosan solution, 117.5 ml of a $CH_3COOH$ solution (pH 4.3) and 7.5 ml of water was taken. The results are shown in Fig. 1-3.

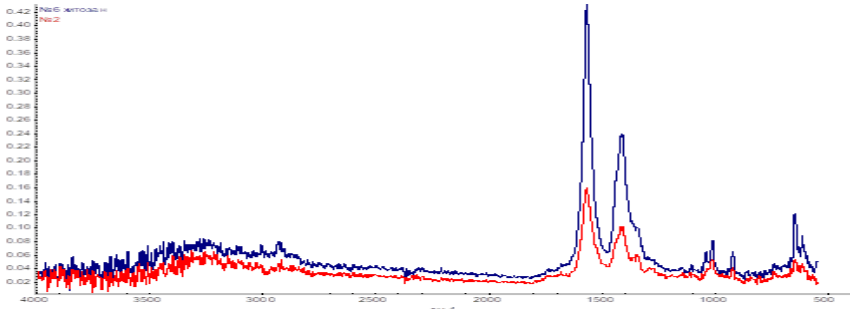

***Fig. 1.*** *Spectrum of the supernatant liquid obtained after the separation of microparticles, in comparison with the chitosan solution with the initial concentration; concentration of solutions for synthesis: pectin 0.093% by weight, chitosan 0.07% by weight, $CaCl_2$ 20 mM*

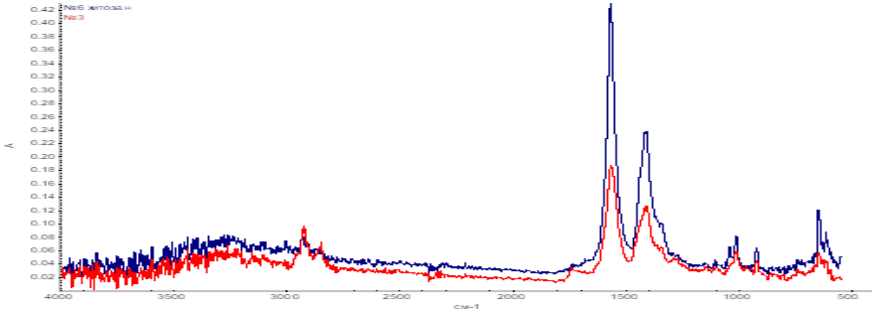

***Fig. 2.*** *Spectrum of the supernatant liquid obtained after the separation of microparticles in comparison with the chitosan solution with the initial concentration; concentration of solutions for synthesis: concentration of solutions for synthesis: pectin 0.093% by weight, chitosan 0.07% by weight, $CaCl_2$ 22 mM*

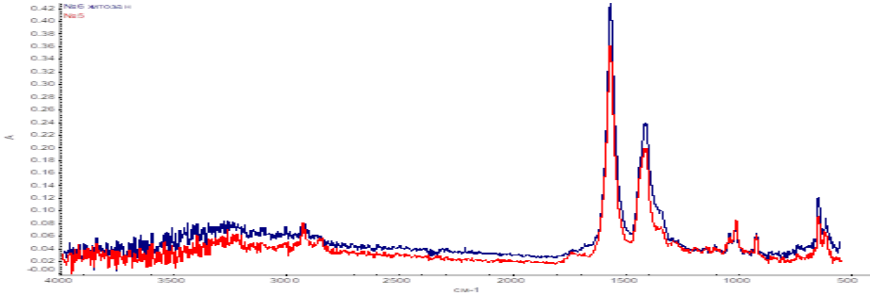

***Fig. 3.*** *Spectrum of the supernatant liquid obtained after the separation of microparticles in comparison with the chitosan solution with the initial concentration; concentration of solutions for synthesis: pectin 0.093% by weight, chitosan 0.07% by weight, $CaCl_2$ 26 mM*

From the data obtained, it can be seen that the most complete binding of chitosan to microparticles is provided at a concentration of the initial calcium chloride solution of 20 mM. The spectrum taken from the supernatant obtained after the separation of microparticles synthesized using a 26 mM calcium chloride solution shows that chitosan, in fact, did not bind to microparticles and almost all remained in the supernatant.

Thus, according to the above criteria, the following initial solutions are optimal conditions for the synthesis of microparticles: 117.5 ml of a 0.093% mass pectin solution, 25 ml of a 0.07% mass chitosan solution and 7.5 ml of a 20 mM calcium chloride solution.

The next stage of the work is to determine the effectiveness of using these microparticles for the inclusion of therapeutic substances in them using doxorubicin as an example. First of all, their capacity for this connection was assessed.

To determine the capacity of microcapsules for doxorubicin when preparing a suspension of microcapsules, the studied antibiotic was added to the pectin solution, varying its concentration in the range of 0.021 - 0.13 mg/ml.

The concentration of the antibiotic not included in the microparticles in the supernatant was monitored by measuring the optical density at 475 nm. Separately, the background was measured - the supernatant obtained after the deposition of unloaded microparticles. The results on the capacity of microparticles for doxorubicin and the degree of its sorption are shown in Fig. 4-5.

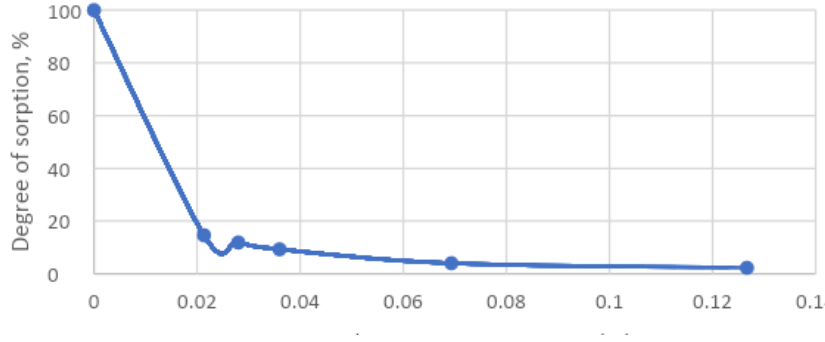


***Fig. 4.*** *Dependence of the degree of sorption of doxorubicin into chitosan-pectin microparticles (synthesized using a 20 mM $CaCl_2$ solution) on its concentration in suspension*

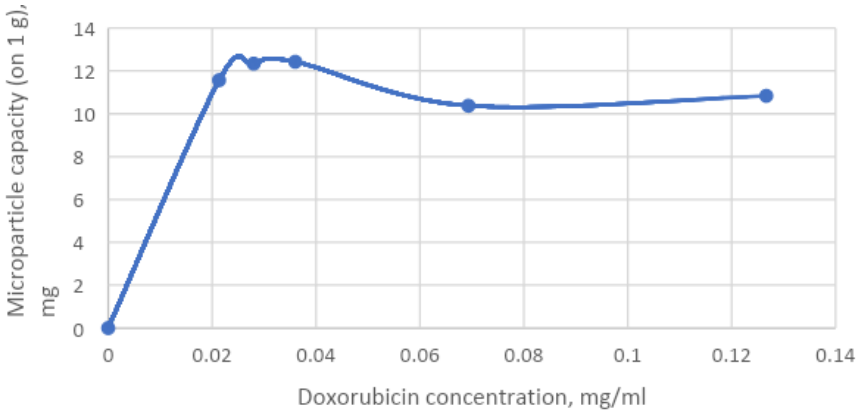


***Fig. 5.*** *Dependence of the amount of doxorubicin included in chitosan-pectin microparticles (synthesized using a 20 mM $CaCl_2$ solution) on its concentration in suspension*

The graphs show that microparticles synthesized using a 20 mM calcium chloride solution have a low capacity for doxorubicin (12.34 mg doxorubicin / g microparticles) and a low degree of sorption of this antibiotic. Therefore, they are ineffective for the inclusion of low molecular weight therapeutic drugs.

For comparison, the capacity of chitosan-pectin microparticles synthesized using a 0.093 wt% pectin solution, a 0.07 wt% chitosan solution and a 22 mM calcium chloride solution was determined. The concentration of doxorubicin in the initial pectin solution was varied in the range of 0.0133 - 0.133 mg/ml. The results on the capacity of microparticles and the degree of sorption of doxorubicin in them are shown in Fig. 6-7.

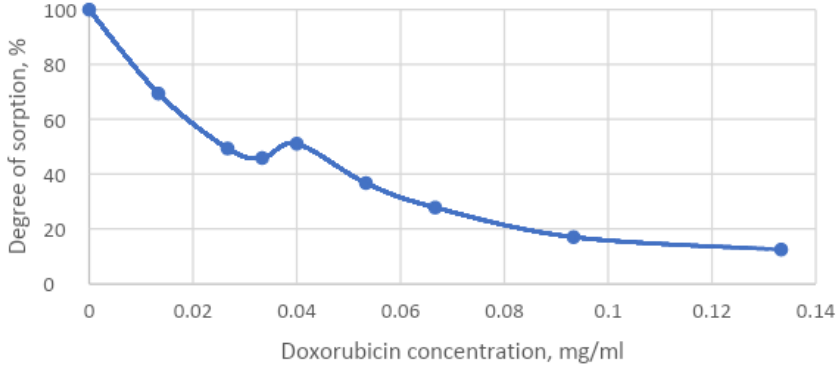


***Fig. 6.*** *Dependence of the degree of sorption of doxorubicin into chitosan-pectin microparticles (synthesized using a 20 mM $CaCl_2$ solution) on its concentration in suspension*

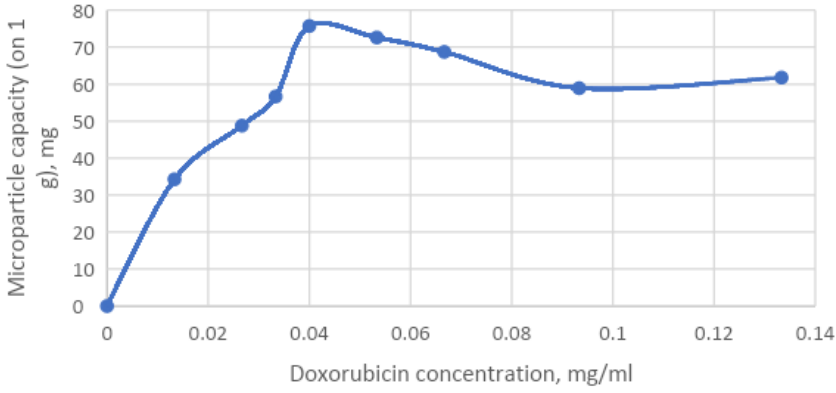


***Fig. 7.*** *Dependence of the amount of doxorubicin included in chitosan-pectin microparticles (synthesized using a 20 mM $CaCl_2$ solution) on its concentration in suspension*

From the obtained dependences it can be seen that these microparticles, in comparison with the previous ones, are able to absorb a larger amount of doxorubicin (the maximum degree of sorption reached 69.4%) and have a higher capacity than the previous ones by 6.4 times (the degree of sorption reaches 77.28 mg of doxorubicin / g microparticles).

These results confirm the feasibility of using these chitosan-pectin microparticles for the inclusion of low-molecular-weight therapeutic drugs. In this regard, the following initial solutions are optimal conditions for the synthesis of microparticles: 117.5 ml of a 0.093% mass pectin solution, 25 ml of a 0.07% mass chitosan solution and 7.5 ml of a 22 mM calcium chloride solution.

## CONCLUSION

Received chitosan-pectin microparticles, the diameter of which was 700-800 nm. The zetta potential of the microparticles was - (35 ± 3) mV, which indicates the absence of adhesion tendencies in microparticles. The spectrum of the supernatant obtained after the separation of microparticles confirms the inclusion of most of the chitosan in the polyelectrolyte complex.

The optimal ratio of the concentrations of structural components in the initial solutions for the synthesis of microparticles was selected: pectin solution - 0.093% by weight; chitosan solution - 0.07% by weight; CaCl2 solution - 22 mM. It was found that the initially established criteria for evaluating the optimal conditions for the synthesis of microparticles do not guarantee their effectiveness and high capacity for therapeutic drugs.

The optimal concentration of doxorubicin in the suspension (0.04 mg/ml), at which the maximum incorporation of this antibiotic into chitosan-pectin microparticles is achieved (degree of sorption is 52.11%), has been determined. Based on the data that the concentration of microparticles in the suspension is 6

mg/ml, and their dry weight is 4.5%, the doxorubicin capacity of microparticles is 77.28 mg/g of dry microparticles.

## REFERENCES

[1] Kravchenko I.A. Methods for introducing drugs into the body, M .: Astroprint, 82 pp., 2009.

[2] Michael Goldberg, Challenges for the oral delivery of macromolecules/ Michael Goldberg, Isabel Gomez-Orellana// Nature Publishing Group – 2003. – Vol. 2. – p. 289 – 295

[3] Kyeongsoon Park, Ick Chan Kwon, Kinam Park. Oral protein delivery: Current status and future prospect, Reactive & Functional Polymers. Vol.71. PP. 280-287, 2011.

[4] E.A. Kirzhanova, M.A. Pechenkin, N.B. Demina, N.G. Balabushevich Micro- and nanoparticles from alginate and chitosan for transmucosal protein delivery, Bulletin of Moscow University. Ser. 2. Chemistry – vol.57/ 2. PP. 103 – 111, 2016.

[5] Vasiliev AV, Grinenko EV, Shchukin AO Infrared spectroscopy of organic and natural compounds. SPb .: SPbSWTA, P.29, 2007.

[6] Knyazev R.A., Trifonova N.V., Polyakov L.M. Transport form of anticancer drugs doxorubicin and melphalan based on apolipoprotein A-I of blood plasma, Journal "Modern problems of science and education". vol. 6, PP. 2016

[7] Russian Federation. Ministry of Health care. On the approval of the rules for the manufacture and dispensing of medicinal products for medical use by pharmacy organizations, individual entrepreneurs who have a license for pharmaceutical activities N 751н dated October 26, 2015.

# HPV GENOTYPES COINFECTIONS AND HEALTH RISK - PRELIMINARY STUDY OF THE EAST ROMANIAN POPULATION

**Ph.D. Student Codrin Gheorghe**[1]
**Assoc. Prof. Dr. Schröder Verginica**[2]
**Assoc. Prof. Dr. Stoicescu Ramona**[3]
**Lecturer Dr. Honcea Adina**[4]
**Assoc. Prof. Dr. Dumitru Irina**[5]
[1, 5] Ovidius University of Constanta, Faculty of Medicine, Constanta, Romania
[3, 4] Ovidius University of Constanta, Faculty of Pharmacy, Constanta, Romania
[5] Clinical Infectious Diseases Hospital, Constanta, Romania

## ABSTRACT

The study aims to identify the degree of infection and co-infection with HPV strains in people of different ages, to assess the risk associated with lack of immunization of the Romanian population. In this study we are looking at the prevalence and relationship of the different types of HPV strains present in the 37 cases with suspected HPV infection that were analyzed, in the period 2018-2019, within the Prodiagnostic analysis laboratory, in Constanța, Romania. Of the total number of people analyzed for the case study, 45.94% (17 out of 37) tested positive for HPV infection. The analysis of the frequency of strains by risk categories shows that the highest percentage was 48% in the case of high-risk strains, followed by the percentage of frequency of strains with unknown risk (44%) and that of low-risk strains (8 %); The analysis by age indicates the maximum infection rate recorded belonging to the age group between 23 and 34 years. The association between strains and the 50% frequency indicates an important aspect of the infection as well as important data for diagnosis and treatment and involves more rigorous monitoring of patients with such associations, the risk increases with the associations.

***Keywords:*** *HPV, co-infections, strains, screening, lesions*

## INTRODUCTION

HPV are double-stranded DNA viruses that infect the stratified epithelium of the skin and mucous membranes. There have been identified approximately 200 strains with potential for induction of transformations. HPV serotypes are differentiated between one another by the genetic sequence of the external L1 protein capsid. Of these, 15 are classified as having high oncogenic risk (16,18, 31, 33, 35, 39, 45, 51, 52, 56, 58, 68, 73 and 82), 3 with probable oncogenic risk (26, 53 and 66) and 12 with low oncogenic risk (6,11, 40, 42, 43, 44, 54, 61, 70, 72, 81, CP6108) [1].

The infection appears to begin with the virus entering through a site of epithelial disruption (microlesion) that allows viral access to the basal epithelial layer. HPV-16 penetration occurs through clathrin-facilitated endocytosis, although other types of HPV may have other mechanisms of cell penetration [2].

Cervical HPV infection with oncogenic risk causes cervical morphological lesions, from normal (normal cytology) to various stages of preneoplastic lesions (CIN 1, CIN 2, CIN 3 / CIS) and invasive cervical cancer. Cervical infection is established by determining HPV DNA in cervical cells by various methods.

Clinically, the most important manifestation of HPV infection in the cervix is considered to be cervical intraepithelial neoplasia (CIN). CIN are cellular lesions with unstable genetic bases, presenting a risk of evolution in extensive cervical cancer, of 30-40%. These untreated lesions, CIN 2 or CIN 3, can cause cervical cancer in a few years or even decades later. The average period of natural evolution to invasive neoplasm is about a few years (12 years) [3].

Certain HPV serotypes more frequently induce oncogenesis, which includes them in the high-risk oncogenic HR-HPV strains, namely serotypes 16, 18 and 45.

These data suggest that in laboratory evaluation, high-risk oncogenic HPV DNA genotyping is a necessary test in suspected lesions and is an important indicator of the risk of developing high-grade or more advanced squamous intraepithelial lesions [4].

Immunohistochemical, cytogenetic and molecular studies [7] have shown that low-risk HPV types do not integrate into the host cell genome, while high-risk types are integrated into the nucleus of epithelial cells in the cervix.

Following integration, the protein product of HPV-16 and 18, proteins E7 and E6 respectively, inactivate the tumor suppressor genes, p53 and the RB-1 gene, allowing uncontrolled cell proliferation. It was possible to document morphological abnormalities in cervical lesions, observing a good correlation with underlying cellular events, by using techniques such as proliferation of cellular antigen (PCNA), expression of p16, p53 and nucleolus organizer region (NOR)[3].

HPV is a necessary cause of cervical cancer, but it is not a sufficient cause. Other cofactors are needed for progression from cervical HPV infection to cancer. Tobacco smoking, high parity, long-term hormonal contraceptive use and HIV co-infection have been identified as established cofactors. Co-infection with *Chlamydia trachomatis* and *Herpes simplex* virus type-2, immunosuppression and certain dietary deficiencies are other likely cofactors [4]. Genetic and immunological host factors and viral factors other than type, such as type variants, viral load, and viral integration, are likely important, but have not been clearly identified [4], [5], [9], [11].

The study aims to identify the degree of infection and co-infection with HPV strains in people of different ages, to assess the risk associated with lack of immunization of the Romanian population.

## MATERIALS AND METHODS

37 cases with suspected HPV infestation were analyzed, in the period 2018-2019, within the Prodiagnostic analysis laboratory, in Constanța, Romania. People were between 23 and 64 years old. The endocervical epithelium was taken and analyzed by HPV DNA detection and genotyping in the specialized laboratory of Matei Basarab Medical Center, Bucharest. The following HPV types were tested:

1. With increased oncogenic risk 14 HR-HPV strains: 16, 18, 31, 33, 35, 39, 45, 51, 52, 56, 58, 59, 66, 68;
2. With low oncogenic risk 3 LR-HPV strains: 6, 11, 42;
3. Other types of HPV: 26.40, 53, 54, 55, 61, 62, 64, 67, 69, 70, 71, 72, 73, 81, 82, 83, 84, IS 39, CP6108.

The results were statistically analyzed and interpreted [12], [13].

## RESULTS AND DISCUSSION

Human papillomavirus (HPV) infection is strongly implicated in the etiology of cervical cancer. High-risk HPV types, most commonly types 16 and 18 and less often types 31, 33, 52 and 58 are present in 70-100% of cervical cancer cases. HPV types 6 and 11 are most commonly found in warts, and mixed HPV types can be found in dysplasia [6].

The analysis of the presence of HPV strains shows that there are 25 different strains, belonging to three categories, taking into account the risk:

1. high-risk HPV strains (61, 52, 31, 56, 66, 16, 51, 39, 58, 18, 35, 59)
2. low-risk strains (6, 42)
3. other strains (81,54, 62, 67, Cp6108, 70, 71, 55, 69, 53, 84).

Of the total number of people analyzed for the case study, 45.94% (17 out of 37) tested positive for HPV infection.

As can be seen in Table 1, most cases indicate that there are several associated strains (co-infection) and with different degrees of risk. It should be noted that 6 of the 17 positive cases analyzed (35.29 %) show the association between 2, 3 or 4 high-risk strains. Another 6 cases show co-infection between high-risk strains and other lesser-known strains (Table1).

***Table 1.*** *Frequency of HPV strains in the group of participants (n = 17) positive and aspects regarding co-infection and frequency of strains (LR = low-risk, HR = high risk)*

| Crt. no. | Strain type | Frequency (%) | Co-infections |
|---|---|---|---|
| | HPV81 | 23.52 | 81, 61, 52, 62 |
| | HPV61 (HR) | 17.64 | 61, 81, 54, 31, 16, 18, 71, 62, 39, 42, 84, CP6108 |
| | HPV 52 (HR) | 29.41 | 52, 54, 62, 31, 62, 35, 59, 55, 69, 35 |
| | HPV54 | 11.76 | 54, 31, 16, 18, 71 |
| | HPV31 (HR) | 17.64 | 31, 56, 66, 16, 18, 71, 62,35,59,55,69 |
| | HPV56 (HR) | 5.88 | 56, 66 |
| | HPV66 (HR) | 5.88 | 0 |
| | HPV62 | 29.41 | 62, 67, 16, 70, 35, 59, 55, 69, CP6108 |
| | HPV CP6108 | 11.76 | CP6108, 62, 67, 61, 39, 42, 84 |
| | HPV67 | 5.88 | 67, CP6109 |
| | HPV16 (HR) | 17. 64 | 16, 70, 39, 58, 18, 71, |
| | HPV70 | 5.88 | 70, 16, 62 |
| | HPV 51 (HR) | 5.88 | 0 |
| | HPV 39 (HR) | 11.76 | 39, 16, 58, 61, 62, CP6109, 42, 84, CP6109 |
| | HPV 58 (HR) | 5.88 | 58, 16, 39 |
| | HPV 6 (LR) | 5.88 | 0 |
| | HPV 18 (HR) | 5.88 | 18, 71, 16, 31, 54, 61 |
| | HPV 71 | 5.88 | 71, 18, 16, 31, 54, 61 |
| | HPV 35 (HR) | 11.76 | 35, 52, 31, 62, 59, 55, 69 |
| | HPV 55 | 5.88 | 55, 35, 52, 31, 62, 59, 69 |
| | HPV 59 (HR) | 5.88 | 59, 55, 35, 52, 31, 62, 69 |
| | HPV 69 | 5.88 | 69, 55, 35, 52, 31, 62, 59 |
| | HPV 53 | 5.88 | 0 |
| | HPV 42 (LR) | 5.88 | 42, 61,81, 54, 31, 16, 18, 71, 62, 39, 84, CP6109 |
| | HPV 84 | 5.88 | 84, 61,81, 54, 31, 16, 18, 71, 62, 39, 42, CP6109 |

As can be seen in the analysis, 21 of the 25 strains (84%) are co-infected, in some cases more than 2 strains being present in the same person (Table 1). These aspects are important for diagnosis and treatment and involve more rigorous monitoring of patients with such associations.

The analysis of the frequency of strains by risk categories highlights the fact that the highest percentage was 48% in the case of high-risk strains, followed by the percentage of frequency of strains with unknown risk (44%) and that of low-risk strains (8 %), Figure 1.

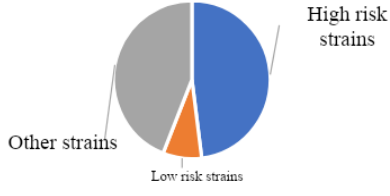


***Fig. 1.*** *Frequency (%) of HPV strains by risk categories, identified in the case of the analyzed group*

Of the total number of strains analyzed, 12 are very high risk (HR-HPV). These strains are found with a frequency between 10- 40%. The most common are HPV52, HPV61, HPV31 and HPV16 from these having 25% frequency (HPV61, HPV31, HPV16) and 41% HPV52, Figure 2.

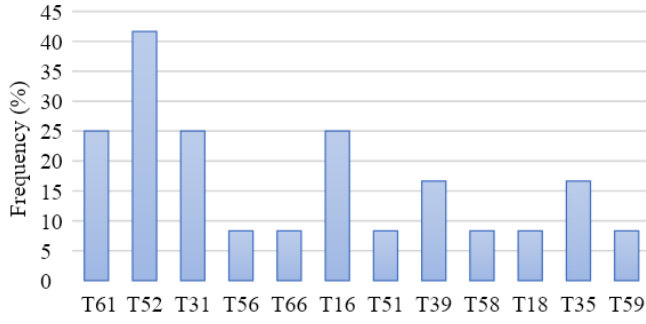


***Fig. 2.*** *Frequency of high-risk HR-HPV strains*

Worldwide, it is generally considered that the most frequently encountered serotypes in patients with CIN 3 or more advanced lesions are HPV 16 and 18. Recent studies have shown large differences in the variation of the serotype 18 prevalence of advanced neoplastic lesions [6], [11].

From the category of strains with unknown or low risk (LR-HPV), only 4 strains (T81, T54, T62, TCP6109) are noted as having a frequency of over 10% (Figure 3).

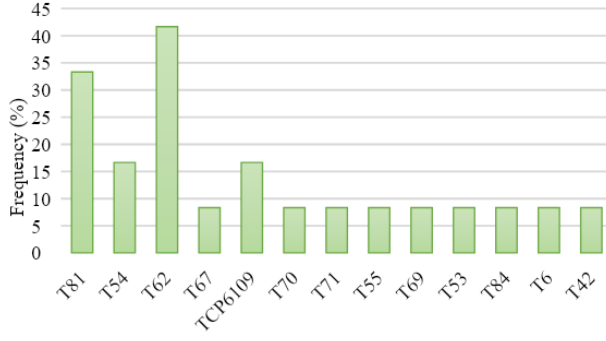


***Fig. 3.*** *Frequency of low-risk (LR-HPV) or unknown risk HPV strains*

The analyzed batch was divided into three classes of age (Fig. 4), a percentage of 25%, the maximum recorded belonging to the group between 23 and 34 years. This result can be associated with conceptual differences in the relationship between partners and education.

There are no known data on the socioeconomic level of people screened or any other factors that would promote the risk of contamination: immunosuppression, smoking, inadequate use of contraceptive methods, infections, sexual behavior, gene polymorphism's [9], [10], [11], [14].

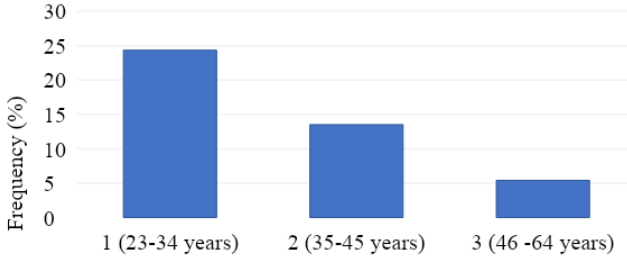


***Fig. 4.*** *Frequency of comparative HPV-positive samples by age classes*

In a similar study from the north Romanian population, prevalence results showed out of the total tested samples, about 37.3% from samples were positive for HPV/DNA. From them 23.3% were single HPV type infections and 14% tested positive for multiple HPV types [6].

The Global strategy towards eliminating cervical cancer as a public health problem adopted by the WHA in 2020, recommends a comprehensive approach to cervical cancer prevention and control. The recommended set of actions should be multidisciplinary[15], including components ranging from community education, social mobilization, vaccination, screening, treatment and palliative care across the life course [9].

Cervical cancer screening involves testing for pre-cancer and cancer, more and more testing for HPV infection is performed. Testing is done among women who have no symptoms and may feel perfectly healthy. When screening detects an HPV infection or pre-cancerous lesions, these can easily be treated, and cancer can be avoided. Screening can also detect cancer at an early stage and treatment has a high potential for cure. Screening has to be linked to the treatment and management of positive screening tests. Screening without proper management in place is not ethical.

The World Health Assembly adopted the global strategy to accelerate the elimination of cervical cancer as a public health problem and its associated goals and targets for the period 2020–2030 [8], [9].

Romania is struggling with a high rate of cervical cancer. The National Screening Program for the early detection of cervical cancer targets a segment of the extended population (about 6 million women). To date, about 700,000 women have benefited from free Babeș Papanicolaou testing services (coverage rate 12%). It is estimated that 49% of all possible cases of cervical cancer have been prevented by population screening.

It is considered that in Romania the information about the risk of cervical cancer is no longer sufficient, and methods of awareness of cervical cancer causes and prevention can reduce risk by 80%, if there is a mass proportion gain [9].

## CONCLUSION

Of the total number of people analyzed for the case study, 45% (17 out of 37) tested positive for HPV infection.

Frequency analysis of strains by risk categories reveals that the largest percentage was recorded in the strains with high risk (48%), followed by the frequency of strains with unknown risk (44%) and that of strains with low risk (8 %).

The analysis by age class indicates the maximum of recorded strains belonging to the age group between 23 and 34 years. This result can be associated with conceptual differences in the relationship between partners and education.

In our study the most common high-risk serotypes were HPV61, HPV31, HPV52, and HPV16. These strains are found with a frequency between 10 - 40%. The most common are HPV52, HPV61, HPV31 and HPV16 having the values of frequency at 25% (HPV61, HPV31, HPV16) and 41% respectively (HPV52).

The association between strains and the 45% frequency indicates an important aspect of the infection as well as important data for diagnosis and treatment and involves a more rigorous monitoring of patients with such associations, the risk increases with the associations.

## REFERENCES

[1] Sabet F., Mosavat A., Ahmadi Ghezeldasht S., Basharkhah S., Shamsian S.A.A, Abbasnia S., Shamsian K., Rezaee S.A., Prevalence, genotypes and phylogenetic analysis of human papillomaviruses (HPV) in northeast Iran. International Journal of Infectious Diseases, 103:480-488, 2021.

[2] Moody C.A., Laimins L.A., Human papillomavirus oncoproteins: pathways to transformation. Nat. Rev. Cancer, 550-560, 2010.

[3] Fernandes J.V., DE Medeiros Fernandes T.A., DE Azevedo J.C., Cobucci R.N., DE Carvalho M.G., Andrade V.S., DE Araújo J.M., Link between chronic inflammation and human papillomavirus-induced carcinogenesis (Review). Oncol. Lett. (3):1015-1026, 2015.

[4] Bruni L., Albero G., Serrano B., Mena M., Gómez D., Muñoz J., Bosch FX., de Sanjosé S., ICO/IARC, Information Centre on HPV and Cancer (HPV Information Centre). Human Papillomavirus and Related Diseases in the World. Report 17, pp 243-244, 2019.

[5] Burd E.M., Human papillomavirus and cervical cancer. Clin. Microbiol. Rev., pp 1-17, 2003.

[6] Ursu RG, Onofriescu M, Nemescu D, Iancu LS., HPV prevalence and type distribution in women with or without cervical lesions in the Northeast region of Romania, Virol J., 2011, 8:558;

[7] Verissimo, J.F., Araújo De Medeiros A.T. F., Veríssimo De Azevedo J.C., Cobucci R.N.O., Freire De M. G., Andrade V.S. and Araújo J.M.G., Link between

chronic inflammation and human papillomavirus induced carcinogenesis (Review), Oncology Letters, 9: 1015-1026, 2015.

[8] https://www.who.int/en/news-room/fact-sheets/detail/human-papillomavirus-(hpv)-and-cervical-cancer;

[9] Bruni L., Albero G., Serrano B., Mena M., Gómez D., Muñoz J., Bosch F.X., de Sanjosé S. ICO/IARC, Information Centre on HPV and Cancer (HPV Information Centre). Human Papillomavirus and Related Diseases in the World. Summary Report 17 June 2019, www.hpvcentre.net.

[10] Georgescu M., Ginghina O., Raita S., Tapaloaga D., Ilie L., Negrei C., Popa D. E, Varlas V., Multescu R., Rosca A.C., Mirica R., Georgescu D., Natural alternative remedies in the background of updated recommendations for the prophylactic and therapeutic approach of *Clostridium difficile* infections, Farmacia, 66, pp 563-572, 2018.

[11] Stefanescu C., Calistru P., Voinea C., Gherlan G., Prevalence and distribution of high-risk genotypes of HPV in women with cervical intraepithelial neoplasia (CIN), in CDT "Victor Babes", Revista Romana de Boli Infectioase, XV, 4, 2012.

[12] E. C. Lupu, S. Lupu, A. Petcu, EB lifetime distributions as alternative to the EP lifetime distributions, Annals of "Ovidius" University from Constanţa, Mathematics Series, 22, (3), pp.115-125, 2014.

[13] A. Leahu, E. C. Lupu, Statistical simulation and prediction in software reliability. Annals of "Ovidius" University from Constanţa, Mathematics Series, 16, 1, pp 81-90, 2008.

[14] Torres-Poveda K., Burguete-García A.I., Bahena-Román M., Méndez-Martínez R., Zurita-Díaz M.A., López-Estrada G., Delgado-Romero K., Peralta-Zaragoza O., Bermúdez-Morales V.H., Cantú D., García-Carrancá A., Madrid-Marina V., Risk allelic load in Th2 and Th3 cytokines genes as biomarker of susceptibility to HPV-16 positive cervical cancer: a case control study. BMC Cancer, 24, 16:330, 2016.

[15] Erdem H, Puca E, Ruch Y, Santos L, Ghanem-Zoubi N, et al. Portraying infective endocarditis: results of multinational ID-IRI study, Eur J Clin Microbiol Infect Dis. 38(9):1753-1763, 2019.

# MATHEMATICAL MODELS FOR THE SYNTHESIS OF PLANT-BASED COMPOSITIONS WITH IMPROVED AMINO ACID COMPOSITION

**Ph.D. Student Irina Gaivoronskaya**[1]
**Prof. Dr. Valentina Kolpakova**[2]
[1, 2] All-Russian Research Institute for Starch Products – Branch of V.M. Gorbatov Federal Research Center for Food Systems of Russian Academy of Sciences, Kraskovo, Russia

## ABSTRACT

The aim of the work was to optimize the process of obtaining multicomponent protein compositions with high biological value and higher functional properties than the original vegetable protein products. Was realized studies to obtain biocomposites on the base of pea protein-oat protein and pea protein-rice protein. Developed composites were enriched with all limited amino acids. For each of the essential amino acids, the amino acid score was 100% and higher. Protein products used in these compositions are not in major allergen list, which allows to use these compositions in allergen-free products and specialized nutrition. To determine biosynthesis parameters for compositions from pea protein and various protein concentrates with the use of transglutaminase enzyme, was studied effect of concentration and exposition time on the amount of amino nitrogen released during the reaction. Decreasing of amino nitrogen in the medium indicated the occurrence of a protein synthesis reaction with the formation of new covalent bonds. Were determined optimal parameters of reaction: the hydromodule, the exposure time, the concentration of EP of the preparation, were obtained mathematical models. Studies on the functional properties of composites, the physicochemical properties of the proteins that make up their composition, and structural features will make it possible to determine the uses in the manufacture of food products based on their ability to bind fat, water, form foam, gels, and etc.

***Keywords:*** *plant-based preparations, transglutaminase, protein compositions, amino acid score, biological value*

## INTRODUCTION

The increase in the population of the planet allows experts today to predict the progressive shortage of protein foods. The shortage of protein on the planet is estimated at 10-25 million tons per year. Approximately half of the world's population suffers from a lack of protein. The lack of food protein is not only an economic, but also a social problem of the modern world [1]. With the help of biotechnological processes with the usage of microorganisms have not yet had any success in obtaining new alternative sources of this mandatory and valuable component of food. This dramatically increases the role of natural proteins, enhances the importance of high-tech technological processes in their production and use in the form of new forms. Plant-based diet containing a complete protein in

the required amount might be created on the base of usage of protein preparations obtained from protein-containing sources with different chemical composition and biological value. Most of the cereals are deficient in lysine, one of the most important from the essential amino acids in human nutrition, while legumes contain this amino acid in sufficient quantity. On the other hand, cereal proteins can supplement legume proteins with the deficient amino acid methionine [2]. Along with soy proteins, with appropriate functional properties, pea, rice and oat proteins also can be successfully used for enrichment and enhancing of the biological value of food products [3]. With the usage of enzyme preparation transglutaminase for the biosynthesis of composite protein products with increased biological value from a technological point of view, it may be important to vary the content of free amino groups in the used plant preparations. Adding proteins with a high content of free amino groups, in particular lysine, to proteins with a low amount of them will increase the reactivity of the latter [4] and form modules with a given composition and functional properties.

*The aim of this work is* an optimization of parameters of biosynthesis multi-protein compositions, created on the base of pea protein with the selection of their composition on the basis of the quantitative content of amino acids in them, and above all, essential, so that the human body received full proteins, and this protein product could be more widely used in the manufacture of food products.

## MATERIALS AND METHODS

The main materials used were samples of pea (Roquette, France), rice (Beneo, Belgium) and oat (Tate & Lyle, Sweden),. The chemical composition of protein concentrates is shown in Table 1. The enzyme preparation used was the enzyme preparation (EP) of the 'classical' transglutaminase (TG) (Novozymes, Denmark).

***Table 1.*** *The chemical composition of protein products*

| Protein product | Humidity, % | Protein, % | Fat, % | Insoluble fibers, % | Carbohydrates, % |
|---|---|---|---|---|---|
| Pea | 10,0 | 84,0 | 5,0 | 1,0 | 0 |
| Rice | 12,0 | 79,0 | 5,0 | 3,2 | 6,0 |
| Oat | 6,0 | 56,0 | 3,0 | 2,0 | 18,0 |

Conclusion about the reaction, with the transglutaminase enzyme, between proteins with different chemical nature was based on the amount of released amine nitrogen. Amine nitrogen was determined by formol titration. To do this, 50 $cm^3$ of distilled water was added to 10 g of the fermented DWG mixture with protein concentrates taken at certain ratios, then the mixture was dispersed for 4-5 minutes at 500 $min^{-1}$. The mixture was centrifuged at 5500 $min^{-1}$ for 20 minutes. The supernatant was decanted, 5 $cm^3$ from it was transferred into a glass beaker, mixed with 20 $cm^3$ of distilled water after has been measured the pH. The pH meter electrodes were loaded into the test suspension. Neutralization of free carboxyl groups was performed with 0.05 N NaOH solution. Alkali was added while stirring, following the readings of the potentiometer. When the pH of the solution reached 7, was added 0.5 $cm^3$ of the formula mixture with phenolphthalein 50 $cm^3$ of 40% formalin + 2 $cm^3$ of 1% alcohol solution of phenolphthalein). The mixture was

titrated with 0.05N NaOH solution to pH 9.1-9.5, which corresponded to the bright red staining of the sample. All reagents were chemically pure.

Amine nitrogen (in mg /%) (N) was calculated by the formula: N = A * 0.7 * 100 / V, where: A -is the amount of $cm^3$ of 0.05N NaOH, followed by titration; V- is the amount of solution for titration; 0.7- is the amount of nitrogen in g, corresponding to 1 $cm^3$ of 0.05 N NaOH solution.

For the preparation of two-component fermented compositions, weighed protein products at their specific ratios were mixed on a stirrer at a speed of 500 $min^{-1}$. Samples of transglutaminase EP were placed in a microbiological test tube with a cap, was added 3,6 $cm^3$ of phosphate buffer solution with predetermined pH, mixed vigorously, and was added 1 g of a mixture of protein products. The tubes were placed in a thermostat, shaken at 170 $min^{-1}$ and a temperature of 50 °C.

For the preparation of two-component fermented compositions, weighed protein products at their specific ratios were mixed on a stirrer at a speed of 500 $min^{-1}$. Samples of transglutaminase EP were placed in a microbiological test tube with a cap, was added 10.5 $cm^3$ of distilled water, in accordance with a given hydromodule, mixed vigorously, and was added 1 g of a mixture of protein products. The tubes were placed in a thermostat, shaken at 170 $min^{-1}$ and a temperature of 50°C, and the proteins were reacted at different flow times and concentrations.

## RESULTS AND DISCUSSION

With the help of the program developed by us on the basis of the Monte Carlo calculation method, were compiled protein compositions with an improved amino acid profile. In time of calculating was used amino acid composition data of protein products for the proposed mixtures, data for the reference protein based on the recommendations of the FAO WHO (2011) [5]. For pea and oat concentrates, the optimum ratio of proteins in the composition was 1: 1 (table 2), for pea and rice concentrates - 1: 0.6 (table 2). These ratios provided the optimal amino acid fastness and were economically feasible.

***Table 2.*** *An amino acid score of proteins from compositions of the protein concentrates,%*

| Indicators | Protein compositions | | | Protein concentrate | |
|---|---|---|---|---|---|
| | PEA | OAT | RICE | PEC/OC | PEC/RC |
| Mass fraction of proteins, % | 84.0 | 56,3 | 79.5 | 70.2 | 81.8 |
| Amino acids | Score, % | | | | |
| Valine | 125 | 65 | 137 | 132 | 157 |
| Leucine | 134 | 62 | 124 | 135 | 158 |
| Isoleucine | 156 | 62 | 113 | 149 | 170 |
| Threonine | 152 | 56 | 176 | 142 | 196 |
| Lysine | 148 | 33 | 147 | 117 | 141 |
| Methionine + cysteine | 151 | 103 | 136 | 181 | 177 |
| Phenylalanine + tyrosine | 47 | 82 | 147 | 101 | 105 |

*Note: PEC – pea concentrate; OC – oat concentrate; RC-rice concentrate*

The data showed that rice concentrate had the highest amino acid scores, oat protein had the lowest values, pea concentrate contained insufficient amounts of sulfur-containing amino acids, which does not contradict the literature data. Amino acid composition of protein compositions with pea concentrate, in comparison with individual samples, was significantly improved due to rice and oat concentrates. This increase is especially valuable in all two-component composites for lysine, threonine, phenylalanine and rytosine, sulfur-containing amino acids, the deficiency of which is noted in most grain crops [6]. The most balanced in terms of amino acids was the PEC/RC composite composition, the most unbalanced (in sulfur-containing amino acids) - the PEC/OC composition composite.

To optimize the parameters of the biosynthesis of compositions from protein concentrates using TG was studied the effect of concentration of EP, exposure time and hydromodule on the amount of amino nitrogen released during the reaction with the enzyme.

Considering that in transglutaminase reactions, the transfer of amino groups - $NH_2$ between molecules occurs with the formation of new covalent bonds, the amount of amino nitrogen in the studied systems decreased, therefore, by the number of unreacted amino groups, it was possible to judge the course of the synthesis process between different types of proteins.

To obtain results on the influence of various factors on the content of amino nitrogen for the composition of pea protein-oat protein, methods of mathematical planning of the experiment were used, with pH = 6.8–7.0 (const), temperature = 50 ° C (const). The exposure time (X3) was changed in the range of 5 ÷ 20 min, the hydronic module (X1) - in the range of 1: 5 to 1: 8, the concentration of EP (X2) - from 0.0015 to 0.003 U / g protein (table 3).

***Table 3.*** *The effect of the concentration of EP, the exposure time and hydromodule on the amount of amine nitrogen in the process of synthesis of the composition of the pea concentrate-oat concentrate*

| № | Concentration of EP, U/g for DS | Exposure time, min | Hydromodule | Amine nitrogen, mg% |
|---|---|---|---|---|
| 1 | 0,0015 | 5 | 1:5 | 7,98 |
| 2 | 0,0015 | 10 | 1:6 | 7,28 |
| 3 | 0,0015 | 15 | 1:7 | 6,16 |
| 4 | 0,0015 | 20 | 1:8 | 7,98 |
| 5 | 0,002 | 5 | 1:6 | 9,38 |
| 6 | 0,002 | 10 | 1:7 | 7,56 |
| 7 | 0,002 | 15 | 1:8 | 6,86 |
| 8 | 0,002 | 20 | 1:5 | 8,4 |
| 9 | 0,0025 | 5 | 1:7 | 6,44 |
| 10 | 0,0025 | 10 | 1:8 | 7,84 |
| 11 | 0,0025 | 15 | 1:5 | 7,14 |
| 12 | 0,0025 | 20 | 1:6 | 8,4 |
| 13 | 0,003 | 5 | 1:8 | 7,7 |
| 14 | 0,003 | 10 | 1:5 | 7,42 |
| 15 | 0,003 | 15 | 1:6 | 7,7 |
| 16 | 0,003 | 20 | 1:7 | 7,7 |

According to the experiment data, using the TableCurve 3D program, were constructed response surfaces for amino nitrogen (Fig. 2). Data processing in programs Matematika and Table Curve 3D

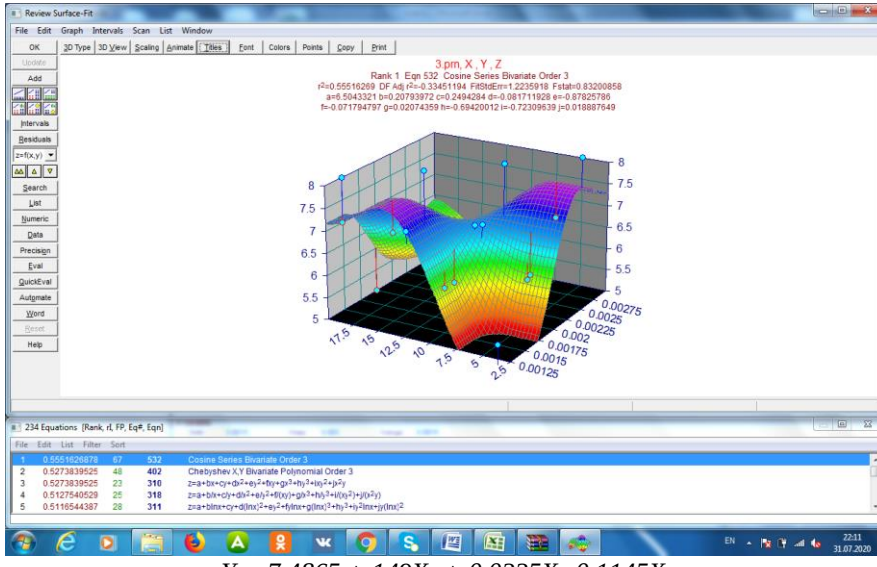


$$Y = 7.4865 + 149X_1 + 0.0335X_2\text{-}0.1145X_3$$

*where x –concentration of EP, g/g of protein; y-time of exposition, min; z- back hydromodule*

***Fig. 2.*** *The dependence of the amount of amine nitrogen on the reaction parameters for the composition of pea concentrate-oat concentrate*

To obtain the results on the influence of various factors on the content of amino nitrogen for the composition of pea protein concentrate-rice protein, were used methods of mathematical planning of the experiment. Taking into account the data obtained during the protein concentrate-rice protein experiment, the most effective reaction parameters were selected: pH - 6.8–7.0 (const), temperature 50°C (const). The exposure time (X3) was changed in the range of 5 ÷ 20 min, the hydromodule (X1) - in the range of 1: 5 to 1: 8, the concentration of OP (X2) - from 0.0015 to 0.003 U / g protein (table 4).

***Table 4.*** *The effect of the concentration of EP, the exposure time and hydromodule on the amount of amine nitrogen in the process of synthesis of the composition of the pea concentrate-rice concentrate*

| № | Concentration of EP, U/g for DS | Exposure time, min | Hydromodule | Amine nitrogen, mg% |
|---|---|---|---|---|
| 1 | 0,0015 | 5 | 1:5 | 7,28 |
| 2 | 0,0015 | 10 | 1:6 | 7,14 |
| 3 | 0,0015 | 15 | 1:7 | 7,14 |
| 4 | 0,0015 | 20 | 1:8 | 6,72 |
| 5 | 0,002 | 5 | 1:6 | 7,28 |
| 6 | 0,002 | 10 | 1:7 | 7,28 |
| 7 | 0,002 | 15 | 1:8 | 7,14 |
| 8 | 0,002 | 20 | 1:5 | 7,84 |
| 9 | 0,0025 | 5 | 1:7 | 7 |
| 10 | 0,0025 | 10 | 1:8 | 7,42 |
| 11 | 0,0025 | 15 | 1:5 | 7,98 |
| 12 | 0,0025 | 20 | 1:6 | 7,98 |
| 13 | 0,003 | 5 | 1:8 | 7,28 |
| 14 | 0,003 | 10 | 1:5 | 8,4 |
| 15 | 0,003 | 15 | 1:6 | 8,26 |
| 16 | 0,003 | 20 | 1:7 | 7,84 |

According to the experiment data, using the TableCurve 3D program, were constructed response surfaces for amino nitrogen (Fig. 3). Data processing in programs Matematika and Table Curve 3D

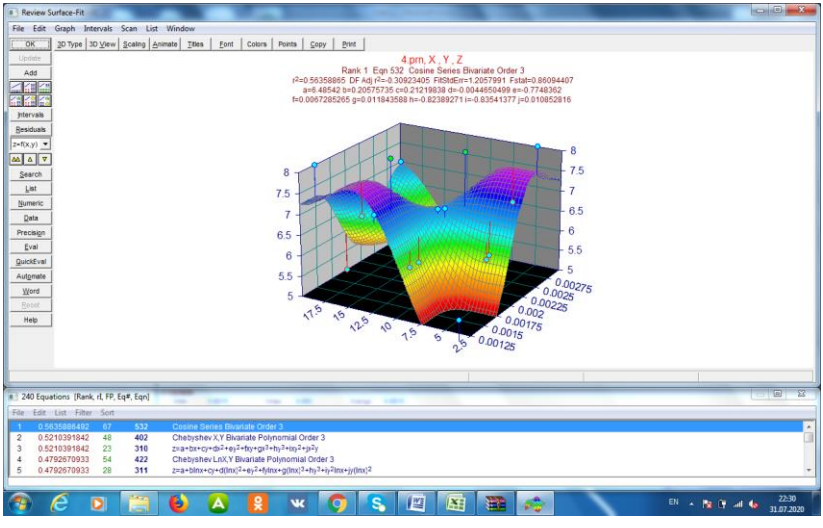


$$Y = 7.5775 + 567X_1 + 0.0245X_2\text{-}0.2555X_3$$

*where x –concentration of EP, g/g of protein; y-time of exposition, min; z- back hydromodule*

***Fig. 3.*** *The dependence of the amount of amine nitrogen on the reaction parameters for the composition of the pea concentrate-rice concentrate*

For the composition of pea concentrate-oat concentrate, the patterns of change in the amount of amine nitrogen in the course of the reaction were similar to the patterns characteristic of the composition of pea concentrate-rice concentrate. The minimum amount of amino nitrogen after reaction with TG in the composition of pea concentrate-oat concentrate was observed in the reaction medium at a concentration of 0.0015 g / g of protein, exposure time of 15 minutes and a water ratio of 1: 7. The minimum amount of amino nitrogen after reaction with TG in the composition of pea concentrate-rice concentrate was observed in the reaction medium at a concentration of 0.0015 g / g of protein, exposure time of 20 minutes and a water ratio of 1: 8.

## CONCLUSION

Due to its unique properties, TG is widely used in the meat and dairy industry for the aggregation of protein molecules in the production of restructured products from raw materials of various qualities [7], [8], [9]. The enzyme is safe, produced by inexpensive sources of biosynthesis, which makes its use wide. Significantly less TG is used in the manufacture of baked goods (bread, biscuits) [4], [10], [11] and isolated studies are known to produce compositions from vegetable proteins [12].

With the help of a program developed on the basis of the Monte-Carlo calculation method, were compiled protein concentrate compositions with improved amino acid composition. Taking into account the mass fraction of protein and the amino acid composition of the concentrates, their ratios and amino acid levels are determined for protein-protein composites obtained from various types of plant materials (peas, rice, oats). Composites are enriched with lysine, threonine, sulfur-containing amino acids in relation to cereals and leguminous crops. Using biotechnological reactions with the participation of the enzyme class transferase (transglutaminase) obtained biocomposites composition: pea concentrate-oat concentrate, pea concentrate-rice concentrate. Experimentally using the method of formol titration according to the amount of amino nitrogen remaining in the reaction medium, the reaction parameters were determined: the duration of its flow and the concentration of the enzyme preparation.

For the composition of pea concentrate-oat concentrate, the minimum amount of amino nitrogen after reaction with TG in a two-component product was observed in the reaction medium at a concentration of 0.0015 g / g of protein, exposure time 20 minutes and a water ratio of 1: 7; for the composition of pea concentrate-rice concentrate, the minimum amount of amino nitrogen was released in reaction with TG at a concentration of 0.0015 g / g of protein, exposure time of 20 minutes and a water ratio of 1: 8. These data indicated a high intensity of the reaction of the synthesis of new forms of proteins. Compositions of concentrates with potato protein did not contain deficient essential amino acids, soon approached the reference protein as much as possible, or it was higher. Further studies will show what functional and technological properties created protein composites will possess and in which food products they can be used.

## REFERENCES

[1] Donchenko L.V. Technology of functional food products: textbook for high schools. — 2nd edition. — Moscow: Jurait, 2018. — pp.101-102

[2] Iqbal A, Khalil IA, Ateeq N and Khan MS, Nutritional quality of important food legumes. Food Chem, 97:331-335 (2006)

[3] Tömösközi S, Lásztity R, Haraszi R and Baticz O, Isolation and study of the functional properties of pea proteins. Nahrung/Food 45:399-401 (2001).

[4] Marco C, Rosell CM. Breadmaking performance of protein enriched, gluten-free breads. Eur Food Res Technol. 2008;227:1205–1213. doi: 10.1007/s00217-008-0838-6.

[5] Dietary protein quantity evaluation in human nutrition: Report of an FAO Expert Consultation.-Rome: FAO,2013-66pp.

[6] Koehler P., Wieser H. Chemistry of Cereal Grains. In: M. Gobbetti and M. Gunzle (eds.). Handbook on Sourdough Biotechnology, 11. 2013. Chapter 2, Springer Science+Business Media New York . DOI 10.1007/978-1-4614-5425-0_2

[7] Kuraishi C., Sakamoto J., Yamazaki K., Susa Y., Kuhara C., Soeda T. Production of restructured meat using microbial transglutaminase without salt or cooking. J. Food Sci. 1997. V. 62. pp. 488–490. doi: 10.1111/j.1365-2621.1997.tb04412.x

[8] Ozer B., Kirmaci H.A., Oztekin S., Hayaloglu A., Atamer M. Incorporation of microbial transglutaminase into non-fat yogurt production. Int. Dairy J. 2007. V. 17. pp. 199–207. doi: 10.1016/j.idairyj.2006.02.007

[9] Lorenzen P.C., Neve H., Mautner A., Schlimme E. Effect of enzymatic cross-linking of milk proteins on functional properties of set-style yoghurt. Int. J. Dairy Technol. 2002. V. 55. pp. 152–157. doi: 10.1046/j.1471-0307.2002.00065.x

[10] Lorenzen P.C., Neve H., Mautner A., Schlimme E. Effect of enzymatic cross-linking of milk proteins on functional properties of set-style yoghurt. Int. J. Dairy Technol. 2002. V. 55. pp. 152–157. doi: 10.1046/j.1471-0307.2002.00065.x

[11] Kuraishi C., Yamazaki K., Susa Y. Transglutaminase: its utilization in the food industry. Food Rev. Int. 2001. V. 17. pp. 221–246. doi: 10.1081/FRI-100001258

[12] Kolpakova V.V., Gaivoronskaya I.S., Gulakova V.A., Sardzhveladze A.S., Composition on the basis of plant-based proteins with the use of transgutaminase // International Multidisciplinary Scientific GeoConference SGEM (Bulgaria, Albena, 2018) – pp.119-126

# METHODS FOR QUANTIFICATION OF THE MAIN CANNABINOIDS IN CBD OIL

**Assoc. Prof. Ph.D. Student Nicoleta Mirela Blebea[1]**
**Prof. Simona Negreș Ph.D.[2]**
[1] Pharmacology and Clinic Pharmacy Department, Faculty of Pharmacy, Ovidius University, Constanta, Romania
[1] Pharmacology and Clinic Pharmacy Department, Faculty of Pharmacy, Carol Davila UMF, Bucharest, Romania
[2] Pharmacology and Clinic Pharmacy Department, Faculty of Pharmacy, Carol Davila UMF, Bucharest, Romania

## ABSTRACT

Cannabidiol (CBD) is an alkaloid present in *Cannabis sativa*, together with tetrahydrocannabinol (THC) and more than 120 other substances belonging to a group of compounds named cannabinoids. Due to the continuous increased usage of CBD oils, it became necessary to be developed efficient methods for the identification of its compounds and especially for the characterization of the cannabinoids from the commercial specimens. Cannabinoids may be detected by many and different analytical methods, including immunoassays (EMIT®, Elisa, fluorescent polarization, radioimmunotest), techniques of flat chromatography: classic thin layer chromatography (TLC), optimum performance laminar chromatography (OPLC) and multiple development automatization (AMD), gas chromatography-mass spectrometry (GC-MS), high-performance liquid chromatography-mass spectrometry (HPLC-MS). Ultraviolet signal (UV) is used for the quantification of major cannabinoids and the mass spectrometer is used for the quantification of minor cannabinoids. The purpose of this study was to compare the performances of TLC, Ultra High-Performance Liquid chromatography with Photodiode Array Detection (UHPLC with PDA) and LC-MS/ MS technique for the qualitative and quantitative determination of cannabinoids in 3 commercial oils with CBD. Having in view that CBD may be found in many forms of oils, on the legal market of the internet, we believe that the development of a method for the qualitative and quantitative determination may be an interesting subject for the pharmaceutical professional persons.

***Keywords:*** *CBD oils, cannabinoids, analytical, THC, quantification.*

## INTRODUCTION

The Cannabis family includes *Cannabis sativa* and *Cannabis indica s*pecies. *Cannabis sativa* contains over 500 unique compounds, including over 120 natural cannabinoids. There were reported many therapeutical properties attributed to their pharmacological characteristics, which leads to a significant interest in their use in nutraceuticals and other consumption products [1]. The *Cannabis* plant was used from the oldest times for producing hemp fibers (for clothes, rope and paper), seeds that may be used as food for animals and also as a medicinal plant. CBD is one of

the main alkaloids from the composition of cannabis plants together with other identified alkaloids [2]. The two major neuroactive compounds from the cannabis plants are: the main psychoactive alkaloid, tetrahydrocannabinol (THC) and non-psychoactive alkaloid CBD [3].

Taking into account the present legislation, there are small differences regarding the quantities of THC admitted in the hemp products, the concentrations varying between 0,05 and 0,6% [4]. In the plant, the cannabinoids are mostly present under the form of acids, which are decompounded by decarboxylation. CBD is widely used although its benefic effects are reported especially based on the casuistical observations [5],[6]. In some countries, the products with CBD are legal, while in other countries they are forbidden, thus aggravating the confusion. At present, CBD is used as an active ingredient in the following products: Epidiolex® - oral solution (contains only CBD), approved in 2018 by Food and Drug Administration (FDA) as a medical product used for the treatment of seizures associated with Dravet and Lennox-Gastaut syndromes and Sativex® - oral-mucosal spray (contains both CBD and THC, in the percentage of 1:1) [7], [8], [9]. More clinical studies are in progress for the potential treatment of neurological and behavioral disorders. As CBD has a complex mechanism of action, there is a high potential of its use in the treatment of different pathologies [4].

The quantification of cannabinoids is essential for the proper labeling of cannabis products, for quality control, as well as for establishing the legality regarding the content of THC. The oils with CBD contain potentially useful nontoxic phyto cannabinoid substances. Together with the increase of the interest of the patients for the oils with CBD, there are indicated more researches for a better understanding of their therapeutic potential and of the safety profile [1], [10], [11], [14].

The present paper describes a series of analytical methods used for the separation of cannabinoids necessary for the analysis of the oils with CBD from the market. Using chromatographic methods we can determine the original composition of cannabinoids in oils by direct analysis [11]. CBD oil is traded for being used by children (for Dravet syndrome, ADHD, autism) [12], old persons (Alzheimer disease, dementia, Parkinson disease, cardiovascular diseases, inflammatory diseases) [13], patients that suffer from complications (cancer, multiple sclerosis, chronic pain, diabetic complications, arthritis, epilepsy) [11] and even for pets (anxiety, appetite, sleep, osteoarthritis) [15]. From this reason, the qualitative and quantitative certification is necessary through a selective, simple and fast method. The oil-rich in CBD became more and more popular and it is administrated under the form of sublingual drops, gelatinous capsules or as unguent local ointment [11]. At present, the market is in the progress of developing towards more sophisticated products, including oral capsules, liposomal products, skin lotions and chewing gums that contain CBD [6], [7].

## MATERIALS AND METHODS

### TLC

With the help of this technique and of the kit from alpha-CAT ® the main ingredients from cannabis may be visualized due to a reaction of a specific coloration, which represents the cannabinoids present in the oils with CBD or from the cannabis product. Up to 4 specimens may be tested for each chromatographical plate.

TLC is the first method used for the chemical analysis of cannabis. It has the advantage of parallel analyses, although it has limits in resolution and sensitivity. The advantages are the reduced costs, the simple preparation of the specimens and the nondestructive method. Moreover, it allows the use of a wide range of chemical reactive substances for detection.

I used 3 modalities of oils traded on the internet, which I named as follows for easier identification: specimen 174 – product declared with a content of 1350 mg/100 ml total concentration of cannabinoids, specimen 175 - product declared with a content of 2, 5% CBD, specimen 181 - product declared with a content of 8% CBD, 4mg/drop.

Whether our specimen has a decreased or increased rate of cannabinoids, we can calculate a factor of multiplication for testing of the rate of THC is decreased or increased in the oils with CBD analyzed. We apply this simple rule based on the weight of the specimen: Factor of multiplication = (100 mg x 2µl) / weight of the specimens (mg) X extraction fluid (µl).

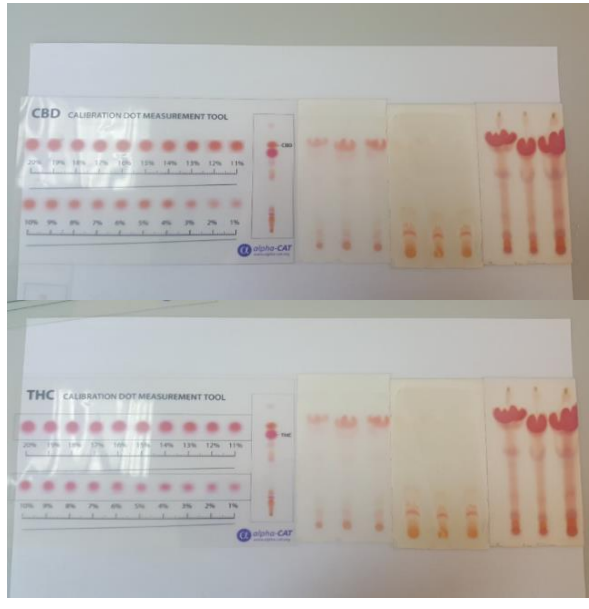


***Fig.1.*** *Comparing with the area cu rigla graphical ruler of cannabinoids alpha-CAT® for CBD and THC, specimens 174, 175, 181.*

At present, TLC is a cheap method for the analysis of cannabinoids approved by the Office of the United Nations for Drugs and Crimes for the routine control of the content of cannabinoids. For the applications that require a high sensitivity for instance in pharmacology, it is not an indicated method.

**UHPLC-PDA**

Through UHPLC technique with PDA detection it was followed the separation and quantitative determination of CBD present in 3 oils. The chromatographical separation was made using a PerkinElmer Brownlee Analytical C18 column (50mm × 4,6mm id, 5µm) or the equivalent, using the evaluation in gradient with 0,1% acid formic in water as mobile phase A and 0,1% acid formic in acetonitrile as mobile phase B. For quantification, the length of detection wave was set at 210 nm.

The method was established and optimized in the following chromatographical conditions: debit-1mL/min, temperature of the column -30°C, injecting volume-5µL, mobile phases - formic acid and formic acid with acetonitrile(V/V).

Solvents, standards and specimens: Solution of cannabidiol, 1,0 mg/ml SLBM6755V; Standard Analytic Standard Sigma Aldrich; Methanol absolute, for HPLC, LiChrosolv®; Acetonitrile, for HPLC, LiChrosolv®; Formic Acid for LC / MS, Fischer Chemical®; 2-propanol, for HPLC, LiChrosolv®; 3 variants of hemp oils from Romania and Netherlands.

***Table 1.*** *Exact Quantification of CBD for the 3 oil specimens*

| **Sample Name** | **Avg. Amount** | **Units** | **Avg. Plates (Foley-Dorsey)** | **Avg. Tailing Factor** | **Avg. Resolution** | **Avg. Area** |
|---|---|---|---|---|---|---|
| Stand CBD 20 ppm | 0.0000 | µg/mL | 11,217 | 1.407 | 2.27 | 2,203,748.7 |
| CBD 174 D100 | 35.2245 | µg/mL | 7,385 | 1.083 | 1.25 | 2,803,382.6 |
| CBD 175 D100 | 48.3351 | µg/mL | N/A | 0.000 | 1.09 | 3,319,760.2 |
| CBD 181 D4500 | 27.3011 | µg/mL | 6,110 | 0.995 | 0.00 | 2,491,310.3 |

The optimized method is a simple, fast, selective, sensitive and useful method for the verification of the stability of CBD in the pharmaceutical forms, may be useful for quality control of the medicine products, both under the form of active substance and pharmaceutical formulations. The perspective of the study consists in applying this method on different pharmaceutical forms but also on different types of specimens (biological, soil, water, etc.)

**LC-MS**

I researched a technique of qualitative and quantitative analysis of CBD and CBG from three commercial hemp oils with the help of a UHPLC device with MS detector. The fluid chromatography system PerkinElmer® Flexar UHPLC connected to a LC/MS PerkinElmer® 5500 QTRAP model detector allows the analysis of different compounds at low concentrations (e.g. pesticides, contaminant, mycotoxin, dopant substances, drugs). The technique combines the separation power of UHPLC and the MS capacity of obtaining information about the mass and structure of the analytes. The mass spectrometer separates ions in gas phase based on m/z (load/mass). The chromatographical separation was performed using a Perkin Elmer Brownlee Analytic DB AQ C18 (1,9 µm 100x2,1 mm) column or an equivalent with elution in gradient, debit 400 µL/min, temperature of the column 40°C, injecting volume 5µL.

The method developed detected the corresponding drops for the two compounds CBD and CBG. The calibration curve was outlined in the interval 10 - 100 ng / mL. The detection limit at the level of 3, 12 ng / mL was validated. The preparation of the specimens eliminates the use of chloroform, which was used regularly in the analysis of cannabinoids, decreasing the costs of materials, using more ecological solvents and improving the safety of the laboratory.

***Table 2.*** *Exact quantification of CBD for the specimen of hemp oil*

| **Product statement** | **CBD content mg/mL** |
|---|---|
| CBD oil 13.5 mg/mL | 3.194 |
| Ozonated hemp oil with 2.5% CBD and terpene oil | 2.250 |
| CBD oil 4 mg/drop | 123.525 |

In the research literature it is widely reported that CBD coelutions with a CBG related cannabinoid but their molecular weights are different [1], [10]. For this reason, the analytic result UHPLC-PDA was confirmed with a MS complementary technique. This analytical method may be used for different applications, for instance for the quantitative and qualitative control of the CBD oil by a selective, simple and fast method.

The content of CBD of the commercial specimens analyzed in this study is not clearly specified by the manufacturer. The analysis of the three specimens of hemp oil revealed the real concentration of CBD from the specimens, highlighting the necessity of this type of analytical method.

## CONCLUSION

The hemp oil from *Cannabis sativa* L. is a natural source rich in important nutritive substances, not only polyunsaturated fat acids and proteins, but also terpenes and cannabinoids, which contribute to the therapeutical benefits of the oil with CBD. Therefore, it is important to exist an analytical method for the

determination and quantification of cannabinoids for establishing the exact concentration from the commercial specimens, an interesting subject for the professionals from the pharmaceutical domain.

HPLC-PDA is widely applied in the quantification of cannabinoids, as the approach is a facile one, robust and cheap. Nevertheless, LC-MS / MS is the most versatile among the methods, both regarding the dynamic range, and related to the offer of a real image of the content of CBD of the oils analyzed. The most frequently are used columns with reverse phase (mainly C18 variant or biphenyl) with a solvent of methanol-water containing 0,1% formic acid. The analytical benefits of the triple-quadrupole LC-MS / MS system are sensitivity, selectivity and identification of the mass. As for the analysis of terpenes, UHPLC-PDA is not able to detect most of the terpenes, the connection to MS being compulsory. Flavonoids may be very well analyzed with all the detection methods connected to LC.

Based on the information presented in this study, ideal quantification method of cannabinoids is LC-MS / MS for the cannabinoids using the PerkinElmer system, especially in clinical research. This analytical method may be used for different applications, quantitative and qualitative control of CBD oil by a selective, simple and fast method.

The perspective of the study is to apply these methods to the different pharmaceutical forms, but also to other types of specimens (biological, soil, water, etc.). It is also an interesting alternative for the routine analyses in the criminalistic sciences. The analytical methods easily characterize and quantify CBD in the oils available from the commercial sources for offering a robust instrument for the determination of the potency, safety and quality, with usages both in human medicine and in the veterinary one.

## ACKNOWLEDGEMENTS

We would like to thank the Scient Research Center for Instrumental Analysis, Tâncăbești, 1 Petre Ispirescu Street, 077167, Tâncăbești, Ilfov, Romania for the equipment provided.

## REFERENCES

[1] Turner S.E., Williams C.M., Iversen L., Whalley B.J., Molecular Pharmacology of Phyto cannabinoids, Progress in the Chemistry of Organic Natural Products, Switzerland, 2017, vol.103, pp.61-101;

[2] Lafaye G., Karila L., Blecha L., Benyamina, Cannabis, cannabinoids, and health, Dialogues in clinical neuroscience, France, 2017, vol. 19/issue 3, pp.309–316;

[3] Ibarra-Lecue I., Mollinedo-Gajate I., Meana J.J., Callado L.F., Diez-Alarcia R., Uriguen L., Chronic cannabis promotes pro-hallucinogenic signaling of 5-HT2A receptors through Akt/mTOR pathway, Neuropsychopharmacology , U.S., 2018, vol.43, pp.2028–2035;

[4] Vlad R.A., Hancu G., Ciurba A., Antonoaea P., Rédai E. M., Todoran N., Muntean D. L., Cannabidiol-therapeutic and legal aspects. Die Pharmazie-An International Journal of Pharmaceutical Sciences, Germany, vol.75 /issue 10, pp.463-469, 2020.

[5] Elliott J., DeJean D., Clifford T., Coyle D., Potter B.K., Skidmore B., Alexander C., Repetski A.E., Shukla V., McCoy B., Wells G.A., Cannabis-based products for pediatric epilepsy: A systematic review, Epilepsy., U.K., 2019, vol.60/ issue 1, pp. 6-19;

[6] Lattanzi S., Brigo F., Trinka E., Zaccara G., Cagnetti C., Del Giovane C., Silvestrini M., Efficacy and Safety of Cannabidiol in Epilepsy: A Systematic Review and Meta-Analysis, Drugs, U.S., 2018, vol.78/issue 19, pp. 1791-1804;

[7] Giacoppo S., Bramanti P., Mazzon E., Sativex in the management of multiple sclerosis-related spasticity: An overview of the last decade of clinical evaluation, Multiple Sclerosis and Related Disorders, U.K., 2017, vol.17, pp. 22–31;

[8] Bartner L.R., McGrath S., Rao S., Hyatt L.K., Wittenburg L.A. ,Pharmacokinetics of cannabidiol administered by 3 delivery methods at 2 different dosages to healthy dogs, Canadian journal of veterinary research, Canada, vol.82/issue3, pp.178–183, 2018.

[9] Sekar K., Pack A., Epidiolex as adjunct therapy for treatment of refractory epilepsy: a comprehensive review with a focus on adverse effects, F 1000 Research, U.K., 2019, vol.8 pp.1–8;

[10] Berman P., Futoran K., Lewitus G.M., Mukha D., Benami M., Shlomi T., Meiri D., A new ESI-LC/MS approach for comprehensive metabolic profiling of Phyto cannabinoids in Cannabis, Scientific reports, U.K., 2018, vol.8/ issue 1, p.14280;

[11] Blebea N.M., Costache T., Negreș S., The qualitative and quantitative analysis of CBD in hemp oils by UHPLC with PDA and applications. Scientific Papers: Series D, Animal Science, The International Session of Scientific Communications of the Faculty of Animal Science, Romania, vol. 62/issue 1, pp.138-142, 2019.

[12] Devinsky O., Patel A.D., Cross J.H., Villanueva V., Wirrell E.C., Privitera M., Greenwood S.M., Roberts C., Checketts D., VanLandingham K.E., Zuberi S.M., Effect of Cannabidiol on Drop Seizures in the Lennox-Gastaut Syndrome, The New England journal of medicine, U.K., vol.378/issue 20, pp.1888-1897, 2018.

[13] Chagas M.H., Zuardi A.W., Tumas V., Pena-Pereira M.A., Sobreira E.T., Bergamaschi M.M., dos Santos A.C., Teixeira A.L., Hallak J.E., Crippa J.A., Effects of cannabidiol in the treatment of patients with Parkinson's disease: an exploratory double-blind trial, Journal of psychopharmacology, U.K., vol.28/issue11, pp.1088-1098, 2014.

[14] Hazekamp A., The trouble with CBD oil, Medical cannabis and cannabinoids, Switzerland, vol.1/issue 1, pp.65-72, 2018.

[15] Gamble L.J., Boesch J.M., Frye C.W., Schwark W.S., Mann S., Wolfe L., Brown H., Berthelsen E.S., Wakshlag J.J., Pharmacokinetics, Safety, and Clinical Efficacy of Cannabidiol Treatment in Osteoarthritic Dogs, Frontiers in veterinary science, U.K., 2018, vol.5 p.165;

# OBTAINING NUCLEIC ACID PREPARATIONS AND THEIR HYDROLYSATES FROM BIOMASS OF METHANE-OXIDIZING BACTERIA

**Prof. Dr. Alla A. Krasnoshtanova**[1]
**Elisaveta K. Borovkova**[2]
[1, 2] D. Mendeleev University of Chemical Technology of Russia, Moscow, Russia

## ABSTRACT

Due to the unfavorable environmental, social and economic situation, the need for the treatment of oncological diseases and diseases associated with impaired activity of the immune system is increasing. A lot of these drugs are made on the basis of nucleic acid components, the industrial production of which is practically non-existent in Russia. Therefore, a task of current interest is to develop the basis of the technology for obtaining components of nucleic acids, which can be widely used in medicine as immunomodulatory, wound-healing, antiviral, and diagnostic medicine, as well as for cancer treatment.

Most of the described in literature methods of isolating nucleic acid components from plant, animal and microbial raw materials are based on the use of toxic and expensive organic solvents, that's why it is impossible to apply these methods outside of laboratory conditions. The most promising source of raw materials for nucleic acids is the biomass of microorganisms (yeast and bacteria) from biomass, since the use of such source makes it possible to quickly obtain a large enough amount of biomass, and, consequently, a larger amount of nucleic acids. This allows obtaining DNA in addition to RNA. RNA and DNA substances can be used to obtain nucleosides and nitrogenous bases, which are also widely used in medicine.

The purpose of these studies was to select the conditions for the extraction of RNA and DNA from the biomass of methane-oxidizing bacteria in one technological cycle, as well as to compare the efficiency of alkaline and acid hydrolysis of microbial RNA and DNA. The need for a two-stage extraction of nucleic acids from the biomass of methane-oxidizing bacteria in order to separately extract RNA and DNA was Substantiated. It was ascertained that at the first stage of extraction at a temperature of 90 ° C, pH 9.0 for 90 min, at least 85% of RNA is extracted. After the separation of the extract by centrifugation, the partially denuclearized biomass must be re-processed under the same conditions in order to extract DNA by at least 83%. The modes of concentration of RNA and DNA solutions by ultrafiltration were selected. It was found that in order to achieve effective deposition of nucleic acids at the isoelectric point, the concentration of the RNA solution must be carried out on the UPM-10 membrane at the concentration degree of 7, and the DNA solution on the UPM-100 membrane at the concentration degree 6. The dynamics of decomposition of nucleic-protein complexes in the medium of monoammonium phosphate was investigated. It was shown that the

transition of NA into solution by at least 80% is achieved at a monoammonium phosphate concentration of 1.7 M, a temperature of 55 ° C for 90 min. The use of 5-fold washing of oligonucleotide substances with acidified water (pH 2.0) to remove excess mineral impurities was substantiated. A comparative assessment of acid and alkaline hydrolysis of RNA and DNA was carried out in order to obtain derivatives of nucleic acids.

***Keywords:*** *methane-oxidizing bacteria, RNA, DNA, acid hydrolysis, alkaline hydrolysis*

## INTRODUCTION

Due to the unfavorable environmental, social and economic situation, the need for the treatment of oncological diseases and diseases associated with impaired activity of the immune system is increasing. A lot of these drugs are made on the basis of nucleic acid components. DNA and RNA preparations of various origins, as well as their derivatives are promising therapeutic and immunomodulatory agents and can be used in food, cosmetic and other industries [1], [2].

In the cell nucleic acids are in a complex with proteins and lipoproteins. Therefore, the complexity of the isolation of nucleic acids lies in separating them from the above impurities, as well as their high degree of destruction under the influence of external factors. In this regard, the choice of reagents for DNA isolation, which inhibit or inactivate cellular nucleases, but leave the native structure of nucleic acids intact, is of great importance [3], [4].

A common method for the isolation of nucleic acids is the destruction of cells of microorganisms and animal tissues. In laboratory conditions, cell disintegration is carried out using liquid nitrogen or mechanical grinding with silicon oxide (or aluminum oxide). This step can be realized directly in a lysis buffer containing nucleases and proteases [5].

After lysis, there are two possible approaches to purifying the target DNA. The first involves processing a DNA solution by extraction with an organic solvent (phenol, chloroform), followed by precipitation of DNA with alcohols and dissolution in water and Tris-EDTA buffer. According to the second approach, differential sorption of DNA is carried out on a solid support (most often, silica gel), after which the sorbent is washed with organic solvents, and then the DNA is washed off with water or Tris-EDTA buffer.

Each of these approaches has advantages and disadvantages. In the first case, it is possible to obtain high molecular weight DNA (more than 15000 nucleotide pairs), however, significant DNA losses are possible, and the resulting preparations contain a significant amount of impurities. In the second case, it is possible to obtain highly purified preparations, however, the isolated DNA turns out to be of low molecular weight.

Known methods for producing RNA from yeast allow the isolation of low-polymer RNA, for example [6], which is used in medicine in the treatment of a wide range of diseases: from viral infections to memory disorders [7].

Work [8] describes a method for obtaining high-polymer RNA from yeast by suspending it in an aqueous 0.3-1.2 M solution of 2-ethylhexanoic acid containing 0.1-0.5 M NaCl at 92-98°C. The disadvantage of this method is the use of a synthetic, expensive and highly toxic lytic agent - 2-ethylhexanoic acid, which requires deep purification of the final product, as a result of which this method is not economical and practically not scalable.

In the article [9], an attempt was made to replace 2-ethylhexanoic acid with a large-tonnage food reagent, which significantly reduces the cost of the process since it makes it practically waste-free and easily scalable.

In the research [10] it is proposed to incubate biological material with pre-treated 3.5-7% solution of hydrofluoric acid for 2-6 hours with finely dispersed meshed glass in a buffer solution containing chaotropic agent, which makes it possible to reduce process duration, increase RNA yield and ensure isolation of both low-molecular and high-molecular RNA fractions.

In a number of works it is proposed to isolate RNA from the blood by sorption on ion-exchange resins in quaternary ammonium form [11], cationite in $H^+$-form [12], from cells of microorganisms, plant and animal tissues by treatment with acid reagents, sorption on cationite in combination with treatment with proteases, desorption of nucleic acids with ionites with buffer solutions [13].

Most of the described in literature methods of isolating nucleic acid components from plant, animal and microbial raw materials are based on the use of toxic and expensive organic solvents, that's why it is impossible to apply these methods outside of laboratory conditions.

The most promising source of raw materials for nucleic acids is the biomass of microorganisms (yeast and bacteria) from biomass, since the use of such source makes it possible to quickly obtain a large enough amount of biomass, and, consequently, a larger amount of nucleic acids. This allows obtaining DNA in addition to RNA. RNA and DNA substances can be used to obtain nucleosides and nitrogenous bases, which are also widely used in medicine.

The purpose of these studies was to select the conditions for the isolation of RNA and DNA from the biomass of methane-oxidizing bacteria in one technological cycle, as well as to compare the effectiveness of alkaline and acidic hydrolysis of microbial RNA and DNA.

## MATERIALS AND METHODS

The object of the study was condensed biomass of methanoacidating bacteria Methylococcus capsulatus, containing 20% dry substances, 10% nucleic acids (including 13.5% DNA), 65% raw protein. The determination of total nitrogen was carried out by the Kjeldahl micrometode. The phosphate ion concentration was determined by the Fiske-Subarrow method. The concentration of nucleic components was determined by Spirin and the concentration of DNA by Dische.

The process of concentrating nucleic acids solutions was carried out on a laboratory ultrafiltration apparatus with a volume of 1000 ml, using membranes of the UPM type (polysulfonamide membranes).

In the analysis of the nucleic acids hydrolysates, the high molecular weight fraction was separated by precipitation with 50% trichloroacetic acid. The low molecular weight fraction was analyzed by the Spirin method.

## RESULTS AND DISCUSSION

Several methods of extracting nucleic components from the biomass of bacteria are known from the literature, but they are often multistage [3] and involve the use of organic solvents, for example, phenol and chloroform.

The most promising is the use of an aqueous alkali solution as an extractant. In these studies, it was proposed to extract nucleic acids from a 20% suspension of biomass of Methylococcus capsulatus bacteria at a pH of 9 and a temperature of 90 ° C. Extraction was carried out for 4 hours. At certain time intervals, suspension samples were taken, biomass was separated by centrifugation at 6000 rpm, and the concentration of total nucleic components in extracts was determined by the Spirin method, DNA by the Dishe method. On the basis of the obtained data, the degree of extraction of total nucleic acids and DNA was determined. The obtained results are shown in Fig. 1, from which it follows that the extraction time providing the extraction of total nucleic acids by not less than 94% should not exceed 180 minutes (3 hours). It should be noted that primarily RNA having a lower molecular weight is extracted from microbial cells, and DNA extraction begins only in the 90th minute of the process.

Thus, it was found that in order to achieve at least 94% recovery of nucleic acids in the form of protein-nucleic complexes, extraction should be carried out at a temperature of 90°C, pH 9.0, extraction time - 3 hours. At the same time, the degree of DNA extraction is 97.6%, and RNA is 94.1%.

According to previous studies, these concentrations of nucleic acids do not allow their effective precipitation at the isoelectric point, therefore, the preliminary concentration of the obtained extract by ultrafiltration is required. To separate the mixture of DNA-protein and RNA-protein complexes, the effectiveness of the ultrafiltration method was evaluated using membranes with cutoff molecular weights of 100 and 10 kDa.

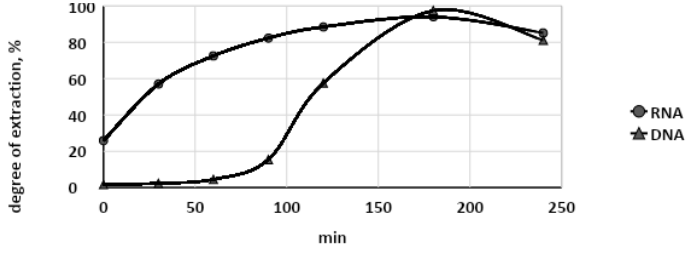


***Fig. 1.*** *Dynamics of extraction of total nucleic acids and DNA from biomass of methanoxic bacteria Methylococcus capsulatus*

Initially, the nucleic extract was concentrated on the membrane UPM-100 to concentrate the DNA-protein complex and reduce the viscosity of the resulting filtrate. To evaluate the effectiveness of the ultrafiltration process, differential and integral selectivity and specific productivity were determined. Figure 2 shows the dependence of the specific productivity of the UPM-100 membrane on the concentration of nucleic acids in the concentrate.

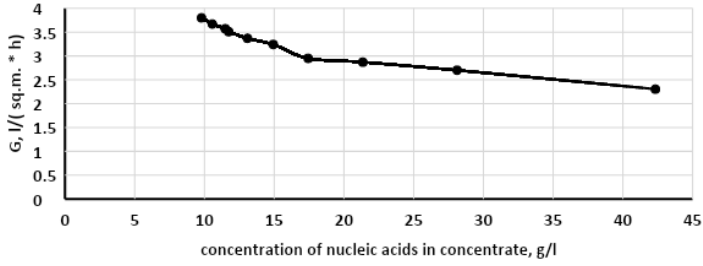


***Fig. 2.*** *Dependence of specific productivity of UPM-100 membrane on the concentration of nucleic acids in concentrate*

From the above data, it follows that a decrease in specific productivity of 1.5 times is observed only at a concentration of total nucleic acids above 30 g/l, which is quite sufficient for subsequent effective precipitation of nucleic acids.

Figure 3 shows the differential selectivity relationships of membrane UPM-100 for nucleic components (2) and for DNA (1). From the data obtained, it can be seen that the values of selectivity for nucleic acids and DNA are close to each other, that is, there is no enrichment of the DNA concentrate. Therefore, a single-step extraction is not feasible, and a 2-step extraction option was studied in the next stage of the studies.

Sequential extraction of nucleic acids from the biomass of methane-oxidizing bacteria was carried out as follows. At the first stage carried out extraction of RNA at a temperature of 90 wasps within 90 min. On the expiration of the specified time biomass was separated centrifugation at 6000 rpm within 30 min. The received extract was directed to an ultraconcentration stage on UPM-10 membrane. The partially denucleinized biomass was suspended in distilled water to obtain a 10% suspension. DNA extraction was carried out at 90 ° C, pH 9.0 for 90 minutes, taking suspension samples at predetermined intervals at which the DNA concentration was determined by Dishe's method. The dynamics of DNA extraction are shown in Figure 4.

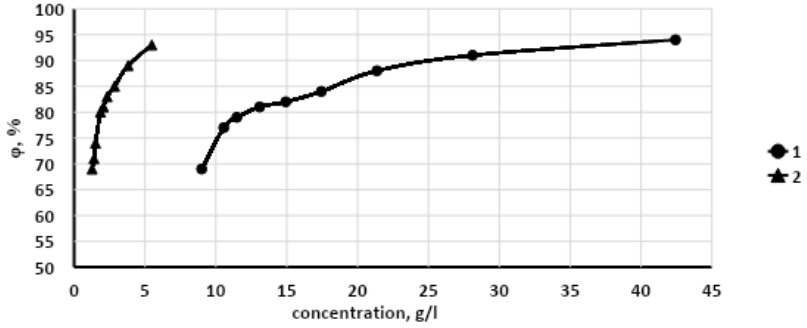


***Fig. 3.*** *Dependence of differential selectivity of the membrane UPM-100 on DNA (1) and nucleic acids (2) on the concentration of nucleic acids and DNA in the concentrate.*

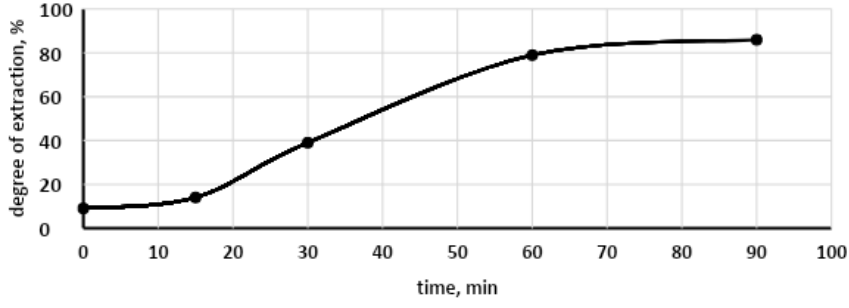


***Fig. 4.*** *Dynamics of DNA extraction from biomass of methane-oxidizing bacteria in 2-stage extraction*

It follows from the figure that in 90 minutes of extraction, a DNA extraction rate of at least 85% is achieved. A further increase in extraction time is not advisable, as this leads to DNA destruction.

Thus, an RNA-containing extract (RNA concentration 8.0 g/l) and a DNA-containing extract (DNA concentration 1.4 g/l) were obtained. The extracts obtained were further concentrated by ultrafiltration on membranes UPM-10 and UPM-100, respectively.

The concentration of the RNA-containing extract was carried out on the membrane of the UPM-10, and the DNA-containing extract on the membrane of the UPM-100.

Similar to the ultra concentration studies described above, specific performance, integral and differential selectivity were determined for the concentration process in both cases. Figures 5 and 6 show the dependencies of specific performance and differential selectivity on the concentration of nucleic acids in the concentrate. From the presented data, it can be seen that a significant decrease in the performance of the ultrafiltration plant is observed at an RNA

concentration in the concentrate of more than 23 g/l, which allows concentrating the RNA-containing extract by at least 6 times. The RNA integral selectivity is not less than 72%.

These data indicate that the DNA concentration process is characterized by high differential selectivity (above 86%), as well as a decrease in the performance of the ultrafiltration device by no more than 1.5 times, which allows concentrating the DNA extract by no less than 6 times.

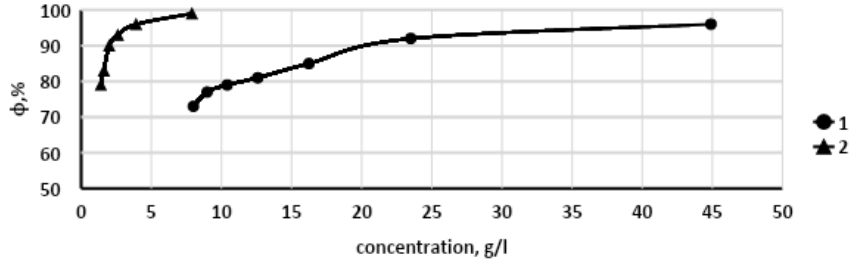


***Fig. 5.*** *Dependence of differential selectivity of membrane UPM-100 on the concentration of DNA (1) and membrane UPM-10 on the concentration of RNA (2) in concentrate*

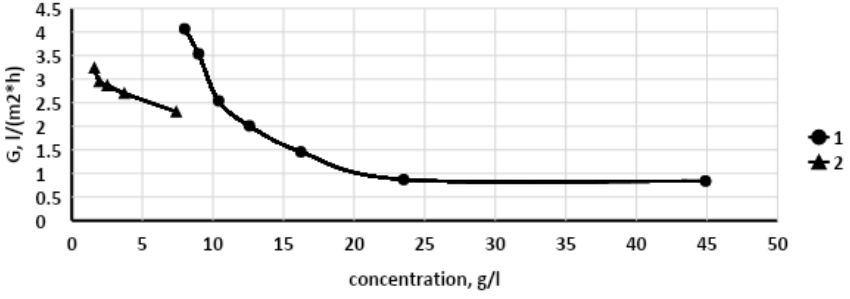


***Fig. 6.*** *Dependence of specific productivity of membrane UPM-100 on the concentration of DNA (1) and membrane UPM-10 on the concentration of RNA (2) in concentrate*

As a result of the ultra-concentration step, an RNA-containing concentrate and a DNA-containing concentrate were obtained, from which the RNA-protein and DNA-protein complexes were precipitated at an isoelectric point.

To this end, the resulting concentrates were cooled to 4-6 ° C, after which the pH of these solutions was set to 1.8-2.0 using a concentrated hydrochloric acid solution. The precipitated DNA-protein and RNA-protein complexes were separated by centrifugation at 6000 rpm for 15 minutes. From the obtained data, the degree of precipitation of nucleoproteins was calculated, the values of which were: for the DNA-protein complex - 80%; for the RNA-protein complex - 83%.

To decompose the protein-nucleic complex, a solution of diammonium phosphate was used, which interacts with the protein of the intracellular protein-nucleic complex and allows the release of nucleic acids in free form. In this case, the protein-phosphate complex precipitates, and nucleic acids pass into solution. The process was carried out at a temperature of 60 ° C, concentration of mmonium phosphate 2.0 mol/l, pH of medium 6.0-6.5. Samples of the suspension were collected periodically, the precipitate was separated by centrifugation at 6000 rpm, and the concentration of RNA in the supernatant was determined by Spirin and DNA by Dishe's method. From the obtained data, the proportion of dissolved nucleic acids from their content in the initial protein-nucleic complexes was determined (Figure 7).

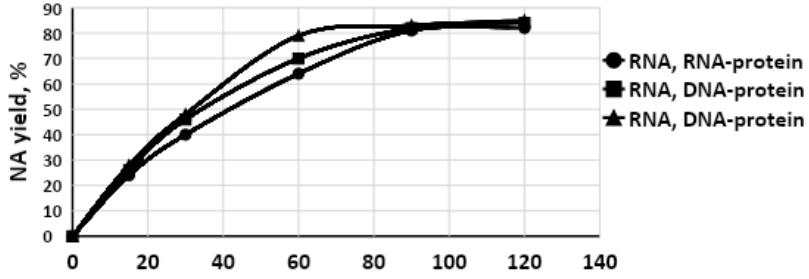


***Fig. 7.*** *Dynamics of nucleic acid dissolution in monoammonium phosphate solution*

From Figure 7 it follows that for both protein-nucleic complexes in 90 minutes, nucleic acid yield to the solution at the level of 80-85% is achieved. Therefore, the optimal processing time of the protein nucleic complexes was assumed to be 90 minutes.

Further, the precipitate of the protein-phosphate complex was separated by filtration, and RNA and DNA were precipitated from the obtained solutions in the same manner as described above. To purify the RNA and DNA precipitates from phosphate ions, they were washed with water acidified to pH 2.0, treated with 96% ethyl alcohol solution and dried at 50 ° C. The RNA preparation contained at least 85% of the main substance, and the DNA preparation contained at least 76%.

As previously noted, RNA and DNA preparations are generally the starting materials for the production of nucleosides and nitrogenous bases. Acid and alkaline hydrolysis are used for their production. Therefore, at the next stage of work, the effectiveness of these hydrolysis methods was compared. from which it follows that both in the case of RNA and DNA, alcaline hydrolysis proceeds with a higher yield under milder conditions.

***Table 2.*** *Effectiveness of acid and alkaline hydrolysis of RNA and DNA preparations*

| Preparation | Hydrolysis conditions | | | Hydrolysis products yield, % |
|---|---|---|---|---|
| | Temperature, °C | Hydrolyzing agent | Concentration of hydrolyzing agent, % | |
| RNA | 90 | Sodium hydroxide | 10 | 14,4 |
| RNA | 115 | Sodium hydroxide | 10 | 20,6 |
| RNA | 90 | Sodium hydroxide | 20 | 20,6 |
| RNA | 115 | Sodium hydroxide | 20 | 13,4 |
| RNA | 90 | Hydrochloric acid | 36 | 9,5 |
| RNA | 115 | Hydrochloric acid | 36 | 11,6 |
| DNA | 90 | Sodium hydroxide | 10 | 27,8 |
| DNA | 115 | Sodium hydroxide | 10 | 28,0 |
| DNA | 90 | Sodium hydroxide | 20 | 27,3 |
| DNA | 115 | Sodium hydroxide | 20 | 25,4 |
| DNA | 90 | Hydrochloric acid | 36 | 27,9 |
| DNA | 115 | Hydrochloric acid | 36 | 25,2 |

## CONCLUSION

The need for two-step extraction of nucleic acids from the biomass of methane-oxidizing bacteria in order to separately extract RNA and DNA is justified. It was found that at the first stage of extraction at a temperature of 90°C, pH 9.0 during 90 minutes, at least 85% RNA is recovered. When partially denucleinized biomass is reprocessed under the same conditions, DNA is extracted by at least 83%.

It has been found that in order to achieve efficient precipitation of nucleic acids at an isoelectric point, concentration of the RNA solution must be carried out on the membrane UPM-10 at a concentration degree of 7, and the DNA solution on the membrane UPM-100 at a concentration degree of 6.

A study of the degradation dynamics of protein-nucleic complexes in the medium of monoammonium phosphate showed that the transition of nucleic acids into a solution of at least 80% is achieved at a concentration of monoammonium phosphate of 1.7 M, a temperature of 55°C for 90 minutes.

It has been established that the hydrolysis of both RNA and DNA is expediently carried out using sodium hedroxide with a concentration of 10% at a temperature of 120° C.

## REFERENCES

[1] Vanyushkin B. F. A spontaneous journalist's gaze at the world of DNA (nucleotide composition, sequences, methylation), Biochemistry, vol. 72./issue 12. PP. 1583-1593, 2007.

[2] Lee Y.K., Kim H.W., Liu C.L., Lee H.K. A simple method for DNA extraction from marine bacteria that produce extracellular materials, Journal of Microbiological Methods. vol. 52/issue 2. P. 245-250. 2003.

[3] In Woo Lee, Han Oh Park. Method for obtaining DNA from fish spermatogonium. Patent US 6759532. 2002.

[4] Tsyrenov V. Zh., Gomboeva S. V., Zakharova M. A. Obtaining low molecular weight DNA from fish milk of the Baikal region, Irkutsk State University Bulletin. Series: Biology. Ecology. vol. 10. PP.3-10. 2014.

[5] Laktionov P.P., Tamkovich S.N., Simonov P.A., Rykova E.Yu., Vlasov V.V. Method for isolating DNA from microorganisms. RU Patent No 2232768.2004.

[6] Yamkovaya TV, Kuzovkova EV, Zheleznova Yu. P., Zagrebel'nyi SN, Panin LE, Yamkova VI A method for obtaining high-polymer RNA from yeast. RF patent No 2392329.2010.

[7] Yamkovaya TV, Vansovskaya IV, Zagrebelny SN, Panin LE, Yamkovaya VI Method of obtaining high-polymer RNA from waste brewer's yeast. RU patent No 2435862.2011.

[8] Laktionov P.P., Tamkovich S.N., Simonov P.A., Rykova E.Yu. Nucleic acid isolation method. RU patent No 2232810.2004.

[9] Sakurai, Toshinari, Hitachinakashi, Kuno, Norihito, Chiyodaku, Uchida, Kenko Chiyodaku, Yokobayashi, Toshiaki. RNA extraction method, RNA extraction reagent, and method for analyzing biological materials. Japan patent EP 1 529 841. 2005.

[10] Yamkovaya TV, Zagrebelny SN, Panin LE, Yamkovaya VI. A method of obtaining a protein-free biologically active preparation of high-polymer RNA from dry baker's yeast Saccharomyces cerevisiae, RU Patent No. 2510854.2014.

[11] Kyoko Kojima, Hino, Satoshi Ozawa, Musashino. Method for isolating and purifying nucleic acids. Patent US No 2002/0192667. 2002.

[12] Khripko Yu. I., Smirnov PN, Bateneva NV Method of isolation of nucleic acids. RU patent No 2584346.2015.

[13] Gabriele Christoffel. Method of isolating purified RNA, Patent US N9487550. 2016.

# PRODUCTION OF ANTIBODIES FROM POULTRY YOLK (IgY) AND INVESTIGATION OF THEIR IMMUNOCHEMICAL PROPERTIES

**Prof. Dr. Alla A. Krasnoshtanova**[1]
**Alesya N. Yudina**[2]
[1, 2] D. Mendeleev University of Chemical Technology of Russia, Moscow, Russia

## ABSTRACT

A particularly important aspect of immunology is to develop non-invasive methods of obtaining antibodies which could be a great alternative to traditional ones that based on the harmful procedure of isolation of immunoglobulins from animal blood sera. That's why the extraction of antibodies from poultry egg yolks (IgY) is the most promising. Due to the fact of variation of IgY structural features that determine the definite immunochemical properties, yolk antibodies in comparison with mammalian immunoglobulins (IgG) does not interact with rheumatoid factor (Rf), contribute to the activation of the complement system, bind to the Fc-receptor (FcR), and also has weak cross-reactivity, which confirms the possibility of their widespread use in medicine and food. Also the presence of phylogenetic distance between chickens and mammalians guarantees immune response against conservative mammalian protein molecules which is highly important for the creation of new generation test systems.

The aim of this work is to develop a selective method of producing high-purity immunoglobulin Y preparations from the yolk of chicken eggs.

There were adopted selective conditions of isolation of IgY under spontaneous thawing procedure at the room temperature of firstly frozen yolk solution in a sodium-phosphate buffer mixed with water (pH 5.0) in a ratio of 1:6, which leads to receiving a water-soluble fraction further precipitated with the sodium chloride at a concentration of 10% of the solution mass and subsequently concentrated using ultrafiltration with membrane UAM-10, that allows achieving the content of IgY not less than 95% per dry substance in immunoglobulin fraction. It is possible to produce a protein fraction with a protein content of at least 9 g/l.

The purity of the immunoglobulin fraction was verified using polyacrylamide gel electrophoresis. The presence of a light chain in the IgY solution was proved to be a low-molecular compound using the method of gel-filtration-chromatography. The immunological activity of IgY was studied with respect to bovine serum albumin (BSA) as an antigen. The enzymatic resistance of IgY against proteolytic enzymes was tested in area of the gastrointestinal tract.

***Keywords:*** *egg yolk, IgY, immune response, gastrointestinal enzymes, ultrafiltration*

## INTRODUCTION

At present time, the development of a new generation of pharmaceuticals based on antibodies' compounds is accelerating. The possibility of their passive administration and the achievement of a rapid therapeutic effect are the main advantages of such drugs.

Egg yolk is a rich source of immunoglobulins(Ig). The total content of gaining Ig is over 100 mg per chicken egg [1], [2]. Most of the yolk immunoglobulins belong to IgY class. Other classes such as IgA and IgM are also antibody components of the yolk but in smaller quantities.

IgY is a systemic immunoglobulin with a molecular weight of approximately 170 kDa. It consists of two heavy (H) and two light (L) chains connected by disulfide bonds and forming a monomeric link (H2L2). The molecular weights of the heavy and light chains are 71 kDa and 26 kDa, respectively [1], [3].

It is known that the variable part of the H-chain encodes a region of the DNA molecule that has variable (V), connective (J), and diversity (D) segments. The rearrangement of these segments doesn't lead to the phenomenon of gene hyperconversion, because of the absence of any development of IgY immunogenetic diversity during the process.

IgY is currently being considered as a promising substitution for mammalian immunoglobulins (IgG). The greatest interest is focused on the variation of IgY structural features which determine the characteristic immunochemical properties. Due to the absence of the hinge region of IgG, chicken antibodies (IgY) are less exposed to proteolytic degradation and fragmentation. There's a limited flexibility zone based on proline and glycine amino acid residues instead of the flexibility zone of the hinge region in IgY [4]. Moreover, IgY does not interact with the Fc-receptor, which is responsible for the implementation of numerous effector functions; they are not able to activate the human complement cascades. Also IgY do not have cross-reactivity and does not bind to the rheumatoid factor (Rf-factor) [5].

Purified yolk antibodies (IgY) are able to conserve their activity for six months at room temperature. In addition, affine-purified and biotinylated IgY retains high activity after five years of storage at 4°C [6].

The technology of production of IgY from the egg yolk requires a specific treatment that provides the isolation of immunoglobulins from the lipophilic matrix of the yolk. This is achievable by a two-step purification procedure of IgY from the yolks. The first stage is the separation of the water- soluble fraction (WF) containing IgY from lipids and lipoproteins. The second stage is based on the segregation of IgY out of the water-soluble protein fraction [7]. To remove the lipophilic components of the yolk, the crude extract of immunoglobulins is precipitated under the action of various reagents (polyethylene glycol, dextran sulfate, alginate, caprylic acid, organic solvents). After that the lipid aggregates could be removed by centrifugation, filtration, diluting of the yolk solution or even by freezing-thawing procedure of the diluted yolk solution. In the second stage, the pure IgY fraction should be prepared from the crude aqueous extract of immunoglobulin. Yolk antibodies are firstly salted out and then purified by chromatography

(exclusive, ion exchange, thiophilic, affinity chromatography). In some cases it's necessary to carry out repeated precipitation of immunoglobulins. Depending on the using purification method the degree of purity and the total yield of the final immunoglobulin preparation are in rang of 85-98% and 1,0-9,8 mg/ml, respectively [7]. These methods for the isolation of IgY are promising for their implementation in technologies for the development of medicines, food additives, functional nutrition, as well as the creation of modern test systems for the early diagnosis and prevention of many diseases, which will reduce the usage of non-invasive therapies on animals aimed to obtain mammalian antibodies (IgG) [8], [9]. That's why the creation of high-quality medicines is required to carry out high degree purification, which guarantees the exact composition of the immunoglobulin fraction.

The aim of this work is directed to the development of a method for obtaining high-purity immunoglobulin Y preparations from the poultry yolk.

## MATERIALS AND METHODS

Poultry eggs of Public Joint Stock Company «Snezhka» plant production were used as the object of the study. The eggs have next characteristics: humidity is about 74%; the fat content of the yolk is 32.6%; the content of phospholipids in egg yolk is 29.6%; the crude protein contents in egg protein fraction and in the yolk are 10.6% and 16.6%, respectively.

Determination of crude protein content was performed by the Kjeldahl method, the concentration of protein content in the solution was measured using the biuret method. The determination of the molecular weight of the protein and the degree of its purification was evaluated by gel-filtration-chromatography and polyacrylamide gel electrophoresis in denaturing conditions.

The process of concentration of IgY solutions was performed using ultrafiltration with UAM-type membranes (ultrafiltration acetate cellulose membranes) with molecular weights cut-off of 100 and 10 kDa.

The immunological activity of IgY was investigated using the method of precipitation antibodies with antigen. Bovine serum albumin (BSA) was chosen as an antigen. BSA was prepared in aqueous solution of distilled water with a concentration of 1 mg/ml. The turbidity of the solution after adding equal aliquots of antibodies and antigen preparations was checked against the control sample at a wavelength of 440 nm in cuvettes with a light-absorbing layer thickness of 10 mm.

The enzymatic resistance of IgY against proteolytic enzymes of the gastrointestinal tract was studied using the parallel profile technique.

To build the parallel profile of the gastrointestinal tract area, aliquots of IgY solution and definite enzyme solution were added to preliminarily prepared sodium-phosphate buffer salt (PBS) solutions and hydrochloric acid (HCl) solution with required value of pH the way shown on Figure 1.

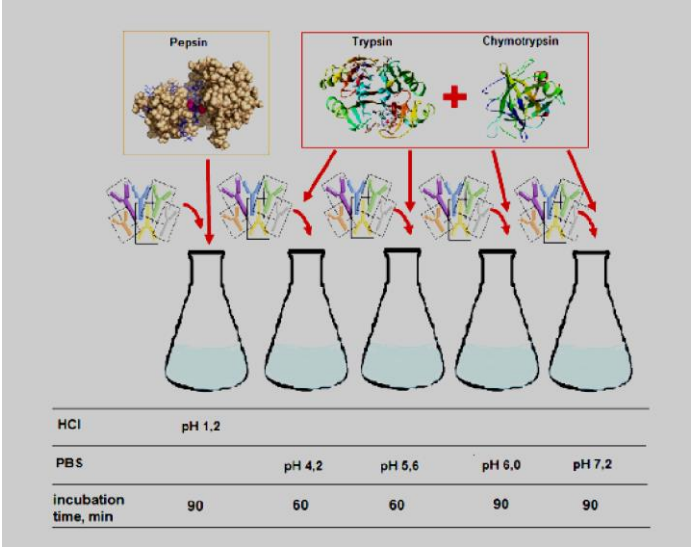


***Fig. 1.*** *Parallel profile of gastrointestinal tract area.*

Consequently, prepared solutions were incubated at 37-40$^0$C being periodically stirred during 60 or 90 minutes depending on gastrointestinal tract section. The dynamics of IgY destruction were constructed by taking samples every 15 minutes from the solutions. All of the above pH values correspond to the acidity values of the human small intestine.

Pepsin was transformed in solution with concentration of 0.1 mass %. According to the literature data average activity of trypsin and chymotrypsin in the human gastrointestinal tract is 15 U/l [10].

Activities of enzymes were defined using the modified Anson method. Degree of IgY destruction was mesuared using the modified Lowry method.

## RESULTS AND DISCUSSION

During the previously conducted methods of isolation of IgY, based on precipitation process to segregate proteins and residual fats from the native and ethanol-treated yolk. However, these methods did not allow to obtain a final product with a protein content of more than 54%.

At the next stage of work, after separating the eggs into white and yolk, the yolk was transferred to filter paper for thorough removal of the protein trace. The yolk-shell was additionally decanted.

Then the yolk mass was mixed with an equivalent volume of sodium-phosphate buffer salt (PBS) solution with a pH of 7.4 using a magnetic stirrer to achieve homogeneity. Aliquots were taken from the prepared solution for subsequent dilutions in tap water adjusted to pH 5.0 using 0.2 N HCl in 6 and 8 times [7]. The mixtures were frozen at temperature of -20$^0$C, and then subjected to spontaneous thawing through a paper filter at room temperature. A transparent protein solution,

called a water-soluble fraction (WF), was obtained after filtration. The protein content in obtained filtrates, depending on the initial dilution of the yolk mass, are shown in Table 1.

***Table 1.*** *Effect of the dilution multiplicity on the protein content in the filtrates*

| № | Dilution multiplicity | Protein content in the filtrates, g/l |
|---|---|---|
| 1 | 6 | 7.2 |
| 2 | 8 | 6.1 |

Based on the small difference between the obtained concentrations in both dilutions, it was not possible to determine the unambiguous dilution multiplicity of the yolk suspension. Therefore, further fractionation of the proteins contained in the WF was carried out by means of specific precipitation with sodium chloride salts added to filtrate solutions in concentrations equal to 5 and 10 mass %. The freshly prepared fractions were kept for a day at 4℃ to induce complexation processes. Filtration through a folded filter was chosen as the primary purification of the target product against ballast proteins and dissolved salts. The protein content of the obtained filtrates was determined using the biuret method. The experimental results are shown in Table 2.

***Table 2.*** *Effect of the degree of dilution of the yolk mass and the content of sodium chloride on the protein yield*

| № | Dilution multiplicity | Content of NaCl, mass % | Protein content , g/l |
|---|---|---|---|
| 1 | 6 | 5 | 8.1 |
| | | 10 | 9.7 |
| 2 | 8 | 5 | 10.3 |
| | | 10 | 10.1 |

Based on the results obtained, it can be concluded that the highest concentration of protein is observed in the filtrate at a dilution ratio of 8 and at a concentration of sodium chloride of 5 mass %.

After that the high-molecular fraction containing immunoglobulin Y was washed from residual salts and ballast proteins using ultrafiltration (UF) on the UAM – 100 membrane. The calculated values of the protein content in solutions after UF and the integral selectivity for protein are presented in Table 3. Consequently, the best dilution of the yolk mass at which the highest value of the index φ is observed, corresponds to 6, and the concentration of the added reagent (NaCl) is 10 mass %.

***Table 3.*** *Effect of dilution multiplicity of the yolk mass and the concentration of sodium chloride on the efficiency of ultrafiltration*

| № | Dilution multiplicity | Concentration of NaCl, mass % | Protein content after cocentration, g/l | Integral selectivity φ, % |
|---|---|---|---|---|
| 1 | 6 | 5 | 3.58 | 56 |
| | | 10 | 3.26 | 66 |
| 2 | 8 | 5 | 4.49 | 56 |
| | | 10 | 3.82 | 62 |

The dilution multiplicity equal to 8 was unsuccessful due to the presence of a strong opalescent effect in the water-soluble fraction, which indicates an incompleted separation of protein and lipid fractions.

According to the literature data, purified yolk antibodies (IgY) are able to maintain their activity for 6 months at room temperature. In addition, affine-purified and biotinylated IgY retains high activity after five years of storage at 4°C [10].

In order to confirm the efficiency of the method for isolating IgY developed at the previous stage of the study, it was advisable to evaluate the fractional composition of the obtained fraction using polyacrylamide gel electrophoresis in denaturing conditions.

During the analysis, the bands corresponding to the molecular weights of the H - and L-chains of IgY were identified. The electrophoresis data is shown on Figure 2.

Electrophoresis data show that the two bands correspond to the molecular weights of the light (28 kDa) and heavy (63 kDa) chains of IgY, which coincides with the literature information [11].

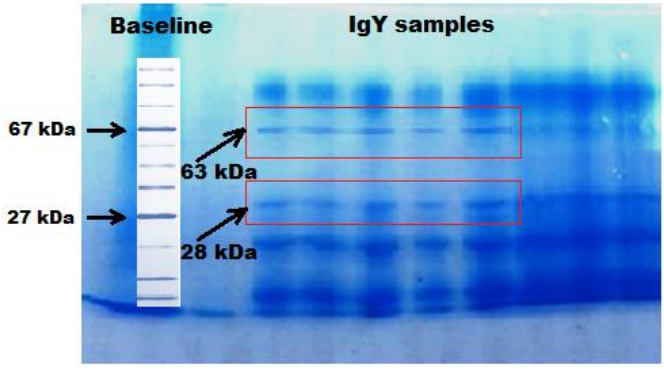


***Fig. 2.*** *Electrophoresis data of IgY*

Since the gel contains several lower bands corresponding to impurity proteins with molecular weights of about 15 kDa, as well as fractions of proteins with molecular weights in the range of 1-100 kDa, it was concluded that the obtained immunoglobulin fraction is not sufficiently pure.

UAM-10 membrane with a lower molecular weight cut-off was tested to purify the target product from low molecular weight fragments by ultrafiltration.

After ultra-concentration, the target product was washed against mineral salts using diafiltration mode. The results of the determination of the best diafiltration multiplicity are shown in Table 4.

The experimental data show that after third diafiltration a solution with a protein content of 12.18 g/l was obtained, which indicates an increase of total protein content in 4.5 times. Based on the content of a dry substance in sample, the

resulting immunoglobulin preparation contained at least 95 mass % of the main substance.

During diafiltration the losses of the target protein is minimal, while the salt concentration in the immunoglobulin concentrate is reduced by 16 times, which allows to recommend the method of ultra-concentration and subsequent diafiltration to obtain purified immunoglobulin Y fraction.

***Table 4.*** *Effect of the diafiltration multiplicity on the physico-chemical parameters of diafiltrates and a protein concentrate*

| Diafiltration multiplicity | Residue content of NaCl in protein concentrate, g/l | Integral selectivity φ, % | Dry substance content of diafiltrate, % | Protein content in concentrate (in respect to dry substance content of diafiltrate), % |
|---|---|---|---|---|
| 1 | 5.0 | 99.8 | 5.6 | 70.4 |
| 2 | 2.5 | 98.8 | 2.4 | 82.5 |
| 3 | 1.3 | 95.3 | 1.6 | 89.9 |
| 4 | 0.6 | 95.8 | 0.8 | 95.0 |

The solution obtained as a result of washing using diafiltration mode on the UAM-10 membrane with protein content of at least 98% of dry weight and with protein concentration of 16.2 g/l was tested using the gel chromatography method for the presence of low-molecular components.

Since the weight of the light chain of immunoglobulins is 26, 000 Da the G-50 sefadex was chosen as the carrier for the separation proteins and peptides, which molecular weights are in the range of 1, 500 – 30, 000 Da.

The result of the protein distribution for fractions is shown on Figure 2.

Based on collected data it follows that the light chain of immunoglobulin is present in the immunoglobulin solution as the only low-molecular compound. According to the calibration graph, its molecular weight is approximately 26 kDa, which corresponds to the literature information.

Consequently, the presence of a light chain and the absence of protein compounds with a lower molecular weight in the IgY solution was proved to be a low-molecular compound using the method of gel-chromatography, which also indicated the effectiveness of chosen purification method by diafiltration.

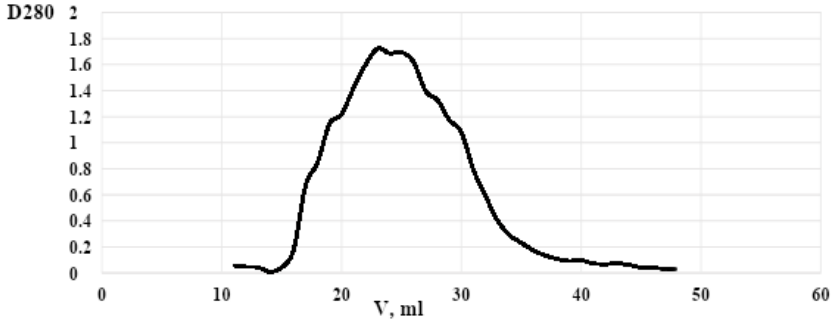


***Fig. 3.*** *Data of gel-chromatography of light chain (L) of IgY*

IgY was proved to be immunologically active by adding bovine serum albumin (BSA) as an antigen. Results of turbidity demonstrated an intensive interaction of precipitants, which confirms the immunochemical properties of the IgY antibodies.

The final experiment was conducted to examine the process of destruction of IgY under the enzymatic conditions of the gastrointestinal tract area. Portions of enzyme preparations with adopted activity values were added into buffer solutions with IgY as previously described on Figure 1 to build the parallel profile of the gastrointestinal tract area. The collected results are shown on Figure 4.

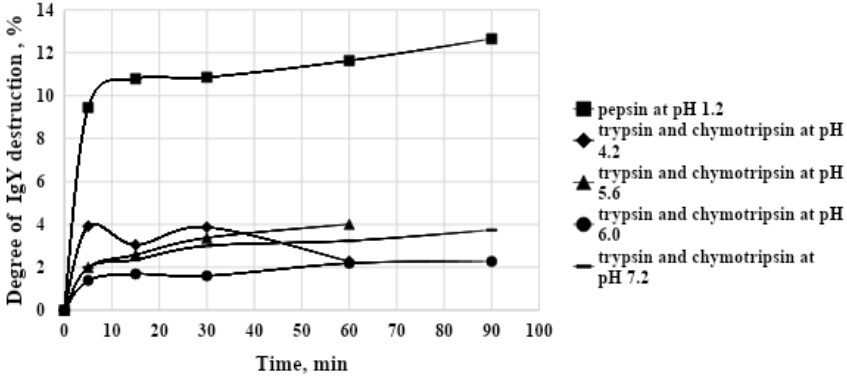


***Fig. 4.*** *Degree of IgY destruction under the enzymatic conditions of the gastrointestinal tract area*

The data of the graph demonstrate brightly expressed degradation of IgY under the influence of pepsin at pH 1.2 and stability of IgY molecule under the influence of trypsin and chymotrypsin, which corresponds to literature [10].

## CONCLUSION

A method for selective isolation of immunoglobulin Y from egg yolk was developed, based on the technology of freezing and spontaneous thawing under conditions that do not cause strong opalescent effect. It is possible to obtain a protein fraction with a protein content at least 9 g/l by diluting the yolk suspension

solution in 6 times and adding sodium chloride as a precipitating agent in amount of 10 mass %.

IgY was purified from low-molecular impurities using diafiltration mode on the UAM-10 membrane, which ensures the protein content at least 98% of dry substance in the preparation.

The purity of the immunoglobulin fraction of the yolk was electrophoretically tested. The presence of a light chain (L) in IgY solution was proved to be a low-molecular compound using method of gel-chromatography.

The immunochemical properties were tested using precipitation with BSA as an antigen.

The construction of a parallel profile of the gastrointestinal tract area proved the destruction of IgY under the influence of pepsin at pH 1.2 and enzymatic resistance of IgY under the influence of trypsin and chymotrypsin at different pH values correspond to the acidity values of the human small intestine.

## REFERENCES

[1] Kaplin V.S., Kaplina O.N. IgY technologies in medicine. Avian yolk antibodies in immunotherapy, International Reviews: Clinical Practice and Health. PP. 59-75. 2016.

[2] Kaplin V.S., Kaplina O.N. IgY technologies. Avian yolk antibodies, Biotechnology, vol.33/issue 2. PP. 29-40. 2013.

[3] Wei Nie, Chao Zhao, Xiaoxiao Guo et. al. Preparation and identification of chicken egg yolk immunoglobulins against human enterovirus 71 for diagnosis of hand-foot-and-mouth disease, Analytical Biochemistry. vol. 573. PP. 44–50. 2019.

[4] E.P.V. Pereira, M.F. van Tilburg, E.O.P.T. Florean, M.I.F. Guedes. Egg yolk antibodies (IgY) and their applications in human and veterinary health: A review. International Immunopharmacology. vol 79. PP. 293-303 2019.

[5] Warr, G.W., Magor, K.E. and Higgins, D.A. (1995). IgY: clues to the origins of modern antibodies, Immunol. Today. vol. 16, PP. 392–398. 1995.

[6] Efremova M.S. Isolation of immunoglobulin Y from blood serum of hens and egg yolk. Mat. conf. "State and prospects for the development of veterinary science in Russia" Veterinary medicine and feeding. vol. 4. PP.34-35. 2013.

[7] P. Hodek, P. Trefil, J. Simunek et. Al. Optimized Protocol of Chicken Antibody (IgY) Purification Providing Electrophoretically Homogenous Preparations, J. Electrochem. Sci. vol.8. P. 113 – 124. 2013.

[8] Yudina A.N., Krasnoshtanova A.A. Selection of the optimal scheme for the isolation of immunoglobulins from the yolk of poultry eggs. "Biochemical Physics", Moscow, PP. 247-250. 2019.

[9] Yudina A.N. A.A. Krasnoshtanova Methods for the isolation of immunoglobulins from the yolk of poultry eggs. Congress materials "Advances in chemistry and chemical technology", D. Mendeleev University of Chemical Technology of Russian. Moscow, vol. 33, PP. 49-50. 2019.

[10] E.P.V. Pereira, M.F. van Tilburg, E.O.P.T. Florean et. al. Egg yolk antibodies (IgY) and their applications in human and veterinary health: a review, International Immunopharmacology. vol. 73. PP. 293-303. 2019.

[11] Hartmann C., Wilhelmson M. The hen's egg yolk: a source of biologically active substances, World's Poultry Sci. J. vol. 57/issue 1. PP. 14–28. 2001.

# QUALITY ASSURANCE IN PHARMACEUTICAL OPERATIONS

**Assist. Prof. Ph.D. Student Blebea Nicoleta Mirela**[1]
[1] Faculty of Pharmacy, Ovidius University of Constanta, Constanta, Romania
[1] Faculty of Pharmacy, University of Medicine and Pharmacy Carol Davila, Bucharest, Romania

## ABSTRACT

The specialized literature does not confer a consensual definition of the quality in the pharmaceutical procedures. Nevertheless, most definitions imply the satisfaction of eth customers' needs. The customers of the pharmaceutical procedures are the patients and also the professional persons from the domain of health that prescribe, issue and administrate medicines. The pharmacist is a professional person who is in direct contact with the patient, being the first professional person to whom the patients address when the affection is a mild one and they need counselling regarding the medication or diagnostic. The more complex the medication of the patient is, the more probable the side effects shall be. The morbidity and mortality may be consequences at the error of medication. The appearance of some medicines increases directly proportional to the errors of prescribing the medication. The quality in using the medication implies the choice of the medicine, the optimization of the compliance of the patient with the treatment, avoiding side effects, assuring the therapeutical objectives. The possibilities of appearing the errors being numerous, it is easy to understand why the assurance and improvement of the quality of the pharmaceutical procedures are important aspects for pharmacists and patients. The present paper has as purpose the qualitative improvement of the pharmaceutical procedures by the help of the pharmacist, thus the pharmacy becoming a supplier of pharmaceutical care of the best quality.

***Keywords:*** *quality assurance, patient care, pharmaceutical operations, pharmacist*

## INTRODUCTION

At the world level, there is the concern for building a new health system adapted to the 21st century. In this regard, the system that assures quality care in pharmacotherapy and assessment of the quality of using the medication represents a guarantee efficient and safe pharmacotherapy for the patient and society. The assurance of quality in pharmaceutical care represents more and more solicited and important concerns for the profession of pharmacist [5].

Quality may seem an ambiguous term, as we can recognize quality when we see it, but the definition of quality is most of the time subjective. In Webster´s Dictionary quality is defined as a level of excellence [11]. This definition helps at analyzing the definitions of the specific quality from the domain of health and supports the idea according to which quality represents continuous excellence.

From the definition given by the Office of Technology Assessment we can assert that in the process of medical care, quality may be measured and used for the care offered to the patients. Although the patients are not always the best arbitrators of the quality of the pharmaceutical care, as they may not know what they want, may not have clear ideas about what they need. Therefore, the pharmacist has the duty to offer services of qualitative care to the patient [1].

***Pharmaceutical services***

The pharmacies take an integral part from the system of health care. The pharmacists are authorized professional persons for assuring pharmaceutical care in health and they develop their activity in conformity with the legislation and regulations in force, as well as the strict and professional rules [12]. This is the vision of the international organizations: World Health Organization (OMS) and the European Commission [15].

The pharmaceutical services represent the assembly of all actions performed by the pharmacist, necessary for warranting the pharmaceutical care of the population. Their purpose is to ensure the best answer to the needs and health problems of the population entirely and of the patient individually. The pharmaceutical services are part of the health system and have as a purpose the improvement of the health condition and increase of life quality of the population [6], [8], [9], [13], [14].

If we focus on the **European Union**, a report of the **Pharmaceutical Group of European Union (PGEU)** classifies the pharmaceutical services according to the frequency of their supply in the member states. Thus, they consider the **release of medicines based on medical prescription as an essential service** performed by the pharmacist, met in all the member states, in some countries being remunerated as a service, in other countries the benefit being related only to the markup (as it is the case of Romania). In the category of the pharmaceutical services frequently supplied, we find the **measuring of the different clinical parameters (**glycemia, body weight, blood pressure, cholesterol), **collecting the expired or not used medicines from the population, programs for giving up smoking, programs for managing different chronic** diseases (diabetes, arterial hypertension, asthma), as well as the night service (on-call). Among the services that begin to take shape in certain states, mainly in countries with developed economy, are found anti-**flu vaccination**, phone or online counseling, as well as the counselling and **monitoring of the patient to the initiation of a new treatment [6], [8], [9], [14].**

The pharmacist is the professional from the domain of health, easily to be approached, who is in direct contact with the patient, being the first professional to whom the patients address when the affection is a mild one and they need counselling related to the medication or diagnostic [1].

***Pharmaceutical care***

Pharmaceutical care consists of the responsible provision of the therapy with medicine for obtaining some clear results that improve or maintain the quality of the patient's life. Pharmaceutical care is a term with international recognition, defined as being the practice in which the pharmacist assumes his responsibility for

the needs of the patient regarding the medicine and is considered responsible for the satisfaction of these needs [1].

Therefore more and more, the task of the pharmacist is to ensure that the treatment with a medicine of a patient is properly indicated, is the most efficient available, the most suitable possible and the most convenient for the patient. By assuming this direct responsibility for the health needs of the patient, the pharmacists may bring a significant contribution to the result of the therapy with medicines and the quality of the patients 'life [2], [6], [8], [9], [14].

***Methods of assuring the quality***

In the domain of pharmacy, the raw materials or the structure for qualitative care are numerous and different: the number of pharmacists on a shift, the area of confidentiality, the quality of the pharmacists, the total area of the pharmacy, the bibliographical materials about medicines and access to on-line information, the stock of medicines and the counselling areas.

As the pharmacists are responsible for all the stages of using the medicines, the processes within the pharmacy may refer to any of these stages: prescribing, release, administration and monitoring. Among the indicators of the processes there are found the compliance with the clinical norms, the percentage of the prescriptions evaluated from the point of view of fairness and the percentage of the patients counseled.

The results represent the stimulant of the management of the therapy with medicines, which determine the pharmacists to assume a role in educating the patients and the management of the chronic diseases. Among these activities, they succeed to improve the pharmaceutical care of the patients through: (1) Increase of the control of the patients on their medical affections [3], [7] and (2) Decrease of using the resources from the budget of the system of health insurances [7]; (3) Improvement of the knowledge of the patients regarding the diseases and their medication [2], [11]; (4) Increase of adopting and maintaining the non-pharmaceutical regime [11]; (5) Increase of satisfaction of patients regarding the care they benefit from [4], [7]; (6) Saving the money of the patients [4], [7]; (7) Improvement of the quality of the patients' life [2], [11].

The capacity of the pharmacists to identify, settle and prevent the problems related to medication, as well as assuming the responsibility in the domain of chronic diseases make the object of many papers, their results representing the final purpose of the therapy and they may be analyzed through more methods [1], [2], [4], [10].

One of the methods, the model "Extension for Community Healthcare Outcomes ECHO®", suggests three types of results of the medical care: economical, clinical and humanistic. The project ECHO® is an approach of managing the disease that has as purpose the increase of the knowledge of the suppliers and standardization of the best practices for screening, care and treatment of a disease. ECHO® is based on a basic principle of learning related on cases, in which the clinicians and the suppliers of pharmaceutical care attend a teleconference meeting hosted by a central team for presenting individual cases, in

order to consult a multidisciplinary team of specialists and for studying the cases. The discussion related on the case are interactive, exploiting the ideas of a multidisciplinary team. The sessions of ECHO® offer the possibility of building a dynamic community of trainees.

The economic results include direct costs and consequences, both medical and nonmedical, and indirect costs and consequences as well as nonmaterial costs. Such an approach is necessary for helping at the optimization of the increasing costs associated with chronic diseases and diseases that may be prevented with the help of pharmaceutical care [5].

The clinical results are medical events that occur after the disease or the treatment. The criteria of the clinical results include morbidity and mortality, the incidence rates or the spread of the symptoms. These criteria represent a direct measure of the quality, but are difficult to assess in the pharmacy. For the evaluation of the results, in pharmacy can be used specific indicators or markers, for instance glycosylate hemoglobin (HbA1C), blood pressure (HTA)-indicator of the probability of a stroke.

The studies emphasize the effect of the advanced pharmaceutical care on the adherence of the diabetic patients to treatment and the efficiency of the therapeutical results related to medicines that improve eventually the quality of the patient's life. More and more important part of the activity of the pharmacist becomes the provision of information related to the modality of using the medicines by each patient, as every person is different, with different particularities, unique affections and needs of medical care [1].

The methods of human evaluation are the methods for the evaluation of the impact of the disease and its treatment on the quality of life based on the health condition of the patient, preferences and satisfaction of the patient and application of the pharmacotherapeutic decisions.

The quality of life was defined as the evaluation of the functional effects of the disease and of the therapy prescribed, as they are perceived by the patient. These effects are physical, emotional and social effects on the patient [5].

The human results are the consequences of the disease or treatment on the functionality of the patient in society or on the actual and future quality of life. These consequences may be classified as positive and negative. An example of a positive result is that the expected effect from a medicine to be manifested accordingly, this being a modality of measuring the efficiency of using the respective medicine. A negative result is the occurrence of a side effect or negative after having used a medicine. The pharmacoeconomic evaluation must include the possibilities of measuring both types of results. The evaluation of the positive results only may mislead with regard to the costs, by excluding the costs caused by the negative results [5].

The human results include criteria of the human aspects, such as the satisfaction of the patients and the quality of life. A survey related to the satisfaction of the patients regarding the services of pharmaceutical care may be useful for the evaluation of the results in case of the patients that benefit from these services. Most

of the surveys include either specific measures for a disease, or general measures for maintaining the health condition. In exchange, an evaluation of the quality of life may be useful for establishing the impact of the therapy with medicine on the patient in general.

Building an economic model may help the pharmacist anticipate the impact that the decisions of using the medicine have on the patient and on the health system and rush the process of reevaluation regarding the management of formulating decisions regarding the policy of using the medicines, while new medicines enter the market and replace the old ones. The most recent application of the pharmacoeconomic principles and methods is for justifying the value of different services of pharmaceutical care [5].

Standardization is considered one of the most powerful instruments for improving quality. When a person does the same thing every time, the chances to make errors decrease significantly. In the pharmacy, standardization is the easiest method, the most widespread and the most efficient for improving quality. In fact, the transition to standardization stimulated the critical ways that are focused not only to prevent errors, but also to optimize the results, the reduction of the costs and obtaining the satisfaction according to the American Pharmacists Association. These supportive systems may be used for alerting the pharmacist regarding the possible problems**.**

Another mechanism that may help the pharmacists is the use of protocols and verification lists, which diminish the confusion according to the Agency for Healthcare Research and Quality. The protocols usually prevent issuing a prescription until it is approved by a final verification by the pharmacist. The policies and protocols diminish the confusion.

The improvement of the access to information leads to the improvement of quality. The studies reveal the fact that the pharmacists take decisions for using the medicines more correctly, if they have access to complex and complete information about the patients, as well as the treatment profile, allergies, comorbidities [13].

## CONCLUSION

If we apply the ideas mentioned above in the pharmaceutical practice, we may state that the qualitative improvements shall produce the clinical results wanted, such as an increased quality of life, as well as a greater satisfaction of the patients. In the end this will make the pharmacy create the image of a supplier of pharmaceutical care of the best quality.

The processes for improving the quality were used for monitoring the errors of medication and for avoiding the errors of prescribing.

In general, the techniques for improving the quality were used in an institutional frame, but they become more and more frequent in eth pharmacies that offer services of assisted care.

Quality represents the essential component of the competent and professional pharmaceutical practice. Many of the changes for improving the quality are simple,

may be fast implemented but they have a massive impact on the quality of the patients' care.

Quality in the domain of the pharmaceutical care reached a position of maximum visibility and the pharmacist is recognized as the key – actor in this process. Therefore, the pharmacists shall be required more and more to be involved in assuring the quality of all the segments within the system of using the medicines.

## REFERENCES

[1] Blebea N.M., Stefănescu E., Zbârcea C.E., Mușat O., Chiriță C., Negreș S., The Evaluation of the Consumption of Dietary Supplements at Diabetic Patients, Proceedings of The Romanian National Congress of Pharmacy – 17th Edition, 21st Century Pharmacy – Between Intelligent Specialization and Social Responsibility , FilodirittoEditore – Proceedings, Romania, pp. 29-34, 2018.

[2] Blebea N.M., Negreș S., The Impact of Pharmaceutical Care on Patients with Chronic Hypertension, Proceedings of the Inaugural Edition of the Virtual Congress with International Participation Nutrition, Diet Therapy & Food Safety in the Context of the COVID-19, NutriTerra, Romania, pp.206-209,2 020.

[3] Clifford R.M., Davis W.A., Batty K.T. et al., Effect of a pharmaceutical care program on vascular risk factors in type 2 diabetes: The Fremantle diabetes study, Diabetes Care, U.S., vol.28/ issue 4, pp.771-776, 2005.

[4] Cranor C.W., Bunting B.A. Christensen D.B., 2003, The Asheville Project: Long –term clinical and economic outcomes oh community pharmacy diabetes care program, Journal of American Pharmacists Association, U.S., vol..43/issue 2, pp.173-184, 2003.

[5] Cristea A.N., Clinical Pharmacy, Romania, vol.2, pp.46-56, pp.509-537, 2017.

[6] European Community Pharmacy Services & Activities, PGEU Database 2015-2016, Pharmaceutical Group of the European Union, Belgium, November 2017.

[7] Garrett D.G., Bluml B.M., Patient self-management program for diabetes: first-year clinical, humanistic, and economic outcomes, J Am Pharm Assoc , U.S., 2005; vol. 45 pp.130–137, 2005.

[8] International Pharmaceutical Federation, Pharmacy: A Global Overview, Workforce, medicines distribution, practice, regulation and remuneration, The Netherlands, 2017.

[9] International Pharmaceutical Federation, Sustainability of Pharmacy Services. Advancing Global Health, The Netherlands, 2015.

[10] Mangiapane S., Schulz M., Community pharmacy-based pharmaceutical care for asthma patients, Annals of Pharmacotherapy, Germany, no39, pp.1817-1822, 2005.

[11] Merriam-Webster , Merriam-Webster's collegiate dictionary, Springfield, Massachusetts, U.S., 2003.

[12] Romanian Parliament, Law No.226/2008 of the pharmacy, Pharmacy law. Romania, 2008 .

[13] Warholak-Juarez T., Rupp M.T., Salazar T.A., Effect of patient information on the quality of pharmacists` drug use review decisions, Journal of the American Pharmacists Association, U.S., vol. 40/issue 4, pp.500-508, 2000.

[14] Wiedenmayer K., Summers S. R., Mackie C.A., Gous A.G.S., Everard M., Tromp D., World Health Organization and International Pharmaceutical Federation, Developing pharmacy practice A focus on patient care, Handbook, Switzerland, Edition 2006.

[15] World Health Organization, Transforming and scaling up health professionals'education and training, Switzerland, 2013.

# RESEARCH ON THE BOTANICAL AND PHARMACOGNOSTIC PARTICULARITIES OF THE INDIGENOUS SPECIES *LYSIMACHIA NUMMULARIA* L.

**Suciu Felicia**[1]
**Arcuș Mariana**[2]
**Roșca Adrian Cosmin**[3]
**Bucur Laura**[4]
**Popescu Antoanela**[5]
**Badea Victoria**[6]
[1, 2, 3, 4, 5] Faculty of Pharmacy, Ovidius University of Constanta, Romania
[6] Faculty of Dentistry, Ovidius University of Constanta, Romania

## ABSTRACT

Preliminary pharmacochemical research on *Lysimachia nummularia* L. was performed by dint of pharmacognostic analysis (macroscopic examination, global chemical analysis, preliminary quantitative determinations).The article includes the analysis of the macroscopic characters of the vegetative organs (root, stem and leaf), as well as of the reproductive organs (flower, fruit, seed) belonging to the spontaneous native species *Lysimachia nummularia* L.

Morphological features were described and discussed. The identification of these aspects was done with the naked eye, but also with the help of a hand magnifier and a binocular magnifier. The results revealed that the external appearance of the plant justifies the species belonging to the genus *Lysimachia*, family *Primulaceae*. They are found in the glabrous and creeping appearance of the plant, opposite, almost round leaves, solitary, yellow flowers, axillary with vigorous pedicels, perianth pentamer, actinomorphic, dialisepal and dialipetal, globular capsule fruit. The semi-hydrophilic nature is found in the presence of adventitious roots that develop both from the rhizome and at the nodes of the stem. The preliminary quantitative determinations performed were loss by drying as well as soluble substances of the species *Lysimachia nummularia* L. Following the global chemical analysis, active principles known in the literature for the antioxidant potential were identified. Following the preliminary quantitative determinations (drying loss, determination of soluble substances) results comparable to those in the literature on the content of volatile substances and soluble substances were obtained.

***Keywords:*** *Lysimachia, macroscopic, pharmacognostic analysis, active principle*

## INTRODUCTION

The paper aims at a broader study both botanical - morphological and histoanatomical, but especially pharmacognostic and phytochemical of the species *Lysimachia nummularia* L. (Fam. *Primulaceae*). The idea of this study started from

the fact that in the literature, the plant has proven, following scientific research, to be beneficial in various diseases, due to the presence of some active principles with phytotherapeutic potential in the structure of its tissues.

Thus, in traditional medicine, it is used internally to treat ulcers, diarrhea, dysentery and tuberculosis, and externally to heal wounds and skin ulcers [1].

In cultured medicine, studies have shown the presence of polyphenolic compounds, flavonoids, anthocyanosides, tannins [2], [3], [4], [5], [7], [8], due to which the plant would have a significant antioxidant potential, as well as a triterpene saponoside - nummulariozide [9], [10], isolated from the underground parts, showing cytotoxic (antitumor) activity important in five human cancer cell lines [6], [12], [13], [14], to which are added the antibacterial, antirheumatic and analgesic effects.

In this article we tried a preliminary study aimed at knowing the macroscopic characteristics of both vegetative (root, stem, leaf) and reproductive (flower, fruit, seed) organs belonging to the native spontaneous species *Lysimachia nummularia* L and preliminary pharmacognostic determinations (chemical analysis qualitative, preliminary quantitative analysis).

## MATERIALS AND METHOD

The working material was represented by the plant *Lysimachia nummularia* L., harvested on July 19, 2020, on the edge of Lake Tău-Brazi in the Roșia Montană area (Fig. 1). Here, the plant in full anthesis, develops on considerable surfaces, forming well-defined associations and dominates the area due to its plagiotropic feature (Fig. 2). The collected specimens were herbivored and determined in the Pharmaceutical Botany Laboratory within the Faculty of Pharmacy, using for this purpose the flora determinants from the laboratory equipment [15]. Several herbaceous specimens are in the custody of the Pharmaceutical Botany Laboratory.

For the preliminary pharmacognostic determinations, the pharmacognostic analysis was used as a working tool (macroscopic examination, qualitative chemical analysis, determination of drying loss, determination of soluble substances).

To establish the macroscopic characters, the species was analyzed with a hand magnifier and a binocular magnifier.

The pharmacognostic analysis consists of two groups of methods: quantitative methods and qualitative methods.

Qualitative methods lead to the determination of the identity of a plant product and include the Examination, macroscopic, microscopic and chemical (microchemical and qualitative chemical).

Quantitative methods aim to determine the purity and quality of a plant product.

For the pharmacognostic analysis were used the vegetal products obtained from the species *Lysimachia nummularia* L.: *Lysimachiae* radix, *Lysimachiae* herba and *Lysimachiae* flores.

The vegetable products were obtained from the species *Lysimachia nummularia* L. after drying and sorting.

The qualitative chemical analysis is based on the successive extraction of the plant product used, with solvents of different polarities and the identification by reactions characteristic of each group of active principles. The reagents used in identifying the active principles are reagents for analysis from various domestic and imported companies.

Determination of drying loss is a preliminary quantitative pharmacognostic method that represents the degree of humidity of plant products, which must be within certain limits, so as to ensure the preservation of plant products.

The working method involves the following technique.

The weighing vials with the vegetable products previously brought to a constant mass, together with the sample taken, are kept in the oven at $105^0$C for 3-4 hours, unless otherwise provided, cooled in a desiccator and weighed. Continue drying for 1 hour, followed by cooling in the desiccator and weighing until the samples reach a constant mass. A KERN ABJ analytical balance was used to weigh the samples.

Determination of soluble substances is the amount of substances that are soluble in a given solvent, per 100 grams of dried vegetable product. This preliminary quantitative determination has indicative value as regards the amount of active principles soluble in a given solvent.

Taking into account the solubility of the active principles known in the literature, as well as the extraction possibilities, we used in this determination three solvents, namely: ethanol 40% (v / v), ethanol 96% (v / v) and water. Thus, the determination of soluble substances was performed for each plant product (*Lysimachiae* radix, *Lysimachiae* herba and *Lysimachiae* flores) in the three solvents mentioned above.

The following working technique was used to determine the soluble substances:

2.5 g of vegetable product, sprayed according to the provisions of the respective monograph, are weighed on the analytical balance and brought into a vial with a ground-in stopper; add 100 g of the solvent provided, shake vigorously several times, leave to soak for 23 hours, shake again for 1 hour and filter, removing the first portions of the filtrate. 10 g of the filtrate are evaporated to dryness on a water bath in a pre-calibrated weighing ampoule. The weighing vial with residue is dried in the oven; at $105^0$ C, for 3-4 hours, cool in the desiccator and weigh.

## RESULTS AND DISCUSSIONS

*Lysimachia nummularia* L., is a herbaceous, perennial plant (Figure 1, Figure 2), spread through meadows and bushes, in forests, streams, wet depressions, through water holes, meadows and on the waterfront, in the plains and hilly regions from all over the country.

***Fig.1.*** *Association with Lysimachia nummularia L.*

***Fig. 2.*** *General appearance of the species Lysimachia nummularia L.*

From a macroscopic point of view, underground, it presents a rhizome with nodes and internodes, with thin adventitious roots starting from the nodes (Figure 3). The stem is sudden, 10-50 cm long, glabrous, simple or weakly branched, in four edges, at nodes with bundles of adventitious roots (Figure 4).

***Fig. 3.*** *Lysimachia nummularia L. – roots with nodes and internodes*

***Fig. 4****. Lysimachia nummularia L.- simple glabrous stems*

The leaves are opposite, round or elliptical, obtuse, with entire edges, very shortly petiolated, with red glandular points (Figure 5).

The solitary hermaphroditic flowers, arranged in the axils of the leaves (Figure 5), have floral pedicels the length of the leaves, sometimes even longer. The floral coating is a perianth made of calyx and corolla.

***Fig. 5.*** *Lysimachia nummularia L. - Opposite round elliptical leave*

***Fig. 6.*** *Lysimachia nummularia L. Solitary flowers in the leaf axils*

The actinomorphic calyx consists of five free sepals, 7 mm long, with cordiform lacinas, separated to the base (dialisepal) (Figure 6, 7).

***Fig. 7.*** *Lysimachia nummularia L. - calyx with cordiform lacinae*

***Fig. 8.*** *Lysimachia nummularia L. - calyx with cordiform lacinas - dialisepal pentamerous corolla*

The corolla is intensely yellow, with a glandular reddish dotted interior, about 15 mm wide, twice as wide as the calyx, divided almost to the base into obovate, obtuse lacrines with full edges. It is pentamerous, actinomorphic, dialisepal (Figure 8).

The androecium consists of five stamens (Figure 9), two to three times shorter than the corolla, with hairy glandular filaments at the base. Stamen length style. The fruit is a capsule only rarely developed, globular, 4-5mm long, shorter than the calyx, whitish yellow, with small red secretory sacs. Blackish seeds, in 3 edges, warty, 1-1.5 mm long.

***Fig. 9.*** *Lysimachia nummularia L. - Androecium of 5 stamens*

Following the general chemical analysis performed, the following types of active principles were identified as follows:

In the roots of *Lysimachia nummularia* L. were identified: volatile oil, sterols (triterpenes), flavonic aglycones, carotenoids, coumarins, tannins (gallic tannins, catechin tannins), flavonosides, coumarins heterozidates, heterozides o, triterpenes, (ortho dihydroxy phenols) ODP, poliosis, polyuronides, saponosides.

The following classes of active principles have been identified in the plant product *Lysimachiae* herba: volatile oil, sterols (triterpenes), flavonic aglycones, carotenoids, fatty acids, coumarins, tannins (Galician tannins, catechin tannins), flavonoids, heterosidium coumarins, heterosides, ODP, reducing compounds, oases, polyoses, polyuronides, saponosides.

Following qualitative chemical analysis, the flowers of *Lysimachia nummularia* L. contain: volatile oil, sterols (triterpenes), flavonic aglycones, carotenoids, fatty acids, coumarins, tannins (gallic tannins, catechin tannins), flavonoids, heteropidate coumarins, ODP, reducing compounds, oases, polyoses, polyuronides.

Comparing the results obtained by us with those mentioned in the literature we found the following:

- the presence of flavonosides is also mentioned in the literature in all parts of the plant *Lysimachia nummularia* L. Thus, throughout the plant were identified rifolin, isoquercitrin, myricitrin, mearnsitrin, syringetin 3-galactoside, kaempferol 3-O-rhamnosyl (1 → 2) galactus, quercetin 3-O-neohesperidioside, rutin, kaempferol 3-O-(2,6-dirhamnosylgalactoside) and quercetin 3-O- (2,6-dirhamnosylgalactoside) [5];
- species of the genus *Lysimachia* contain kaempferol, quercetin and myricetin in: L. vulgaris, L. *nummularia*, L. *punctata*, L. *christinae*, L. *ciliata* and L. *clethroides*, respectively, which demonstrates the presence of flavonic aglycones identified by us [7];

- polyphenolic compounds were also determined in species of the genus Lysimachia sp, *Lysimachia nummularia* L., *Lysimachia vulgaris* L. and *Lysimachia punctata* L [6].
- Thus, the identification of the constituents from the groups of active principles highlighted in the researched plant product will be possible also through the correlation between metabolism and phylogeny.

The loss results for the plant products *Lysimachiae* radix, *Lysimachia*e herba and *Lysimachiae* flores are summarized in the table below:

***Table 1.*** *Results of preliminary determinations*

| Nº | **Vegetable product** | **Loss on drying Quantity (g% ± SD)** |
|---|---|---|
| 1. | *Lysimachiae radix* | 8,6043 ±0,5125 |
| 2. | *Lysimachiae herba* | 8,54086±0,1070 |
| 3. | *Lysimachiae flores* | 7,4941±0,5408 |

The values of the loss by drying show that the vegetal product taken in work falls within the limits allowed by FR X and Ph. E. 10.0 (3 - 13%) in terms of the content of volatile substances at 100ºC, to ensure their good shelf life. Regarding the content of soluble substances in different solvents, it is observed that most substances are soluble in 40% ethanol.

***Table 2.*** *Results of preliminary determinations - soluble substances*

| **Crt. no.** | **Vegetable product** | **Determination of soluble substances in different solvents** | **Soluble substances (g% ± SD) Dried vegetable product** |
|---|---|---|---|
| 1. | *Lysimachiae radix* | Ethanol soluble substances 40% | 54,1038±0,4055 |
| | | Ethanol soluble substances 96 % | 23,5023±0,7913 |
| | | Water soluble substances | 41,3076±0,6882 |
| 2. | *Lysimachiae herba* | Ethanol soluble substances 40% | 62,9067±1,1140 |
| | | Ethanol soluble substances 96 % | 27,6922±0,4269 |
| | | Water soluble substances | 54,5582±0,3369 |
| 3. | *Lysimachiae flores* | Ethanol soluble substances 40% | 81,4685±1,3784 |
| | | Ethanol soluble substances 96 % | 53,6120±0,9132 |
| | | **Water soluble substances** | 66,6908±1,2166 |

## CONCLUSION

The analysis of the macroscopic characters of the studied species confirms that the plant is *Lysimachia nummularia* L. from the *Primulaceae* family, because these characteristics are in accordance with the description of the species in the literature, respectively in the flora determinants in Romania. Among these characters are the plagiotropic feature, the glabrous appearance of the vegetative organs, the opposite position of the almost round leaves, the solitary, axillary yellow flowers.

The presence of several groups of active principles in all organs of the species *Lysimachia nummularia* L. leads us to the conclusion that the species is of interest and can be researched for therapeutic recovery purposes.

The product does not contain cardiotonic alkaloids and heterosides (toxic compounds) or anthracenosides (laxative compounds). The values of drying loss show that the vegetable products used correspond to their preservability.

As the largest amount of substances are soluble in 40% ethanol, it determines us in the following research to take extracts obtained in 40% ethanol.

## REFERENCES

[1] Pârvu C., Enciclopedia plantelor, vol. I, Tehnică, București, 2003, 67.

[2] Neli K. O., Studiul extractelor vegetale – mai mult decât analize fitochimice, Universitatea de Vest „Vasile Goldiș" Arad, Iulie 2018.

[3] Tóth A., Riethmüller E., Alberti Á., Végh K., Kéry Á., Comparative phytochemical screening of phenoloids in *Lysimachia species*, European Chemical Bulletin, Vol. 1, nr. 1-2, 2012.

[4] Toth A., Toth G., Kerya A., Polyphenol Composition and Antioxidant Capacity of Three *Lysimachia Species*, Natural Product Communications, Vol. 9 (10) 2014, 1473-1478.

[5] Toth, A., Riethmuller, E., Vegh, K., Alberti, A., Beni, S., & Kery, A.. Contribution of individual flavonoids in *Lysimachia species* to the antioxidant capacity based on HPLC-DPPH assay. Natural product research, 32(17), 2018, 2058-2061.

[6] Luczak S., Swiatek L., Daniewski M, Phenolic acid in herbs *Lysimachia nummularia* L. and L. vulgaris., Acta Polonie Pharmaceutica, 1989.

[7] Yasukawa K., Ogawa H., & Takido M., Two flavonol glycosides from *Lysimachia nummularia*, Phytochemistry, 29(5), 1990, 1707-1708.

[8] Podolak I., Kokzurkiewicz P., Michalik M., Galanty A., A new cytotoxic triterpene saponin from *Lysimachia nummularia* L., Cercetarea carbohidraílor, Volume 375, 28 iunie 2013, 16-20.

[9] Podolak I., Koczurkiewicz P., Galanty A., Michalik M., Cytotoxic triterpene saponins from the underground parts of six *Lysimachia* L. species., Biochem. Syst. Ecol. 2013; 47, 116–120.

[10] Hanganu D., Kinga O. N., Mocan A., Vlase L., Benedec D., Raita O., Toma C. C., Conținut polifenolic comparativ și activități antioxidante ale două specii de lizimachie românești, Revista de Chimie –București, 2016.

[11] Yildirim A. B., Guner B., Karakas F. P., Turker A. U., Evaluation of antibacterial, antitumor, antioxidant activities and phenolic constituents of field-grown and in vitro-grown *Lysimachia vulgaris* L., Afr. J. Tradit. Complement Altern. Med 14(2), 2017, 177–187.

[12] Csepregi R., T. Viktória, Das S., Ágnes Alberti, Proprietăți și efecte citotoxice, antimicrobiene, antioxidante asupra migrației celulare a compușilor fenolici ai plantelor medicinale transilvane selectate, Antioxidanți, 2020, 9, 166.

[13] *** Flora României, 1952-1976, vol. VII, Acad. R.P.R.-R.S.R., 42-46.

[14] Ciocârlan V., Flora ilustrată a României. Pteridophyta et Spermatophyta, Ceres, București, 2009, 1067.

[15] ***Farmacopeea Română, editia a X-a, Medicala, Bucuresti, 2021.

# SARS-COV-2 CORONAVIRUS: NOMENCLATURE, CLASSIFICATION, STRUCTURE, HISTORY, SYMPTOMS EPIDEMIOLOGY, PATHOGENESIS, ETIOLOGY, DIAGNOSES, TREATMENT, AND PREVENTION

**Hanan Al-Khalaifah**[1]
**Mohammad Al-Otaibi**[2]
**Abdulaziz Al-Ateeqi**[3]
[1, 2, 3] Kuwait Institute for Scientific Research, Environment and Life Sciences Research Center, Kuwait

## ABSTRACT

With the onset of the coronavirus pandemic in December 2019 in China, and the alarming rate at which it has spread across the world has unleashed not only fear, but has taken a toll on social, economic, health, and governing capabilities of the various countries infected with the virus. The pandemic is affecting all aspects of life, including industries such as the animal production industry all over the world. This includes plant, livestock and poultry production. Food security is accordingly impacted, as these industries are vital elements that are contributing to securing food to populations worldwide. In this review, light is shed on the origin of coronaviruses with special emphasis on COVID-19. It also includes introduction of symptoms, epidemiology and pathogenesis, etiology, and prevention. As the disease progresses, scientists are working around the clock in the hope of an effective vaccine, and they managed to introduce some to the worldwide populations. The world faces challenges on a day-to-day basis until most people are vaccinated.

***Keywords:*** *coronaviruses, COVID-19, epidemiology, vaccine*

## INTRODUCTION

The COVID-19 pandemic has affected people worldwide and is the fifth pandemic after the Spanish flu of 1918. It originated in Wuhan, China, and has now escalated to more than 200 countries and has infected individuals of almost all ages. The onset of the disease progresses with milder symptoms such as fever, upper respiratory tract symptoms, shortness of breath, and diarrhea and some individuals are asymptomatic. In those patients with severe infection, pneumonia, multiple organ failure, and death have been reported. The pandemic has now claimed the lives of millions and has gained the attention of public health researchers worldwide [1], [2], [3].

The world has previously also suffered epidemics due to coronaviruses in the form of severe acute respiratory syndrome (SARS)-CoV which emerged in Guangdong province of China and again, in September 2012, the Middle East respiratory syndrome (MERS)-CoV. These viruses have a natural and zoonotic

origin which can be reflected in the SARS-CoV-2. The Covid-19 pandemic has not only disrupted physical health but has also negatively impacted mental health, economy, and social framework and large healthcare systems of the world .Government authorities of the world are putting their heads together to determine the safety and precautionary measures. Scientists are continually and tirelessly researching probable diagnostics and vaccines to curb the spread of this pandemic which has proven to be more than a challenge. Currently, there exist only therapeutic and preventive ways to deal with the outbreak [4].

**Nomenclature and classification**

Coronaviruses belong to the largest group of RNA viruses and are enclosed with positive-strand genomes of 26-32 kb in length. They are abbreviated as "CoVs" due to their crown-like appearance when scanned under an electron microscope [5]. They are classified under the Nidovirales order and include other families such as Coronaviridae, Arteriviridae, Mesoniviridae, and Roniviridae. The Coronaviridae family is again subdivided into Coronavirinae and the Torovirinae [6]. Based on the genetic differences and serological cross-reactivity, the Orthocoronavirinae subfamily is further divided into Alphacoronavirus, Betacoronavirus, Gammacoronavirus, and Deltacoronavirus [7]. The Betacoronavirus group was earlier divided into four lineages: A, B, C, and D. Although recently these have been reclassified and renamed as Embecovirus, Sarbecovirus, Merbecovirus, and Nobecovirus. A fifth subgenus, Hibecovirus, has also been added [6].

The alpha-CoVs consists of human and animal viruses, the beta-CoVs, consists of murine and human viruses, the gamma-CoVs consists of viruses from cetaceans and birds and delta-CoVs consists of viruses from pigs and birds [8]. CoVs have traversed the species barriers and have become transmissible to humans. To date, seven human CoVs (HCoVs) have been identified from which two, HCoV-229E and HCoV-NL63 are α-CoVs and the rest β-CoVs which include HCoV-OC43, HCoV-HKU1, severe acute respiratory syndrome coronavirus (SARS-CoV), Middle East respiratory syndrome coronavirus (MERS-CoV) and SARS-CoV-2. These HCoVs have originated from bats, mice, or domestic animals [5].

**Structure of coronaviruses**

The coronaviruses have a diameter of about 120 nm along with club-shaped protein spikes protruding from the surface, appearing like a solar corona. They possess four principal structural proteins which are; spike (S; 1160–1400 amino acids), membrane (M; 250 amino acids), envelope (E; 74–109 amino acids), and nucleocapsid (N; 500 amino acids) proteins, all of which are encoded within the 3′ end of the viral genome [6]. The S glycoprotein (~150 kDa) is a class I fusion protein and directs attachment to the host receptor. This S protein is cleaved by a host cell protease into distinct subunit, S1, and S2. The former constitutes the major receptor-binding domain of the S protein whereas the latter makes up the stalk of the spike molecule. The M protein is present in abundance, it is small (~25–30 kDa) and gives shape to the virion. The E protein (~8–12 kDa) is present in minute quantities in the virion and the N protein is unique due to its presence in the nucleocapsid [9].

**A brief history of discovery of human coronaviruses (HCoVs)**

One of the first strains to be isolated from infected individuals with respiratory problems in 1966 was HCoV-229E. The symptoms observed in infected patients were common cold, headache, sneezing, malaise, sore throat, fever, and cough. The following year, HCoV-OC43 strain was isolated from organ cultures. The infections caused by these strains were closely similar to those caused by HCoV-229E. These two strains are actively transmitted during winters. The incubation time of these viruses is on average less than a week and an illness period of two weeks. Studies on human volunteers showed that healthy and fit persons infected with the HCoV-229E strain showed mild flu-like symptoms and a few patients showed acute respiratory tract infection. Phylogenetic evidence has indicated that these strains have originated from bats or rodents [5].

The severe acute respiratory syndrome or more commonly known as SARS was the third HCoV to be discovered and the first to be well-documented. It is otherwise called atypical pneumonia. It was first traced back to Guangdong Province of China in November 2002. The World Health Organization (WHO) reported 8096 infections and 774 casualties in just a span of one year in more than 30 countries. There was a 50% mortality rate observed in the elderly subjects. This virus is believed to have originated from the SARS-CoV found in wild feline animals such as the palm civet in the markets of China and was transmitted to humans by contact when handling these creatures. However, it was later observed that palm civets from the wild or farms were negative for SARS-CoV which could be an indicator that they only served as intermediate hosts and the natural animal host was Chinese horseshoe bats [5]. It is transmitted in humans through cough droplets or mucosae which contain infected fomites. The virus originated in China and then spread to other parts of the world via interpersonal transmission from hospitals, medical institutions, homes, workplaces, and public transport [10]. The symptoms for SARS-CoV were muscular pain, headache, fever, weakness, and chills, followed by dyspnoea, cough, and respiratory discomfort as of late symptoms. On a cellular level, alveolar damage, epithelial cell proliferation, and an increase in macrophages were observed in infected individuals. About 20-30 % of patients needed intensive care and ventilation. The HCoVNL63 strain was more widespread among young children, the elderly, and those with respiratory sicknesses. The underlying symptoms observed were coryza, conjunctivitis, fever, and bronchiolitis. Its rate of incidence was high during early summer, spring, and winter. Another strain, HCoV-KKU1 was linked with acute asthmatic exacerbation in the elderly [5].

The MERS coronavirus (MERS-CoV) was initially isolated in Jeddah, Saudi Arabia from an infected person in September 2012 who was suffering from acute pneumonia and renal failure. The WHO reported 288 deaths, with a mortality rate of 34.5% between September 2012 till July 2014. The virus was contracted by a man returning from Saudi Arabia to South Korea and led to the outbreak of the disease with deaths numbering 36 and a mortality rate of 19.4%. The spread of the MERS-CoV infection is believed to be zoonotic as genomic analysis showed that the virus originated from a bat, which was then transmitted to dromedary camels, the intermediate hosts for transmission to humans [10].

**The COVID-19 coronavirus- A pandemic**

**A brief background**

The last twenty years have seen the emergence of several viral diseases as mentioned previously like the SARS-CoV, H1N1, and the MERS-CoV. We now know that these respiratory diseases caused by CoVs can cross species barriers and cause severe illnesses in humans [4].

The COVID-19 pandemic has taken the world by storm since its emergence in December 2019. It originated from Huanan Seafood Market in Wuhan City, Hubei province of China, one of the most densely populated cities with a population crossing 11 million. The wet market traded not only fish but various live animals such as poultry, bats, marmots, and snakes [11]. Hospitals started receiving patients showing severe pneumonia-like symptoms of unknown origin. Surveillance systems installed post the SARS epidemic were again set in motion and throat swab samples collected from infected individuals were tested and on December 31st, 2019, China through the WHO declared the outbreak of the virus. The virus was confirmed to be a CoV. It was found to have a similarity of more than 95% with the bat coronavirus and more than 70% with the SARS-CoV. Samples obtained from the seafood market confirmed the presence of the virus indicating its origin from that place. Cases of infected persons skyrocketed and several cases were reported even though they did not have any exposure to the market. The first fatality was reported on 11th January 2020. The epidemic became explosive during the Chinese New Year when reports of cases started emerging from people returning from Wuhan. Hubei province was soon placed under lockdown and extended to other cities as well. The infection was transmissible from those individuals who did not show any sign of sickness (asymptomatic) and also before the initiation of symptoms [12].

The upsurge of the COVID-19 pandemic which started in China was officially declared by WHO as a state of Public Health Emergency of International Concern (PHEIC) on 30th January 2020. They stated that the spread of the virus could be slowed down employing timely detection, isolation, quick and speedy treatment, and rapid and efficient system to trace contacts [12]. By this time, the virus had already extended to 18 countries and four countries reported cases that spread from human contact. The virus was previously termed 2019-nCoV, the ICTV termed it as the SARS-CoV-2 virus due to its similarity with SARS-CoVs that caused the SARs outbreak. The Director-General of WHO, Dr. Tedros Adhanom Ghebreyesus stated on February 11, 2020, that the disease would be termed ‘COVID-19”, which is the acronym of "coronavirus disease 2019". The situation spiraled out of control on the 11th of March when the number of cases out of China increased 13 times, the countries with infected individuals had tripled with 118,000 cases in 114 countries and more than 400 deaths. This is when the WHO declared the COVID-19 situation as a pandemic [4], [13].

**Symptoms of COVID-19**

The symptoms of the infection start appearing post-incubation interval of an average of 5.2 days. The onset of the symptoms until death (if happens) ranges from 6-41 days. This duration is conditioned based on the age and overall immune system of the patient. It is lower in older patients, greater than 60 years in comparison with younger individuals and people with underlying diseases (i.e., hypertension, chronic obstructive pulmonary disease, diabetes, cardiovascular disease). The familiar symptoms at the start of the disease are fever in some people, cough, fatigue, and varies with sputum production, headache, hemoptysis, diarrhea, dyspnoea, and lymphopenia [14]. The clinical features range from asymptomatic to acute respiratory distress syndrome (ARDS) and multiorgan failure [12]. The uniqueness of COVID-19 as compared to previous beta-CoVs is that it affected lower airways which resulted in rhinorrhoea, sneezing, and sore throat [14].

**Epidemiology and pathogenesis**

As per the report of the WHO COVID-19 dashboard, currently, there are 108,918 new cases, 7,127,753 confirmed cases and 407,159 deaths globally as of 10:47 am CEST June 2020. The data for case comparison of confirmed cases in the WHO regions is as follows: Americas- 3,415,174; Europe- 2,303,361; Eastern Mediterranean- 677,338; South-East Asia- 392,674; Western Pacific- 193,178 and Africa- 145,287. Infection is spread through numerous ways but most commonly from sizable droplets when coughing and sneezing from symptomatic and asymptomatic people, by touching contaminated surfaces and then touching the facial area. The virus may be found in the stools and contaminated water sources. It can remain viable on surfaces for several hours or days [12]. The duration for which the virus can last on several surfaces is plastic- 2-3 days, stainless steel- 2-3 days, cardboard- 1 day, copper- 4 hours. Aerosol transmission of the virus occurs in case of prolonged exposure in closed spaces. People who are either pre- or asymptomatic can be responsible for at least 80% transmission. In intensive care units (ICUs) contamination is dangerously higher than general wards and is known to be present on floors, computers, trash can, sickbed rails, and up to 4 meters from patients. These CoVs can be immobilized by the use of lipid solvents and fumigants like ether (5%), ethanol, and disinfection with chlorine, peroxyacetic acid, and chloroform. Data collected from primary investigations in Wuhan conducted by China CDCs showed that the doubles weekly and basic reproduction number (R0 - R naught) is 2.2 [4].

Human-to-human transmission initially occurred in Wuhan within families, and also among relatives and friends who came in contact with infected persons. It was reported that 31.3% of patients were those who visited Wuhan and 72.3% of patients who came in contact with people from Wuhan. The rate of transmission among medical personnel took place at 3.8% COVID-19 patients [15].

**Etiology of COVID-19**

The SARS-CoV-2 originates from the betaCoV genus, it is round or elliptic with a diameter of about 60-140 nm. The genome isolated from a patient from Wuhan showed that the virus had an 89% nucleotide which identifies with bat

SARS-like- CoVZXC21 and 82% with human SARS-CoV which is why it is given the name SARS-CoV-2. It contains 29891 nucleotides encoding 9860 amino acids [4].

**Diagnosis of COVID-19**

Diagnosis is carried out by molecular testing on samples such as throat swabs, nasopharyngeal swab, sputum, endotracheal aspirates, and bronchoalveolar lavage. Some laboratory investigations are non-specific. The white blood cell count is generally less. A possibility of lymphopenia; a lymphocyte count of less than 1000 is normally indicative of chronic disease. The platelet count is either within range or low. The C-reactive protein (CRP) and erythrocyte sedimentation rate (ESR) are slightly higher but procalcitonin levels are normal. A high procalcitonin level can indicate bacterial co-infection. The ALT/AST, prothrombin time, creatinine, D-dimer, CPK, and LDH may rise and high levels are associated with severe disease [12]. An X-ray of the chest area shows bilateral multifocal alveolar opacities, in advanced infection but is normal in early stages. Chest computed tomography (CT) is used for COVID-19 pneumonia in initial stages [4].

**Treatment of COVID-19**

To date, there is no antiviral treatment or vaccine available against COVID-19. Presently treatments that exist mainly rely on symptomatic and respiratory parameters. The detection and treatment of pneumonia caused by COVID-19 as issued by the National Health Commission of China recommend oxygen therapy and extracorporeal membrane oxygenation (ECMO) to patients with refractory hypoxemia. Several antiviral drugs and systemic corticosteroid treatments including oseltamivir, peramivir, zanamivir, ganciclovir, acyclovir, and ribavirin, as well as methylprednisolone, are not recommended. Based on previous experiences with dealing with the SARS-CoV and MERS-CoV, several drugs have been used for treating COVID-19. The US has reported that its first case of the virus was successfully treated using the drug Remdesivir. Chloroquine which is used to treat malaria in combination with Remdesivir had proven to be effective [15]. The use of non-invasive (NIV) and invasive mechanical ventilation (IMV) is required during times of respiratory failure caused due to resistance to oxygen therapy [4]. Besides all of the aforementioned, the first step that should be taken in isolation to prevent transmission of the virus to any other person. Mild symptoms can be controlled at home and through proper hydration and nutrient-rich diet [12].

**Prevention of COVID-19**

As there is no confirmed treatment for this disease, prevention is of utmost importance. For mild symptoms, isolation at home is recommended with proper ventilation and sufficient sunlight [12]. The WHO along with other organizations recommend the following [4]:

- Keep away from persons having acute respiratory infections
- Washing of hands for a minimum of twenty seconds, particularly after contact with infected individuals or environment

- Using sanitizer and avoiding contact with face or mouth after touching contaminated surfaces
- Avoid exposure to domestic or wild animals
- Persons with any respiratory symptoms should avoid crowds, wear a mask, follow proper etiquettes of covering their mouth when coughing or sneezing with disposable tissues or clothes

Healthcare workers face the biggest threat in COVID-19 transmission. They should take the utmost care by following all necessary protocols, starting with wearing a surgical mask or N95 masks and protective gear and goggles if they need to be near a patient and following the recommended hygiene practice of handwashing after a duration of 15 minutes or so. They should also be checked regularly for the onset of the symptoms. Patients can only be discharged if they have no fever for three days and two consecutive negative molecular tests of a one-day sampling interval. Lockdowns have been incorporated in all affected countries, people were asked to stay away from crowded places and limit travel. Although the use of masks for healthy people is not recommended by WHO as it has not been shown to protect against the disease but in China, the government has enforced wearing masks [12].

The COVID-19 outbreak has disrupted the economic, medical, and public health of the majority of the world. Health care workers are being overworked, frustrated, and exhausted besides facing high risks of infection [15]. The scenario brought about by the COVID-19 pandemic is constantly changing and is reflective of the mortality rates, research, and the never-ending search for a potential vaccine. The world will be able to normalize only as time progresses and every country is free of COVID-19.

## CONCLUSION

Through the numerous literature sources and documents released since the outbreak of this pandemic in December 2019 in China, this paper offers a structured point of view of the CoVs, in terms of classification, history, and detailed review of the COVID-19 disease. Such publications introduce the newcomer to the public that should be aware of the current pandemic. With each day passing, the virus brings out a new angle of public and global health. It has wreaked havoc in the world with so many questions still unanswered and what seems to be a never-ending search for a vaccine making and development. The medical personnel has been facing the ever-challenging side of this virus along with governments to contain and provide all necessary resources to sustain human life and minimize losses. The public worldwide should be trained on practices to reduce infection and face the virus. All people with all ages and sectors should cooperate to face the pandemic and save their lives.

## ACKNOWLEDGMENT

The author expresses her gratitude to the Kuwait Institute for Scientific Research (KISR) and Kuwait Foundation for the Advancement of Sciences (KFAS) for their constant technical and financial support.

## REFERENCES

[1] Park M, Cook AR, Lim JT, Sun Y, Dickens BL. A systematic review of COVID-19 epidemiology based on current evidence. Journal of Clinical Medicine. 2020;9(4):967.

[2] Al-Khalaifah H, Al-Nasser A, Abdulmalek N, Al-Mansour H, Ahmed A, Ragheb GJFiVS. Impact of SARS-Con-V2 on the Poultry Industry in Kuwait: A Case Study. 2020;7:656.

[3] Al-Khalaifah H. Modulatory Effect of Dietary Polyunsaturated Fatty Acids on Immunity, Represented by Phagocytic Activity. Frontiers in Veterinary Science. 2020;7:672.

[4] Cascella M, Rajnik M, Cuomo A, Dulebohn SC, Di Napoli R. Features, evaluation and treatment coronavirus (COVID-19). Statpearls [internet]: StatPearls Publishing; 2020.

[5] Ye Z-W, Yuan S, Yuen K-S, Fung S-Y, Chan C-P, Jin D-Y. Zoonotic origins of human coronaviruses. International journal of biological sciences. 2020;16(10):1686.

[6] Li X, Luk HK, Lau SK, Woo PC. Human Coronaviruses: General Features. Reference Module in Biomedical Sciences. 2019.

[7] de Wit JS, Cook JK. Avian coronaviruses. Taylor & Francis; 2020.

[8] Burrell CJ, Howard CR, Murphy FA. Fenner and White's Medical Virology: Academic Press; 2016.

[9] Fehr AR, Perlman S. Coronaviruses: an overview of their replication and pathogenesis. Coronaviruses: Springer; 2015. p. 1-23.

[10] Fong I. Emerging animal coronaviruses: First SARS and now MERS. Emerging Zoonoses: Springer; 2017. p. 63-80.

[11] Sohrabi C, Alsafi Z, O'Neill N, Khan M, Kerwan A, Al-Jabir A, et al. World Health Organization declares global emergency: A review of the 2019 novel coronavirus (COVID-19). International Journal of Surgery. 2020.

[12] Singhal T. A review of coronavirus disease-2019 (COVID-19). The Indian Journal of Pediatrics. 2020:1-6.

[13] Al-Khalaifah HS, Khalil AA, Amer SA, Shalaby SI, Badr HA, Farag MFM, et al. Effects of Dietary Doum Palm Fruit Powder on Growth, Antioxidant Capacity, Immune Response, and Disease Resistance of African Catfish, Clarias gariepinus (B.). 2020;10(8):1407.

[14] Rothan HA, Byrareddy SN. The epidemiology and pathogenesis of coronavirus disease (COVID-19) outbreak. Journal of autoimmunity. 2020:102433.

[15] Guo Y-R, Cao Q-D, Hong Z-S, Tan Y-Y, Chen S-D, Jin H-J, et al. The origin, transmission and clinical therapies on coronavirus disease 2019 (COVID-19) outbreak–an update on the status. Military Medical Research. 2020;7(1):1-10.

# STUDIES OF MUCOADHEZIVE MATRIXES BASED ON CHITOSAN AND *LYTHRUM SALICARIA* L. PLANT EXTRACT

**Ph. D. Student Irina Mihaela Iancu**[1]
**Assoc. Prof. Dr. Laura Adriana Bucur**[2]
**Assoc. Prof. Dr. Verginica Schröder**[3]
**Dr. Eng. Manuela Rossemary Apetroaei**[4]
**Assist. Dr. Valeriu Iancu**[5]
**Prof. Dr. Victoria Badea**[6]
[1, 6] Ovidius University of Constanta, Faculty of Dental Medicine, Department of Microbiology, Constanta, Romania
[2, 3, 5] Ovidius University of Constanta, Faculty of Pharmacy, Constanta, Romania
[4] Mircea cel Batran Naval Academy, Faculty of Navigation and Naval Management, Constanta, Romania

## ABSTRACT

The *Lythrum salicaria* L. plant, from the *Lythraceae* family, has multiple beneficial effects on the human body, through pharmacological properties imprinted by its secondary metabolites, namely tannins.

Chitosan-based biomedical materials are of increasing interest precisely due to the uniqueness of their properties, namely biocompatibility, nontoxicity, biodegradability, antimicrobial and antioxidant nature. The combination of chitosan with the plant extract aimed at obtaining new matrices, with clearly superior characteristics, compared to each material (chitosan and plant extract). This could be due to the presence of amino groups in the structure of chitosan, known to be active at a pH slightly acidic and which could be chemically bound to the phenolic groups of tannic acids (the predominant components of the plant extract).

The study aimed to obtain for the first-time mixtures of different concentrations of aqueous solutions of *Lythri herba* plant extract with standard chitosan 1 % in lactic acid (1 %) solution, which allowed achieving compatible and stable membranes. Microscopic evaluation of the membranes were made, following the uniformity of the surfaces, the homogeneity, the distribution of chitosan relative to the extract, and their stability in PBS saline buffer. The behavior of these membranes gives us a perspective on their use in dentistry and pharmaceuticals.

In addition, the current paper has shown the existence of chitosan in the composition of the obtained membranes and their ability to maintain constant hydration and flexibility over a certain period.

***Keywords:*** *chitosan, Lythri herba, membranes, epifluorescence microscopy*

## INTRODUCTION

*Lythrum salicaria* L. is a well-known medicinal plant since ancient times, used for conditions such as diarrhea and dysentery. Its name comes from the Greek word *lithron*, which means coagulated blood and probably refers to its hemostatic properties or the color of its flower and *salicaria* due to the shape of the leaves similar to that of willow species (Salix sp.) [1].

*Lythrum salicaria* L. is a rich source of polyphenols, including ellagitannins, flavonoids, flavan-3-oils, phenolic acids, and anthocyanosides [1], which adds value to the extracts of this plant species for medical applications.

At present, the scientific interest in the development of biodegradable films through elementary and easy methods has increased. Natural polymers, such as chitin, chitosan, cellulose, or gelatin have become an acceptable choice; due to the different advantages they have [2]. Chitosan is the most used biopolymer in medical fields due to its non-toxic, biodegradable, biocompatible, antimicrobial, antioxidant nature [3], as well as for its abundant availability and its low-cost [4].

Recent studies evaluate chitosan-based membranes in which plant extracts, or their secondary metabolites have been incorporated [5], precisely due to the increased ability of chitosan to form membranes [6] and its mucoadhesive property [7]. The ease of processing into gels, nanoparticles, microparticles, membranes, nanofibers, and even in the form of sponges is another advantage of chitosan [8].

Given the properties of the biopolymer and the reactivity of its amino groups, membranes made for the first time from weakly acidic solutions of standard chitosan (lactic acid 1%) in which were incorporated the aqueous extract with various concentrations of *Lythri herba*, are to be evaluated in terms of surface characteristics, stability, and hydration.

## MATERIALS AND METHODS

The materials used in this study were dry *Lythri herba* extract, obtained by the concentration method with rotavapor and lyophilization of the aqueous extract from the floral tips of *Lythrum salicaria* L. (harvested in August 2019, from Năvodari area, Dobrogea, Romania), and standard chitosan powder (from Sigma Aldrich) with medium molar mass (300-400 kDa) and deacetylation degree (DDA) between 75% - 85%.

*Obtaining membranes with 1% standard chitosan concentration in diluted lactic acid solutions and aqueous Lythri herba extract*

The mixture obtained from 1% standard chitosan (CS) in 1% lactic acid solution was poured on a Teflon support and placed in the oven at a temperature of 50 °C, for 3 hours. The standard chitosan membrane (1 %) obtained has a yellowish, uniform appearance and was chosen as a reference in this study. Similarly, by slightly mixing the acidic chitosan solutions with aqueous plant extract (v / v = 1: 1), standard chitosan membranes (1%) were obtained mixed with *Lythri herba* extract, of different concentrations (0.5 g/L, 1 g/L, and 2 g/L) and their colors were ranged from light brownish to the dark brown.

*Microscopic evaluation of new membranes obtained*

In order to perform this evaluation, fragments of a few mm from each membrane were sectioned, making preparations, which were subsequently observed with the Optika Microscopes Italy epifluorescence microscope, Series B-350, model B-353LD2 at magnitude X200, used in the field of fluorescence B (ex 450-480 nm.).

*The percentage hydration (%) determination of new membranes*

The hydration properties of the membranes were measured by evaluating their hydration degree using the improved method of Al-Dhubiab *et all*, (2016) [9]. The surfaces of 1 $cm^2$ with initial weight ($m_i$) were cut from membranes, immersed into a small volume of saline PBS phosphate-buffered and kept in an incubator at 37 °C temperature for 10, 20, and 30 minutes. After each time interval, the small pieces of membranes were removed from the solution, dried slightly, and weighed again ($m_f$). The percentage of membrane hydration was determined using the equation of Nair *et all*, (2013) [10]:

$$\text{Hydration (\%)} = \frac{m_f - m_i}{m_f} \cdot 100, \text{ where:}$$

$m_i$ = initial mass of the membrane, $m_f$ = final mass of the membrane after being kept in the buffer solution.

## RESULTS AND DISCUSSIONS

*Obtaining membranes with 1% standard chitosan concentration in diluted lactic acid solutions and aqueous Lythri herba extract*

The obtained membranes are mixtures of diluted acidic solutions with standard chitosan (1%) and aqueous *Lythri herba* extracts of different concentrations (0.5 g/L, 1 g/L and 2 g/L). Known for its many benefits, including regeneration [11], the plant offers potential in terms of developing products with mucoadhesive applications and gives protective, antibacterial and healing action in case of lesions of the oral mucosa.

Solubilized chitosan in the diluted lactic acid solutions (through the amino groups from its structure) has combined with extract components and the membranes obtained have a uniform appearance, slightly brownish color, due to the presence of tannins from the extract composition (Figure 1).

Suitable for the working protocol, the membranes obtained are according to Figure 1.

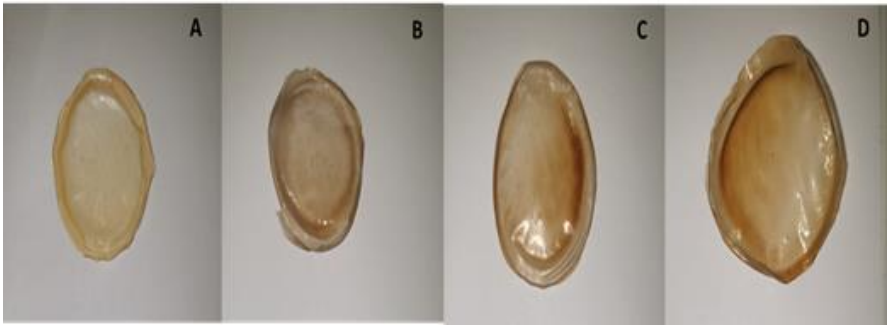


***Fig. 1.*** *1 % standard chitosan membranes (CS) in lactic acid and aqueous Lythri herba extract.* ***A****. 1 % CS membrane in lactic acid,* ***B.*** *1 % CS membrane in lactic acid with 0.5 g/L Lythri herba,* ***C.*** *1 % CS membrane in lactic acid with 1 g/L Lythri herba,* ***D.*** *1 % CS membrane in lactic acid with 2 g/L Lythri herba*

*Microscopic evaluation of new membranes obtained*

The microscopic analysis confirms the presence of chitosan in membranes, due to its ability to emit autofluorescence at the wavelengths specified above, stating that for this analysis no specific dyes are used. Furthermore, the epifluorescence microscopy clearly highlights the details of the multilamellar arrangement in parallel layers and the oblique arrangement of filaments specific to chitosan structures (Figure 2). In addition, the microstructure of these membranes has numerous porosities and the colored components of *Lythri herba* are visibly included in the membranes.

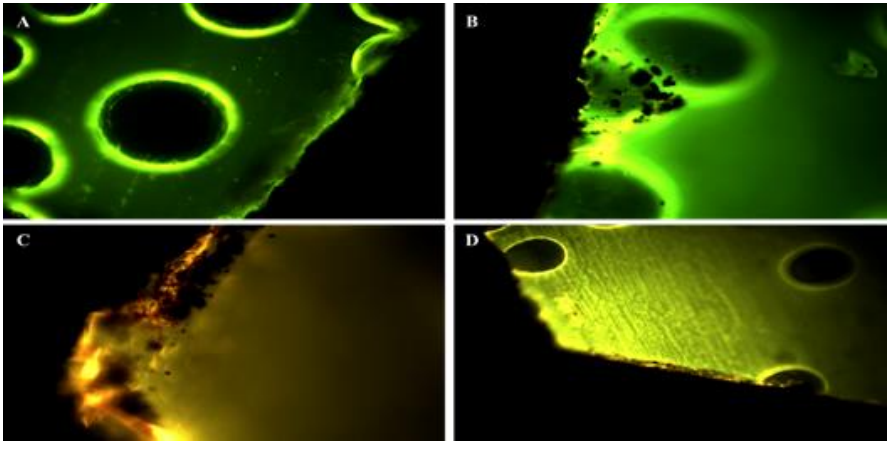


***Fig. 2.*** *Chitosan membranes in 1 % lactic acid solution under the epifluorescence microscope (x200),* ***A*** *–CS (1 %) membrane,* ***B*** *–CS (1 %) membrane with Lythri herba extract (0.5 g/L),* ***C*** *– CS (1 %) membrane with Lythri herba extract (1 g/L),* ***D*** *–CS (1 %) membrane with Lythri herba extract (2 g/L)*

*The percentage hydration (%) determination of new membranes*

In mucoadhesive applications, knowing the hydration degree for membranes is especially useful, as it could be an important preliminary aspect for other tests, such as biocompatibility. Our study highlights the structural stability and the possibility to establish a contact time between chitosan-extract mixtures and mucoadhesive surfaces.

Following exposure of the membranes in PBS buffer, an increase in their hydration was observed in the first 10 minutes after exposure, followed by stagnation in terms of weight in the following time intervals (Figure 3) compared to CS (1 %) membrane, chosen as a reference sample.

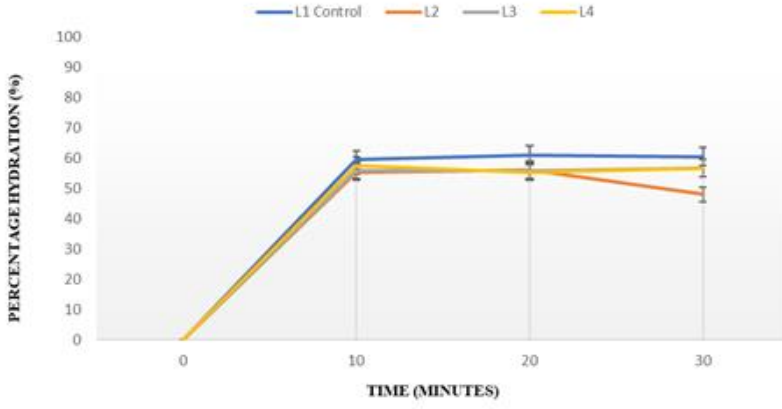


***Fig. 3.*** *Degree of hydration of CS (1 %) membranes in lactic acid solution tested as a function of time (minutes) (± SD).* ***L1*** *(CS in 1 % lactic acid ),* ***L2*** *(a mixture of CS 1 % in lactic acid + Lythri herba extract 0.5 g / L),* ***L3*** *(mixture of CS 1 % in lactic acid + Lythri herba extract 1 g/L),* ***L4*** *(mixture of CS 1 % in lactic acid + Lythri herba extract 2 g/L)*

At the time interval of 10 minutes, the membranes in lactic acid solution (1 %) appeared to be stable, without deformations, and showing a tendency to roll. The colors of the tested membranes, during hydration, did not have any noticeable change, which denotes the stability of the bonds (of chemical nature) between chitosan and the components of the analyzed extract.

At the time interval of 20 minutes all tested membranes in diluted lactic acid solution (1 %) exhibit stability, without deformations, but visibly they are much more flexible. Membrane L1, the reference sample (standard chitosan in 1 % lactic acid) is softer and more flexible than membranes with aqueous *Lythri herba* extracts (L2, L3, L4) incorporated. Compared to the membranes that remained in the alkaline buffer PBS for 10 minutes, it is no longer observed the same tendency of rolling of the edges; except for this observation of the L4 membrane is making (Figure 4).

At the hydration time interval of 30 minutes, the membranes in 1% lactic acid solution are visibly softer, without deformations, and no longer show the same

tendency to roll as the membranes after the time interval of 10 minutes, except for this observation making the L3 membrane, whose edges have rolled more.

Low mechanical resistance in water of standard chitosan (1 %) membranes were common points of the various studies performed [12], [13], a statement also proven in the current paper on the L1 membrane of standard chitosan (1 %) in 1 % lactic acid solutions.

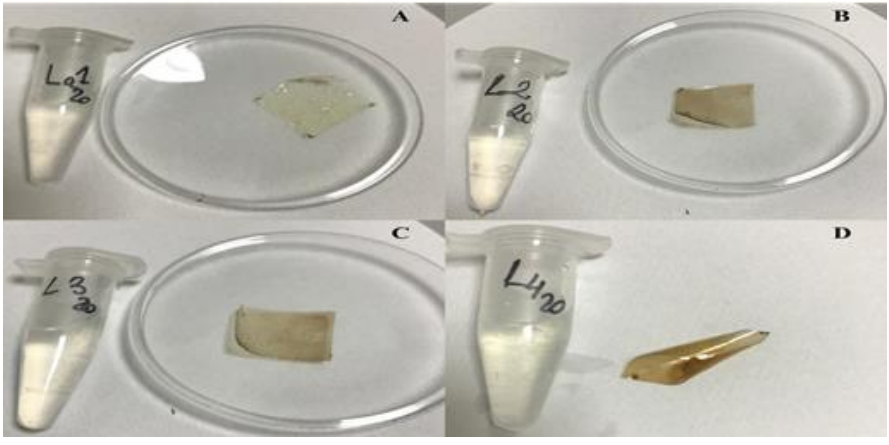


***Fig. 4.*** *CS membranes in 1% lactic acid tested.* ***A*** *- L1 (CS in 1 % lactic acid),* ***B*** *- L2 (mixture of CS 1 % in lactic acid + Lythri herba extract 0.5 g/L),* ***C*** *- L3 (mixture of CS 1 % in lactic acid + Lythri herba extract 1 g/L),* ***D*** *- L4 (mixture of 1 % CS in lactic acid + Lythri herba extract 2 g/L)*

This study presents strong stability and flexibility of the membranes made from the mixture of chitosan with *Lythri herba* extract. The results obtained confirm the hypothesis of the study to create from chitosan a favorable matrix for the compounds of the analyzed plant, to promote obtaining a resistant, and flexible system, but also with therapeutic potential induced by the components of Lythri herba extract.

The correlation between extract concentration and hydration stability of membranes reveals an interaction with chitosan, which is even higher as the extract quantity increases. This information is supported by data from the literature according to which chitosan interacts, through its amino groups, with some groups of polyphenols contained in plant extracts [14].

Our studies on the cytotoxic activity of the extract [15] showed low toxicity of *Lythri herba* solutions, which further strengthens the potential support that the extract could induce.

As a result, our study focused to obtain stable chitosan-extract membranes with promising applications for the therapy of mucosal surfaces or those interacting with aqueous solutions.

## CONCLUSION

To the best of our knowledge, this is the first time when membranes with potential in therapeutic applications are obtained by mixing in a compatible and stable ratio of solutions of standard chitosan (1%) in lactic acid (1%) with the aqueous solutions of *Lythri herba* plant extract.

Epifluorescence microscopy confirmed the presence of fluorescent chitosan in membranes and clearly showed its multilamellar, oblique, and superficial layer arrangement.

The membranes obtained for the first time showed constant hydration over time and had a flexible, elastic, and deformation-free behavior, these features are necessary for mucoadhesive biomaterials, to their use in the medical and pharmaceutical field.

Following the analyses carried-out, our study showed the therapeutic potential of *Lythrum salicaria* L., which could be improved by combining with chitosan, at appropriate concentrations in the form of membranes (mucoadhesive films), in order to increase the number of pharmaceutical or biomedical applications.

## REFERENCES

[1] Piwowarski, J. P.; Granica, S.; Kiss, A. K. Lythrum salicaria L. Underestimated medicinal plant from European traditional medicine. A review. *Journal of ethnopharmacology*, 2015, 170: 226-250.

[2] Sakthiguru, N., & Sithique, M. A. (2020). Fabrication of bioinspired chitosan/gelatin/allantoin biocomposite film for wound dressing application. *International journal of biological macromolecules*, 152, 873-883.

[3] İlk, S., Ramanauskaitė, A., Bilican, B. K., Mulerčikas, P., Çam, D., Onses, M. S., ... & Zang, L. S. (2020). Usage of natural chitosan membrane obtained from insect corneal lenses as a drug carrier and its potential for point of care tests. *Materials Science and Engineering*: C, 110897.

[4] Hu, Q., & Luo, Y. (2016). Polyphenol-chitosan conjugates: Synthesis, characterization, and applications. *Carbohydrate polymers*, 151, 624-639.

[5] Kaya, M., Khadem, S., Cakmak, Y. S., Mujtaba, M., Ilk, S., Akyuz, L., ... & Deligöz, E. (2018). Antioxidative and antimicrobial edible chitosan films blended with stem, leaf and seed extracts of Pistacia terebinthus for active food packaging. *RSC advances*, 8(8), 3941-3950.

[6] Bajić, M., Ročnik, T., Oberlintner, A., Scognamiglio, F., Novak, U., & Likozar, B. (2019). Natural plant extracts as active components in chitosan-based films: A comparative study. *Food Packaging and Shelf Life*, 21, 100365.

[7] Khutoryanskiy, V. V. Advances in mucoadhesion and mucoadhesive polymers. *Macromolecular bioscience*, 2011, 11.6: 748-764.

[8] Ahmed, S., & Ikram, S. (2016). Chitosan based scaffolds and their applications in wound healing. *Achievements in the life sciences*, 10(1), 27-37.

[9] Al-Dhubiab, B. E., Nair, A. B., Kumria, R., Attimarad, M., & Harsha, S. (2016). Development and evaluation of buccal films impregnated with selegiline-loaded nanospheres. *Drug Delivery*, 23(7), 2154-2162.

[10] Nair, A. B., Kumria, R., Harsha, S., Attimarad, M., Al-Dhubiab, B. E., & Alhaider, I. A. (2013). In vitro techniques to evaluate buccal films. *Journal of Controlled Release*, 166(1), 10-21.

[11] Jouravel, G., Guénin, S., Bernard, F. X., Elfakir, C., Bernard, P., & Himbert, F., New biological activities of *Lythrum salicaria* L.: Effects on keratinocytes, reconstructed epidermis and reconstructed skins, Applications in dermo-cosmetic sciences. *Cosmetics*, 2017, 4(4), p. 52

[12] De Masi, A., Tonazzini, I., Masciullo, C., Mezzena, R., Chiellini, F., Puppi, D., & Cecchini, M. (2019). Chitosan films for regenerative medicine: fabrication methods and mechanical characterization of nanostructured chitosan films. *Biophysical Reviews*, 1-9.

[13] Hps, A. K., Saurabh, C. K., Adnan, A. S., Fazita, M. N., Syakir, M. I., Davoudpour, Y., ... & Dungani, R. (2016). A review on chitosan-cellulose blends and nanocellulose reinforced chitosan biocomposites: Properties and their applications. *Carbohydrate polymers*, 150, 216-226.

[14] Jing, Y., Diao, Y., & Yu, X. (2019). Free radical-mediated conjugation of chitosan with tannic acid: Characterization and antioxidant capacity. *Reactive and Functional Polymers*, 135, 16-22

[15] Iancu, I., M., Bucur, L., A., Schroder, V., Mireșan, H., Mihai, S., Iancu, V., Badea, V., Phytochemical evaluation and cytotoxicity assay of Lythri herba extracts, *Farmacia*, 2021, 69(1), 51-58

# STUDIES ON THE MORPHO-ANATOMICAL PARTICULARITIES OF *LYSIMACHIA NUMMULARIA* L.

**Suciu Felicia**[1]
**Arcuș Mariana**[2]
**Roșca Adrian Cosmin**[3]
**Bucur Laura**[4]
**Popescu Antoanela**[5]
**Badea Victoria**[6]
[1, 2, 3, 4, 5] Faculty of Pharmacy, Ovidius University of Constanta, Romania
[6] Faculty of Dentistry, Ovidius University of Constanta, Romania

## ABSTRACT

The objective of the study was the histo-anatomical analysis of the root, stem and leaf belonging to the species *Lysimachia nummularia* L. from the *Primulaceae* family.

The plant is native to Europe, but has been introduced to North America, where it is considered an invasive species in some areas. It aggressively spreads in favorable conditions, such as low wet ground or near ponds. It is moderately difficult to remove by hand pulling. Any tiny piece left behind will regrow. The research results led to the following assessments: root with primary structure and beginning of secondary structure, the presence of calcium oxalate druze in the bark, endoderm and primary type conducting bundles. The results of the study also demonstrated the existence of the stem with four prominent ribs, a meatic-type bark with small secretory channels and a central cylinder with a secondary structure. Another element studied from a histo-anatomical point of view; leaf with dorsi-ventral bifacial structure, with heterogeneous asymmetrical structure, collateral free-woody bundle, without periectors. From the morpho-anatomical data described, it can be concluded that the species *Lysimachia nummularia* L. belongs to the family *Primulaceae* and is related to other species of the genus *Lysimachia.*

***Keywords:*** *Lysimachia, Primulaceae, microscopy, vegetative organs.*

## INTRODUCTION

*Lysimachia nummularia* L. (*Primulaceae*) (Figure 1), is a herbaceous, perennial, chamefite plant, widespread in our country, in wetlands, in meadows and on the waterfront, through bushes and meadows, ditches and micro-depressions in mountain, hill and plain regions. Globally it is found in Europe, the Caucasus, introduced in Japan and North America.

According to the classification system proposed by Cronquist [2], Takhtajan [3] and Zimmerman [4], accepted by Ehrendorfer [5, 6] and adopted and supplemented by I. Pop et al., *Lysimachia nummularia* L. [7], has the following systematic classification [8]: *Magnoliophyta*, Class *Magnoliatae*, Subclass

*Dilleniidae*, Order *Primulales*, Family *Primulaceae*, Genus *Lysimachia*, Species *nummularia* L.

Known since antiquity, the plant was discovered by Lysimachus (in Pliny the Elder), and its name is also found in Dioscorides as Lysimacheios, indicating a species of the genus *Lysimachia*, probably given in honor of the Thracian king, Lysimachus. The green parts of the plant contain hemolytic saponosides, tannins, flavonosides, phenolic acids, polyuronides, which is why it has medicinal uses both internally and externally [9].

Popularly known as yolk or straight, *Lysimachia nummularia* L, has a sudden, glabrous stem, round opposite leaves and solitary, yellow axillary flowers [10].

In the present study, we aimed to identify and describe the anatomical structure of vegetative organs in order to identify the peculiarities of *Lysimachia nummularia* L, necessary to differentiate the peculiarities of the plant species from other species of the genus *Lysimachia*.

## MATERIAL AND METHOD

The fresh plant was harvested on July 19, 2020, from the edge of Lake Tău-Brazi in the Roșia Montană area of Alba County (Figure 2), where the yolk forms large associations (Figure 1). In order to research from a histo-anatomical point of view, the material represented by the vegetative organs (root, stem and leaves) was subjected to several stages of work. Fixation and preservation of the fresh material was performed in 70% ethyl alcohol. The sectioning was done manually, with the help of the hand microtome and the botanical razor, using as support the elderflower marrow.

The obtained sections were subjected to the bleaching process (with sodium hypochlorite) for 20-35 minutes, after which they were washed with acetic water and distilled water [11], [12]. The sections were then stained with iodine green and ruthenium red (staining used in plant histo-anatomical studies) as follows: The sections were first stained with iodine green (1 minute), washed with 90% ethyl alcohol, and then stained with ruthenium red (1 minute) and finally washed with distilled water [13], [14].

The colored sections were mounted in drops of glycerol gelatin, between the slide and the slide, thus making permanent preparations. After the preparations thus obtained, color photographs were taken with the OPTIKA photon microscope, with Canon A540 digital camera. Scale for photographs = 100 μm.

***Fig. 1.*** *Plant association with straight*

***Fig. 2.*** *Lysimachia nummularia L.*

## RESULTS AND DISCUSSIONS

***Cross section through the root***

The following characters are distinguished:

- the contour of the section is circular, slightly wavy (Figure 3);
- the structure is primary with the beginning of secondary structure, due to the presence of a multilayered suber formed of cells with thin walls (Figure 4);

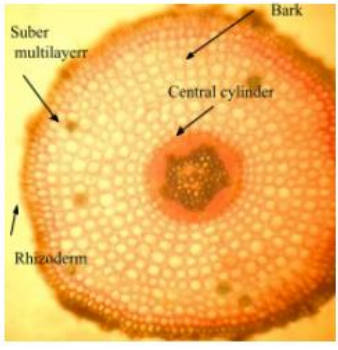


***Fig. 3.*** *Cross section through the root of Lysimachia nummularia L. (6x)*

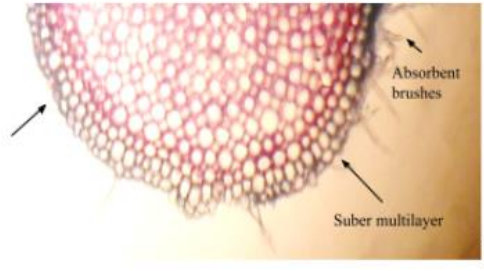


***Fig. 4.*** *Cross section through the root of Lysimachia nummularia L. (10x) -detail*

On the outside there is a rhizoderm, formed by a single layer of cells with external walls slightly thicker than the others, covered by a cuticle that forms a characteristic relief; some cells turned into single-cell absorbent hairs. The primary bark is very thick, comprising 8-10 layers of round oval cells, with thin cellulosic walls and intercellular spaces; it is differentiated into exoderm, cortical parenchyma and endoderm; the cells are larger in the middle of the bark and smaller outwards and inwards (Figure 4).

The exoderm, well highlighted, is unistratified, with large cells, slightly elongated radially, with moderately thickened and suberified walls.

The cortical parenchyma is compact and moderately cholenchymatized to the exoderm, but for the most part it has cells of circular contour, with thin walls, leaving small intercellular spaces between them, forming a true meatic parenchyma; cells with calcium oxalate dredges are observed in some places:

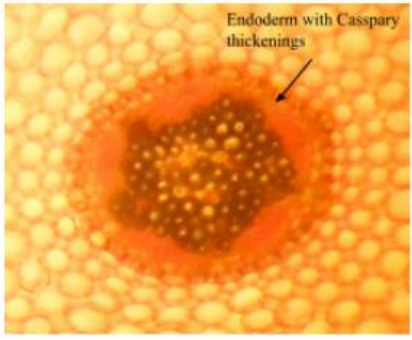


***Fig. 5.*** *Cross section through the root of Lysimachia nummularia L. Endoderm with Casspary thickenings (100x)*

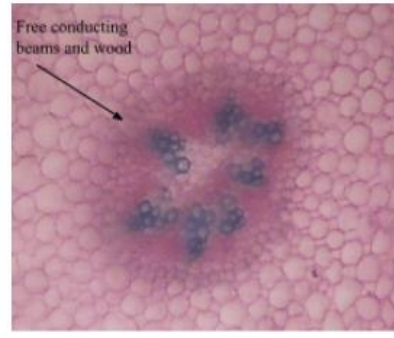


***Fig. 6.*** *Cross-section through the root of Lysimachia nummularia L. Free-conducting beams and wood (100x)*

The last layer of the bark is a primary type endoderm, with the cells elongated tangentially and arranged in an orderly manner, alternating with those of the pericycle; shows obvious lenticular thickenings (Casspary thickenings) (Figure 5);

The central cylinder, located deep, starts with a unilayered pericycle, on which 5-7 wooden beams rest, alternating with as many free beams included in the fundamental parenchyma of the central cylinder (Figure 6); the liber consists of Liberian vessels (sieved tubes), attachment cells and Liberian parenchyma; the wooden fascicles are formed by wooden vessels of meta and protoxylem and very few wooden parenchyma cells; the metaxillem vessels go to the center of the root, occupying part of the spinal cord; the marrow, interrupted by a group of metaxillem vessels, consists of medullary parenchyma of the meatic type.

***Stem cross section***

The cross section through the stem has the following characters:

The contour of the cross section is elliptical-oval, with four visibly prominent ribs at the ends (Figure 7); on the outside there is a single-layered epidermis, formed by isodiametric cells, with domed external walls; they have a round-square shape, are uniformly thickened all around and covered by a thin ribbed cuticle; from place to place there are stomata formed by cells slightly smaller than the cells of the epidermis (Figure 8);

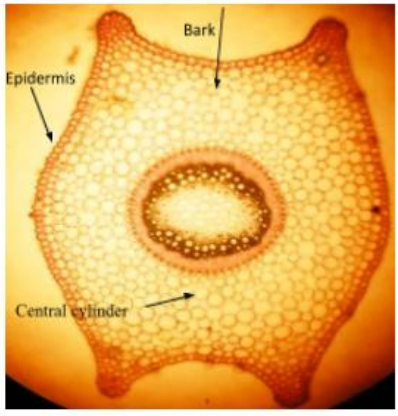


***Fig. 7.*** *Cross section through the stem of the species Lysimachia nummularia L. (100x)*

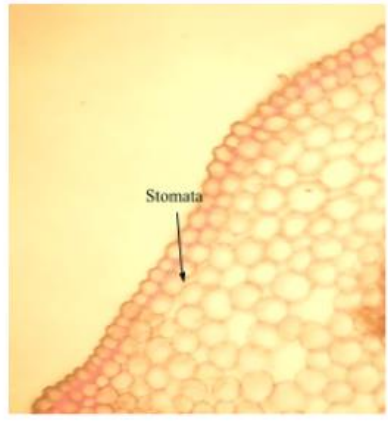


***Fig. 8.*** *Cross section through the stem of the species Lysimachia nummularia L. Detail from the epidermis (100x)*

The bark is parenchymal-cellulose of meatic type, with rounded cells, bigger and bigger inwards; from place to place it has wide air spaces between cells and small secretory canals; the hypodermic layer, slightly cholenchymatized consists of cells smaller than the rest of the bark; near the ribs the thickening process is more pronounced than in the rest of the hypodermis;

The innermost layer of the bark is a primary type endoderm, with its thickening of the Casspary visible and made up of cells of different sizes; the central cylinder consists of conductive tissues of secondary origin, arranged in an annular and represented by an outer ring of free secondary and an inner ring of secondary wood, which arose from the activity of the bill of exchange; it does not start with a special type of danger; the free ring is slightly thinner than the wooden one; the wooden ring has discontinuities, in which thicker areas, consisting of several vessels, alternate with thinner portions, consisting of fewer vessels and of smaller caliber.

The secondary free ring consists of sieved tubes, attachment cells and Liberian parenchyma cells.

The wooden ring consists of protoxilem vessels, towards the outside and metaxilem vessels, towards the center of the cord; the vessels are arranged in series, in order and are surrounded by cellulosic woody parenchyma; the medullary rays are narrow, relatively unobvious.

The marrow is thick, parenchymal-cellulosic, meatic type, consisting of two types of cells: very large, in the center of the spinal cord and very small at its periphery, some cells at the periphery of the spinal cord are oxaliferous (Figure 8).

***Leaf cross section***

The leaf cross section has the following characters:

- in cross section, the median rib is prominently visible at the abaxial face of the tongue, and at the adaxial face there is a slightly deepened groove (Figure 9);
- at the level of the nerve there is a single hypodermic layer of colenchyma, a fundamental parenchyma formed by large isodiametric cells with thin parts and large intercellular spaces, and in the center, a large, free-wood beam with primary structure, next to which appears a beam of very small dimensions (Figure 10);
- the conducting beam is surrounded by a unilayered parenchyma sheath, formed by uniformly arranged cells; it consists of a free cord, towards the lower epidermis and a wooden cord, towards the upper epidermis; under the free cord is a sclerenchyma sheath;

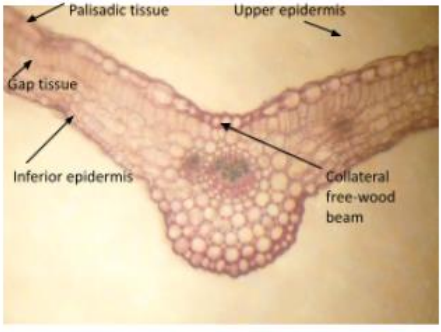


***Fig. 9.*** *Cross section through the leaf of the species Lysimachia nummularia L. (100 x)*

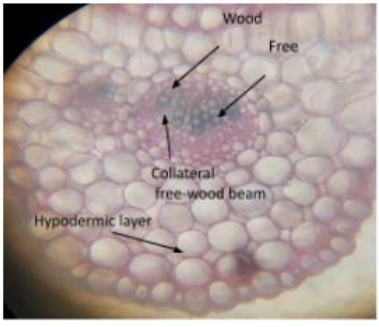


***Fig. 10.*** *Cross section through the leaf of the species Lysimachia nummularia L. Detail of the median rib (100x)*

- the release cord has sieved tubes, attachment cells and Liberian parenchyma;
- the wooden cord consists of radial rows of proto- and metaxillem vessels, separated by cellulosic woody parenchyma (Figure 8);
- the upper epidermis consists of a single layer of very large, vesicular cells, of different sizes, with the outer wall thicker than the others and covered by a very thin cuticle; from place to place there are stomata, less than in the lower epidermis; tector brushes are missing (Figure 10);
- the lower epidermis, formed by a single layer of cells, has larger cells at the level of the median nerve, but of different sizes, and at the level of the tongue, much smaller cells; all are interrupted by stomata.

- the mesophile has 5-6 layers of cells and consists of a unistratified palisade on the upper face (the cells being 3-4 times higher than wide) and a lacunar multilayered parenchyma on the lower face;
- the limb has a dorsoventral bifacial structure.

## CONCLUSION

The analysis of the cross sections through the vegetative organs of the species *Lysimachia nummularia* L. showed that the analyzed species has a structure characteristic of the group to which it belongs, respectively of the *Primroses*. Thus, the root has a primary structure with a little developed central cylinder, the 6-7 wooden bundles, alternating with the free ones.

The endoderm has lenticular thickenings (Casspary punctuation); the primary endoderm shows obvious Casspary scores.

The bark is of the meatic type with large intercellular spaces and cells with calcium oxalate dredges.

The stem has the contour of the elliptical-oval cross section, at the ends with four visibly prominent ribs. The leaf has epidermis covered by an obvious cuticle, asymmetric heterogeneous mesophilic, is devoid of periectors and has a dorsiventral bifacial structure with unistratified palisade tissue.

The conducting beam is of the collateral type, consisting of a free cord, towards the lower epidermis and a wooden cord, towards the upper epidermis; under the free cord there is a sclerenchymal sheath.

## REFERENCES

[1] Săvulescu T. et al., Flora R.P.R., vol. VII, Acad. R.P.R., 1960, 42-46.

[2] Cronquist A., The evolution and classification of flowering plants, Botanical Garden, New York, 1988.

[3] Takhtajan A.L., Diversity and classification of flowering plants, Koeltz, Konigstein, 1996.

[4] Zimmermann W., Die phylogenie der Pflanzend, G. Thieme Verlag, Stuttart, 1959.

[5] Ehrendorfer F., Closing remarks: systematics and evolution of Centrospermous families, Plant Syst. And Evol., Volume 126, 1971, 99-105.

[6] Ehrendorfer F., Samenpflanzen, Strasburger, s Lehrbuch der Botanik, 32, Aufl. Stuttgart, New York, 1983.

[7] Pop I., Hodișan I., Mititelu D., Lungu L., Cristurean I., Mihai Gh., Systematic Botany, Didactics and Pedagogy, Bucharest, 1983, p. 419.

[8] Ștefan N., Ivănescu Lăcrămioara, Elements of morphology and vegetal taxonomy, Univ. Al. I. Cuza, Iași, 2002, p. 345.

[9] Pârvu C., Enciclopedia plantelor, volume II, Tehnică, București, 2003, 77.

[10] Ciocârlan V., The illustrated flora of Romania. Pteridophyta et Spermatophyta, 3rd ed., Ceres, Bucharest, 2009, 1067.

[11] Sîrbu I., Ștefan N., Oprea A., Vascular plants from Romania, illustrated field determiner, Victor B, Bucharest, p. 554.

[12] Andrei M., Paraschivoiu R. M., Botanical Microtechnics, Niculescu, Bucharest, 2003.

[13] Șerbănescu-Jitariu G., Andrei M., Mitroiu-Rădulescu Natalia, Petria Elena. Practicum of plant biology, Ceres Publishing House, Bucharest, 1983.

[14] Toma C., Gostin I., Vegetal H., Junimea Publishing House, Iași, 2000.

# TESTING THE BIOLOGICAL ACTIVITY OF *LYTHRI HERBA* EXTRACT FOR APPLICATIONS IN MEDICAL BIOTECHNOLOGIES

**Ph. D. Student Irina Mihaela Iancu**[1]
**Assoc. Prof. Dr. Laura Adriana Bucur**[2]
**Assoc. Prof. Dr. Verginica Schröder**[3]
**Dr. Eng. Manuela Rossemary Apetroaei**[4]
**Assoc. Prof. Dr. Horațiu Mireșan**[5]
**Prof. Dr. Victoria Badea**[6]
[1, 6] Ovidius University of Constanta, Faculty of Dental Medicine, Department of Microbiology, Constanta, Romania
[2, 3, 5] Ovidius University of Constanta, Faculty of Pharmacy, Constanta, Romania
[4] Mircea cel Batran Naval Academy, Faculty of Navigation and Naval Management, Constanta, Romania

## ABSTRACT

Nowadays we are witnessing an increased interest in phytotherapy and implicitly for herbal products that have lower side effects. One medicinal plant whose popularity has decreased significantly in recent years is *Lythrum salicaria* L., loosestrife, known in Romanian traditional medicine for its beneficial effects against gastrointestinal diseases.

The aim of this study is to evaluate the biological activity of three different extracts (aqueous, alcoholic, acetonic) from the flower tips of *Lythrum salicaria* L. using the BSLA (Brine Shrimp Lethality Assay) test and the antimicrobial activity of the extracts on two reference bacterial strains which are important for the medical field (*Staphylococcus aureus* and *Escherichia coli*) through the diffusimetric method.

We demonstrated the fact that the *Lythri herba* plant product extracts (aqueous, alcoholic, and acetonic) lack acute toxicity, as well as the moderate antibacterial effect on the *Gram-positive* reference strain, *Staphylococcus aureus*, thus highlighting the possibility of using the plant in biomedical applications.

***Keywords:*** *Lythri herba, antibacterial activity, Artemia salina.*

## INTRODUCTION

Medicinal plants are rich sources of biologically active compounds, are easy to procure, and are inexpensive. For these reasons, they continue to have a growing interest in the research and development of new antibacterial and antifungal products, for which no resistance has developed.

Basically, the chemicals produced by plants are divided into two categories, primary and secondary metabolites. Primary metabolites are involved in the

synthesis of the basic elements of the plant, while secondary metabolites are involved in the defense mechanism of the plant against various microbial infections. Important secondary metabolites in medicine include flavonoids, alkaloids, terpenes, tannins, and phenolic compounds. Unlimited opportunities for drug discovery have been offered by plant extracts, whether they are pure compounds or standardized extracts, due to their chemical diversity [1].

*Lythrum salicaria* L. (*Lythraceae* family) is a plant species known in traditional European medicine for its healing effects against dysentery, diarrhea, intestinal inflammation, hematuria, leukorrhea, epistaxis, dysmenorrhea, lupus, eczema, anemia, urogenital inflammation, hemorrhoids, diseases of the gastrointestinal tract, colitis and stomatitis [2].

Studies on the bioactivity of extracts from the *Lythrum salicaria* L. plant began in the nineteenth century and highlighted pharmacological effects such as antidiarrheal, anti-inflammatory, antioxidant, antimicrobial, hemostatic, metabolic, antihypertensive, and hypoglycemic effects [3].

The antimicrobial activity of *Lythrum salicaria* L. plant extracts was investigated against pathogenic species such as *Candida albicans*, *Micrococcus luteus*, *Bacillus subtilis*, *Escherichia coli*, *Pseudomonas aeruginosa*, *Staphylococcus aureus*, *Staphylococcus epidermis*, *Proteus mirabilis* [4].

Cytotoxicity studies are the first useful step in determining the potential toxicity of a test substance, including plant extracts or biologically active compounds isolated from plants. Minimal or no toxicity is essential for the successful development of pharmaceutical or cosmetic preparation and, in this regard, cell toxicity studies to play crucial roles [5].

The low cytotoxic activity of extracts (aqueous and hydro-ethanolic) from the *Lythrum salicaria* L. (*Lythri herba*) plant, highlighted by the BSLA (Brine Shrimp Lethality Assay) test in previous studies, allowed important assessments of the possibility of using the extract in biomedical applications [6].

Starting from these data, the current paper aimed to evaluate the biological effects induced by extracts (aqueous, ethanolic, and acetonic) from the floral tips of the *Lythrum salicaria* L plant species.

The study was performed on the "*in vivo*" model BSLA (Brine Shrimp Lethality Assay) to indicate cytologically induced manifestations, as well as on two bacterial strains of medical importance (*Staphylococcus aureus* and *Escherichia coli*) [7] for the preliminary evaluation of antimicrobial activity and modern perspectives [8].

## MATERIALS AND METHODS

*Obtaining plant extracts*

The floral tops of the Lythrum salicaria L. plant, harvested in July 2020 from the Năvodari area, Constanța, Romania, were cleaned and then dried at room temperature, in the shade. The plant material was then extracted with different

solvents (water, 96% ethyl alcohol, and pure acetone) by refluxing for two hours and then filtered through filter paper. After filtration, the aqueous extractive solution was concentrated by rotavapor and lyophilized, and the alcoholic and acetonic extractive solutions were left in porcelain capsules to evaporate under a niche. The dry extracts obtained were stored in sealed glass vials in the desiccator until the next evaluations could take place.

Evaluating the cytotoxicity of the plant extracts by BSLA test

The larvae were obtained by incubating cysts of *Artemia* sp. (Hobby, Grafschaft, Germany), in artificial salt water (35 ppm), with aeration and continuous lighting. The larvae from stage I naupliar, obtained after hatching, in the first 24 hours, were introduced in the test vessels. Between 15 - 20 specimens of stage, I larvae were transferred to each well of the test microplates and evaluated under a stereomicroscope (Optika B-350, Italy) every 24h.

Concentrations of 50, 100, 200, 250, 300 µl / mL of each extract were analyzed in a total volume of 1 mL. Larvae introduced into saline without extract were evaluated as negative control samples.

The plant extracts (alcoholic and acetonic) were solubilized in 0.1 % dimethylsulfoxide solvent (DMSO), achieving a ratio of 1:20 (v:v). The *Artemia salina* L. larvae were not fed throughout the test period (48 hours), thus avoiding interaction between test solutions and their food. The larvae were assessed for motility, survival, or mortality within 24 hours of testing. Statistical analysis was performed with StatPlus Mac Pro, version v6, Analyst Soft Inc statistical analysis program for MacOS.

Microscopic observations were made on living organisms, the preparations being analyzed directly, the larvae being transparent.

Antimicrobial evaluation of plant extracts, using the diffusimetric method

Two reference bacterial strains were chosen, namely *Staphyloccocus aureus*, a *Gram-positive*, aerobic, unencapsulated coke, also called "superbacteria", because it no longer responds to the action of many antibiotics, and *Escherichia coli*, a *Gram-negative* bacterium from the enterobacteria group. Further information on microbial strains is provided in **Table 1**.

***Table 1.*** *Microbial species, reference source, cultivation medium and assay medium*

| Microbial species | Reference source | Cultivation medium | Assay medium |
|---|---|---|---|
| *Staphylococcus aureus* | ATCC* 29213 | Columbia + 5 % sheep blood** | Mueller-Hinton*** |
| *Escherichia coli* | ATCC* 25922 | Columbia + 5 % sheep blood** | Mueller-Hinton*** |

Note:*ATCC - American Type Culture Collection,
** Columbia + 5 % sheep blood – Lot 64379472,
*** Mueller-Hinton – Lot 64372104.

The antimicrobial activity was determined by the diffusion method in a culture medium seeded with the reference strains we mentioned in the table above.

On the Petri dishes, each bacterial strain used was seeded in the Mueller-Hinton medium, then the plate was divided into four equal parts in which sterile filter paper rounds impregnated with constant volumes (10 µl) were applied with sterile tweezers from each test solution (negative control solvent DMSO 10%, aqueous extract, ethanolic and acetonic solubilized in DMSO 10%). The plates were then thermostated at 37°C for 24 hours. Following this, each diameter of the inhibition area around the filter paper impregnated in the test substance was recorded. The expression was performed using the grades "sensitive" (S), "intermediate" (I), and "resistant" (R) to the action of the extracts tested by *Lythri herba*.

## RESULTS AND DISCUSSIONS

*Obtaining plant extracts*

*Lythri herba* plant product extracts (aqueous, alcoholic, acetonic) were obtained according to the following image (**Figure 1**) and their phytochemical composition was synthesized in **Table 2** depending on the nature of the solvent according to the literature.

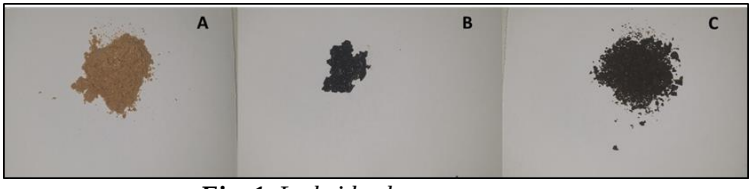


***Fig. 1.*** *Lythri herba extracts*
***A*** *– Aqueous extract,* ***B*** *– Alcoholic extract,* ***C*** *– Acetonic extract.*

*Table 2 – Phytochemical profile of the Lythri herba extracts*

| *Lythri herba* extracts | Contents | References |
|---|---|---|
| Aqueous | • total polyphenols (16.39 %)<br>• tannins (10.53 %)<br>• anthocyanins (0.3598 %) | [6] |
| Alcoholic | • total polyphenols (8.3-27.3 %)<br>• tannins (6.6-21.9 %) | [4] |
| Acetonic | • total polyphenols (278 ± 3.04 mg gallic acid equivalents/g extract)<br>• flavonoids (4.38 ± 0.13 mg rutin equivalents/g extract)<br>• hydroxycinnamic acids (69.6 ± 0.81 mg caffeic acid equivalents/g extract)<br>• condensed tannins (not detected) | [9] |

*Evaluating the cytotoxicity of the plant extracts by BSLA test*

The plant is known to have a complex composition. It is appreciated due to its polyphenols, tannins, flavonoids, phenolic acids, etc. content [3].

At the same time, more and more studies reveal different pharmacological effects given both the solvent used in the extraction and the model ("*in vivo*" or "*in vitro*") used for evaluation [10].

The effects observed during the experiment show differences which correlate with the level of concentrations (**Figure 1**), for both extracts. Important and quantified manifestations were those related to the motility of the tested organisms, respectively the reduction of swimming and the appearance of jerky, spasmogenic movements. The changes were identified after 20 hours of exposure and persisted in the same percentage until the end of the experiment (24 hours).

Sublethal manifestations of larvae were recorded during the observations. The lack of acute toxicity is explained by the low toxicity of the *Lythri herba* extract, but also by the dilutions obtained in DMSO.

The alcoholic extract (ALCLy) analyzed induced percentage increases of quantified effects (jerky movements), but below the 50% mark, at concentrations between 50 µl / mL and 250 µl / mL. However, the decreases of these manifestations at the maximum tested concentration of 300 µl / mL are surprising. The explanations can be given by the high level of carbohydrates and proteins [10] which, possibly, blurred the discomfort created to the larvae by other phytochemicals.

The jerky motility can be compared to muscle spasms, the larvae have cells similar to myocytes with which they ensure swimming movements. In the literature, the spasmogenic effects of the extract have been mentioned and studied. Thus, the "*in vivo*" studies of Bencsik, T., from 2014 correlated the contractions of the smooth intestinal muscles with the level of caffeic acid or catechin in the extract. It has also been observed that alcoholic extract of *Lythri herba* induces acetylcholinesterase (ACE) inhibition [10]. ACE inhibition may also be possible in these tested organisms, which would explain the altered movements of the larvae.

The enzyme acetylcholinesterase (ACE), is present in these organisms since the embryonic period and has a significant increase in the early stages of larval development [11].

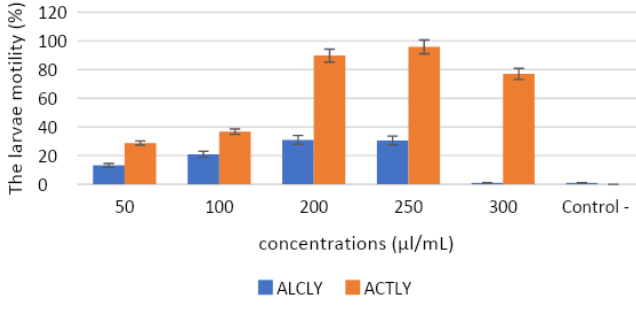


***Fig. 1.*** *The larvae abnormal motility evaluated (%), after 24 h exposure (ALCLy- alcoholic extract of Lythri herba, ACTLy – acetonic extract of Lythri herba)*

The acetone extract is less known in terms of its biological effect. Observations show an increase in abnormal manifestations of motility (**Figure 1**), in a significant proportion (76-95%). The effects are recorded at high concentrations (200, 250, 300 µl / mL) (**Figure 1)**, compared to larvae exposed to 50 and 100 µl / mL, as well as to control samples, without extract.

Statistical analysis indicates a linear stimulus-effect correlation for organisms exposed to concentrations between 50-250 µl / mL of alcoholic extract - ALCLy (Fig. 2 A), ($p < 0.001$) and at concentrations between 50-300 µl / mL of acetonic extract -ACTLy (Fig. 2 B), and the prediction has statistical significance [12], [13].

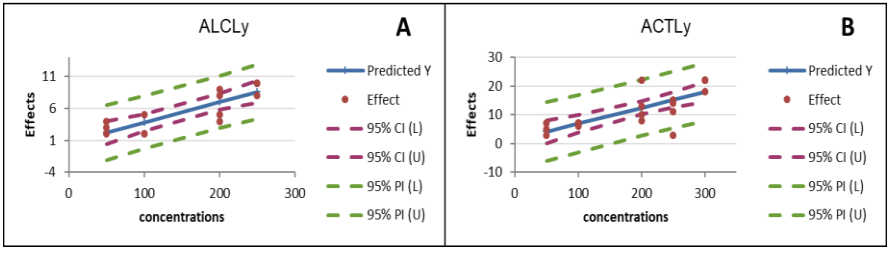


***Fig. 2.*** *Representation of the tested larvae response* ***A*** *- in the alcoholic extract (ALCLy) by linear regression (CI - 95% Confidence Interval, PI -95% Prediction Interval, p - value = 0.00037),* ***B*** *- in the acetonic extract (ACTLy) by linear regression (CI - 95% Confidence Interval, PI - 95% Prediction Interval, p-value = 0.00016*

In addition to the response related to the change in larval motility, observations on cytomorphology were made. The analysis was relevant by observing general changes in the larval body as well as inhibiting organogenesis and appendicular buds, respectively (**Figure 4, A-F**).

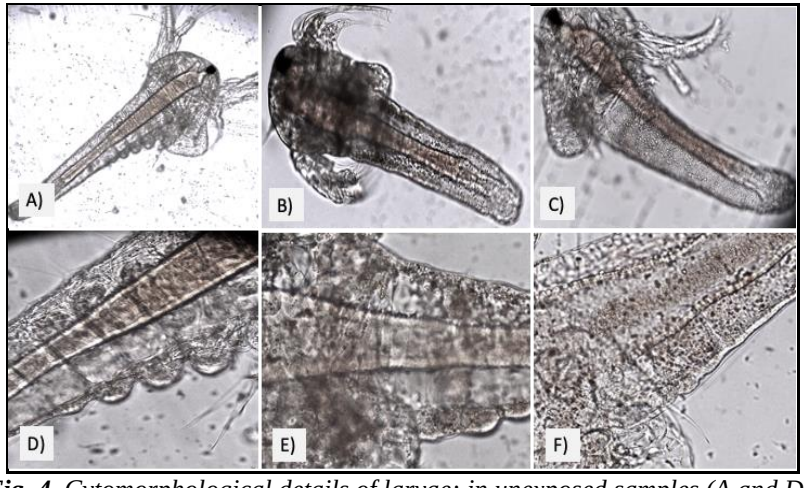


***Fig. 4.*** *Cytomorphological details of larvae: in unexposed samples (A and D), exposed in ALCLy (B, E), and acetone (C, F); magnification x100 (A); x200 (B, C); x400 (D, E, F)*

*Antimicrobial evaluation of plant extracts, using the diffusimetric method*

The results obtained from the evaluation of the antibacterial action of the *Lythri herba* aqueous, ethanolic, and acetonic extracts are summarized in **Table 3**.

***Table 3.*** *Diameters of inhibition areas (mm) of Lythri herba extracts and control on bacterial cultures (mean ± SD)*

| Microbial species | ATCC | DMSO (mm) | Aqueous extract (mm) | Ethanolic extract (mm) | Acetonic extract (mm) |
|---|---|---|---|---|---|
| *Staphylococcus aureus (G+)* | 29213 | 0 | R (9.66 ± 1.52) | R (9.66 ± 2.08) | S (17.66 ± 1.52) |
| *Escherichia coli (G-)* | 25922 | 0 | R (< 5 mm) | R (< 5 mm) | R (< 5 mm) |

*Note: 10 % DMSO solvent has no inhibitory effect, R – resistant, S – sensitive.*

As can be seen in **Table 3**, all three *Lythri herba* extracts do not generate areas of inhibition for the *Gram-negative* species studied, namely *Escherichia coli*. In the case of the *Gram-positive* species (*Staphylococcus aureus*) only the acetonic extract has the largest inhibitory zone, unlike the much smaller inhibitory diameters and resistant mutants of the aqueous and ethanolic extracts. The 10 % DMSO solvent used to solubilize the extracts obtained did not show an inhibitory effect.

These observations are also supported by the following conclusive images (**Figure 5**).

In the review of Piwowarski J. (2015) it was observed that the inhibition area for *Escherichia coli* of various *Lythri herba* extracts is between 0 - 15 mm, and for *Staphylococcus aureus* it is between 0 - 30 mm. The differences between the values of the areas of inhibition on these bacterial strains are due to the extraction methods and the various solvents used on the *Lythrum salicaria* L. plant [3].

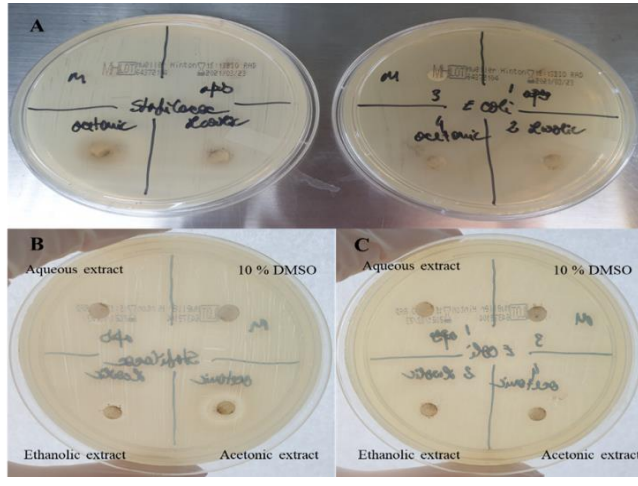


***Fig. 5.*** *Lythri herba extracts (aqueous, ethanolic, and acetonic) effects on Staphylococcus aureus and Escherichia coli (**A**), Staphyloccocus aureus (**B**), Escherichia coli (**C**)*

The values obtained in this paper are similar to the results of the 2021 study by Turker A. U. et all. [2] in which *Staphyloccocus aureus* was shown to be sensitive

to the action of aqueous and alcoholic *Lythri herba* extracts, and the representative of *Gram-negative* bacteria, namely *Escherichia coli*, to demonstrate total resistance to both extracts (aqueous and alcoholic) solubilized in DMSO.

## CONCLUSION

Evaluating the biological activity of *Lythri herba* extracts (aqueous, alcoholic, and acetonic), using BSLA, highlighted their lack of acute toxicity thus allowing the use of extracts in future biomedical applications.

The biological changes identified "*in vivo*" induced by the action of the compounds contained in the extract on the *Artemia salina* L. larvae are associated with behavioral changes, such as jerky movements, and cellular changes such as the inhibition of appendicular primordia growth areas. Both ALCLy and ACTLy extracts induced a gradual increase in larval discomfort, correlated with the level of concentration of the extract to which the organisms were exposed.

The *Lythrum salicaria* L. plant showed, through its extracts (aqueous, alcoholic, and acetonic), antibacterial activity on the *Gram-positive* reference bacterium, *Staphylococcus aureus* (ATCC 29213) and total resistance to the *Gram-negative* reference bacterium, *Escherichia coli* (ATCC 25922). These results are similar to those in the literature; the differences between the areas of inhibition can be explained by the diversity of extraction methods, the nature of the solvents used, and the structural specificity of the cell walls of *Gram-positive* and *Gram-negative* bacteria.

## REFERENCES

[1] Tahir, L., & Nazir, R. Dental Caries, Etiology, and Remedy through Natural Resources. *Dental Caries-Diagnosis, Prevention and Management*, Zühre Akarslan, IntechOpen, 2018, DOI: https://doi. org/10.5772/intechopen, 75937, 19.

[2] Turker, A. U., Yildirim, A. B., Tas, I., Ozkan, E., & Turker, H. chemical profile, antibacterial and antioxidant potentials. *Biotechnol Lett*, 2021, 26(2), 2499-2510.

[3] Piwowarski, J. P., Granica, S., & Kiss, A. K.. Lythrum salicaria L.—Underestimated medicinal plant from European traditional medicine. A review. *Journal of ethnopharmacology*, 2015, 170, 226-250.

[4] Al-Snafi A., E., Chemical constituents and pharmacological effects of Lythrum salicaria- A review, *IOSR Journal of Pharmacy*, 2019, 9.6, pp. 51-59.

[5] Mcgaw, L. J., Elgorashi, E. E., & Eloff, J. N. (2014). Cytotoxicity of African medicinal plants against normal animal and human cells. *In Toxicological survey of African medicinal plants*, 2014, pp. 181-233, Elsevier.

[6] Iancu, I., M., Bucur, L., A., Schroder, V., Mireșan, H., Mihai, S., Iancu, V., Badea, V., Phytochemical evaluation and cytotoxicity assay of *Lythri herba* extracts, *Farmacia*, 2021, 69(1), 51-58.

[7] Erdem H, Puca E, Ruch Y, Santos L, Ghanem-Zoubi N, et al. Portraying infective endocarditis: results of multinational ID-IRI study. Eur J Clin Microbiol Infect Dis. 2019 Sep;38(9):1753-1763. doi: 10.1007/s10096-019-03607-x. Epub 2019 Jun 11. PMID: 31187307.

[8] Octav Ginghina, George Traian Alexandru Burcea- Dragomiroiu, Bianca Galateanu, Ariana Hudita, Silvia Dragomir, Doina Draganescu, Andra Balanescu, Cosmin Adrian Rosca, Carmen Giuglea, Daniela Elena Popa, Anca Pantea-Stoian, Carolina Negrei- Long –term safety of biosimilar medicinal products-key for administration? Revista Farmacia, 2019, Vol. 67, 1, 18-26.

[9] Lopes, A., Rodrigues, M. J., Pereira, C., Oliveira, M., Barreira, L., Varela, J., ... & Custodio, L.. Natural products from extreme marine environments: Searching for potential industrial uses within extremophile plants. *Industrial Crops and Products*, 2016, 94, 299-307.

[10] Bencsik, T. Comparative histological, phytochemical, microbiological, and pharmacological characterization of some Lythrum salicaria L. Populations, 2014, unv. Diss. University of Pécs.

[11] Raineri, M.; Falugi, C. Acetylcholinesterase activity in embryonic and larval development of Artemia salina Leach (Crustacea Phyllopoda). *Journal of Experimental Zoology*, 1983, 227.2: 229-246, https://doi.org/10.1002/jez.1402270207

[12] Lupu, E., C., Lupu, S., Petcu, A., *EB lifetime distributions as alternative to the EP lifetime distributions*, Analele Univ. Ovidius Constanţa, Seria Matematică, Vol. 22(3), 2014, ISSN 1224-1784, p.115-125 (I.F. 0.333, I.S. 0.088).

[13] Leahu, A., Lupu, E., C., Statistical simulation and prediction in software reliability. Analele Univ. Ovidius Constanţa, Seria Matematică, vol. XVI (1), 2008, ISSN 1224-1784, p 81-90.

# THE DIFFERENT SCREENING METHODS FOR THE CERVICAL LESION DIAGNOSTIC AND THE ECONOMIC AND SOCIAL IMPLICATIONS OF SCREENING AMONG FEMALE POPULATION

**Ph.D. Student Codrin Gheorghe**[1]
**Assoc. Prof. Dr. Schröder Verginica**[2]
**Assoc. Prof. Dr. Stoicescu Ramona**[3]
**Assoc. Prof. Dr. Dumitru Irina**[4]
[1, 4] Ovidius University of Constanta, Faculty of Medicine, Constanta, Romania
[2, 3] Ovidius University of Constanta, Faculty of Pharmacy, Constanta, Romania
[3, 4] Clinical Infectious Diseases Hospital, Constanta, Romania

## ABSTRACT

The study aims to compare different screening methods that are currently being used to confirm a cervical intraepithelial lesion (CIN) underlying the inherent advantages of the varied examination procedures. In this study we are looking at the quality contrast of the different paraclinical examinations relative to the cost, invasiveness and cultural acceptance of such procedures. Every year, more than 100,000 women in EU countries are diagnosed with cervix uteri cancers (CCU). This type of cancer can be prevented if precancerous cells are detected and treated. HPV is found in over 90% of cervix uteri cancers. In Europe, more than half of the countries have implemented screening programs for cervical cancer, and most European countries now have national HPV vaccination programs, however target populations vary depending on the epidemiological evidence and the budgetary level of each countries health system.

In this study we evaluated and compared the current and modern techniques used for cervix cellular diagnostics. Also, this study helps improve the understanding on the economic and social implications of screening among female population and the impact it has on healthcare system relieving. Romania recorded an incidence of 22.6 cases of cervix uteri cancers / 100.000 women (age standardized rate), and a mortality of 9.6 / 100.000, ranking second highest in the EU zone.

***Keywords:*** *screening, cervical cancer, HPV, spectroscopy, Raman*

## INTRODUCTION

Cervical cancer is among the most preventable cancers. Pre-cancerous lesions can easily be detected through screening before they become cancerous. When screening detects pre-cancerous lesions, these can be treated and thus the cancer can be avoided.

Human papillomavirus (HPV) is the essential driver of cervical malignant growth. More than 3/4 of sexually active women get it in the span of their lives. The prevalence of HPV increases with severity of the lesion. There are over 200 types of HPV with potential for induction of cellular transformations, but two of these strains, HPV-16 and 18, the two vaccine-preventable types contribute to over 70% of all cervical cancer cases, between 41%-67% of high-grade cervical lesions and 16-32% of low-grade cervical lesions. After HPV-16/18, the six most common HPV types are the same in all world regions, namely 31, 33, 35, 45, 52 and 58; these account for an additional 20% of cervical cancers worldwide. The HPV vaccine is almost 100% effective in preventing the persistent HPV infections that cause cervical cancer [1], [2].

Since the introduction of the Papanicolau's smear and cervical cancer screening, there have been other attempts to update and develop new screenings methods as minimally invasive as possible that would bring benefits to different economic regions of the world.

**BURDEN OF HPV RELATED DISEASE**

About 604,127 new cervical cancer cases are diagnosed annually globally (estimates for 2020) ranking in 3rd place as the most common cancer site in females. It is established that well-organised cervical screening programs or widespread good quality cytology can reduce cervical cancer incidence and mortality [3].

Screening methodologies contrast between nations. Some countries have population-based programs where in each round of screening women in the target population are individually identified and invited to attend screening. This type of program can be implemented nationwide or only in specific regions of the country [2].

As the European Guidelines recommend, a program with an organized population-based nature may substantially improve the accessibility and equity of screening access while simultaneously improving effectiveness and cost-effectiveness. The vital elements to be determined inside such a program are the target age, screening spans, and screening algorithm. The latter alludes to the essential screening test and the ensuing administration of results at each progression of the algorithm [4].

**SCREENING OF CERVICAL TISSUE**

Conventionally cervical cancers are diagnosed by visual inspection with acetic acid (VIA), HPV testing, polar probe, Pap smear (PAP) and colposcopy. However, these methods are not providing high sensitivity and specificity; furthermore, the diagnostic potential is highly subjective as it depends on the skills and experience of the persons who were analyzing the samples (Figure 1). Although biopsy and resulting histopathology are considered as the gold standard strategy for cancer diagnosis, it is an intrusive technique and has numerous impediments particularly for mass screening of patients with multiple suspicious lesions. In this context, extensive studies are under progress in the development of real-time, non-invasive and cost-effective molecular diagnostic modality using various techniques [5].

Present studies are centered around concurrent multispectral analysis which provides higher sensitive and accurate diagnosis.

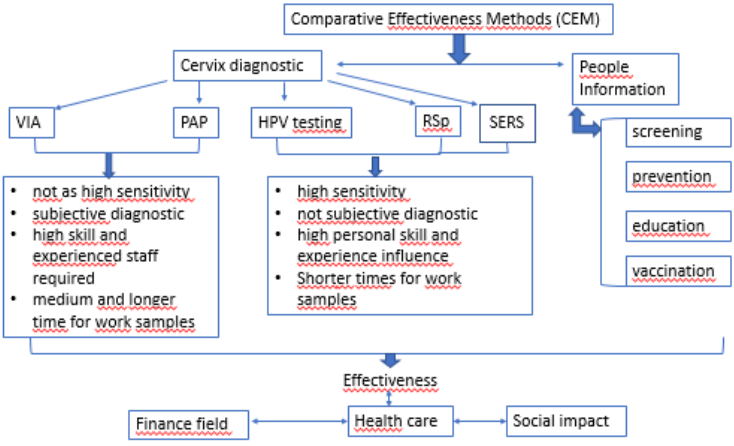


***Fig. 1.*** *Comparative effectiveness methods (CEM) system for cervix diagnostic*

**Diffuse Reflectance Spectroscopy**

Steady-state reflectance spectroscopy (RSp) is a technique where light after multiple scattering in the tissue is collected and studied for qualitative and quantitative information. A study of reflectance spectroscopy involving 324 sites of 164 precancerous patients carried out by Mirabal et al. has found the discrimination ability between squamous normal and high-grade squamous intraepithelial lesions with sensitivity and specificity of **72**% and **83**% respectively. In spite of the fact that DRS has many advantages, even the slightest error like probe-to-tissue pressure can alter the accuracy of the spectra [6].

**Surface-Enhanced Raman Spectroscopy (SERS)**

Since the Raman effect is a weak phenomenon, researchers around the globe have tried to enhance the weak effect. One such novel technique is enhancing the Raman signals by nanoparticles known as SERS. The aid of multivariate statistical analysis is inevitable to glean meaningful inferences from the enormous data set obtained from these spectroscopic studies [6].

**Spectro-cytology by label-free surface-enhanced Raman fingerprints and chemometrics**

Varsha Karunakaran et al. explored a spectroscopic modality in which different spectral fingerprints were obtained by utilizing label-free ultrasensitive surface-enhanced Raman scattering (SERS) technique on exfoliated cell samples of the cervix. Three different approaches i.e. single-cell, cell-pellet and extracted DNA from oncology clinic as confirmed by Pap test and HPV PCR were employed. Gold nanoparticles as the SERS substrate favored the increment of Raman intensity exhibited signature identity for Amide III/Nucleobases and carotenoid/glycogen

respectively for establishing the empirical discrimination. Moreover, all the spectral invention was subjected to chemometrics including Support Vector Machine (SVM) which furnished an average diagnostic accuracy of **94**%, **74**% and **92**% of the three grades (LSIL, HSIL, Cervical Cancer) [7].

Cervical cancer has been well studied by conventional Raman spectroscopy in the past several years for differentiating normal and abnormal subjects using blood serum, cells, tissues, in vivo etc. When contrasted with the regular Raman spectroscopy, SERS is a ultrasensitive strategy requiring less acquisition time, better signal-to-noise ratio, increased fold intensity, specificity and Raman cross section. Employing SERS in exfoliated cell samples for cervical cancer detection will provide direct understanding into the cause of abnormalities offering some unmistakable advantages over different procedures like less time preparing the samples and minimal influence of water bands [7], [8].

**Raman spectroscopic detection of high-grade cervical cytology**

In a study done by Jing Wang et al., 210 ten tissue sections from 210 patients (Among them, 60 were diagnosed as cervicitis, 30 as CIN I, 30 as CIN II, 30 as CIN III, 30 as cervical squamous cell carcinoma, and 30 were diagnosed as cervical adenocarcinoma by pathological diagnosis) which yielded 157 spectra of CIN I tissue, 138 of CIN II tissue, 155 of CIN III tissue, 166 of cervical squamous cell carcinoma tissue, and 201 of cervical adenocarcinoma tissue, totaling 1110 spectra [8]. The spectra was analyzed and interpreted then using the SVM algorithm to build an efficient diagnosis model to classify the six tissues.

The main Raman characteristic peaks of the cervical tissues were summarized, and the differences of biochemical components of the 6 types of cervical tissues were analyzed. After rehashed tests, the characterization impact was improved. The accuracy of the cervical tissues was **85.7**% which indicated that Raman spectroscopy combined with support vector machine could be used to successfully classify the different types of samples [7], [8].

**Rapid screening using Raman spectroscopy based on GA-SVM**

In a study conducted by Chen Chen et al., 196 HPV negative secretion samples and 58 HPV positive samples were analyzed using Raman spectroscopy and multivariate statistical analysis.

By using algorithms for noise reduction, the background of the Raman spectras were normalized and the processed spectras were used to build a model for analysis (The airPLS-PLS-GA-SVM hybrid model process) which further improved the accuracy and quality of the data extracted.

Because this technology has the advantages of being fast, noninvasive, and low cost, it has broad application prospects. The accuracy of using airPLS-PLS-GA-SVM to diagnose cervical diseases was up to **98.6**%, which indicates the great potential of using Raman spectroscopy to screen cervical diseases and prevent cervical cancer in the future [8].

## SOCIAL AND ECONOMIC CONCERNS

In low and middle-income countries (LMICs), where cervical cancer burden is highest, screening coverage is much lower. In these settings, low Pap screening accessibility (due to limited resources, infrastructure, and trained personnel) and poor sensitivity of the existing low-cost cervical cancer screening option, visual inspection with acetic acid (VIA), are boundaries to effective screening [9].

Primary HPV screening has advantages over Pap that can benefit both high and low-income settings. HPV testing has higher sensitivity than Pap to detect cervical pre-cancers, allowing broadened screening intervals, and HPV testing requires less training for sample collection. Figure 1

Some studies proposed HPV tests using self-collected samples which were shown to have comparable sensitivity to clinician-collected samples for detecting cervical intraepithelial neoplasia grade 2 or higher (CIN2+), making HPV self-sampling (HPV-SS) a feasible screening option. Women of different ages, ethnicities, and nationalities reported HPV-SS to be highly acceptable [9].

Cervical cancer remains a significant public health problem in Romania. It ranks third in the country after breast and colorectal cancer. Unfortunately, the first attempt of campaign vaccination in Romania proved short to deliver.

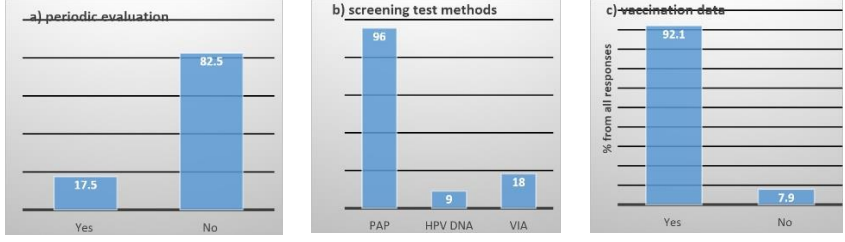


***Fig. 2.*** *HPV information - responses of a survey conducted online a) periodic evaluations of cervix lesions, b) methods used for screening, c) vaccination data for 21-30 ages groups*

In a survey conducted online, 116 of 126 (92.1%) participants responded that they did not get any HPV vaccines (Figure 2) even though most of them talked about it with their medical practitioners. Furthermore, our survey found that 82.5% of the participants did not get any form of cervical examination (Figure 2). The highest rate of respondents was in the age group of 21-30 (75 of 126 or 59.5%).

## DISCUSSION

The lack of cost-effectiveness studies outside of Western Europe, especially in LMICs, that include data on real-world implementation scenarios, represents an important gap in the literature. Future cost-effectiveness studies within screening programs should model the impact of new triage strategies, the development of HPV-SS outreach materials, and increasing HPV vaccination rates [9].

The research community is in pursuit of molecular fingerprinting which differentiates samples between different biological conditions with emphasis on

real-time, minimal invasiveness and high-thorough analysis. One such analysis is that of the SERS combined with multivariate statistical analysis which proves to be a high specificity, low-cost analysis which could be employed in all types of economical regions.

Furthermore there is also the need of educating the population about the dangers of HPV. Comparative studies have shown that vaccination and regular screening against HPV even though imply national programs which require some additional spending, on the long run surpass the cost of treating the possible cervical cancer patients.

## REFERENCES

[1] Sabet F., Mosavat A., Ahmadi Ghezeldasht S., Basharkhah S., Shamsian S.A.A, Abbasnia S., Shamsian K., Rezaee S.A., Prevalence, genotypes and phylogenetic analysis of human papillomaviruses (HPV) in northeast Iran. International Journal of Infectious Diseases, 103:480-488, 2021.

[2] Bruni L., Albero G., Serrano B., Mena M., Gómez D., Muñoz J., Bosch F.X., de Sanjosé S. ICO/IARC, Information Centre on HPV and Cancer (HPV Information Centre). Human Papillomavirus and Related Diseases in the World. Summary Report 17 June 2019, www.hpvcentre.net

[3] International Agency for Research on Cancer, WHO, https://gco.iarc.fr/

[4] Chrysostomou, A.C.; Stylianou, D.C.; Constantinidou, A.; Kostrikis, L.G. Cervical Cancer Screening Programs in Europe: The Transition Towards HPV Vaccination and Population-Based HPV Testing. *Viruses* **2018**, *10*(12):729, 2018.

[5] Pappu Raja, Prakasarao Aruna, Dornadula Koteeswaran, Singaravelu Ganesan, Characterization of blood plasma of normal and cervical cancer patients using NIR Raman spectroscopy, Vibrational Spectroscopy, Volume 102, 2019.

[6] Daniel A., Savarimuthu W.P. (2019) Current Advances in Optical Screening for Cervical Cancer. In: Farghaly S. (eds) Uterine Cervical Cancer. Springer, 2019.

[7] Varsha Karunakaran, Valliamma N. Saritha, Manu M. Joseph, Jyothi B Nair, Giridharan Saranya, Kozhiparambil G. Raghu, Kunjuraman Sujathan, Krishnannair S. Kumar, Kaustabh K. Maiti, Diagnostic spectro-cytology revealing differential recognition of cervical cancer lesions by label-free surface-enhanced Raman fingerprints and chemometrics, Nanomedicine: Nanotechnology, Biology and Medicine, Volume 29, 2020.

[8] Wang, J., Zheng, CX., Ma, CL. *et al.* Raman spectroscopic study of cervical precancerous lesions and cervical cancer. *Lasers Med Sci*, 2021.

[9] Colin Malone, Ruanne V. Barnabas, Diana S.M. Buist, Jasmin A. Tiro, Rachel L. Winer, Cost-effectiveness studies of HPV self-sampling: A systematic review, Preventive Medicine, Volume 132, 2020.

Section

# ENVIRONMENTAL GEOLOGY

Protectional and Conservation of the Geological Heritage
Regional and structural geology
Petrology and hydrogeology
Sedimentology

# ASSESSMENT OF ENVIRONMENTAL CHANGES DURING MINING OF FELDSPAR DEPOSITS IN UKRAINE

**Dr. Geol.-Mineral. Sci., Dr. Geogr. Sci., Dr. Eng. Sci., Prof. Georgii Rudko**[1]
**Assoc. Prof. Ph.D. Mariia Kurylo**[2]
**Ph.D. Student Maksym Ozerko**[3]
[1] State Commission of Ukraine on Mineral Resources, Kyiv, Ukraine
[2, 3] National Taras Shevchenko University of Kyiv, Kyiv, Ukraine

## ABSTRACT

Possible negative impacts on the environment during mining of feldspar deposits with open-pit and underground mine are defined. The main changes have been identified, which are as follows: air pollution, soil destructions, change of relief, a local decrease in groundwater level, pollution by sewage and waste.

Destructions of the soil cover are fixed under the dumps of the quarry and in the path of the movement of quarry equipment. Through the development of a pit and dumps, the primary relief acquires significant changes and the action of forces caused primarily by gravity is activated, aimed at smoothing out negative and positive relief forms.

An increase in the height difference from the dump ridge to the bottom of the quarry and the formation of a significant, pronounced depression of the relief redirects the surface runoff, increases its speed, and reduces infiltration into the soil. Mining development caused drainage of groundwater due to its release to the surface and evaporation.

Air pollution has a bigger scale than other components of negative impacts. The main impact of mining activities is due to emissions of pollutants into the atmosphere as a result of blowing dust from the surface of dumps and emissions from quarry transport and their deposition on the soil and storage of industrial waste. The main pollutants are inorganic dust with content of $SiO_2$ - 65-82% and $Al_2O_3$ - 11-21%.

Separately, the article discusses the impact on the environment during multi-components deposits` exploitation, where feldspar concentrates are produced as by-products. Several deposits in Ukraine belong to the group: Bakhtyn (fluorite ores), Nosachivske (titanium-ilmenite ores), Perzhanske deposits of rare metals, Mazurivske (tantalum and niobium ores). Most of them are planned to be mined underground, which saves more land resources in comparison with open workings. The placement of mine shafts and industrial sites for their maintenance requires an area of about 30 hectares. All of them have a complex ore processing with the separation of several concentrates, which necessitates the use of flotation and other reagents. The development of such deposits involves the organization of tailings and circulating water supply of the processing plant.

***Keywords:*** *feldspar deposits, environmental changes, mining, assessment*

## INTRODUCTION

The relevance of assessing the impact of feldspar mining on the environment is associated with an increase in the scale of production. In Ukraine, dozens of deposits are mined for use in the construction and production of ceramics. Globally feldspar consumption has been gradually increasing in ceramics, glass industry for solar panels, housing, and building construction.

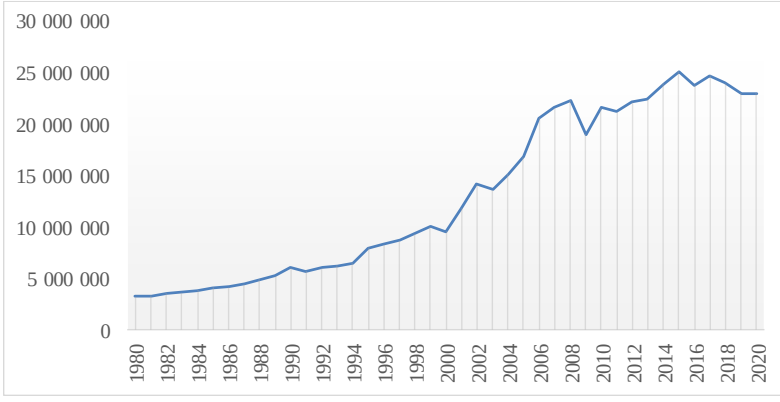


***Fig. 1.*** *Feldspar global production dynamics in metric tons (according to statistical data usgs.gov [6])*

The total production of feldspar raw materials in Ukraine amounted to 634.63 thousand tonnes in 2019.

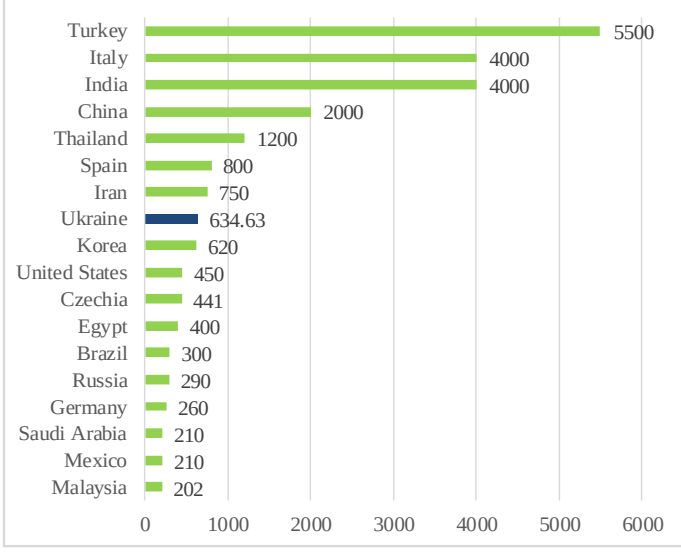


***Fig. 2.*** *Feldspar production in 2019 by country (according to statistical data usgs.gov [6], and statistical data for Ukraine - State Information Geological Fund of Ukraine [1] )*

Environmental impact assessment is mandatory in Ukraine for mining enterprises [7] and for feldspar, deposits have their peculiarities. The main source of feldspar raw materials in Ukraine is multi-component deposits. These objects belong to different genetic and mining types, which determine the impact on the environment that occurs during development. The following diagram illustrates the features of mining methods and the processing of feldspar raw materials by the type of deposits (figure 3).

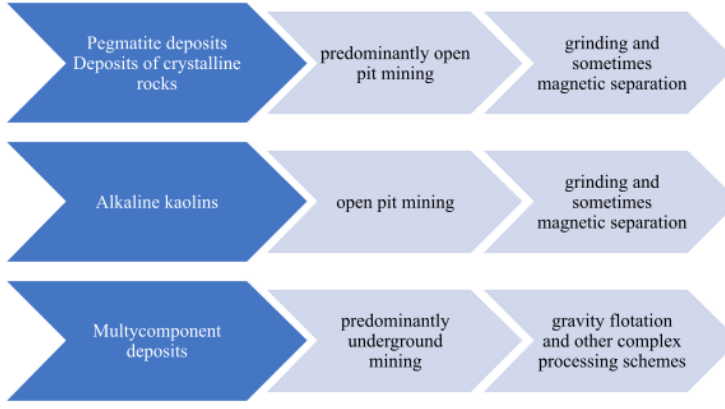


***Fig. 3.*** *Features of mining methods and processing of feldspar raw materials by the type of deposits*

Possible negative impacts on the environment during *open-pit mining* of feldspar deposits are as follows: air pollution, soil destructions, change of relief, a local decrease in groundwater level, pollution by sewage, and waste. The area of disturbed land and the volume of waste with the open method depends on the size of the reserves and the stripping ratio. As a rule, this ratio is less than 1, which has a positive effect on the profitability of mining. The soil is less than 10% of the total overburden volume and the enterprises store it separately for further reclamation. As a rule, the production capacity of mining enterprises ranges from 50 to 200 thousand tons per year, which provides at least 20 years of operation.

Destructions of the soil cover are fixed under the dumps of the quarry and in the path of the movement of quarry equipment. Through the development of a pit and dumps, the primary relief acquires significant changes and the action of forces caused primarily by gravity is activated, aimed at smoothing out negative and positive relief forms.

The main impact of mining activities is due to emissions of pollutants into the atmosphere as a result of blowing dust from the surface of dumps and emissions from quarry transport and their deposition on the soil and storage of industrial waste. The main pollutants are inorganic dust with a content of $SiO_2$ - 65-82% and $Al_2O_3$ - 11-21% [5].

An increase in the height difference from the dump ridge to the bottom of the quarry and the formation of a significant, pronounced depression of the relief

redirects the surface runoff, increases its speed, and reduces infiltration into the soil. Mining development caused drainage of groundwater due to its release to the surface and evaporation.

Air pollution has a bigger scale than other components of negative impacts. During the mining operation, a significant amount of gaseous substances of spent fuel and other technological substances, as well as suspended particles of the quarry rock, are emitted into the air.

The influence of mining activity on the disturbance of landscapes and biocenosis should be studied separately. These factors depend on the availability of those items on the territory and the scale of land alienation.

Deposits of crystalline rocks often require preliminary disintegration using drilling and blasting operations. In such cases, the stability of the geological environment and its assimilation potential must be assessed. The boundaries of the development of the deposits in the plan ensure compliance with the 500-meter sanitary protection zones.

Other features of the impact on the environment are multi-components deposits, where feldspar concentrates are produced as by-products. Several deposits in Ukraine belong to the group: Bakhtyn (fluorite ores), Nosachivske (titanium-ilmenite ores), Perzhanske deposits of rare metals, Mazurivske (tantalum and niobium ores).

Most of them are planned to be mined underground, which saves more land resources in comparison with open workings. The placement of mine shafts and industrial sites for their maintenance requires an area of about 30 hectares. All of them have a complex ore processing with the separation of several concentrates, which necessitates the use of flotation and other reagents. The development of such deposits involves the organization of tailings and circulating water supply of the processing plant.

The impact on the atmosphere is different from open-pits since dust pollution from mining is less due to production volumes and is concentrated in underground buildings. Processing can be a source of air pollution and pollutants depend on the composition of enrichment reagents.

For the Nosachivske, Bakhtyn, and Perzhanske deposits listed above, it is planned the mining system with backfilling. Considering the underground mining, overburden rocks in a large volume will not be, and those crystalline rocks that will be raised to the surface will be used in the construction of a mining and processing complex. For these deposits, it`s proposed to organize the recycling water supply system of the processing plant. A decrease in the level of groundwater in the adjacent territories is possible [3], [4].

In terms of land resources, it is planned to withdraw land and change their intended purpose for the placement and operation of main, auxiliary, and auxiliary buildings and structures associated with the use of subsoil for mining. Contamination of the soil with oil products from faulty equipment is assumed;

violation of the soil cover during the surface construction of the mining and processing complex.

The planned activities are considered to have a minor and tolerable impact on flora and fauna. Sources of increased noise from mining operations may cause minor impacts on habitats, breeding conditions, and animal migration routes. As a result of the implementation of the planned activities, an insignificant permissible impact on the spatial, species, population diversity of flora objects is possible.

Individual design solutions are directed to the processing and use of production waste. On the example of the Mazurivske deposit, the production of feldspar concentrate is associated with processing stored waste. It allows us to free up large areas of tailings and eliminate the source of potential environmental hazards given the existing connection of tailings with the river Kalchyk basin. However, a base of feldspar raw materials can be created for the ceramic industry quite quickly and without significant investment. Such production will become a testing ground for the preparation of the complex development of the Mazurivske deposit [2].

Generalized objects of influence on the environment for the named types of deposits are shown in Table 1.

***Table 1.*** *Main objects of influence on the environment for feldspar deposit un Ukraine*

| Type of deposit | List of feldspar deposit un Ukraine | The main objects of influence on the environment |
|---|---|---|
| Pegmatite deposits | Bilchakivske, Ustia village, Hruzlivetske, Lozuvatske, Volodymyrivske, Balka Velykoho Taboru | Open-pit, drilling and blasting operations, crushing plant, overburden dumps |
| Deposits of crystalline rocks | trachytes of the Verbova site, microgranodiorites of the Dubrynetske deposit | |
| Alkaline kaolins | Prosianivske, Pershozvanivske, Biliayivske, Katerynivske | Open-pit, crushing, and grinding plant, overburden dumps, processing plant for dry, wet, and electromagnetic separation, tailings |
| Multicomponent deposits | Bakhtyn (fluorite ores), Nosachivske (titanium-ilmenite ores), Perzhanske deposits of rare metals, Mazurivske (tantalum and niobium ores) | underground mine, processing plant (gravitation, flotation, and electromagnetic separation), tailings |

## CONCLUSION

Objects of negative impact for different types of deposits are highlighted:

1. for pegmatite deposits and deposits of crystalline rocks it is open-pit, drilling and blasting operations, crushing plant, overburden dumps;
2. for kaoline deposits it is (except for the above) processing plant for dry, wet, and electromagnetic separation, tailings;
3. for multicomponent deposits - underground mine, processing plant, tailings.

Possible negative impacts on the environment during open-pit mining of feldspar deposits are air pollution, soil destructions, change of relief, a local decrease in groundwater level, pollution by sewage, and waste. For underground mines, important changes are disturbances in the rock mass and its stability, changes in the regime and composition of surface and ground waters. For all facilities where there are processing plants, the development and condition of tailing dumps and the possibility of processing waste are critical.

Important and effective measures for improving facilities are the reduction of disturbed mining areas and their early reclamation, backfilling during underground mining, the maximum extraction, and processing of all useful components of minerals, which reduces the amount of production waste.

## REFERENCES

[1] Balance of mineral reserves of Ukraine. Issue 72. Feldspar raw materials. Kyiv, State Research and Production Enterprise “State Information Geological Fund of Ukraine”, 2018. *(in Ukrainian)*

[2] Cherniyenko N.M. Complex use of ores of the Mazurivske deposit, Pryazovia region, http://ea.donntu.org:8080/jspui/bitstream/123456789/7226/1/215-222.pdf *(in Ukrainian)*

[3] Conclusion on environmental impact assessment of mining Nosachivske deposit// http://eia.menr.gov.ua/uploads/documents/2522/reports/ 9846711dd23548eb3c49153d17086c5f.pdf *(in Ukrainian)*

[4] Conclusion on environmental impact assessment of extraction and processing of the Perzhanske deposit//http://eia.menr.gov.ua/uploads/documents/3271/reports /420b60111f02a021002d13c0d8614294.pdf *(in Ukrainian)*

[5] Conclusion on environmental impact assessment of the development of the Pyatyrichanka site of the Dubrivka alkaline kaolin deposit//http://eia.menr.gov.ua/uploads/documents/6682/reports/q5utEyl1tK.pdf *(in Ukrainian)*

[6] Feldspar Statistics and Information. National Minerals Information Center. USGS// https://www.usgs.gov/centers/nmic/feldspar-statistics-and-information

[7] On environmental impact assessment. Law of Ukraine. Vedomosti Verkhovnoi Rady (VVR), 2017, № 29, p.315. *(in Ukrainian)*

# LONG-PERIOD SURFACE-RELATED MULTIPLE SUPPRESSION IN 2D MARINE SEISMIC DATA USING PREDICTIVE DECONVOLUTION AND COMBINATION OF SURFACE-RELATED MULTIPLE ELIMINATION AND PARABOLIC RADON FILTERING

**Pimpawee Sittipan**[1]
**Assoc. Prof. Dr. Pisanu Wongpornchai**[2]
[1, 2] Department of Geological Sciences, Chiang Mai University, Thailand

## ABSTRACT

Some of the important petroleum reservoirs accumulate beneath the seas and oceans. Marine seismic reflection method is the most efficient method and is widely used in the petroleum industry to map and interpret the potential of petroleum reservoirs. Multiple reflections are a particular problem in marine seismic reflection investigation, as they often obscure the target reflectors in seismic profiles. Multiple reflections can be categorized by considering the shallowest interface on which the bounces take place into two types: internal multiples and surface-related multiples. Besides, the multiples can be categorized on the interfaces where the bounces take place, a difference between long-period and short-period multiples can be considered. The long-period surface-related multiples on 2D marine seismic data of the East Coast of the United States-Southern Atlantic Margin were focused on this research. The seismic profile demonstrates the effectiveness of the results from predictive deconvolution and the combination of surface-related multiple eliminations (SRME) and parabolic Radon filtering. First, predictive deconvolution applied on conventional processing is the method of multiple suppression. The other, SRME is a model-based and data-driven surface-related multiple elimination method which does not need any assumptions. And the last, parabolic Radon filtering is a moveout-based method for residual multiple reflections based on velocity discrimination between primary and multiple reflections, thus velocity model and normal-moveout correction are required for this method. The predictive deconvolution is ineffective for long-period surface-related multiple removals. However, the combination of SRME and parabolic Radon filtering can attenuate almost long-period surface-related multiple reflections and provide a high-quality seismic images of marine seismic data.

***Keywords:*** *Long-period multiple reflections, Marine seismic reflection survey, Multiple reflections, Petroleum exploration, Surface-related multiple reflections*

## INTRODUCTION

The Marine seismic reflection method is widely used in the petroleum industry to map and interpret the potential of petroleum reservoirs. The marine zones of marine seismic exploration include the shallow-water areas (water depth of less than

30 to 40 meters) and the deep-water areas associated with seas and oceans. When the energy of the seismic wave travels through the water surface and reflects back to receivers, each reflected signal in the seismic record theoretically has only one reflection point, it is called primary reflection. Many problems limit the ability of marine seismic exploration and generate noise even if they are random noise from environment activities or coherent noise such as swell noise, generated by streamer cables, and the big problem; multiple reflections, due to the strong reflector with a reflectivity close to unity. Multiple reflections are the events in the seismic record and have the reflection point more than one before traveling to the receivers. They are treated as unwanted events. Multiple reflections can be classified by considering the shallowest interface on which the bounces take place [1]. Two subdivisions of multiples are internal multiples and surface-related multiples. The internal multiples have a downward bounce at the reflector below the surface. The surface-related multiples have a downward bounce at least one at the surface. Besides, the multiples can be categorized on the interfaces where the bounces take place, a difference between long-period and short-period multiples can be made. The long-period or long-path multiples having the distinct arrival times from the primaries are the multiple events that can be differentiated from the primary events. On the other hand, short-period or short-path multiples generated by thin layer and interfering with the primaries are the multiples that cannot be separated from the primaries.

Due to the multiples being the unwanted events, subsurface imaging without removing them may be the big problems and misunderstanding for the interpreters. Several multiple removal techniques are used in seismic data processing. However, the well-known techniques, predictive deconvolution, surface-related multiple eliminations (SRME) and parabolic Radon filtering will be discussed in this research.

Predictive deconvolution can remove not only the seismic wavelets but also the repetitive events [2]. However, predictive deconvolution becomes less acceptable as the water depth increases and the complex structure. The large of the multiple reflection period and the complexity of structure yield the poor estimation of the periodic events [3], [4]. SRME [5], [6], [7], [8], [9] and Parabolic Radon filtering [8], [9], [10], [11] are the complementary methods effectively removing the surface-related multiple reflections for the complex geological setting data.

This research attempt to eliminate the surface-related multiples on marine seismic data. The two separated flows will be used for multiple removals. The first processing flow includes predictive deconvolution. The other contains SRME and parabolic Radon filtering.

## METHODOLOGY

### Predictive Deconvolution

The recorded seismic signal is considered as the convolutional model in the time domain. The source wavelet, $w(t)$, is sent through the subsurface and convolved with the Earth response (Earth's reflectivity), $r(t)$, to produce the seismic traces. Random noise, $n(t)$ is generated by activities in environment while

the seismic acquisition is working. The seismic records, $s(t)$, can be mathematically expressed as

$$s(t) = w(t) * r(t) + n(t) \quad (1)$$

Deconvolution is the inverse of the convolution process. The inverse filter operator, $h(t)$, estimated from seismic traces is convolved with the seismic records, $s(t)$. In principle, the deconvolution process sharpens the seismic traces by removing source wavelet and yields only the Earth's reflectivity.

$$r(t) = h(t) * s(t) \quad (2)$$

In practice, because the seismic data is not noise-free data, this condition may reduce the effectiveness of the deconvolution process and cause errors.

Predictive deconvolution is the most commonly used technique in seismic processing. This procedure not only removes the source wavelet but also suppresses the repetitive events in seismic data. Fig. 1 shows the autocorrelation functions of seismic traces containing long-period multiples. The $\alpha$ parameter indicates the repetition of the seismic events. In predictive deconvolution, the prediction lag $\alpha$ must be designed to predict and suppress the multiples [12].

In Fig. 2, the prediction lag $(\alpha)$ and prediction operator length $(n)$ were designed.

The shorter prediction lags yield more compression of the source wavelet. While the prediction lag increases, the effectiveness the compression wavelet is reduced [12].

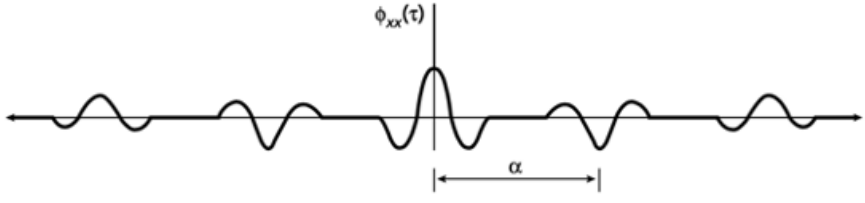


***Fig. 1.*** *Autocorrelation functions of seismic traces containing with long-period multiples, [modified from [13]].*

The shorter length of $n$ is the length of the first-order event and the longer length of $n$ is the length of the second-order event. The prediction operator length $(n)$ can be defined in order to suppress one or more orders of multiples. The autocorrelation of the output trace shows the very low energy of repetitive patterns after the deconvolution process.

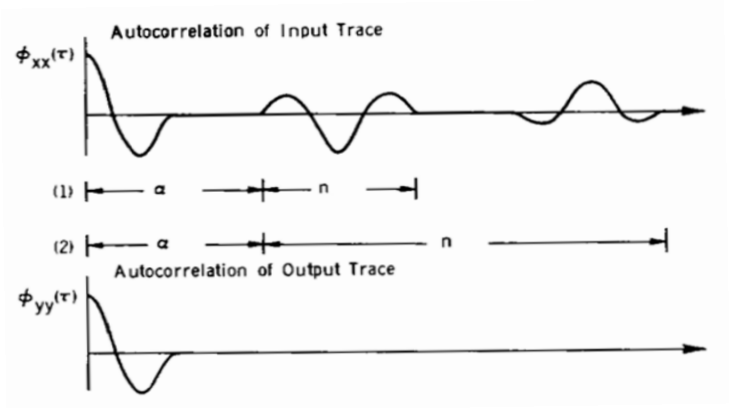


***Fig. 2.*** *Upper diagram illustrates the autocorrelation of trace with long-period multiples. Lower diagram illustrates the autocorrelation output after applying predictive deconvolution, [modified from [2]].*

**Surface-related Multiple Elimination (SRME)**

The principle of SRME process is that multiples are a combination of primaries. First-order multiples are the spatial convolution of primaries and primaries, second-order multiples are the spatial convolution of primaries and the first-order multiples, and so on. These steps are referred to the prediction of the multiple reflection model.

First, the forward model of surface-related multiples for the 1D situation is explained. The impulse response of the Earth is defined by and contains all primary and multiple reflections. When these events hit the free surface, they all reflect back into the medium. Hence each event in the primary response acts as a new source wave for the complete round trip. Each event from the impulse response will be convolved with the complete impulse response to become a sequence of the first-order multiples. The construction of the first-order surface-related multiples can be expressed as [1].

$$m_1(t) = -x_0(t) * x_0(t) \tag{3}$$

where the minus sign describes the reverse phase of the signal. Next, these events arrive at the surface again, and each first-order multiple acts as a source for the second-order multiples. Thus, the second-order multiples can be written as

$$m_2(t) = -x_0(t) * m_1(t) = x_0(t) * x_0(t) * x_0(t) \tag{4}$$

The total response *x(t)* with all surface-related multiples becomes a series as

$$x(t) = x_0(t) - x_0(t) * x_0(t) + x_0(t) * x_0(t) * x_0(t) - \ldots \tag{5}$$

The surface-related multiples response from the full wavefield can be expressed by a series of auto-convolutions as

$$x_0(t) = x(t) + [(x)t * x(t)] + [x(t) * x(t) * x(t)] + [x(t) * x(t) * x(t) * x(t)] + \ldots \quad (6)$$

For the 2D situation, the integral expression of multiple prediction is given by

$$M_0(x_r, x_s, f) = -\sum_{x_k} X_0(x_r, x_k, f) P(x_k, x_s, f) \quad (7)$$

where $X_0$ is the primary impulse response function, $P$ is the total recorded field, $x_s$ is the source location, $x_r$ is the receiver location and $x_k$ is the lateral coordinate over which the data are summed [14]. Fig. 3 illustrates the construction of the first-order multiple for 2D seismic data.

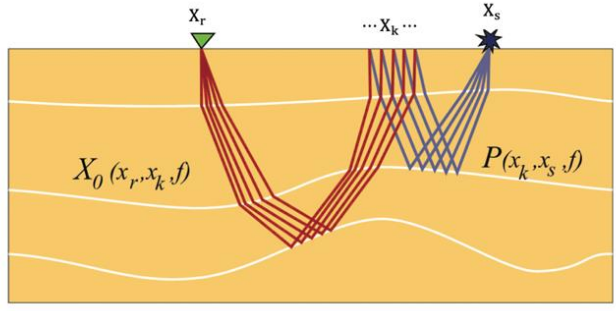


***Fig. 3.*** *The construction of the first-order multiple [1].*

The model of multiple reflections from (7) is subtracted from the input data using a least-square method with a matching operator *A(f)* expressed as (8). The operator $A(f)$ is an inverse source property relating between data with and without multiples. The correct operator $A(f)$ obtains the minimum energy of multiples in the output [15].

$$P_0(x_r, x_s, f) = P(x_r, x_s, f) - A(f) M(x_r, x_s, f) \quad (8)$$

**Parabolic Radon Filtering**

The Radon transform is a mathematical technique having been widely used in the seismic data processing. This method transforms the input data from the offset-time (x-t) domain to the Radon domain, where it is modified and then transform back to the x-t domain. In this research, the parabolic Radon filtering is used for multiple removals. The forward parabolic Radon transform is expressed as

$$m(q, \tau) = \sum_{n=1}^{N} d(x_n, t = \tau + q x_n^2) \quad (9)$$

where $d(x_n, t)$ is the data in offset-time *(x-t)* domain, *N* is the number of traces and $m(q, \tau)$ is the data in parabolic Radon domain [10]. The transformed data are a

function of the curvature $q$ and the zero offset intercept time $\tau$. After a temporal Fourier transformation, the parabolic Radon transform is calculated for each temporal frequency component $\omega$. The forward and inverse transform are expressed in (10) and (11), respectively [10].

$$M(q,\omega) = \sum_{n=1}^{N} D(x_n,\omega) exp(j\omega q x_n^2) \quad (10)$$

$$D(x_n,\omega) = \sum_{i=1}^{N_q} M(q_i,\omega) exp(-j\omega q_i x_n^2) \quad (11)$$

where $M(q,\omega)$ and $D(x_n,\omega)$ are the temporal Fourier transform of $m(q,\tau)$ and $d(x_n,t)$, respectively, and $N_q$ is the number of $q$ values.

Parabolic Radon filtering is the process based on the moveout differences between primary and multiple reflections in common depth point (CDP) gather. The schematic of parabolic Radon filtering is illustrated in Fig. 4. The normal moveout (NMO) correction with the velocities of primary reflections is applied to input CDP gather. After NMO correction, the primary reflections turn into straight lines and the multiple reflections turn into parabolas. The NMO corrected CDP gather is transformed to the $\tau - q$ domain by parabolic Radon domain transform, the primaries and multiples can be discriminated, and the multiples are muted out. The muted data is transformed back to the CDP domain, and the inverse NMO correction is applied to obtain the data without multiples.

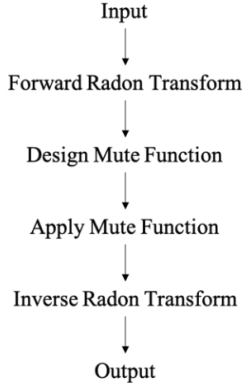


***Fig. 4.*** *The procedure of parabolic Radon filtering.*

**2D MARINE SEISMIC DATA**

The 2D marine seismic data of the East Coast of the United States-Southern Atlantic Margin used for this research are the open data and available on the U.S. Geological Survey website. A number of survey lines were carried out approximately 25,000 km with multichannel seismic reflection survey between 1974 and 1978 to address hydrocarbon resource potential and stratigraphic history. The used dataset is a second quarter part of line number 31. The details of shot and receiver parameters collected from the USGS report and observer's log are shown in Table 1.

***Table 1.*** *The information of 2D marine seismic data*

| | |
|---|---|
| Line number | 31 |
| Distance | 52250 m |
| Number of shots | 999 |
| Number of receivers | 48 |
| Shot interval | 50 m |
| Group interval | 50 m |
| Minimum offset | 359 m |
| Maximum offset | 2709 m |
| Trace length | 12 s |
| Sampling rate | 4 ms |
| Fold coverage | 24 |

## RESULT AND DISCUSSION

2D marine seismic data contain the long-period surface-related multiple reflections. Predictive deconvolution, surface-related multiple eliminations (SRMEand parabolic Radon filtering were conducted to remove surface-related multiple reflections. Predictive deconvolution was limited to suppress the long period of multiple reflections and dipping reflectors in 2D marine seismic data. The multiple reflections are remained as shown in Fig. 5 and Fig. 6 and indicated by the rectangle and the ellipse.

SRME and parabolic Radon filtering can efficiently remove surface-related multiple reflections. While SRME successfully removed near-offset multiple reflections, however far-offset multiple reflections had remained. For the reason that the construction of multiples model uses an approximate velocity from the input data. The amplitude between the estimated model of multiples and the original input data are different, especially in far offset. Thus, this situation limits the ability of SRME. However, the residual far offset multiple reflections were removed by parabolic Radon filtering.

The random noise appearing in 2D marine seismic data was very problematic. Due to this troublesome noise, the performance of multiple removal methods was limited. The stacked section at CDP numbers around 12000 to 13200 contains the noise obscuring the reflectors. SRME and parabolic Radon filtering could remove the most of multiple reflections, however they have remained. The residual multiple reflections in noisy data are shown in Fig. 7 and indicated by the rectangle. Nevertheless, Fig. 8 displays the results from the success of SRME and parabolic Radon filtering. The long period multiples reflections were almost removed, the results will not give any misunderstandings in the interpretation.

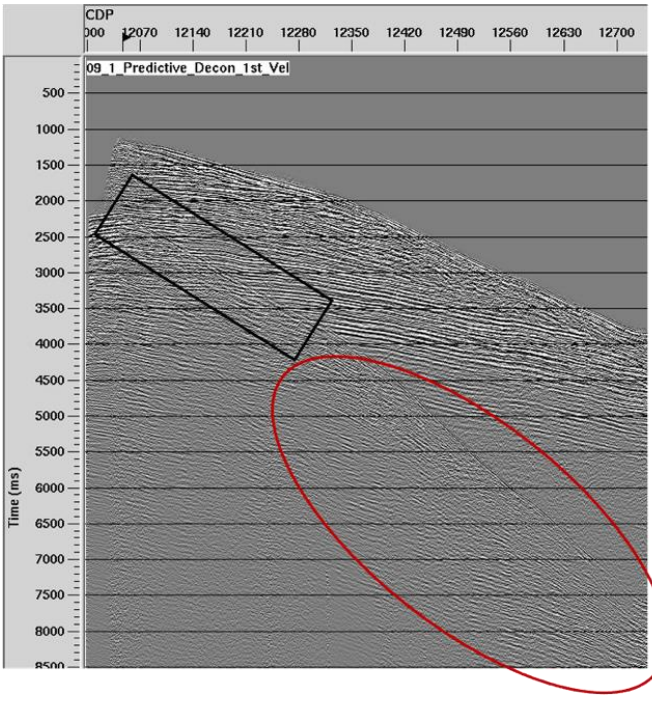


***Fig. 5.*** *The stacked section of 2D marine seismic data at CDP numbers 12000 to 12730 from multiple removals by the predictive deconvolution.*

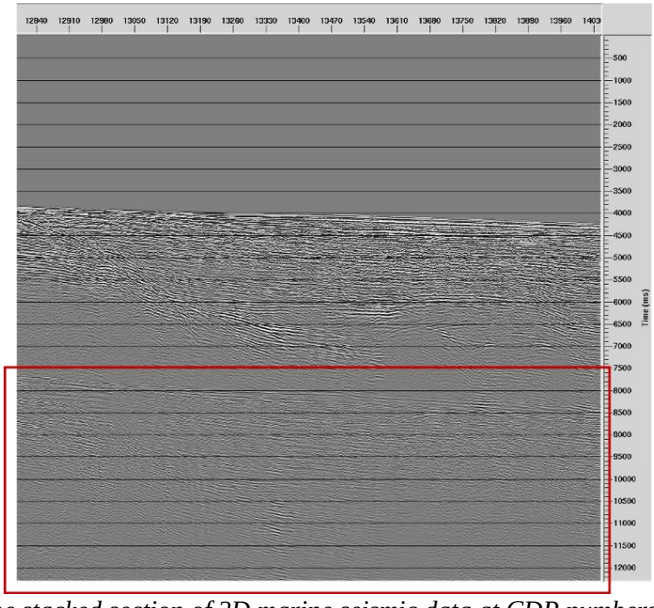


***Fig. 6.*** *The stacked section of 2D marine seismic data at CDP numbers 12800 to 14030 from multiple removals by predictive deconvolution.*

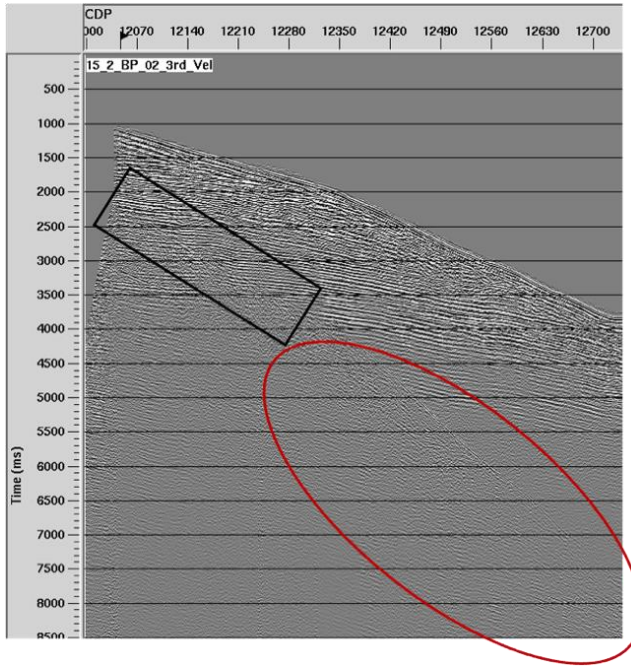


***Fig. 7.*** *The stacked section of 2D marine seismic data at CDP numbers 12000 to 12730 from multiple removals by the combination of SRME and parabolic Radon filtering, respectively.*

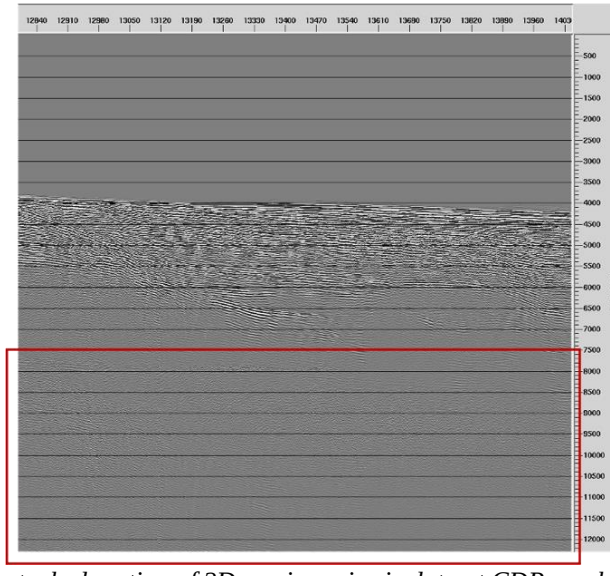

***Fig. 8.*** *The stacked section of 2D marine seismic data at CDP numbers 12800 to 14030 from multiple removals by the combination of SRME and parabolic Radon filtering, respectively.*

## CONCLUSION

This research used three multiple removal methods in order to analyze the long-period surface-related multiple reflections. The predictive deconvolution cannot attenuate the long-period multiple reflections in seismic data. The performance of the predictive deconvolution process is degraded when the multiple period changes, such as the dipping reflectors and the complexity of geological structures. SRME and parabolic Radon filtering are effective in removing long-period surface-related multiple reflections. The combination of these two methods increases signal-to-noise ratio. The near-offset multiples are effectively removed by SRME. The residual far-offset multiples are suppressed by parabolic Radon filtering. However, the performance of multiple removal methods is limited by the random noises obscuring the signals. The more noise is cleaned, the better results will be.

## ACKNOWLEDGEMENTS

We would like to thank Halliburton for SeisSpace® ProMAX 2D software support and the U.S. Geological Survey for the dataset used in this research.

## REFERENCES

[1] Verschuur D.J., Seismic multiple removal techniques: past, present and future. EAGE, Houten, 2013.

[2] Peacock K.L., Treitel S., Predictive deconvolution: Theory and practice, Geophysics, vol. 34, no. 2, pp 155-169, 1969.

[3] Schoenberger M., Houston L.M., Stationarity transformation of multiples to improve the performance of predictive deconvolution, Geophysics, vol. 63, no. 2, pp 723-737, 1998.

[4] Jian X., Zhu S., Predictive deconvolution for attenuation of multiple reflections in marine seismic data processing, Journal of Coastal Research, vol. 73, pp 310-314, 2015.

[5] Verschuur D.J., Berkhout A.J., Wapenaar C.P.A., Adaptive surface-related multiple elimination, Geophysics, vol. 57, no.4, pp 1166-1177, 1992.

[6] Naidu P., Santosh, Chand S., Saxena U.C., Surface related multiple elimination: A case study from east coast India, in Proc. 10th Biennial International Conference & Exposition, Kochi, 2013, p 217.

[7] Kim T., Jang S., Increasing signal-to-noise ratio of marine seismic data: A case study from offshore Korea, Journal of Applied Geophysics, vol. 134, pp 136-145, 2016.

[8] Hadidi M.T., Baumstein A.I., Kim Y.C., Surface-related multiple elimination on wide-tow marine data, The Leading Edge, vol. 21, no. 8, pp 787-790, 2002.

[9] Lester R., McIntosh K., Multiple attenuation in crustal-scale imaging: examples from the TAIGER marine reflection data set, Marine Geophysical Research, vol. 33, pp 289-305, 2012.

[10] Hampson D., Inverse velocity stacking for multiple elimination, in SEG Technical Program Expanded Abstracts, 1986, pp 422-424.

[11] Abbadi S., Jaiswal P., Attenuating ling-period multiples in short-offset 2D streamer data: Gulf of California, in SEG Houston 2013 Annual Meeting, 2013, pp 4201-4205.

[12] Dondurur D., Acquisition and processing of marine seismic data. Elsevier, Amsterdam, 2018.

[13] Kearey P., Brooks M., Hill I., An introduction to geophysical exploration. Third Edition, Blackwell Science Ltd, Oxford, 2002.

[14] Berkhout A.J., Seismic migration, imaging of acoustic energy by wave field exploration, Part A: theoretical aspects. Elsevier, Amsterdam, 1982.

[15] Berkhout A.J., Verschuur D.J., Integrated multiple elimination and source wavefield estimation, in SEG Technical Program Expanded Abstracts, 1993, pp 1095-1098.

# MULTICOMPONENT DEPOSITS WITH BY-PRODUCT AS THE MAIN SOURCE OF FELDSPAR RAW MATERIALS FOR MODERN TECHNOLOGIES

**Dr. Geol.-Mineral. Sci., Dr. Geogr. Sci., Dr. Eng. Sci., Prof. Georgii Rudko**[1]
**Assoc. Prof. Ph.D. Mariia Kurylo**[2]
**Ph.D. Student Maksym Ozerko**[3]
[1] State Commission of Ukraine on Mineral Resources, Kyiv, Ukraine
[2, 3] National Taras Shevchenko University of Kyiv, Kyiv, Ukraine

## ABSTRACT

Feldspar is raw materials with a growing volume of production every year, as well as a price for it. Feldspar consumption has been gradually increasing in ceramics, glass industry for solar panels, housing, and building construction.

Feldspar raw materials include intrusive, effusive rocks, weathering crust of crystalline rocks, sedimentary altered and altered rocks, as well as partially medium and basic aluminosilicate rocks. It was defined an industrial application for each species of feldspar. Potassium feldspars (orthoclase, microcline, sanidine) are used in electroceramic, electrode, abrasive, and ceramics industries. For these productions, the potash module is fixed in a ratio of 2: 1. For some industries, in particular the manufacture of high-voltage ceramics, the necessary feldspars are as close as possible to pure potassium (with a modulus of at least 4: 1, which corresponds to 80% of the orthoclase component). Potassium-sodium raw materials, from a potassium modulus of at least 0.9, are used for building construction. Sodium minerals with non-standardized potassium modulus are used for the glass industry, the production of enamels, and products such as vitreous porcelain. Calcium feldspars, represented by plagioclase of higher numbers, have limited practical application and their presence in feldspar concentrates is undesirable.

According to mineral associations, all types of feldspar raw materials can be divided into five types: 1) feldspar (syenites, trachitis); 2) quartz-feldspar (pegmatites, granites, sands, etc.); 3) nepheline-feldspar (nepheline syenites, alkaline pegmatites); 4) quartz-sericite-feldspar (shales, secondary quartzites); 5) quartz-kaolinite-feldspar (sands, alkaline kaolins, secondary quartzites).

It is shown on the example of Ukrainian deposits of feldspar minerals that complex deposits with by-products become the main source for production. Especially if these are new mining operation facilities. The authors have identified three main types of such complex multicomponent deposits: 1) deposits of intrusive rocks where weathering crust of crystalline rocks are mined as a byproduct; 2) complex deposits, where feldspar rocks are enclosing or overburden and can also be considered as byproducts; 3) deposits where feldspar concentrate can be produced as a product of ore components processing.

***Keywords:*** *feldspar minerals, by-product, multicomponent deposit, Ukraine*

## INTRODUCTION

Feldspar is raw materials with a growing volume of production every year, as well as a price for it. Feldspar consumption has been gradually increasing in ceramics, glass industry for solar panels, housing, and building construction.

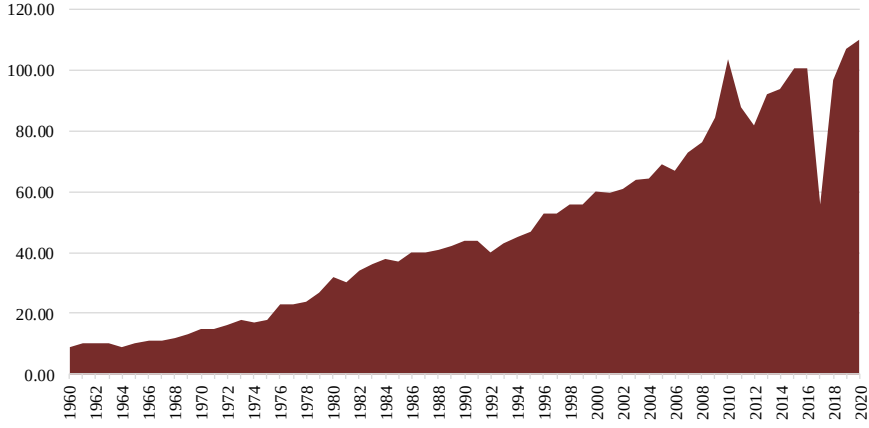


***Fig. 1.*** *Feldspar price dynamics (according to statistical data usgs.gov [3])*

Feldspars deposits are divided into three main groups: potassium feldspars - (orthoclase, microclines) $K_2OAl_2O_3{\times}6SiO_2$, sodium feldspars - (albites) $Na_2OAl_2O_3{\times}6SiO_2$ and calcium feldspars - (anortites) $CaOAl_2O_3{\times}2SiO_2$, which are present to varying degrees in all crystalline rocks. Potassium feldspar is the primary rock-forming mineral of many igneous metamorphic and sedimentary rocks. In addition to the main groups, there are other feldspars, such as barium feldspar – $BaOAl_2O_3{\times}2SiO_2$ (celsian), but they are rarely used in ceramics. The primary parameter that characterizes feldspar concentrates is the potassium modulus (ratio $K_2O$:$Na_2O$).

According to modern concepts, feldspar raw materials include intrusive, effusive rocks, weathering crusts of crystalline rocks, sedimentary unaltered and altered rocks, as well as partially medium and basic aluminosilicate rocks.

Each type of feldspar has its field of industrial application:

- potassium feldspars (orthoclase, microcline, sanidine) are used in the electroceramic, electrode, abrasive and porcelain-earthenware industries. The potassium modulus for the porcelain-earthenware industry has been established in the ratio of 2:1. Feldspars as close as possible to pure potassium (with the modulus not less than 4:1 corresponding to 80% of the orthoclase component) are essential in several productions, particularly the production of high-voltage porcelain;
- potassium-sodium raw materials, with a potassium modulus of at least 0.9, are used in ceramic building materials;

- sodium raw materials with non-standardized potassium modulus are used in the glass industry, the production of enamels and products such as vitreous china;
- calcium feldspars represented by plagioclase of higher numbers have limited practical application, and their presence in feldspar concentrates is undesirable.

According to mineral associations, feldspar raw materials can be divided into five types:

- feldspar (syenite, trachyte);
- quartz-feldspar (pegmatites, granites, sands, etc.);
- nepheline-feldspar (nepheline syenites, alkaline pegmatites);
- quartz-sericite-feldspar (shales, secondary quartzites);
- quartz-kaolinite-feldspar (sands, alkaline kaolins, secondary quartzites).

Total balance reserves of feldspar raw materials as of 01.01.2020 amounted to 49109.07 thousand tonnes by categories A+B+$C_1$, cat. $C_2$ – 192703.8 thousand tonnes, off-balance – 192.91 thousand tonnes. The total production of feldspar raw materials in Ukraine amounted to 634.63 thousand tonnes in 2019 [1], [6], [7]. It is comparable to major global producers.

There are the following types of deposits in Ukraine:

1. Pegmatite deposits: Bilchakivske, Ustia village, Hruzlivetske, Lozuvatske, Volodymyrivske, Balka Velykoho Taboru;
2. Deposits of crystalline rocks: trachytes of the Verbova site, microgranodiorites of the Dubrynetske deposit;
3. Alkaline kaolins: Prosianivske, Pershozvanivske, Biliayivske, Katerynivske;
4. Multicomponent deposits (feldspar raw materials as a by-product): Bakhtyn (fluorite ores), Nosachivske (titanium-ilmenite ores), Perzhanske deposits of rare metals, Mazurivske (tantalum and niobium ores).

Currently, only the pegmatite deposit “Balka Velykoho Taboru” is being developed, and a special permit for the extraction of pegmatites from the “Hirne” deposit is invalid.

Feldspar raw materials were extracted from crystalline rocks - Dubrynytske deposit of microgranodiorite (Transcarpathian region), which occurs in the flysch rocks of the Carpathian Mountains in the form of a dyke-like body. The deposit was developed by OJSC “Steatyt”. Also, work was conducted to study trachytes of the Verbova site in the Telmanovo district of Donetsk region.

According to the analysis of feldspar raw material production, it is noted that the increase in feldspar raw material production is observed primarily in complex multicomponent deposits - the Piatyrichka section of the Dubrivske deposit and the Novakivska site of the Maidan-Vilske deposit, where alkaline kaolins, hard feldspar

and feldspar crystalline rocks (granites, migmatites, plagiogranites, pegmatoid granites) are developed.

The most significant object of additional study of feldspar raw materials is the Piatyrichka site of the Dubrivske deposit, which is being exploited. The Piatyrichka site of the Dubrivske alkaline kaolin deposit is located at a distance of about 400 m north of Hlynianka village (until 2016 - Piatyrichka) in the Baranivka district of Zhytomyr region.

Until 2019, the Piatyrichka site of the Dubrivske deposit was developed as a deposit of primary kaolins approved in 1991 by the protocol of the CCMR SE "Ukrbudmaterialy" in the amount of 614 thousand tonnes as raw materials for the production of refractory bricks. During 2019-2020, it was performed a geological and economic reassessment of primary kaolins as alkaline kaolins at the Piatyrichka site of the Dubrivske deposit with their reevaluation associated with a new direction of use and additional exploration of the lower part of the kaolin deposit – feldspar scree as feldspar raw materials, as well as underlying crystalline rocks (granites, migmatites, plagiogranites, pegmatoid granites) as feldspar raw materials. The quality of alkaline kaolins, feldspar scree and underlying crystalline rocks were determined by the content of $SiO_2$, $Al_2O_3$, $Fe_2O_3$, $TiO_2$, $K_2O$ and $Na_2O$. In addition, the quality of crystalline rocks (granites, migmatites, plagiogranites, pegmatoid granites) as feldspar raw materials was previously studied.

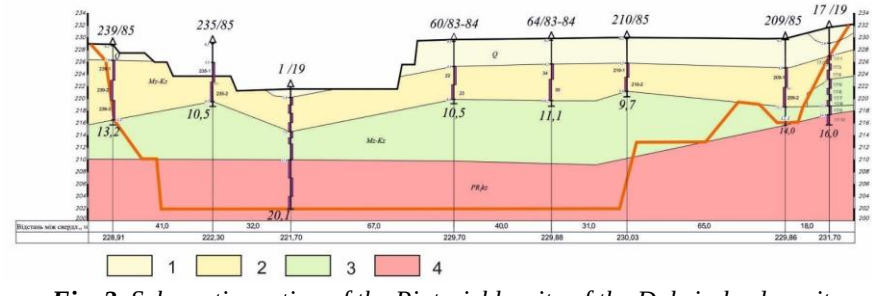


***Fig. 2.*** *Schematic section of the Piatyrichka site of the Dubrivske deposit (according to data of the PC "Geolog")*

1 – sedimentary rocks (Q), 2 – alkaline kaolins (Mz-Kz), 3 – feldspar scree (Mz-Kz), 4 – feldspar crystalline rocks (granites, migmatites, plagiogranites, pegmatoid granites).

***Table 1.*** *The quality of alkaline kaolins, feldspar scree, and underlying crystalline rocks of the Dubrivske deposit*

| № | Component (indicator) | Content of the component (value of the indicator) | | |
|---|---|---|---|---|
| | | alkaline kaolin | feldspar scree | crystalline rock |
| Chemical composition (for calcined substance) | | | | |
| 1. | $SiO_2$ content, % | 72,05-75,75 | 72,87-74,81 | 71,16-73,96 |
| 2. | $Al_2O_3$ content, % | 17,55-18,63 | 15,33-16,17 | 15,12-15-64 |
| 3. | $Fe_2O_3$ content, % | 0,64-0,68 | 0,61-1,16 | 1,10-1,15 |
| 4. | $TiO_2$ content, % | 0,13-0,15 | 0,07-0,09 | 0,07-0,09 |
| 5. | $K_2O+Na_2O$ content, % | 6,07-6,86 | 7,71-7,96 | 8,40-8,56 |
| Mineralogical composition | | | | |
| 6. | Feldspar, % | 30-40 | 40-60 | 55-65 |
| 7. | Quartz, % | 20-30 | 20-30 | 20-30 |
| 8. | Mica, % | 2-5 | 2-5 | 2-5 |
| 9. | Kaolinite, % | 30-40 | 5-25 | 0-5 |

It has been noted that the content of feldspars decreases from the bottom up due to the kaolinization of plagioclase, the content of alumina increases from the bottom up and accumulates in alkaline kaolins. The content of iron oxide is low. The refractory value of alkaline kaolins at the Piatyrichka site of the Dubrivske deposit was 1380-1710 C, feldspar scree – 1320-1580 C, and crystalline rocks – not determined.

Technological tests of laboratory-technological samples to check technological parameters of feldspar masses production in the industrial conditions were carried out at the ISU “Ceramic tile plant” of LLC Epicenter K in ceramic masses with the following content of raw materials.

***Table 2.*** *Technological parameters of feldspar masses production*

| № ceramic mass | Content index | | | |
|---|---|---|---|---|
| | clay PJSC “Vesko” | alkaline kaolin site “Piatyrichka” | feldspar scree site “Piatyrichka” | pegmatite |
| Ceramic mass № 1 | 40,0 | 5,0 | 15,0 | 40,0 |
| Ceramic mass № 2 | 40,0 | 10,0 | 10,0 | 40,0 |

Obtained ceramic masses were ground up and demagnetized from ferrous and weakly magnetic materials using a rod magnet. A mixture of masses was prepared; its technological parameters met the production and state technological requirements B B.2.7-117-2002 “Ceramic tiles for floors. Technical conditions”. Currently, the ISU “Ceramic tile plant” of LLC Epicenter K uses both alkaline kaolin and feldspar raw materials for the manufacture of ceramic tiles [7], [9].

One of the complex multicomponent deposits of feldspar raw materials is the Mazurivske deposit of rare metal nepheline-feldspar ores (niobium, tantalum, zirconium) with approved reserves. It is one of the first discovered zircon deposits, where the industrial significance of the discovered ores was established in the course of exploration works in 1934-1948. The Mazurivske deposit was considered as a formation containing 2 ore types: zircon ores of the alkaline complex and

ilmenite ores of basic and ultrabasic rocks. The deposit was operated until 1967 when it was preserved with the advent of cheaper raw materials of the Vilnohirsk Mining and Metallurgical Plant. Due to the absence of an economic technological enrichment scheme, metals were not processed and were sent in the form of sludge (99% of the initial volume of ore) to dumps, where they were stored. About 2 million tonnes of ore were processed. Currently, accumulated "tailings" of the enrichment plant contain nepheline, feldspar, pyrochlore, rare metal, and rare earth minerals, and it is a technogenic deposit – a potential source of feldspar.

44 ore bodies were found at the deposit (Mazurivske ore node), including 10 within the studied area (within the project quarry). Ore bodies are traced at considerable distances, often more than 1000 m for some bodies. Their width is mostly more than 300 m, and the thickness varies from 1 to 45-80 m. Contacts of ore bodies with host rocks are clear, rapid, well-mapped visually in the core holes [4], [5], [8].

The deposit belongs to the geological-industrial type of rare metal albitite associated with nepheline syenites. The main industrial type of ore is disseminated, complex tantalum-niobium-zircon ore. The main carrier of niobium and tantalum is pyrochlore, zirconium – zircon. According to the content of conditional tantalum pentoxide, the generalizing conditional indicator that takes into account the contribution of each basic component to the cost of production, poor (common in various bodies from 16 to 33%), ordinary (28-58%), rich (15-55%) and very rich ores (0-2%) were identified within the deposit. Average contents of useful components (niobium, tantalum pentoxides and zirconium dioxide) in ores of the whole deposit were: 0.118%; 0.0057% and 0.47%, respectively; in the bodies of the detailed block - 0.116%; 0.004% and 0.49%. The distribution of niobium, tantalum and zirconium oxides in industrial bodies was uneven and extremely uneven.

During 2003-2004, state geological enterprise "Donetskgeologiya" carried out exploration works for geological and industrial assessment of technogenic enrichment wastes of the Mazurivske rare metal deposit on the area of 8.5 hectares. In 2005, the SCMR estimated the amount of feldspar raw materials in the dumps of the Eastern part of the deposit in the amount of 1133.5 thousand tonnes. Besides, the presence of associated mineral resources in the processing waste was detected in the amount of niobium pentoxide - 1053 tonnes, with the average content of $Nb_2O_5$ in the mineral - 0.09%, zirconium dioxide - 1313 tonnes, with the average content of $ZrO_2$ in the mineral - 0.11%.

During 2014-2016, LLC "Azov-Mineraltekhnika" carried out researches and developed technological regulations for feldspar raw materials. Test results showed the suitability of the material for the colored packaging glass production. Following the test results, LLC "Azov-Mineraltekhnika" developed technical conditions "Alkaline aluminosilicate flux".

Tests of feldspar concentrate with a low content of iron oxides in the ceramic tile and sanitary ware production showed that the material contains impurities, which give a darker color of the ceramic mass when firing ceramics, compared to feldspar materials of other manufacturers ( with the same iron oxide content). Thus, feldspar concentrates from the enrichment waste of weathered ores of the

Mazurivske deposit with $Fe_2O_3$ content up to 0.5% in ceramic production are of limited use - for the production of ceramic products that are covered with opaque glaze. Calculations of technical and economic indicators characterize the economic feasibility of reserve development of the Eastern section of the weathered ore enrichment waste storage of the Mazurivske rare metal deposit [4], [5], [8].

As of 2020, balance reserves of feldspar raw materials of the Eastern section of the weathered ore enrichment waste storage amount to 826 thousand tonnes. Besides, $ZrO_2$ reserves in the amount of 510.8 tonnes with an average content of 0.172% and $Nb_2O_5$ - 283.3 tonnes, with an average content of 0.095% were calculated.

Processing stored waste allows us to free up large areas of tailings and eliminate the source of potential environmental hazard given the existing connection of tailings with the river Kalchyk basin. However, a base of feldspar raw materials can be created for the ceramic industry quite quickly and without significant investment [2]. Such production will become a testing ground for the preparation of the complex development of the Mazurivske deposit.

Due to the growing demand for rare metal raw materials, the Perzhanske ore field, within which there is the Perzhanske beryllium deposit, is of particular interest; it is represented so far by the only industrial-genetic and technological type of high-quality phenakite-genthelvin ores in alkaline (feldspar) metasomatites.

Two sites have been explored at the field: Pivnichna (5,5x1,5 km) and Krushynska (4,0x2,0 km). Ore zones occur with the extension of basic structural elements of the Sushchano-Perzhanska zone, their length reaches 5 km with a width of up to 35-100 m. Ore zones have been traced up to 400 m in depth. Each ore zone consists of a series of en echelon ore bodies with a thickness of a few meters up to 20-30 m. Ore bodies are composed of feldspar and mica-quartz-feldspar metasomatites, they form lenticular and vein-like formations of complex shape (characteristic swellings, obtuse wedging) deposits with rich genthelvite (genthelvite – $Zn_4$ $(BeSi_2)_3S$) mineralization (average BeO content is 0,55 %, maximum content - 8%). Ore bodies are bordered by a strip of 5-30 m of granite with blue newly formed quartz. The upper parts of ore bodies are composed primarily of albite-microcline metasomatites, the lower parts – mica-quartz-feldspar metasomatites. Phenakite mineralization, which is formed at an early stage of mineral formation, is spatially separated from the genthelvite one and localized primarily in the western part of endocontact of the Perzhanskiy granite massif forming a poor (average BeO content - 0.2%) impregnated mineralization. Cassiterite, columbite, and zircon are present as accessory minerals [10], [11].

The Perzhanske ore field is located in the central part of the Sushchano-Perzhanska tectonic-metasomatic zone of the north-eastern extension (north-western part of the Volyn megablock of the Ukrainian Shield), at its junction with the latitudinal North Ukrainian linear zone of tectonic activation [4]. This ore field together with Yastrubetske, Yurivske and Sushchanske ore-bearing fields form the Perzhanskiy ore district within the Sushchano-Perzhanska structural-metallogenic zone [10], [11].

Studies of the chemical composition of rocks in the Perzhanskiy ore node have shown that the amount of $K_2O+Na_2O$ is 6,9-12,8 % in hydrothermal-metasomatic formations (syenites, granites, metasomatites) with a potassium modulus of 0,6-1,9, and they can serve as a material for feldspar concentrates, which will increase economic attractiveness.

One way to increase the investment attractiveness of deposits is the complex development of various ore objects in the ore field by one mining and processing plant, which would allow producing commodities for different purposes (beryllium oxide, zinc sulfide, ilmenite, apatite, disthene, zircon, rare earth, fluorite and feldspar concentrates) to ensure the development of electronic, nuclear, automotive and aviation industries and highly profitable agriculture.

It should be noted that the Mazurivske and Perzhanske deposits of rare metals are classified as priority development objects.

There are other multicomponent deposits with feldspar raw materials as a co-product - Bakhtyn (fluorite ores), Nosachivske (titanium-ilmenite ores).

Bakhtyn fluorite deposit is located in Murovanokurilovetsky district of Vinnytsia region. The deposit is confined to the Olchedaevsky and Yampolsky feldspar-quartz sandstones of the Vendian age. Deposit consists of two ore bodies (upper and lower) of a sheet-like form, consisting of disconnected lenticular bodies on an area of 700 x 1200 m, the depth of occurrence is 21.3–118.5 m. The total thickness of fluorite-containing sandstones varies from 0,4 to 4.7 m, and the fluorite content in them ranges from 5 to 48.9% (average 15%). Fluorite in sandstones is a typical epigenetic mineral replacing cement, partly quartz and feldspars. The Bakhtyn fluorite deposit is planned to be developed with an underground mine with a life of mine more than 20 years. During the operation of the deposit and flotation processing of ores, more than half of the commodity product will be feldspar concentrates.

Nosachivske apatite-ilmenite deposit is located in the Smelyansky district of the Cherkasy region of Ukraine. The deposit consists of two elongated sheet-like deposits. The length of ore bodies along the strike is up to 2000 m, the width across the strike is from 450 to 1000 m. Taking into account the mining and geological conditions of the deposit ( the dip angle of deposits is 45º - 75º, the development depth is below 700 m from the earth's surface), the need to preserve the earth's surface with the existing high-grade objects and rational use of the subsoil, the most acceptable and economically feasible is the underground method of development. The output of the feldspar concentrates will be more than 2 million tons with planned productivity of 4 million tons of ore.

## CONCLUSION

It is shown on the example of Ukrainian deposits of feldspar minerals that complex deposits with by-products become the main source for production. Especially if these are new mining operation facilities. The authors have identified three main types of such complex multicomponent deposits: 1) deposits of intrusive rocks where weathering crust of crystalline rocks are mined as a byproduct; 2)

complex deposits, where feldspar rocks are enclosing or overburden and can also be considered as byproducts; 3) deposits where feldspar concentrate can be produced as a product of ore components processing.

The production of feldspar concentrates as by-products with ore processing of multicomponent deposits is one of the ways of increasing their profitability. This is due to the large production volume of feldspar products and an increase in raw material prices. The price of feldspar products is not as high as that of the main components - metals, fluorite, apatite, but the huge output of these products affects the final deposit value as well as the prices of the main components.

## REFERENCES

[1] Balance of mineral reserves of Ukraine. Issue 72. Feldspar raw materials. Kyiv, State Research and Production Enterprise "State Information Geological Fund of Ukraine", 2018. *(in Ukrainian)*

[2] Cherniyenko N.M. Complex use of ores of the Mazurivske deposit, Pryazovia region// http://ea.donntu.org:8080/jspui/bitstream/123456789/7226/1/215-222.pdf *(in Ukrainian)*

[3] Feldspar Statistics and Information. National Minerals Information Center. USGS// https://www.usgs.gov/centers/nmic/feldspar-statistics-and-information

[4] Haletskiy L.S., Shevchenko T.P., Cherniyenko N.M. New concepts about the geological structure and metallogeny of the territory of Ukraine // Geological Journal. № 3, pp. 74–83, 2008. *(in Ukrainian)*

[5] Haletskiy L.S., Naumenko U.Z., Cherniyenko N.M. Main types of ore-bearing structures of Ukraine // Mineral resources of Ukraine. № 4, pp. 12-19, 2016. *(in Ukrainian)*

[6] Mineral resources of Ukraine, Kyiv, State Research and Production Enterprise "State Information Geological Fund of Ukraine", 270p., 2014. *(in Ukrainian)*

[7]. Mineral resources of Ukraine, Kyiv, State Research and Production Enterprise "State Information Geological Fund of Ukraine", 270p., 2020. *(in Ukrainian)*

[8] Mostyka Yu.S., Shpylioviy K.L., Miakyshev V.M., Shpylioviy L.V. Substantiation of geological-economic, technological and ecological possibilities of industrial development of technogenic deposit of feldspar raw materials // Modern economic possibilities of development and sales of mineral resource base of Ukraine and Russia in the conditions of globalization of the mineral raw material market. IGS NAS of Ukraine. Kyiv,- pp. 219-222, 2005. *(in Russian)*

[9] Rudko H.I., Ozerko V.M., Shepel I.V. Geology and geological-economic assessment of kaolin deposits in Ukraine. Ed. by H.I. Rudko. Kyiv. 2015. *(in Ukrainian)*

[10] Voynovskiy A.S., Bochay L.V., Nechayev S.V. et al. Complex metallogenic map of Ukraine. Scale 1:500 000. Explanatory note. Kyiv, UkrDGRI,

State geological service of the Ministry of Natural Resources of Ukraine, 336 p., 2002. *(in Ukrainian)*

[11] Vysotskiy B.L., Lykov L.I., Prykhodko V.L. et al. Geological and economic assessment of the Perzhanske ore field // Collection of scientific proceedings of UkrDGRI, № 1. pp. 172–179, 2005. *(in Ukrainian)*

Section

# SOIL SCIENCE

Plant and soil science
Soil management
Soil Biology

# ASSESSMENT OF STRONTIUM, RUBIDIUM AND SCANDIUM STATUS IN SOILS AFFECTED BY SOLID WASTE DEPOSITS

**Prof. Dr. Luminita Pirvulescu**[1]
**Assoc. Prof. Dr. Despina-Maria Bordean**[2]
**Lecturer Dr Loredana Copacean**[3]
**Lecturer Dr. Narcis Gheorghe Baghina**[4]
**Assoc. Prof. Dr. Carmen Petcu**[5]
**Dr. Diana Obistioiu**[6]
[1, 2, 3, 4, 6] Banat's University of Agricultural Sciences and Veterinary Medicine "King Michael I of Romania" from Timisoara, Timisoara, Romania
[5] University of Agronomic Sciences and Veterinary Medicine of Bucharest, Bucharest, Romania

## ABSTRACT

The aim of the study was to assess the level of contamination of soil with strontium, rubidium and scandium in the solid waste deposits. The study was performed on soil samples collected from Moldova Noua, southwest of Romania, an area with historical anthropogenic history. The soil analysis was performed using X-ray fluorescence (XRF). The samples were collected from five collection points using a random pattern from around the illegal waste deposit and all analyses were performed in triplicate. To assess the influence of wastes on the soils concentration levels of strontium (Sr), rubidium (Rb) and scandium (Sc), were calculated contamination factors (CF), and pollution index ($PI_L$) by reporting the concentration of the investigated elements of the upper earth crust concentrations and geo-accumulation index ($I_{geo}$) calculated by reporting the elements concentration values to a control sample, used as reference. The reference sample was collected from an area close to the waste deposit but located in a protected green area. The results show that from the investigated elements, scandium is the element of concern, the soil presenting a moderate contamination level with this element.

***Keywords:*** *heavy metals, contamination factors, pollution index, geo-accumulation index*

## INTRODUCTION

The rising number of illegal waste dumps represents a global problem and is the result of the increase of waste production correlated with the ever-growing population. Even if official waste disposal sites are available, illegal waste dumps occur everywhere around the world, most commonly on the periphery of colonized areas, forest margins, as well as at other places, contaminating the environment and degrading land [15]. The metal concentration and behavior of metals associated with various industrial, mines or municipal wastes in soil systems is much higher and affects metal mobility, being decidedly dependent on the waste type. The modifications in time of the environmental conditions, such as changes in pH, the

degradation of the organic waste matrix, or soil solution composition, may modify metal mobility [10].

The aim of the study was to assess the level of contamination of soil with strontium, rubidium and scandium on disposed solid wastes. Contaminations are less investigated in rubidium, strontium and scandium soils. Compared to the number of studies related to hazardous heavy metals, strontium occurs in nature, is estimated to approximately 320 ppm in the upper Earth's crust [12]. Rubidium is an alkali metal, almost as abundant as zinc. According to Rudnick et al, in the upper earth crust are approximately 84 ppm rubidium [12]. Rubidium is easily taken up by plants, similar to potassium and generally is concentrated in flowers and young leaves [6]. It is appreciated by a recent study as the best predictor variable for estimating the clay content and salinity of soils [14]. Scandium is a naturally occurring element in the soil and its concentrations vary across geographic regions. In the earth's crust, Sc is varying from 16 ppm [8] to 25 ppm [2]. The soils as well as the natural and/ or mineral water [7] have a specific natural content of metal cations, which depend on the background concentrations specific to the investigated area. The control area was chosen, as it is a protected area and due to its natural potential and ecological value. The Romanian territory shelters a huge variety of habitats, of national as well as European interest.

## MATERIALS AND METHODS

*Description of the Study Site:* The investigated area is located in the southwest of Romania, close to Moldova Noua city and close to the Danube.

The study was conducted on soil samples from an area where an illegal waste deposit was identified and compared to soil samples from a vegetation area, practically a protected area, which is considered as a control area. All samples were collected using a random pattern from around the waste deposit (Figure 1).

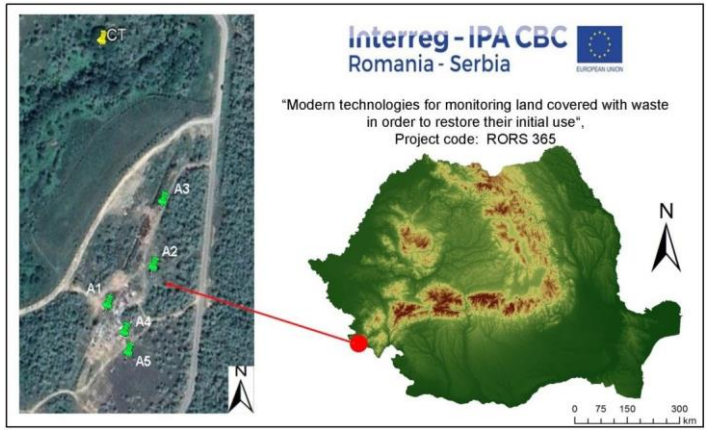


***Fig. 1.*** *Map of the investigated experimental area [4], [5]*

*Legend: A1, A2, A3, A4, A5 - Soil sampling collection points, CT – Soil sampling control point*

The soil samples was collected from the topsoil (0-20 cm depth) using a standard auger. For evaluating the soil status of the experimental area (Table 1) were established five collection areas (A1, A2, A3, A4, and A5). From each collection area were sampled three replicates, which were thoroughly mixed to obtain a homogenous soil mixture.

*Preparation of soil samples for analysis*

For the accuracy of the analysis results, the fragments of leaves and small stones were removed and the soil samples were dried until the water content became less than 10%, and ground into a fine powder (~ 100μm). For XRF analysis, the soil sample is analyzed in a sample cup with a thin built-in polypropylene film.

***Table 1.*** *GPS Stereo coordinates of the soil samples collection points*

| Samples Area | Sample code | x | y |
|---|---|---|---|
| Illegal waste deposit | A1 | 362637.919 | 234144.254 |
| | A2 | 362679.914 | 234201.804 |
| | A3 | 362754.786 | 234216.725 |
| | A4 | 362605.614 | 234163.640 |
| | A5 | 362582.523 | 234167.162 |
| Control sample, area with vegetation | CT | 362947,015 | 234151,003 |

*Legend: A1, A2, A3, A4, A5 - Soil sampling collection points, CT – Soil sampling control point*

*Soil analysis*

The analysis of the soil samples were performed using X-MET8000 - X-Ray Fluorescence Analyzer. The apparatus is factory calibrated. All analysis were done in triplicate and result were shown as average ± SD

*Contamination indices*

Soil contamination with strontium, rubidium and scandium, was evaluated using pollution indices (contamination factor, pollution index of soil loadings ($PI_L$) and geo-accumulation index ($I_{geo}$)) presented in Table 2. Soil Contamination Factor (CF) represents a quantification of the contamination level relative to upper earth crust composition of the investigated metals as shown in Table 2.

In this paper, we used separately, both, the concentration of elements in the Earth's crust as well as concentration of the control samples as reference values. The concentration of elements in the Earth's crust are presented in Table 3 [1], [13].

The Geo-Accumulation Index ($I_{geo}$) of a sample site was calculated according to the relation shown in Table 2 [9]. The classifications of contamination level based on CF, $PI_L$ and $I_{geo}$ are presented also, in Table 2.

Statistical Analysis

The experimental data were statistically evaluated using Excel 2007, PAST Version 2.17c and Statistica 13.5.0.17 Tibco Software Inc.

***Table 2.*** *The classification of pollution level based on soil pollution indices*

| Crt. No | Pollution index and classification of pollution level | Formula | Parameters |
|---|---|---|---|
| 1 | Soil Contamination Factor (CF) [3]:<br>• CF < 1, low pollution;<br>• 1<CF<3, moderate pollution;<br>• 3<CF<6, high pollution;<br>• CF>6, very high pollution [1] | $CF^i = \frac{C^i_{0-1}}{C^i_n}$ | $C^i_{0-1}$ = the mean content of investigated metals from three to five sampling sites<br>$C^i_n$ = the concentration level of the individual metal before depositing waste, practically the concentration of elements in the Upper Earth's crust |
| 2 | Pollution Index of Soil Loadings (PIL) [13]<br>• $PI_L$< 1 no contamination with the studied metals;<br>• $PI_L$= 1, baseline levels of pollutants are present<br>• $PI_L$>1 metal concentrations are above the permissible level, which is producing a deterioration of the soil quality | $PI_L = (CF_1 \cdot CF_2 \cdot \ldots \cdot CF_n)^{1}$ | n = the number of studied metals (three in this study) and CF is the contamination factor calculated as described<br>$CF_1, CF_2, \ldots, CF_n$ are the contamination factors calculated as described before |
| 3 | The Geo-Accumulation Index ($I_{geo}$) [9]<br>• $I_{geo}$≤ 0 no contamination with the studied metals;<br>• 0 <$I_{geo}$≤1 mild to moderate contamination<br>• 1<$I_{geo}$≤2 moderate contamination<br>• 2<$I_{geo}$≤3 moderate to high contamination<br>• 3<$I_{geo}$≤5 high contamination<br>• $I_{geo}$≥5 exceptionally high contamination | $I_{geo} = \log_2 \frac{c^i_n}{k \cdot c^i_{ref}} = \log$ | $c^i_n$ = the measured concentration of heavy metals in the soil (mg/kg),<br>$c^i_{ref}$ = The background concentration of the metals, specific to the studied area<br>Constant k = 1.5 is a correction coefficient that specifies the influence of natural fluctuations and of anthropic sources. |

***Table 3.*** *Concentration of elements in the earth's crust [12]*

| Sample site | Symbol | Heavy metals concentration (ppm) | | |
|---|---|---|---|---|
| | | Sr | Rb | Sc |
| Upper Earth Crust | UEC | 370 | 90 | 22 |

## RESULTS AND DISCUSSIONS

The level of concentrations of the investigated soil samples are presented in Figure 2. The concentrations of Sr, Rb and Sc in the upper earth crust are appreciated in accordance with Rudnick and Gao, 2003 [12]. As we can observe Rb content is much higher in the upper earth crust and slightly higher in the control sample, which was sampled from an area with vegetation, registered as protected area. The samples with the codes A1-A5 are soil samples collected from an area where illegal wastes are deposited. Comparing the obtained heavy metals concentration values, it is visible that the highest scandium content (202 ppm) is shown by soil sample A2, while for strontium (370 ppm) and rubidium (90 ppm), the highest concentration values mentioned, are those in the upper earth crust [12]. The transfer factors for the evaluated heavy metals for all sampling areas are presented in Table 4.

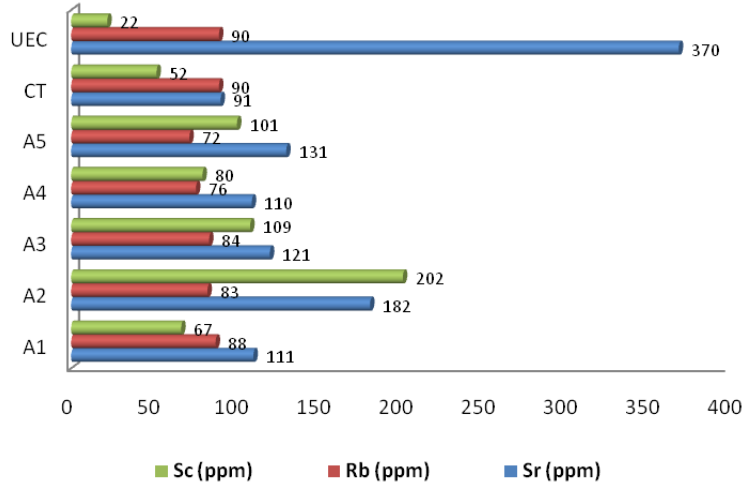


***Fig. 2.*** *Mean values of the concentration of Sr, Rb and Sc in soil samples*

*Legend: A1-A5 and CT, soil sample codes, CT – soil control sample, UEC – upper earth crust concentration values.*

***Table 4.*** *Individual Transfer Factors (CF) and Pollution Index of Soil Loadings ($PI_L$) for Sr, Rb and Sc in soil*

| Sample code | $CF_E$ (Sr) | $CF_T$ (Sr) | $CF_E$ (Rb) | $CF_T$ (Rb) | $CF_E$ (Sc) | $CF_T$ (Sc) | $PI_L$ |
|---|---|---|---|---|---|---|---|
| A1 | 0.35 | 1.22 | 1.05 | 0.98 | 4.79 | 1.29 | 1.209 |
| A2 | 0.57 | 2 | 0.99 | 0.92 | 14.43 | 3.89 | 2.01 |
| A3 | 0.38 | 1.33 | 1 | 0.93 | 7.79 | 2.10 | 1.43 |
| A4 | 0.34 | 1.21 | 0.90 | 0.84 | 5.71 | 1.54 | 1.21 |
| A5 | 0.41 | 1.44 | 0.86 | 0.8 | 7.21 | 1.94 | 1.36 |
| CT | 0.28 | 1 | 1.07 | 1 | 3.71 | 1 | 1.04 |
| UEC | 1 | - | 1 | - | 1 | - | - |

*Legend: A1-A5 and CT, soil sample codes, CT – soil control sample, UEC –upper earth crust, $CF_T$= CF of the metal reported to the background value, $CF_E$ = CF of metal reported to the earth crust value*

The transfer factors of the individual metals were calculated both in respect to control ($CF_T$) as well as to the concentration of elements in the Upper Earth's crust ($CF_E$). In both situations, the soil samples prove to be contaminated with scandium. The contamination factors for Sr, Rb and Sc were calculated by reporting the individual concentration media for each area to two reference concentration values (CT and UEC) in order to identify the historic pollution due to mining activities of Moldova Noua area and the new pollution area created by depositing the solid wastes. The mines present in Moldova Noua area have a long history of (the Stratigraphic age of Late Cretaceous–Paleocene) Porphyry copper deposits [11].

Based on the recommendations of Ahamad et al, 2020 (Table 2), $CF_E$ (Sc) shows high ($3<CF<6$) and very high pollution ($CF>6$), while $CF_T$(Sc) shows moderate ($1<CF<3$) to high pollution ($3<CF<6$). $CF_E$ (Sr) shows low pollution ($CF < 1$) while $CF_T$(Sr) shows moderate pollution, which might confirm that strontium is less in the soil of Moldova Noua area compared to the concentration specific to the upper earth crust. $CF_E$(Rb) and $CF_T$(Rb) are similar. Irrespective of the concentration values used to calculate CF, the pollution level of Scandium is high.

$PI_L$ for Sr, Rb and Sc in soil was calculated only for CFT (Figure 3), in order to evaluate the pollution level created as a result of solid waste deposits.

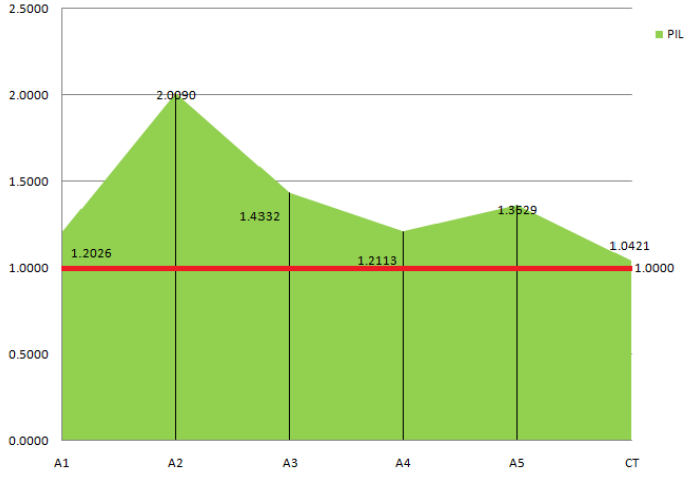


***Fig. 3.*** *Graphical representation of Pollution Index of Soil Loadings ($PI_L$) for Sr, Rb and Sc*

*Legend: A1-A5 and CT, soil sample codes, CT – soil control sample, $PI_L$ - Pollution Index of Soil Loadings*

$PI_L$ shows that the entire investigated area poses a high level of pollution ($PI_L$ > 1), even for the control area, due to the elevated level of scandium in the soil, which is causing deterioration of the soil quality.

The geo-accumulation index shows moderate contamination ($1 < I_{geo} \leq 2$) for scandium and zero contamination for strontium and rubidium (Table 5).

***Table 5.*** *Geoaccumulation indices of Sr, Rb and Sc, for the collected soil samples*

| Sample code | Igeo(Sr) | Igeo(Rb) | Igeo(Sc) |
|---|---|---|---|
| A1 | -0.2983 | -0.6174 | -0.2193 |
| A2 | 0.4150 | -0.7018 | 1.3728 |
| A3 | -0.1739 | -0.6845 | 0.4828 |
| A4 | -0.3114 | -0.8289 | 0.0365 |
| A5 | -0.0593 | -0.9069 | 0.3728 |
| CT | -0.5850 | -0.5850 | -0.5850 |

*Legend: A1-A5 and CT, soil sample codes, CT – soil control sample, Igeo – Geo-Accumulation Index of soil*

## CONCLUSION

The investigated soil samples, collected from the area with solid waste deposits shows a lower content of rubidium and strontium compared to the normal concentrations of these metals in the upper earth crust, but comparable with the control samples. On the other hand, scandium is present in big quantities in the soil covered by wastes, and less in the control samples. The pollution indices, CF, $PI_L$ and Igeo demonstrate that the pollution with scandium is degrading the soil quality and is a cause for concern.

## ACKNOWLEDGEMENTS

All authors are principal authors and have contributed evenly to this paper. Corresponding author: despinabordean@usab-tm.ro.

This research paper was funded by Interreg–IPA Cross–border Cooperation Romania-Serbia Programme - financed by the European Union under the Instrument for Pre-accession Assistance (IPA II) and co-financed by the partner states in the Programme, through the project "Modern technologies for monitoring land covered with waste in order to restore their initial use", 2019–2021, code e-MS: RORS 365.

## REFERENCES

[1] Ahamad, M.I.; Song, J.; Sun, H.; Wang, X.; Mehmood, M.S.; Sajid, M.; Su, P.; Khan, A.J., Contamination level, ecological risk, and source identification of heavy metals in the hyporheic zone of the Weihe River, China, International journal of environmental research and public health, Switzerland, 17/3, 1070, 2020.

[2] Bordean D.M., Cojocariu A., Horablaga M., Cojocariu L., Alda S., Nica D., Alda L., Borozan A.B., Scandium, element of surprises**,** Ecology, Economics, Education and Legislation, Conference Proceedings, Bulgaria,vol. I, pp 865-872, 2013,doi:10.5593/SGEM2013/BE5.V1/S20.113, http://sgem.org/sgemlib/spip.php?article3365;

[3] Bordean, D.M.; Borozan, A.B.; Nica, D.; Alda, S.; Cojocaru, L.; Horablaga, M.; Gergen, I. Assessment of soil, copper, cobalt and chromium contamination in old mining areas from Romania, International Multidisciplinary Scientific GeoConference: SGEM, Albena, Bulgaria, 5, 101–108, 2012, June 17–23 http://toc.proceedings.com/19962webtoc.pdf.

[4] European Environment Agency (EEA): Digital Elevation Model (DEM) with spatial resolution at 25 m, Produced using Copernicus data and information funded by the European Union - EU-DEM layers; owned by the Enterprise and Industry DG (DG-ENTR) and the European Commission, Denmark, 2017,

https://www.eea.europa.eu/data-and-maps/data/copernicus-land-monitoring-service-eu-dem

[5] Geospatial database of the Real Estate Cadastre and Advertising Agency, Romania, http://geoportal.ancpi.ro/geoportal/catalog/download/download.page;

[6] Greger M., Uptake of nuclides by plants, Technical Report TR-04-14, Department of Botany, Stockholm University, Sweden, 2004, https://skb.se/upload/publications/pdf/TR-04-14.pdf.

[7] Heghedűş-Mîndru, G., Biron, R.C., Perju, D.M., Rusnac, L.M., Riviş, A., Ştef, D.S., Cation contents in natural mineral waters of Romania determined with the HPIC method, Journal of Food, Agriculture and Environment, Finland, 6, pp: 506–509, 2008, https://doi.org/10.1234/4.2008.1395.

[8] Kenneth Barbalace, Periodic Periodic Table of Elements - Scandium - Sc. EnvironmentalChemistry.com. 1995 - 2021. https://EnvironmentalChemistry.com/yogi/periodic/Sc.html

[9] Khaled, A., Abdel-Halim, A., El-Sherif, Z., Mohamed, L. A., Health risk assessment of some heavy metals in water and sediment at Marsa-Matrouh, Mediterranean Sea, Egypt, Journal of Environmental Protection, 8(01), 74, 2017

[10] McLean, J. E., Bledsoe B. E. Behavior of metals in soils (EPA/540/S-92/018). U.S. Environmental Protection Agency, Washington, D.C., USA, 1992.

[11] Porter, K. E., U.S. Bureau of Mines, Moldova Noua, Geologic information, Romania, https://mrdata.usgs.gov/mrds/show-mrds.php?dep_id=10133958.

[12] Rudnick, R.L., Gao, S., The Composition of the Continental Crust. In: Holland, H.D. and Turekian, K.K., Eds., Treatise on Geochemistry, Vol. 3, The Crust, Elsevier-Pergamon, Oxford, England, 1-64, 2003.

[13] Thomilson D.C., Wilson D.J., Harris C.R., Jeffrey D.W., Problem in heavy metals in estuaries and the formation of pollution index, Helgolander Meeresunters, Germany, 33**,** 566–575 (1980).

[14] Tóth, T., Kovács, Z. A., Rékási, M. XRF-measured rubidium concentration is the best predictor variable for estimating the soil clay content and salinity of semi-humid soils in two catenas, Geoderma, Elsevier, 342, pp. 106-108, 2019.

[15] Vaverková, M. D., Maxianová, A., Winkler, J., Adamcová, D., Podlasek, A., Environmental consequences and the role of illegal waste dumps and their impact on land degradation, Land Use Policy, Elsevier, 89(C), 2019.

Section

# WATER RESOURCES

Water resource management
Water use, standards
Hydrology, irrigation and drainage science and technology management
Water quality and hydraulic engineering

# FLOCCULATION OF FINE APATITE AIMED AT REDUCING ENVIRONMENTAL WATER USE PROBLEMS IN MINERAL PROCESSING PLANTS

**Alexandr V. Artemev**[1]
**G. V. Mitrofanova**[2]
[1, 2] Mining Institute of the Kola Science Centre of the Russian Academy of Sciences, Apatity, Russia

## ABSTRACT

Water treatment technologies involving pre-treated industrial effluents without transporting them to the tailing dump are of interest primarily from an environmental point of view, as they reduce the environmental burden. The paper studies the possibility of purification of process waters from apatite concentrate production from suspended particles and water-soluble impurities using polyacrylamide flocculants.

By studying the processes of adsorption of $H^+$ and $OH^-$ ions from aqueous solutions, the acid-base properties of the surface of the solid phase of the most polluted technological product - the drain of the apatite concentrate thickener - the mineral composition of which is 90% apatite have been studied. The influence of the reagents present in the processing technology on the quantitative ratio of acid-base centers on the apatite surface has been evaluated. It has been shown that the interaction of these reagents with the mineral creates prerequisites for a greater efficiency of the anionic flocculant.

The electro-surface properties of apatite treated with various reagents were studied using the laser Doppler electrophoresis method. The mechanism of fixation of ions present in the dispersion medium on the surface of apatite was studied by infrared spectroscopy.

In order to determine the conditions under which various flocculants are in the most ionized state, studies were conducted on the change in the viscosity of the polyelectrolyte solution at different pH values. The position of the isoionic point for samples of cationic and anionic flocculants in the presence of reagents used in the apatite flotation and dehydration of apatite concentrate was studied.

A research has been carried out on "model" and real suspensions in circulating water for a number of cationic, anionic and nonionic flocculants. The kinetic and concentration dependences of the flocculating capacity of the studied reagents were determined, which confirmed the high efficiency of the anionic type reagents.

***Keywords:*** *water-preparation process, reagents-flocculants, flotation, phosphorus-containing ores*

## INTRODUCTION

At present, water treatment technologies are of some interest in order to involve pre-treated wastewater from mineral processing plants without transporting them to the tailing pond. The study of the composition of various waters from mineral processing plants working with apatite-containing ores has shown that the main impurities affecting the technological parameters of obtaining conditioned apatite concentrate are suspended particles and calcium ions [1]. The most contaminated processing product transported to the tailing dump is a drain of the apatite concentrate thickener which is characterized by high hardness, increased concentration of polyvalent ions and a high content of suspended particles due to applying of an inorganic coagulant.

A well-known and widely practiced way to reduce the amount of suspended particles is the use of organic flocculants [2]. The flocculation process and its efficiency are influenced by many parameters and in each case the choice of the optimal flocculant should be based on the study of the surface properties of the dispersed phase, the ionic composition of the dispersion medium and the characteristics of the flocculant itself (molecular weight, ionicity, etc.).

## MATERIALS AND METHODS

The substantiation and selection of the most effective flocculant for the purification of industrial waters of apatite-nepheline processing plant were carried out on the drain of the apatite concentrate thickener, the most contaminated product. According to X-ray phase analysis, the mineral composition of the thickener's drain solid phase is almost 90% represented by apatite sludge (Table 1). The efficiency of water treatment largely depends on the surface properties of this mineral; therefore apatite was used as the solid phase of the model system.

***Table 1***. *Results of X-ray phase analysis of solid phase of apatite concentrate thickener drain*

| ***Mineral*** | ***Content, %*** |
|---|---|
| Fluorapatite | 88.42 |
| Nepheline | 5.38 |
| Aegirine | 0.96 |
| Aegirin-augite | 0.7 |
| Arfvedsonite | 0.8 |
| Orthoclase | 1.02 |
| Sodalite | 0.29 |
| Natrolite | 0.55 |
| Titanite | 1.09 |
| Ilmenite | 0.55 |
| Annite | 0.24 |

The surface properties of apatite were studied by the following methods: the acid-base surface properties were researched by investigating the adsorption of $H^+$ and $OH^-$ ions from aqueous solutions; the electro-surface properties were studied by laser Doppler electrophoresis on Malvern Zetasizer Nano-ZS laser analyzer (Great Britain). The zeta potential measurements were carried out in the apatite suspension

in distilled water in the presence of an indifferent electrolyte (KCl 0.01 M). The particle size distribution of apatite used in the research was determined on a laser granulometer Malvern Mastersizer 3000 (Great Britain) and shown in Figure 1.

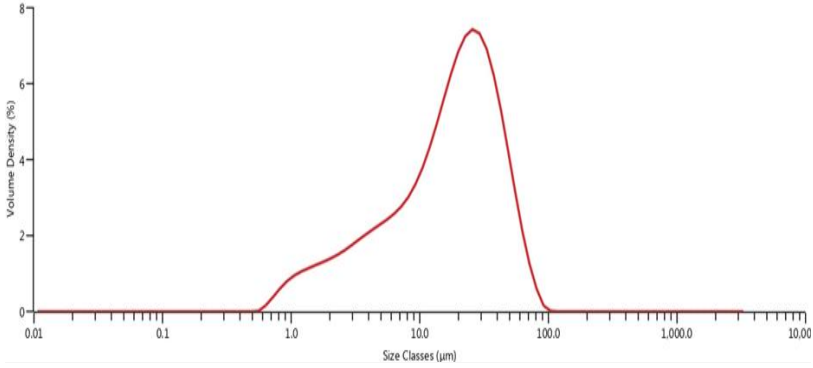


***Fig. 1.*** *The apatite particle size distribution*

Flocculants' efficiency was evaluated on a "model" disperse system, which was a suspension of fine apatite concentrate particles with a dispersed phase content of 2% prepared in circulating water. The suspension was prepared with the apatite concentrate (particle size -0.071 mm) with a $P_2O_5$ content of 39.34%.

For flocculation of fine apatite particles the authors studied polyacrylamide cationic (FO series) and anionic (AN series) SNF flocculants (France) with various ionicity.

## RESULTS AND DISCUSSION

The surface of apatite is heterogeneous and bifunctional and bears both acidic and basic centers of different strength. It is known [3], that H+, OH-, CO32- ions are potential-forming ions for apatite; therefore the surface properties were studied using the pH-metric method based on the study of the adsorption from aqueous solutions of H+ and OH- ions. The method is to measure the suspension effect (SE), which is the difference between the concentrations of counter-ions in the suspension (dispersed system) and the filtrate. According to the theory [4], the SE value allows estimating which centers dominate on the mineral particles surface and characterizes the exchange processes occurring between the liquid phase and the surface, depending on the characteristics of the dispersion medium.

The SE evaluation in a suspension of apatite particles prepared in distilled water (Fig. 2) showed the predominance of the basic centers on the apatite surface. This creates the prerequisites for the interaction of positively charged reagents with the apatite surface.

Zeta potential measurements results also show that the potential-forming layer on the apatite surface is formed by anions. According to the composition and apatite structure, anions are represented with phosphate and hydroxylic groups [5]. Evaluation of the zeta potential of apatite under the action of cationic and anionic flocculants (Fig. 3) has shown that both anionic and cationic flocculants are fixed

on the apatite surface in the absence of any polyvalent cations. A cationic flocculant, which has a lower ionicity, more strongly changes the zeta potential of the apatite surface, recharging it, compared with a decrease in the zeta potential in the case of anionic flocculant fixing on the surface. To put in another way, the fixation of the flocculant on the mineral surface due to the interaction of differently charged groups determines the greater amount of the adsorbed reagent.

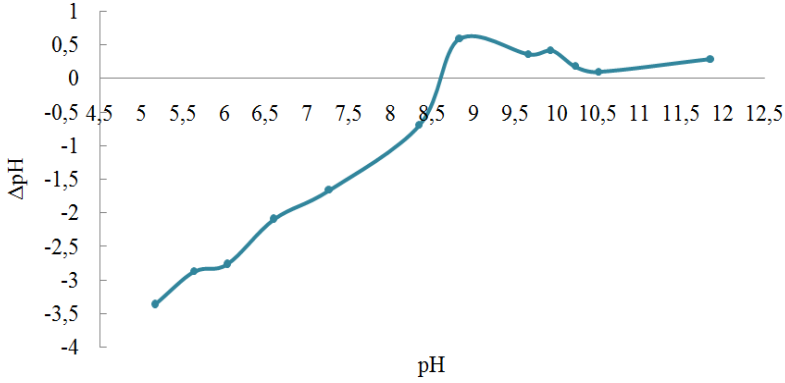


***Fig. 2.*** *Dependence of the SE on pH in apatite suspension in distilled water*

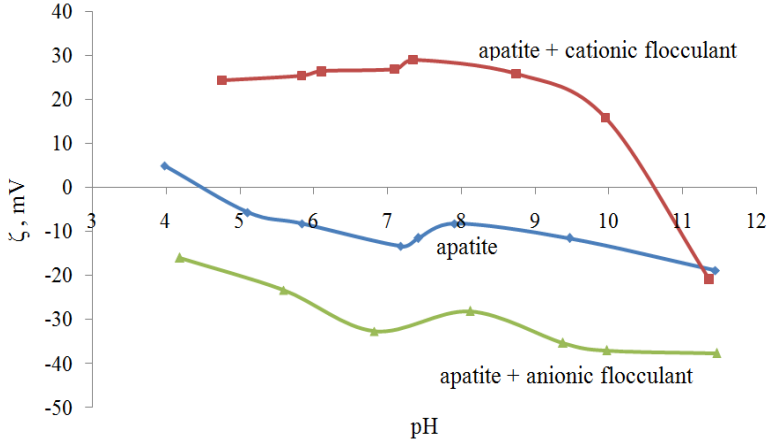


***Fig. 3.*** *Dependence of the zeta-potential of apatite under the action of cationic and anionic flocculants at different pH values*

It is known that the circulating water of processing apatite-nepheline ores plants contains a large amount of polyvalent metal cations, which will also interact with the basic apatite surface. Evaluation of the electro-surface properties of apatite in the presence of calcium and iron salts (Fig. 4) has shown that the adsorption of calcium cations with a concentration of 40 mg/l $Ca^{2+}$ decreases the negative value of the zeta potential and shifts the zero point of charge to a higher pH range. A further increase of calcium ions concentration can lead to a complete recharge of the surface and change the sign of the apatite surface to positive [6], [7]. Iron cations, which have a higher positive charge, neutralize negatively charged groups

on the apatite surface to a greater extent, and even at $Fe^{3+}$ concentration of 40 mg/l the apatite surface is recharged.

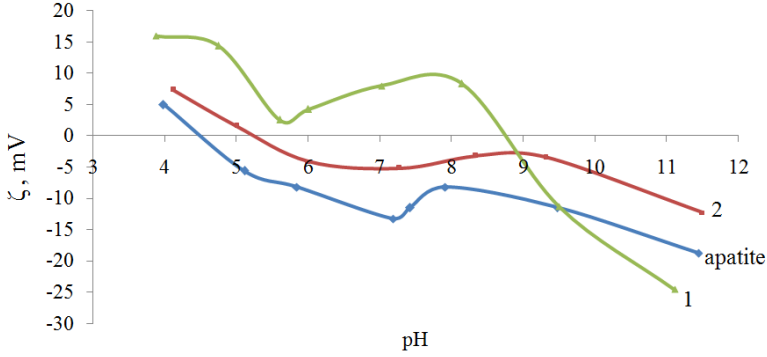


***Fig. 4**. The impact $Fe^{3+}$ ions (1) and $Ca^{2+}$ (2) ions on zeta potential of apatite: $Ca^{2+}$ - 40 mg/l, $Fe^{3+}$- 40 mg/l*

Thus, it can be assumed that in the circulating water contaminated with salts of polyvalent metals positive ions are fixed on the apatite surface and prerequisites for more effective action of the anionic flocculant are produced.

The higher efficiency of flocculation is known to depend on the characteristics of the used organic polymer, the more charged flocculant is used. It is important to understand to which pH range corresponds this flocculant being in the most ionized state. This state determines more expanded conformation of molecules due to the mutual repulsion of equally charged parts of the polymer chain [8].

Evaluation of the solution viscosity of the cationic and anionic polyacrylamide has shown (Fig. 5) that the anionic flocculant has the maximally expanded state in the alkaline pH range. For a cationic flocculant the regularities are different: when pH value increases, the charges of the polycation will be bound. Consequently, in the alkaline region the cationic flocculant molecule is in unexpanded state, which is ineffective for bridge-type flocculation.

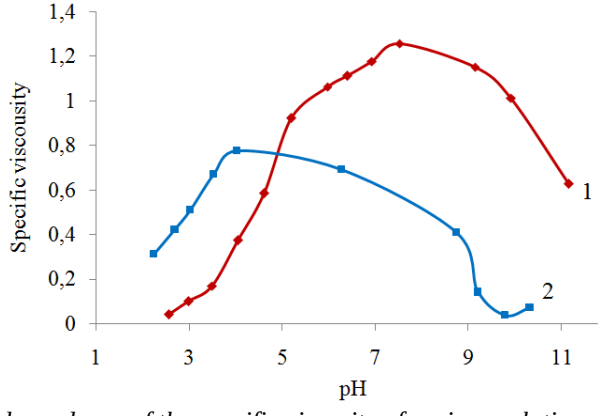


***Fig. 5**. The dependence of the specific viscosity of various solutions of flocculants depending on pH ( 1 - anionic flocculant, 2 - cationic flocculant)*

The obtained concentration and kinetic curves of the clarification degree of the "model" suspension (Fig. 6) confirm anionic flocculants to be more effective and much lower costs for anionic flocculants are required to achieve the similar characteristics of water clarification. The advantage of the anionic flocculant appears more in the first minutes of clarification. Among anionic flocculants, reagents with a higher ionicity (from 30%) have a higher efficiency.

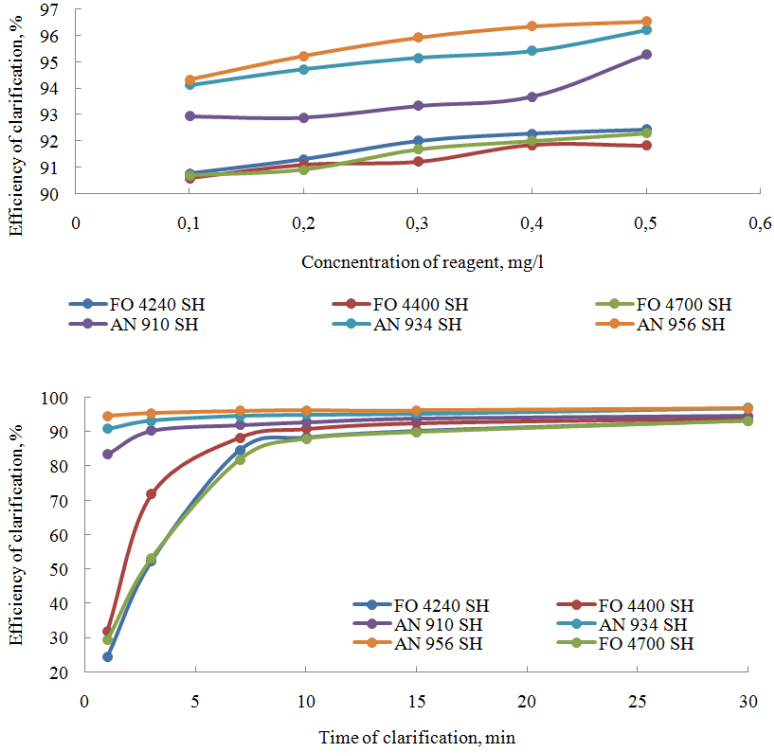


***Fig. 6.*** *Concentration and kinetic curves of the clarification degree of a model suspension of apatite concentrate in recycled water for a number of cationic (FO series) and anionic (AN series) flocculants*

## CONCLUSION

The authors have studied the effect of anionic and cationic organic flocculants during cleaning the drain of the apatite concentrate thickener as the most contaminated product obtained in the apatite-nepheline ores processing. It was found that the influence of the applied reagents and ions of the liquid phase changes the surface properties of the dispersed phase. Polyvalent metal cations are fixed on the surface of apatite providing conditions for the effective application of anionic polyacrylamide flocculant.

The authors have analyzed the results and assumed the following mechanism of action of an anionic flocculant:

- oleate ion is adsorbed on apatite particles;
- iron ions (or its hydroxocomplexes) are fixed under the action of ferrous sulfate making a positive charge to the particle surface;
- anionic flocculant due to the formation of complex compounds with iron ions is fixed on the particles of the dispersed phase;
- the calcium ions present in the solution also enhance the flocculating effect due to the formation of complex bridges of the "particle - macroion - $Ca^{2+}$ - macroion - particle" type, thereby increasing the effective size of the flocculant molecule.

## ACKNOWLEDGEMENTS

This publication has been produced with the assistance of the European Union. The contents of this publication are the sole responsibility of the following authors: A.V.Artemev, Mitrofanova G.V. and can in no way be taken to reflect the views of the European Union.

## REFERENCES

[1] Golovanov V.G., Petrovsky A.A., Brylyakov Yu.E., Introduction of recycled water supply at ANOF-2 // Gornyi Zhurnal. - 1999. - № 9. - pp. 48-50.

[2] Gandurina L.V. Wastewater treatment using synthetic flocculants. M.: DAR/VODGEO, 2007. 197 p.

[3] Brylyakov Yu.E. Development of the theory and practice of complex beneficiation of apatite-nepheline ores of the Khibine deposits: Ph.D.in Eng. Thesis: 25.00.13: Kirovsk, 2004. - 358 p.

[4] Ikonnikova K.V., Ikonnikova L.F., Minakova T.S., Sarkisov Y.S. Theory and practice of pH-metric determination of acid-base properties of solid surfaces: textbook - Tomsk: Publishing house of Tomsk Polytechnic University, 2011. - 85 p.

[5] - Skwarek E., Janusz W. / The Influence of Carbonate Ions on the Structure of the Electrical Double Layer at the Interface of Hydroxyapatite/Electrolyte Solution / Materials Science, Vol. 22, No. 2. 2016, pp. 174-178, https://doi.org/10.5755/j01.ms.22.2.7817

[6] Yaoyang Ruan, Zeqiang Zhang, Huihua Luo, Chunqiao Xiao, Fang Zhou and Ru-an Chi / Effects of Metal Ions on the Flotation of Apatite, Dolomite and Quartz / *Minerals* 2018, *8*(4), 141; https://doi.org/10.3390/min8040141

[7] Fang Zhou, Qi Liu, Xu Liu, Wanchun Li, Jian Feng and Ru-an Chi / Surface Electrical Behaviors of Apatite, Dolomite, Quartz, and Phosphate Ore / Front. Mater., 18 February 2020; https://doi.org/10.3389/fmats.2020.00035

[8] Holmberg K., Jönsson B.,. Kronberg B,. Lindman B / Surfactants and polymers in liquid solutions / BINOM. Laboratory of knowledge, 2007 - 528 p.

# REDUCTION OF THE VOLUME OF PUMPING OF LIQUID WASTE FROM THE PRODUCTION OF APATITE CONCENTRATE DUE TO THE TECHNOLOGY OF PARTIALLY CLOSED WATER CIRCULATION

**Alexandr V. Artemev**[1]
**Valentin V. Biryukov**[2]
[1, 2] Mining Institute of the Kola Science Centre of the Russian Academy of Sciences, Apatity, Russia

## ABSTRACT

The use of recycled water supply technology in mineral dressing plants solves current environmental and economic problems for the mining and processing industry. Usually, water treatment takes a long time and requires constructing large-volume tailing dumps.

The paper proposes a technology of a partially closed water circulation with the purification of watered production waste from suspended particles and water-soluble impurities that negatively affect the flotation process, based on the regularities describing the interaction of flocculants with the phases of a heterogeneous system of process waters.

The authors have determined the most effective reagents providing optimal indicators of recycled water. The proposed technology is implemented in hardware in a radial thickener and eliminates the discharge of process water into an external tailings dumps facility, which will reduce the area occupied by production waste.

Based on the particle size distribution data for various preliminary treatment options, differential and integral particle size distribution curves have been obtained. Analytical expressions of the obtained curves have been used to create discrete functions of volume fractions of particles with different sizes when constructing a model of the initial feed.

The hydrodynamic processes of highly diluted suspension flows in the thickener's body were studied using computational experiments on a model developed in the ANSYS Fluent software package, which is based on the real 3D geometry of a radial thickener. To build the geometry, the authors used a standard module GAMBIT. A computational experiment on cleaning the apatite concentrate discharge was performed on a virtual stand. The distributions of the concentrations of volume fractions of particles and the velocities of their movement in the thickener's volume were obtained.

The results of laboratory studies and computer simulation data allow the authors to tell about the prospect implementation of the technology of intra-plant water circulation, which will reduce by 10% the amount of wastewater discharged into the tailing dump. The use of the most efficient reagents will provide optimal

water parameters for the content of suspended particles and hardness cations and, ultimately, will increase the technological and environmental performance of the Khibiny apatite-nepheline ores processing.

***Keywords:*** *water-preparation process, reagents-flocculants, flotation, apatite-nepheline ores, computer simulation*

## INTRODUCTION

Along with the indisputable advantages, the introduction of recycled water supply at the mineral dressing plants has a number of problems affecting on the technological process. The ionic composition of water plays a specific role in using recycled waters for apatite-nepheline ores flotation. It has been found that the main components of recycled water are $Ca^{2+}$, $Mg^{2+}$, $Fe^{2+}$, $K^{+}$, $Na^{+}$ cations and $Cl^{-}$, $SO_4^{2-}$, $CO_3^{2-}$, $HCO_3^{-}$, $SiO_3^{2-}$ anions, as well as sludge and organic components [1].

The experience of the mineral dressing plants has revealed that the greatest influence on the change in the surface properties of minerals composing apatite-nepheline ores is exerted by suspended solids and Ca2 + cations. The particle size of suspended solids is usually in the range of 0.1-300 microns, i.e., from course to colloidal particles. The negative effect of sludge on the flotation process is the sorption of the collector on itself, a change in the ionic composition of the pulp and contamination of the apatite concentrate due to the mechanical removal of sludge into the froth. The study of the influence of $Ca^{2+}$ cations on the apatite flotation has shown their interaction with soaps of fatty acids with the formation of sparingly soluble salts as colloidal dispersed formations and reducing the CMC (critical micelle concentration) of collectors. During flotation, cations activate the minerals' surface, violate selectivity, and deteriorate the concentrate quality [2,3]. Earlier works have proved that the ultimate value of calcium cations content in flotation water should not exceed 20 mg/l [4]. According to the experience of the dressing plants processing apatite-nepheline ores, the optimum amount of suspended particles is up to 900 mg/l.

Mining and processing enterprises use tailings ponds to treat process water for its further application. The water is clarified there under the action of gravitational forces. However, it takes considerable time and volumes of the tailings pond to achieve equilibrium of the processes occurring in the tailings dump. At present, the mining enterprises are interested in increasing the technological efficiency and environmental safety of ore processing by involving pre-treated process water of the processing plant without discharging it into the tailings pond.

The most promising source of water, which can be used in in-plant water circulation, is a discharge of the apatite concentrate thickener. The study of the characteristics of this product (Table 1) has shown the excess of the maximum permissible values by several times, which excludes its potential involvement in the technological process without additional purification.

***Table 1.*** *Characteristics of the apatite concentrate thickener discharge*

| Content of $Ca^{2+}$, mg/l | Content of suspended particles, g/l |
|---|---|
| 52.2 | 27.363 |

The authors have proposed a technology of intensification of suspended particle separation by means of polyacrylamide flocculants, hardware implemented in the radial thickener [5].

Due to the complexity of industrial tests, the most perspective method to research the influence of technological parameters of the suspension on processes of thickening of the apatite concentrate discharge is a computational model experiment.

## MATERIALS AND METHODS

At the first study stage the authors have assessed the efficiency of various organic flocculants differing by molecular weight, origin and quantity of ionogenic groups, in particular, the SNF company reagents, representing polyacrylamides of high molecular mass with various ionicities (Table 2).

***Table 2.*** *Characteristic of reagents-flocculants*

| Reagent class | Name | Ionicity | Molecular mass |
|---|---|---|---|
| Anionic flocculants | AN 956 SH | High, 50% | $(13.4\text{-}16.1)*10^6$ |
| | AN 934 SH | High, 30 % | $(13.8\text{-}16.75)*10^6$ |
| | AN 923 SH | Average, 20% | $(12.2\text{-}14.1)*10^6$ |
| | AN 910 SH | Very low, 10% | $(11.6\text{-}13.75)*10^6$ |
| Cationic flocculants | FO 4700 SH | High,70% | $(4.9\text{-}7.25)*10^6$ |
| | FO 4400 SH | Average,30% | $(5.0\text{-}7.55)*10^6$ |
| | FO 4240 SH | Low,16% | $(6.2\text{-}8.25)*10^6$ |

The flocculation activity of the studied polymeric reagents was determined on model and real disperse systems. As a model system the authors used a suspension of fine dispersed apatite concentrate particles (particle size -0.071 mm, $P_2O_5$ content - 39.34%) with the content of dispersed phase 2%, prepared on distilled and recycled water.

The hydrodynamic processes of highly diluted suspension flows were studied by means of computational experiments over a model developed in the ANSYSFluent software package. The main research task was to study the influence of technological parameters of the suspension on thickening processes and on the kinetics of the thickening process using polyacrylamide flocculants.

Proceeding from the fact, that the water treatment technology is proposed to be realized by a radial thickener in ANSYSFluent software package (license of Mining Institute KSC RAS), the mathematical model of working space of a 30-meter thickener was developed. The model is based on the real 3D geometry of a radial thickener with a central drive. The standard GAMBIT module was used to build the geometry of the radial thickener. The model is constructed of two main parts: a stationary volume (the thickener's body) and a dynamic volume (a prismatic element - thickener rake). The raking mechanism of the thickener is designed to

move the deposited disperse particles to a discharge port and consists of a central axis and four radial rakes with blades. It was modeled using "SlidingMesh" technology. This technology allows the interaction of any rotationally and progressively moving components with multiphase fluid medium and vice versa. In this case, the rotating blades of the thickener's raking mechanism at a controlled speed transmit effort to the medium consisting of dispergating and several dispersed phases of the suspension.

The computational grid of 3D geometry of the virtual stand, as close as possible to the real Outotec thickener with a diameter of 30 meters has 670,000 tetrahedral elements. Feeding of the initial suspension and discharge into the model is performed through the upper and lower nipples of the cylindroconical body. It is possible to control the flow rates of supply and discharge of the suspension. The clarified water is drained through the upper section of the model. The flow of a highly diluted suspension was simulated in the working space of the thickener by multiphase Euler equations for one dispergating and several dispersed phases.

## RESULTS AND DISCUSSION

The influence of ionicity on flocculation of fine disperse apatite concentrate particles was studied through concentration and kinetic dependences of the degree of clarification of the model apatite concentrate suspension in recycled water for a number of cationic and anionic flocculants (Fig. 1).

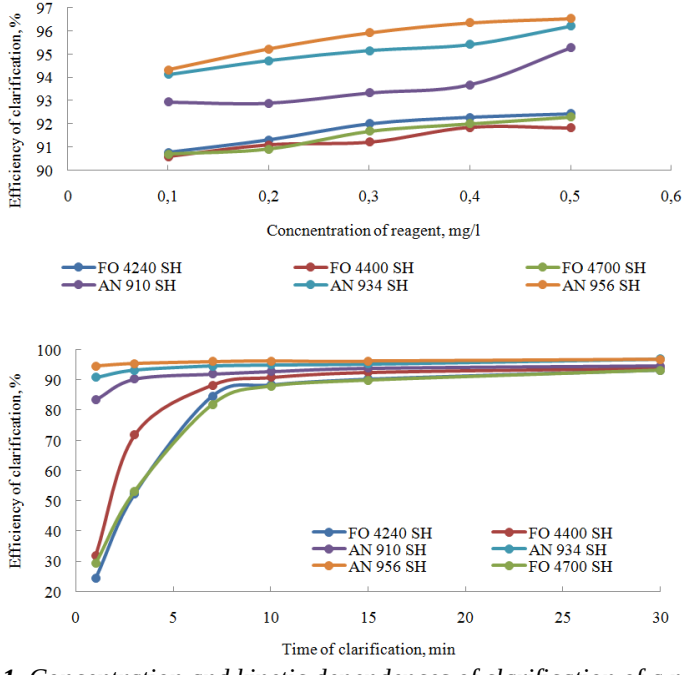


***Fig. 1.*** *Concentration and kinetic dependences of clarification of a model apatite concentrate suspension in recycled water for a number of cationic (FO series) and anionic (AN series) flocculants*

The data show that anionic flocculants are more effective in their action. The advantage of an anionic flocculant is mainly seen in the first minutes of clarification. The anionic reagents-flocculants with a higher degree of ionicity (from 30 %) have a higher efficiency.

Further studies were aimed at creating models of initial feed for different preparation regimes. The real discharge of apatite concentrate's thickener was taken as a basis. As the majority of disperse systems, it contains particles of different sizes, and their content is not equal. Determination of particle sizes of the disperse phase and construction of the curves of particle size distribution is the essence of the sedimentation analysis.

Its use is limited by conditions of the Stokes equation application. To meet these conditions, the industrial thickener discharge with suspended particle content of 109.3 g/l was diluted with distilled water. The concentration of dispersed phase obtained is 1%. The sedimentation analysis was carried out according to known methods [6].

The studies were carried out in two modes:

- sedimentation of the apatite concentrate thickener's discharge without the use of chemical reagents;
- sedimentation of the apatite concentrate thickene's discharge using the developed technology: input of 0.2 mg/l of anionic flocculant AN 934 SH into the initial feed at pH-11.

The relative mass (share) of the sediment of the dispersed phase of the low-concentration suspension of the apatite concentrate thickener's discharge, accumulated during the sedimentation time $\tau$ is described by the following empirical functions:

- for a test without chemical reagents:
$$F(\tau) = 100(1 - e^{-0.25\tau}) - \tau(25e^{-0.25\tau})$$
- for a test with flocculant AN 934 SH at pH-11:
$$Z(\tau) = 100(1 - e^{-0.68\tau}) - \tau(68e^{-0.68\tau})$$

To characterize the fractional composition of the settling suspensions, the authors have plotted the integral and differential curves of particle size distribution, which show the mass share of each fraction (Fig. 2). The distribution curves were plotted by an analytical method [7].

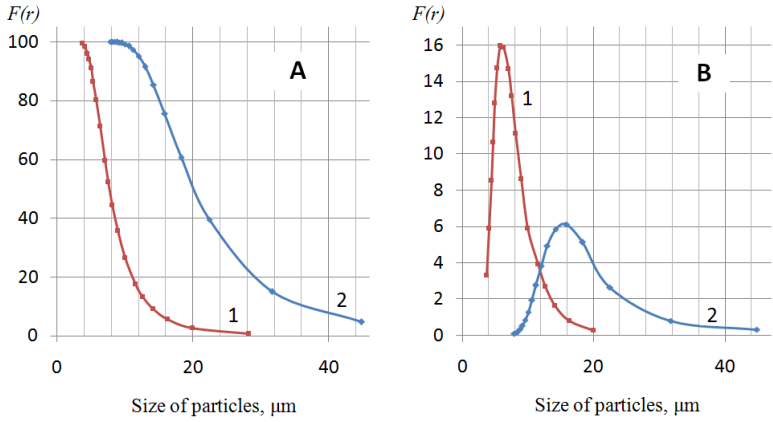


***Fig. 2.*** *The integral (A) and differential (B) curves of particle size distribution form the apatite concentrate's discharge: 1 – without a flocculant, 2 - 0.2 mg/l AN 934 SH at pH-11*

The analytical expressions of the differential curves of particle mass distribution of the suspension by equivalent radius were obtained by differentiating the analytical expression of the integral distribution curves by the variable r. For a test without chemical reagents: $F(r) = -(16.129\tanh(0.323r - 2.226)^2 - 16.129$; for a test with flocculant AN 934 SH at pH-11: $F(r) = -(14{,}706\tanh(0.294r - 2.206)^2 - 14{,}706$

The obtained expressions were used to create discrete functions of volume fractions of particles with different particle sizes when constructing models of initial feed of each water preparation mode.

The computational experiments on the research of sedimentation of the apatite concentrate thickener's discharge under conditions of using a flocculant effectively binding apatite particles (anionic flocculant AN 934 SH with a degree of ionicity 30%) and without reagents (particles sedimentation by gravity) were set on the virtual bench.

The authors have obtained the distributions of concentrations of volume fractions of particles (Table 3, Fig. 3,4) and velocities of their movement in the volume of the thickener (Fig. 5).

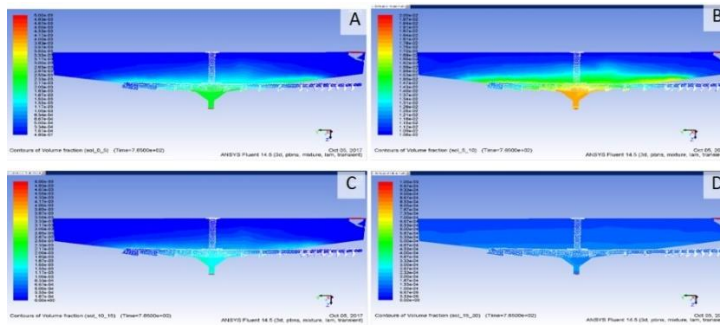


***Fig. 3.*** *Fields of volume concentrations of solid phases of different coarseness of the suspension on the vertical section of the thickener's model (at sedimentation without reagents-flocculants);*

A - coarseness $0 – 5 \cdot 10^{-6}$ m; B – $5 \cdot 10^{-6} – 1 \cdot 10^{-5}$m; C – $1 \cdot 10^{-5}$ - $1.5 \cdot 10^{-5}$m; D - $1.5 \cdot 10^{-5} – 3 \cdot 10^{-5}$m

***Table 3.*** *Distribution of volume fractions of particles*

| Fract-ion of initial sus-pension, μm | Concentration of volume fractions, kg/s | | | Fract-ion of initial suspen-sion, μm | Concentration of volume fractions, kg/s | | |
|---|---|---|---|---|---|---|---|
| | Test without chemical reagents | | | | Test with AN 934 SH at pH-11 | | |
| | Initial feed | Sands of thick-ener | Dis-charge of thick-ener | | Initial feed | Sands of thicken-er | Dischar-ge of thicken-er |
| water | 60,43 | 3,91 | 79,99 | water | 77,78 | 3,16 | 76,80 |
| 0-5 | 0.232 | $5.88 \cdot 10^{-5}$ | $4.36 \cdot 10^{-10}$ | 0-20 | 0.12 | 0.00168 | 0.02278 |
| 5-10 | 3.121 | 0.0039 | 0.0286 | 20-70 | 1.55 | 0.034 | 0.208 |
| 10-15 | 0.1032 | $2.66 \cdot 10^{-5}$ | $1.86 \cdot 10^{-10}$ | 70-85 | 0.65 | 0.034 | 0.041 |
| 15-30 | 0.000258 | $3.48 \cdot 10^{-7}$ | $1.93 \cdot 10^{-6}$ | 85-120 | 0.82 | 0.0776 | 0.0248 |
| | | | | 120-170 | 0.499 | 0.0965 | 0.0064 |
| | | | | 170-250 | 0.2699 | 9.4745 | 0.2327 |
| | | | | 250-500 | 0.19 | 7.4389 | 0.34105 |
| | | | | 500-850 | 0.0699 | 5.8578 | 0.1355 |

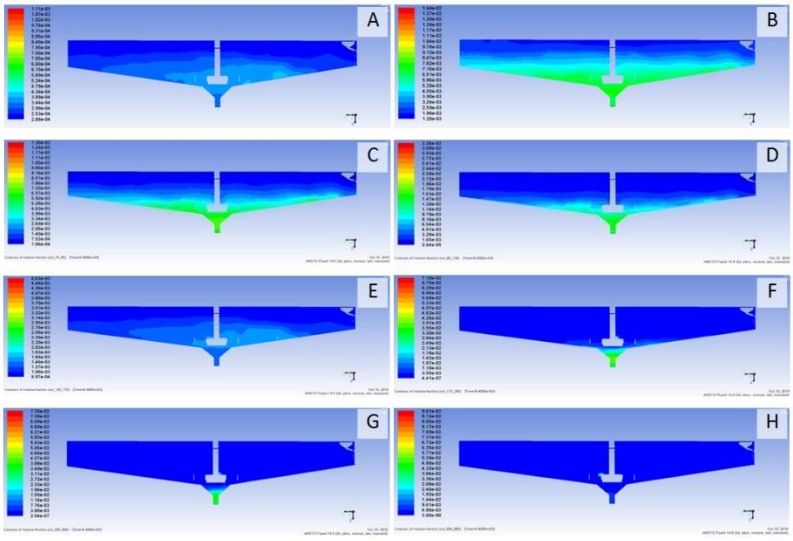


***Fig. 4.*** *Fields of volume concentrations of solid phases of different coarseness of the suspension on the vertical section of the thickener's model (at sedimentation with flocculant AN 934 SH):*

A – coarseness 0 – $2 \cdot 10^{-5}$m; B - $2 \cdot 10^{-5}$ – $7 \cdot 10^{-5}$m; C - $7 \cdot 10^{-5}$ – $8.5 \cdot 10^{-5}$m; D – $8.5 \cdot 10^{-5}$ – $1.2 \cdot 10^{-4}$m; E – coarseness $1.2 \cdot 10^{-4}$ – $1.7 \cdot 10^{-4}$m; F – $1.7 \cdot 10^{-4}$ – $2.5 \cdot 10^{-4}$m; G – $2.5 \cdot 10^{-4}$ – $5 \cdot 10^{-4}$m; H - $5 \cdot 10^{-4}$ – $8.5 \cdot 10^{-4}$m

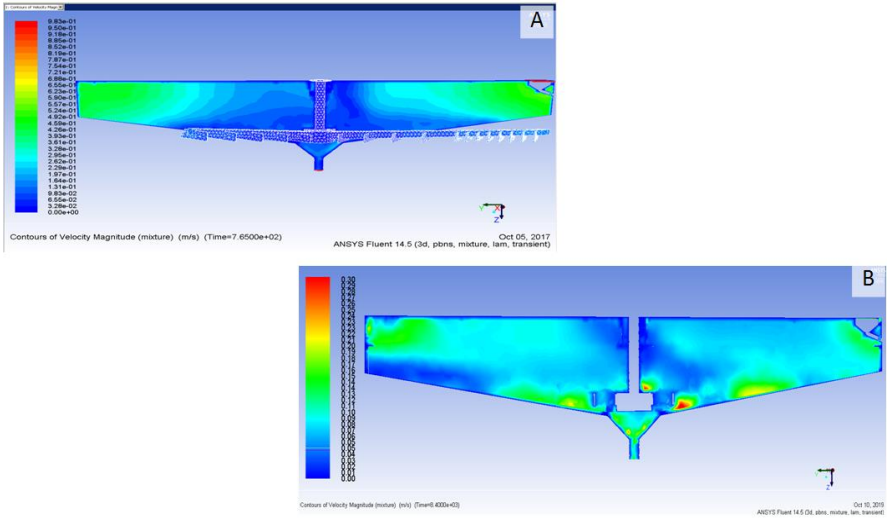


***Fig. 5.*** *The velocity field of the suspension on the vertical section of the thickener's model*

A – at sedimentation without flocculants, B - at sedimentation with flocculant AN 934 SH

## CONCLUSION

The authors have analysed the data obtained at this study stage and according to their conclusion, if the reagents-flocculants are not used, the main mass of volume fractions of the initial suspension accumulates on the inclined plane of the thickener's bottom and only a small part comes out through the discharge hole due to transportation with the rakes, but the sands of the thickener are heavily watered.

Thus, water preparation in a radial thickener cannot be carried out without flocculants due to the difficulty of achieving acceptable specific loads on solids. In case of using flocculants, according to the computational experiment results, there is an increase in particle settling velocities, due to enlargement of finely dispersed apatite particles and the density of the resulting thickener's sands. Rotating rotor rakes facilitate the movement of the sedimented suspension to the discharge hole of the thickener, and form the necessary operating mode which can provide mixing and amount of particle collisions necessary for floc formation.

The results of laboratory studies and computer simulation data allow to tell about the prospect implementation of the technology of intra-plant water circulation, which will reduce by 10% the amount of wastewater discharged into the tailing dump.

## ACKNOWLEDGEMENTS

This publication has been produced with the assistance of the European Union. The contents of this publication are the sole responsibility of the following authors: A.V.Artemev, V.V. Biryukov and can in no way be taken to reflect the views of the European Union.

Kolarctic CBC
EU FINLAND NORWAY RUSSIA SWEDEN

## REFERENCES

[1] Malinskaya I.S., Bacheva E.D. Research of features of selective apatite flotation under recycled water supply conditions. - Processing of oxidized ores. - M: Nauka, 1985. - pp. 205-211

[2] Golovanov G.A. Flotation of the Kola apatite ores. - M: Chemistry, 1976. - 216 p.

[3] Golovanov V.G., Petrovsky A.A., Brylyakov Yu.E., Introduction of recycled water supply at ANOF-2. - Gornyi Zhurnal. - 1999. - № 9. - pp. 48-50.

[4] Gershenkop A.Sh., Mukhina T.N., Artemev A.V. Features of the mineralogical composition of apatite-nepheline ore from the Oleniy Ruchey deposit and their impact on the processing performance. - Ore beneficiation, No. 3, 2014, pp. 33-36.

[5] Mitrofanova, G.V. Ivanova, V.A. Artemev A.V. Use of reagents-flocculants in water-preparation processes during phosphorous-containing ore

processing. - 17th International Multidisciplinary Scientific GeoConference SGEM 2017, SGEM2017 Conference Proceedings , June 29 - July 5, 2017, Issue 11, Vol. 17, 1143-1150 pp.

[6] Practicum on colloidal chemistry, edited by I.S. Lavrov. - M: Higher School, 1983. - 206 p.

[7] Zimon, A.D., Leshchenko N.F. / Colloidal Chemistry. - M: Agar, 2001. - 318 p.